

**Evaluation of Acute Cardiorespiratory Disease: Integrating
Metabolite-wide Analysis and Lung Mechanics
Pathophysiology**

Thesis submitted for the degree of
Doctor of Philosophy
at the University of Leicester

by

Masarrah Aljarroof

June 2023

Abstract

Evaluation of Acute Cardiorespiratory Disease: Integrating Metabolite-wide Analysis and Lung Mechanics Pathophysiology

Author: Masarrah Aljarroof

Challenges in studying acute life-threatening events and a knowledge gap in biomarker exploration for overlapping cardio-respiratory conditions necessitate further investigation. This thesis aims to bridge the gap by identifying additional biomarkers using metabolomics and physiological measures in acute cardio-respiratory conditions. Our hypotheses aim to test the differentiation power of plasma metabolomic profiles, characterize ventilation heterogeneity, and identify of metabolic dysfunction in lipid mediators in acute cardiorespiratory conditions.

Methods: We employed a multidimensional approach using LC-MS and GC-MS platforms to analyze plasma, breath, and sputum samples from the same population. The following studies were conducted: (1) Metabolite analysis in blood plasma samples of $n = 54$, in which $n = 20$ acquired from acute exacerbations of chronic obstructive pulmonary disease (AECOPD) patients and $n = 20$ acquired from acute heart failure (AHF) patients, compared to $n = 14$ samples acquired from healthy volunteers. (2) Breath data analysis for ventilation heterogeneity involved 310 subjects using the FOT test, with a subgroup of 208 with published VOC measurements (1, 2), The analysis aimed to investigate the association between identified VOC metabolomics disturbances and respiratory impedance. (3)

Prospective study using n = 141 sputum samples of AECOPD, acute asthma, pneumonia patients, and healthy control group targeting 13 metabolomic markers of inflammation resolution and comparing the results to a sub-cohort of n = 45 during stable status.

Results: (I) Mass spectral analysis identified 2193 compounds in plasma samples of AECOPD, AHF, and healthy subjects. Biomarker scores of 19 metabolites (9 features associated with AECOPD and 10 with AHF) demonstrated $\geq 70\%$ sensitivity and specificity in distinguishing between AECOPD, AHF, and health. (II) Resistance at 5 and 5-19 Hz as well as reactance at 5 Hz, area under the reactance AX, and resonant frequency were significantly different ($p < 0.000$) between all groups; moreover, ($p < 0.05$) indicated the significant impact of respiratory system compliance on the recovery of O, N, and S VOCs in exhaled breath. (III) Group comparisons revealed significant differences in lipid mediator PGE2 levels ($p < 0.01$), with no significant differences observed in stable cohorts. Correlation analysis showed a negative association between eosinophil count and PGE2 levels (coefficient = -0.21, $p < 0.05$) and a positive association between neutrophil count and PGE2 levels (coefficient = 0.24, $p < 0.05$).

Conclusion: This research highlights the potentials of metabolomics, both in targeted and untargeted approaches, along with the integration of bioinformatic statistical models in effectively differentiating between conditions with an overlapping pathology in an acute exacerbation's events and healthy volunteers. Additionally, the study demonstrates the feasibility of utilizing handheld FOT as a valuable tool for assessing respiratory system mechanics in the acute care setting. Furthermore, examining the relationships between the analysed metabolites and other clinical observations adds to our understanding of acute

cardio-respiratory conditions. These findings provide valuable insights that can contribute to the development of improved diagnostic strategies in the future.

Acknowledgments

To my family, who have been a constant source of love and encouragement, I am forever grateful. My parents' unwavering support and belief in my abilities have been instrumental in my academic pursuits. Their sacrifices and reassurance have been the cornerstone of my success, and I am truly blessed to have them by my side. I would also like to extend my deepest gratitude to my beloved and supportive siblings for always being there and motivating me throughout my journey.

To my loving husband, and my wonderful children, I am profoundly thankful for your understanding, patience, and support throughout this thesis journey. Your love, belief in me, and mere presence in my life have brought immense joy and happiness and have been a blessing that provided the motivation and strength to overcome challenges and reach this milestone. I am grateful for the countless sacrifices you have made and the countless hours you have dedicated to supporting my dreams.

I would like to extend my heartfelt appreciation to my supervisors for their invaluable guidance and support throughout the completion of this thesis. Firstly, I express my deep gratitude to my first supervisor, Dr. Neil Greening for his expert advice, insightful feedback, and continuous encouragement. His expertise and mentorship have played a crucial role in shaping this research and ensuring its academic rigor.

I am also deeply thankful to my second and third supervisors, Prof. Toru Suzuki and Prof. Salman Siddiqui, for their dedicated involvement in this project. Their valuable contributions, constructive criticism, and thoughtful suggestions have greatly enhanced the quality and depth of this work. Their diverse perspectives and expertise have broadened my understanding and enriched my research journey.

I am deeply grateful to the Royal Embassy of Saudi Arabia Cultural Bureau for their sponsorship of my PhD studies, which has been instrumental in enabling my academic pursuits.

I express my sincere gratitude to Dr. Erol Gaillard and Dr. Yassine Amrani, esteemed members of my progress review panel. Their guidance, insightful discussions, and unwavering support have been instrumental in ensuring the continued progress and quality of my research.

I would also like to express my appreciation to the academic and administrative staff at Leicester university and at the respiratory science department particularly. Their assistance, resources, and support have been invaluable in facilitating the research process and ensuring a conducive learning environment.

I would like to express my deepest gratitude to the EMBERS clinical research team for their invaluable contributions throughout this study. Their diligent efforts in collecting clinical data, blood samples, breath samples, sputum samples, and performing the FOT test have been indispensable to the success of this research.

I extend my heartfelt appreciation to Prof. Toru Suzuki and his team, especially Dr. Zubair Israr, from the Cardiovascular Biomedical Research Unit at Glenfield Hospital (LCBRU). Their expertise in mass spectrometry techniques and their meticulous work in running the plasma samples and generating the data matrix.

I would like to acknowledge the exceptional statistical expertise provided by Matthew Richardson. His insights and skills in visualizing high-dimensional data and fitting the elastic net have been invaluable to the research.

Dr. Ibrahim Wadah's diligent work within EMBER and with breath sampling using the RECIVA method in specific has been instrumental in capturing and reporting crucial breath metabolomic data which further utilized in my analysis of the VOC study. His contribution in this aspect of my studies is highly appreciated.

I extend my gratitude to Liesl Carr and Dr. Ibrahim Wadah for providing me with training and guidance in collecting breath samples. Their expertise and support enhanced my understanding of standardized procedures and the acquisition of reliable breath samples.

I would like to express my sincere appreciation to Dr. Michael Wilde and Dr. Rebecca Cordell who run the breath samples using comprehensive two-dimensional gas chromatography-mass spectrometry (GCxGC-MS). Providing me with orientations and training on breath samples preparations and operating GCGC MS sampling has proven immensely valuable.

Their expertise has significantly contributed to the acquisition of high-quality data and enhanced my understanding around the topic.

I am immensely grateful to Dr. Luke Baker for his exceptional support and guidance throughout the laboratory work. His expertise in solid face extraction and sample preparation has been invaluable in ensuring the accuracy and reliability of the results. I am particularly grateful for the extensive training he provided, which equipped me with the necessary skills and knowledge to perform all laboratory techniques effectively. His continuous supervision and commitment to excellence have significantly contributed to the success of this research project, and I am truly thankful for his invaluable support.

Dr. Singh Rajinder's invaluable support and expertise in setting up the LC-MS targeted method, providing training, and offering technical assistance throughout the sampling process have been instrumental in the successful implementation of the targeted metabolomic analysis. His guidance and assistance have not only facilitated the development of the MS targeted methods but also ensured their effective implementation, further enhancing the accuracy and reliability of the study's results.

The contributions of these individuals and groups have been essential to the success of this research project. Finally, I would like to acknowledge all those who have directly or indirectly contributed to this research endeavor and shaped my understanding and enriched my academic experience.

I am humbled and honored to have had the privilege of working with such remarkable individuals and being surrounded by such a supportive network. This thesis would not have been possible without their invaluable contributions.

Thank you from the bottom of my heart.

Masarrah Aljarroof

Statement of work personally performed

Within the scope of this thesis, I worked closely with my supervisory team and actively worked in to the development and execution of four studies.

In Study (I), I conducted an inclusive search for the significant metabolites featured in the study. Using metabolomics libraries and databases, I matched these metabolites based on their m/z ratio and reported their classes and subclasses. Additionally, I calculated biomarker scores for the extracted biomarkers using cumulative sum of linear regressions, enabling me to proceed to the assessment of diagnostic accuracies of these biomarkers through ROC curves.

For Studies II and III, my responsibilities included generating equations for reference values of respiratory impedance. By applying multiple linear regression models that accounted for subjects' demographic variables, I derived these equations using data from the recruited healthy control group. Subsequently, I created data columns for FOT predicted and % predicted values based on the normative values obtained from the constructed equations. I also worked on integrating the clinical and VOCs data with the FOT data, then conducted regression modeling to investigate the influence of resistance (R) and reactance (AX) on VOCs peak area.

In Study IIII, I independently performed all solid-phase extractions and sample preparations required prior to the LC-MS analysis. I meticulously transferred the prepared samples from the biology Laboratory to the Mass-spectrometry Laboratory on a daily basis. There, I

managed all samples loading, initiated the LC-MS analysis, and utilized specialized software to generate all chromatography data, peaks selections, and ultimately generating the SPMs data base matrix.

Throughout the research process, I performed all data computation for the clinical characteristics' tables, including descriptive and analytical statistical tests to compare groups and derive clinical observations in all four studies. Additionally, I executed data interpretation, figure and table creation, and results synthesis across the studies. This involved critically analyzing findings, synthesizing complex information, and presenting it in a clear and concise manner.

In summary, my substantial involvement in data computation, biomarker score calculations, data matrix generation, regression modeling, sample preparation, LC-MS analysis, data interpretation, and results synthesis demonstrates a comprehensive contribution to the research conducted in this thesis.

Changes on thesis development and COVID impact

Throughout the program period, the aims and direction of my Ph.D. have been subject to dynamic revisions and updates, which were grounded through thorough discussions in regular supervisory meetings. These changes were documented on various occasions via the university's postgraduate student platform, My PGR, as part of the supervisory meetings' output. A summarized timeline of these modifications is provided in the figure below.

Undoubtedly, the COVID-19 pandemic has exerted a significant influence on the progression of my thesis. Initially, the research involved investigating breath biomarkers in patients with an infective phenotype of AECOPD by conducting prospective diagnostic accuracy study, along with a literature review on the subject of "Metabolomics in COPD exacerbation phenotypes with a secondary focus on LRTI in COPD ". However, due to the national lockdown and the prioritization of COVID-related trials, this work was disrupted. In response, alternative options were considered, such as diverting the breath study to identify COVID patients in pneumonia cases or delaying the study setup. Considering the extensive number of established COVID studies at the time, personal interests, and the associated health risks specially giving my personal responsibility as the primary caregiver for two children who moved overseas with me as an international student, a collective decision was made, supported by my supervisory team, not to proceed with a COVID study. Instead, the setup of the breath study was postponed, prioritizing the health and safety of myself and my family. This change in direction necessitated a revised study timeline, with data collection rescheduled for June 2021.

With the ongoing pandemic and the uncertainties, it posed, the prospective diagnostic accuracy study project was ultimately withdrawn. The limited availability of staffing and resources, impacted by the pandemic, rendered the feasibility of conducting a new prospective study challenging. Consequently, a conscious decision was made to leverage existing resources effectively by utilizing the comprehensive data available from EMBER's or biobank samples. This approach allowed for the exploration of plasma metabolic biomarkers, markers of ventilation heterogeneity (VH) in acute breathlessness using Forced Oscillation Technique (FOT) and the correlation of FOT with breath metabolomics profiling. In light of the revised research plan, the initial intention to conduct a review article on became less relevant. Instead, the focus shifted towards properly reporting the results chapters of the revised projects. However, the established work on metabolomics in COPD phenotypes, including the secondary focus on LRTI, still integrated into the background knowledge and thesis introduction.

By adapting the research plan and mitigating the risks associated with the COVID-19 pandemic, I have continued to make progress towards the updated objectives of the thesis. The positive feedback received from the PRP panel during the regular meeting affirmed and acknowledged the potential risks and the alternative approaches to mitigate them. The panel recognized that completing the prospective diagnostic accuracy study, might be challenging under the circumstances. However, they expressed confidence that the work already conducted provided substantial material for a Ph.D. without the completion of this specific aim. This constructive feedback validated our decision to prioritize available rich data utilize existing resources. It demonstrated recognition of the challenges imposed by

the pandemic and the efforts made to adapt while ensuring the safety and well-being of all involved.

As pandemic restrictions gradually eased and the majority of the population became fully vaccinated, my passion for exploring the intricacies of metabolomics intensified. Taking advantage of the newfound opportunities, I embarked on establishing the laboratory infrastructure and initiating a prospective study. This phase of my research involved conducting meticulous laboratory investigations specifically focused on analyzing specialized pro-resolving mediators (SPMs) within sputum samples what was collected and stored from the same target population of the previous work. The culmination of previous studies, combined with the evolving circumstances, propelled me to delve deeper into metabolomics and expand the horizons of my research.

The changes made to the thesis's direction and aims have been carefully considered, ensuring that the research remains robust and relevant despite the challenges posed by the COVID-19 pandemic. The alterations were thoroughly discussed and documented in regular supervisory meetings, exemplifying our proactive and adaptive approach to the evolving circumstances. I am sincerely grateful for the continuous support and guidance of my supervisory team throughout these challenging times. Their assistance has been instrumental in strengthening the overall quality and relevance of my research.

This timeline illustrates the sequential modifications and decisions made in response to the COVID-19 pandemic.

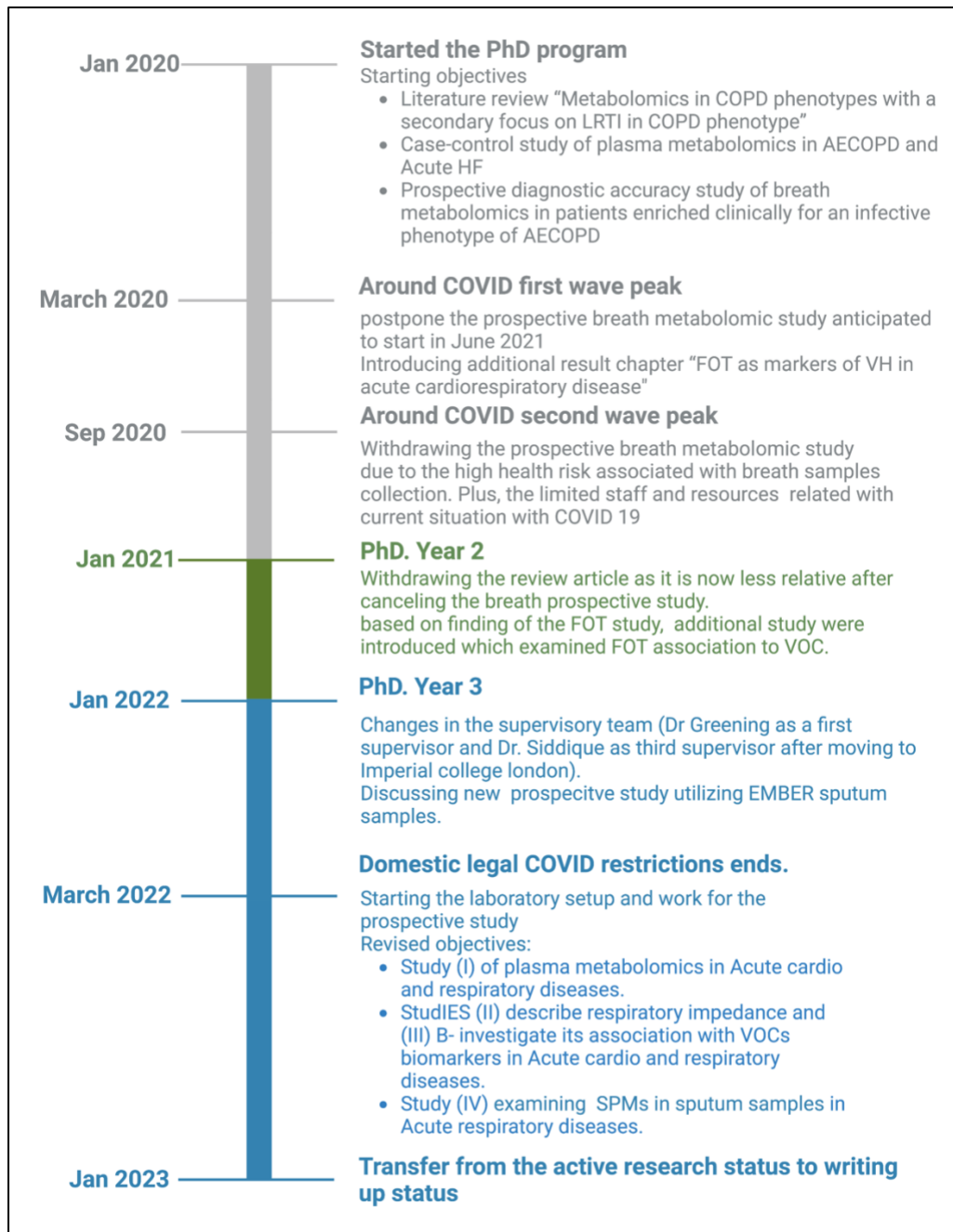


Table of Contents

Abstract.....	ii
Acknowledgments	v
Statement of work personally performed	x
Changes on thesis development and COVID impact	xii
List of abbreviations.....	xxii
Chapter 1 Introduction	1
1.1 Overview.....	1
1.2 Acute exacerbation of cardiorespiratory diseases	2
1.2.1 Definitions, prevalence, and healthcare burden of cardiorespiratory diseases	2
1.2.2 Shared pathogenesis pathways and pathophysiology in cardiorespiratory diseases.....	5
1.2.2.1 Inflammation and immune dysfunction	5
1.2.2.2 Vascular dysfunction.....	10
1.2.2.3 Metabolism dysfunction	11
1.2.2.4 Pathophysiological mechanisms.....	16
1.2.3 Microbiological tests and biomarkers	23
1.2.3.1 Molecular technique and microbiological tests	23
1.2.3.2 Common clinical biomarkers	25
1.2.3.3 Lipid mediators: Pro-inflammatory and specialized pro-resolving mediators	31
1.3 Metabolomics.....	38
1.3.1 Metabolomics contributes to advances in medical practice	38
1.3.2 Current technology.....	39
1.3.3 Biological Samples Used in Metabolomics Studies	41
1.3.4 Plasma metabolomic biomarkers in acute cardiorespiratory diseases.....	43
1.3.4.1 Profiling systemic metabolic changes: The value of plasma analysis in metabolomics studies	43
1.3.4.2 Plasma metabolomic biomarkers and pathways in cardiorespiratory conditions	43
1.3.5 Breathomics and VOCs	47
1.3.5.1 Unveiling the potential of VOCs for clinical utilization	47
1.3.5.2 VOCs from exhaled breath: Collection to data analysis	49
1.3.5.3 Challenges and considerations in breathomics research and VOC composition: Toward clinical applications.....	52
1.4 Oscillometry.....	55
1.4.1 Respiratory mechanics: Understanding pressure gradients, resistance, and compliance in the respiratory system.....	55
1.4.2 Oscillometry and respiratory impedance	60
1.4.2.1 Concept and measurements.....	60
1.4.2.2 Current technologies	62
1.4.2.3 Interpreting results	63
1.4.2.4 Potential and limitations	64
1.4.3 Clinical implications	65
1.5 Thesis.....	67
1.5.1 Introduction summary	67
1.5.2 Hypotheses and aims.....	69
Chapter 2 Methods	71
2.1 Overview.....	71

2.2 Integration of data and leveraging resources through the EMBER project.....	71
2.3 Participants.....	72
2.4 Lab analysis platforms and equipment	76
2.4.1 Mass spectrometry platforms	76
2.4.1.1 MS instruments.....	76
2.4.1.2 MS output parameters	80
2.4.1.3 Automated extraction and drying for sample preparation prior to MS.....	83
2.4.1.4 Levels of chemical identification	88
2.4.2 Handheld FOT	89
2.5 Statistical methods.....	91
2.5.1 Software utilized for statistical analysis and visual representation	91
2.5.2 High-dimensional data.....	92
2.5.3 Regression models.....	92
2.5.4 ROC curve and its performance measures	99
2.5.5 Association and correlation coefficient.....	100
2.5.6 Standard descriptive and statistical tests.....	100
Chapter 3 Studies; Blood Plasma Metabolome Signatures Differentiate Acute Exacerbations of COPD and Decompensated Heart Failure in Hospitalized Patients	102
3.1 Abstract	102
3.2 Introduction	104
3.3 Methods.....	106
3.3.1 Study design and participants	106
3.3.2 Instrumentation and sample processing.....	106
3.3.3 Statistical analysis.....	108
3.4 Results	110
3.4.1 Baseline characteristics	110
3.4.2 High-dimensional data visualization.....	112
3.4.3 Significant plasma biomarkers	114
3.4.4 Classifying the significant compounds	120
3.5 Discussion	122
Chapter 4 Studies; Forced Oscillometry Technique (FOT) to Assess Ventilation Heterogeneity (VH) During Hospital Admission for Acute Cardiorespiratory Illness	126
4.1 Abstract	126
4.2 Introduction.....	128
4.3 Methods.....	130
4.3.1 Study design and participants	130
4.3.2 Forced oscillation technique	130
4.3.3 FOT parameters and normative values	131
4.3.4 Statistical analysis.....	133
4.4 Results	136
4.4.1 Feasibility of FOT in acute settings	136
4.4.2 Baseline characteristics	136
4.4.3 Measures of lung mechanics during acute illness.....	138
4.4.4 Association between lung mechanics, clinical parameters, and blood biomarkers	140
4.4.5 Lung mechanics and healthcare utilization	145
4.5 Discussion	146

Chapter 5 Studies; Do Lung Mechanics Affect the Volatile Organic Compound Composition in the Breath of Patients with Cardiorespiratory Breathlessness?	152
5.1 Abstract	152
5.2 Introduction	153
5.3 Methods.....	155
5.3.1 Study design and participants	155
5.3.2 Exhaled breath VOCs	157
5.3.3 Forced oscillation technique (FOT).....	158
5.3.4 Statistical methods	158
5.4 Results	159
5.4.1 Clinical characteristics	159
5.4.2 VOCs vs FOT.....	161
5.5 Discussion and conclusions.....	164
Chapter 6 Studies; Assessment of Specialized Pro-resolving Lipid Mediators (SPMs) in Asthma, COPD, and Pneumonia Patients through Hospital Admission, Acute Exacerbation, and Recovery	172
6.1 Abstract	172
6.2 Introduction	174
6.3 Methods.....	178
6.3.1 Study design and participants	179
6.3.2 Solid-phase extraction and sample preparation for SPM detection.....	181
6.3.3 LC–MS targeted analysis.....	186
6.3.4 Statistical analysis.....	190
6.4 Results	191
6.4.1 Clinical characteristics	191
6.4.2 SPMs during acute events of inflammatory respiratory diseases.....	193
6.4.3 Associations between PGE2 and clinical parameters in acute illness of respiratory disease.....	196
6.4.4 SPMs during stable cardiorespiratory disease	197
6.5 Conclusions and discussion.....	200
Chapter 7 Discussion, Conclusions, and Future Work	208
7.1 Overview of thesis	208
7.2 Results chapters.....	210
7.3 Converging insights: Implications for field advancement and clinical applications.....	212
7.4 Future work	215
7.5 Concluding remarks.....	216
References.....	217
Appendices.....	238
7.1 Appendix (A) Statistical methods	238
7.2 Appendix (B): SPMs Targeted Methods Optimization on LC-MS.....	254
7.3 APPENDIX (C): Postponed work due to COVID- 19 impact.....	277
7.4 APPENDIX (D): Additional documents; Research passport, certificates for Good Clinical Practice (GCP) training, research essentials and informed consent training.....	291

List of figures:

Figure 1-1 ReCIVA breath sampler device utilizing sorbent tubes	50
Figure 2-1 Total study population and sub-cohorts	75
Figure 2-2 Gas chromatography oven at the chemistry laboratories of the University of Leicester	77
Figure 2-3 Components of the comprehensive GCxGC MS system.....	78
Figure 2-4 Components of the LC–electrospray ionization tandem MS system	80
Figure 2-5 Chromatograms of the examined targeted SPMs within the lipidomic standards mix.....	82
Figure 2-6 The automated nitrogen evaporator system, TurboVap® LV system	85
Figure 2-7 Automated extraction system, Biotage® PRESSURE+	86
Figure 2-8 Laboratory centrifuges	87
Figure 2-9 Laboratory PH meter	87
Figure 2-10 Scatterplot of FOT data to visualize the relationship between variables	94
Figure 2-11 Diagnostic plots of reference values’ models.....	96
Figure 2-12 Summary of the model development process	98
Figure 3-1 TDA visualization of plasma metabolomics across the AECOPD, AHF, and healthy control groups.....	113
Figure 3-2 AECOPD and AHF plasma biomarker score box plots.....	115
Figure 3-3 Receiver operating characteristics (ROC) curve analysis and area under the curve (AUC) for plasma metabolomic biomarker scores.....	118
Figure 3-4 Receiver operating characteristics (ROC) curve analysis and area under the curve (AUC) for plasma metabolomic biomarker scores and clinical blood biomarkers	119
Figure 3-5 Proportions of the chemical classes of the putative metabolites extracted	121
Figure 4-1 Box and whiskers plots of % predicted measures of lung mechanics across healthy volunteers and acutely unwell in COPD, asthma, pneumonia, and heart failure patients. ...	139
Figure 4-2 Box and whiskers plots of selected lung mechanics across breathlessness and wheeze scores.....	143
Figure 4-3 Box and whiskers plots of selected lung mechanics and clinical parameters.....	144
Figure 4-4 Box and whiskers plots of selected lung mechanics and blood biomarkers	145
Figure 5-1 Abstract illustration of the study workflow.....	156
Figure 5-2 VOCs categorized according to their functional groups.....	157
Figure 5-3 Scatter plots with regression lines and 95% CI for significant VOCs’ functional groups vs AX %predicted values for subjects’ height and BMI.....	163
Figure 6-1 Illustration of the study process; sample collection, preparation, and analysis..	178
Figure 6-2 Summary of sample selection and inclusion/exclusion criteria for the acute cohort of the study.....	180
Figure 6-3 Summary of sample selection and inclusion/exclusion criteria for the stable cohort of the study	181
Figure 6-4 PGE2 reported peak area across healthy controls and AECOPD, acute asthma, and pneumonia patients.....	195
Figure 6-5 Scatterplots of PGE2 association with blood immune cell counts	197
Figure 7-1 Evaluation of acute cardiorespiratory disease: Integrating metabolite-wide analysis and lung mechanics pathophysiology	209

List of tables:

Table 1-1 Common biomarkers of cardiorespiratory conditions and their limitations.....	30
Table 1-2 Pro-inflammatory biomarkers across cardiorespiratory diseases.....	33
Table 1-3 Families and specific molecules of specialized pro-resolving mediators (SPMs)	34
Table 1-4 SPMs in acute cardiorespiratory conditions	37
Table 1-5 Comparison of sample types for metabolomics analysis	41
Table 1-6 Plasma metabolites investigated in patients with COPD, asthma, HF, or pneumonia	47
Table 2-1 Software parameters reported for patients, which were used to generate the study data matrix.....	90
Table 2-2 Statistical tests to examine the model ($R5 \sim \text{Height} + \text{BMI}$) according to the of multiple linear regression assumptions.....	96
Table 3-1 LC–MS parameters utilized in the analysis workflow	107
Table 3-2 Cohort clinical characteristics	110
Table 3-3 Biomarker score summary	114
Table 3-4 Sensitivity, specificity, negative, and positive predictive values of biomarker scores	116
Table 4-1 Demographics and baseline oscillometry data for the healthy subjects included for reference value calculations	132
Table 4-2 Comparison of reference values: Current study vs. Oostveen et al.....	133
Table 4-3 Univariate analysis using linear regression for each measure	134
Table 4-4 Multivariate linear regression for normative values	135
Table 4-5 Final prediction equations for normal values of FOT measures.....	135
Table 4-6 Cohort clinical characteristics	137
Table 4-7 Measures of FOT in healthy controls and acutely unwell patients with different cardiorespiratory conditions.....	138
Table 4-8 Correlation coefficients between FOT and symptoms, clinical parameters, and blood biomarkers.....	140
Table 4-9 Measures of FOT across symptoms, clinical parameters, and blood biomarkers.	141
Table 5-1 Cohort clinical characteristics	160
Table 5-2 Multivariate linear regression for VOC sets and FOT	161
Table 5-3 Chemical assignment of significant features	162
Table 6-1 Comprehensive description of the solid-phase extraction (SPE) protocol and parameters for the automated evaporator and automated extraction system	185
Table 6-2 Lipidomic standards and internal standard, including concentrations and volumes utilized for method validation of the LC–MS analysis.	187
Table 6-3 MS parameters, software, and targeted methods for data generation.....	188
Table 6-4 Clinical characteristics of the study population.....	192
Table 6-5 SPMs across acute illness of respiratory disease patients and healthy controls ..	194
Table 6-6 Correlation analysis between PGE2 Levels and clinical parameters	196
Table 6-7 SPMs across stable and recovered respiratory illness patients and healthy controls	198
Table 6-8 SPMs across acute and stable respiratory disease groups and healthy controls..	199
Table 6-9 Visual comparison of SPM patterns in acute and stable phases of respiratory diseases using control group methodology.....	204

Table 6-10 Control analysis of lipidomic standards mix: Pre- and post-analysis performance206

List of abbreviations

ACQ	Asthma Control Questionnaire
AECOPD	Acute Exacerbations of Chronic Obstructive Pulmonary Disease
AHF	Acute Heart Failure
AHR	Airway Hyperresponsiveness
ALI/ARDS	
ANOVA	One-way Analysis of Variance
APCs	Activate Antigen-Presenting Cells
ARDS	Acute Respiratory Distress Syndrome
(AT-RvD1)	Aspirin-triggered resolvin D1
ATP	Adenosine Triphosphate
ATS/ERS	American Thoracic Society/European Respiratory Society.
AUC	Area Under the Curve
AX	The area under the reactance curve
BALF	Bronchoalveolar Lavage Fluid
BCAAs	Branched-chain amino acids
BMI	Body Mass Index
BUN	Creatinine and blood urea nitrogen
CAP	Community-Acquired Pneumonia
CAP	Community-Acquired Pneumonia
CE	Capillary Electrophoresis
CHF	Chronic Heart Failure
CID	collision-induced dissociation
COPD	Chronic Obstructive Pulmonary Disease
COX	Cyclooxygenase
CRDS	Cavity Ring-Down Spectroscopy
CRP	C-Reactive Protein
CSF	Cerebrospinal Fluid
CT	Computed Tomography
CYP	Cytochrome P450
DAMPs	Damage-Associated Molecular Patterns
DNA	Deoxyribonucleic Acid
E-nose	Electronic nose
EI	Electron Ionization
ERS	European Respiratory Society
ESI	Electrospray Ionization
$F_{inertia}$	Forces of Inertia
F_{el}	Forces of Elasticity
FeNO	Fractional exhaled nitric oxide
FEV1	Forced Expiratory Volume in one second
FFAs	Free fatty acids
FID	Flame Ionization Detection
FOT	Forced Oscillation Technique
F_{Raw}	Forces of Airway Resistance
FRC	Functional Residual Capacity
Fres	Resonant Frequency
FRS	Forces in Respiratory System
GC	Gas Chromatography

GC MS	Gas Chromatography Mass Spectrometry
He	Helium
HF	Heart Failure
hs-CRP	High-Sensitivity C-Reactive Protein
HTS	High-Throughput Screening
Hz	Hertz
IgE	immunoglobulin E
IL-10	Interleukin-10
IL-13	Interleukin -13
IL-4	Interleukin-4
IL-5	Interleukin-5
IL-8	Interleukin-8
IMS	Imaging Mass Spectrometry
IOS	Impulse Oscillation
IOS	Impulse oscillometry
IT-MS	Ion Trap Mass Spectrometry
LC	Liquid Chromatography
LC-MS	Liquid Chromatography-Mass Spectrometry
LCI	Lung Clearance Index
LCI	Lung Clearance Index
LDA	Linear Discriminant Analysis
LOX	Lipoxygenase
LTB4	Leukotriene B4
LTE4	leukotriene E4
LXA4	Lipoxin A4
LXB4	Lipoxin B4
MALDI	Matrix-Assisted Laser Desorption/Ionization
MaR1	Maresin 1
MaR2	Maresin 2
MBW	Multiple-Breath Gas Washout
MEWS	Modified Early Warning Score
MI	Myocardial Infarction
MLTT	Mean Lung Transit Time
MRI	Magnetic Resonance Imaging
MS	Mass Spectrometry
MSI	Metabolic Standards Initiatives
N2	Nitrogen
NAFLD	Nonalcoholic Fatty Liver Disease
NMR	Nuclear Magnetic Resonance
NO2-AA	Nitro-Arachidonic Acid
NO2-FAs	Electrophilic Nitro-Fatty Acids
NO2-LA	Nitro-Linoleic Acid
NO2-OA	Nitro-Oleic Acid
NT-proBNP	Aminoterminal Pro-B-type Natriuretic Peptide
P_{el}	Elastic recoil pressure of the lungs
$P_{inertia}$	Pressure needed to overcome the inertia of the respiratory system.
PAMPs	Pathogen-Associated Molecular Patterns
PCA	principal Component Analysis
PCF	Poorly Communicating Fraction
PCR	Polymerase chain reaction
PCT	Serum Procalcitonin

PD1	Protectin D1
PD2	Protectin D2
PDX	Protectin DX
PG2a	prostaglandin 2a
PGD2	prostaglandin D2
PGE2	prostaglandin E2
PRaw	Pressure required to overcome the resistance of the airways
Prs	Pressure in the respiratory system
PUFA	Polyunsaturated Fatty Acid
QC	Quality control
Q-TOF	Quadrupole-Time of Flight
R	Resistance
R19	Resistance at frequency of 19 Hertz
R5	Resistance at frequency of 5 Hertz
R5–R19	Resistance at 19 Hertz minus Resistance at 5 Hertz
ReCIVA	Respiration Collector for in Vitro Analysis
ROC	Receiver Operating Characteristic
ROS	Reactive Oxygen Species
rRNA	16S Ribosomal RNA
RvD1	Resolvin D1
RvD2	Resolvin D2
RvD3	Resolvin D3
RvD4	Resolvin D4
RvD5	Resolvin D5
RvE1	Resolvin E1
RvE2	Resolvin E2
RvE3	Resolvin E3
S(acin)	Acinar Ventilation Heterogeneity Index
S(cond)	Conductive Ventilation Heterogeneity Index
SF6	Sulfur Hexafluoride
SPECT	Single-Photon Emission Computed Tomography
SPME	Solid-Phase Microextraction
TD	Thermal Desorption
TDA	Topological Data Analysis
SPE	Solid Face Extraction
SPMs	Specialized Pro-resolving Mediators
TGF- β	Transforming Growth Factor-beta
TLC	Total Lung Capacity
TNF-alpha	Tumor Necrosis Factor-alpha
TQ-MS	Orbitrap Mass Spectrometry
Tregs	Regulatory T cells
TXB2	Thromboxane B2
UMAP	Uniform Manifold Approximation and Projection
VA	Alveolar Volume
VAS	Visual Analog Scale
$\dot{V}A: \dot{Q}$	Ventilation-Perfusion
VDP	Ventilation Defect Percent
VH	Ventilation Heterogeneity
VOCs	Volatile Organic Compounds
WHO	World Health Organization
X	Reactance

X5
Zrs

reactance at 5 Hertz
Impedance of respiratory system

Chapter 1 Introduction

1.1 Overview

Research into the acute events of cardiorespiratory diseases is challenging as these conditions can quickly become life-threatening. This thesis will examine the role of metabolomics and lung physiology studies in exploring the markers of cardiorespiratory diseases during acute events. A range of analytical technologies, including mass spectrometry platforms, metabolomic analyses and bioinformatics models, and pulmonary function testing, were employed to identify and differentiate acute cardiorespiratory conditions based on the pathogenesis of the underlying disease.

This chapter begins with the definitions, prevalence, and healthcare burden of the examined cardiorespiratory conditions which highlight the importance of accurate and early differentiation. We will then elaborate with the shared biological pathways between the studied conditions, including the inflammation process, metabolomic disturbance, and ventilation heterogeneity. This section is followed by a comprehensive outline of the current clinical diagnostic and prognostic tools and their margins, in addition to the potential biomarkers suggested in the literature, including their extended roles in the resolution of inflammation within the context of cardiorespiratory conditions. Next, to establish the thesis perspective, an overview of advances within the metabolomics field, including available methods and platforms, is covered and elaborated with an overview of the existing literature on plasma metabolomics biomarkers in cardiorespiratory diseases during acute

status. Finally, we provide a focused description of the force oscillation technique, current applications, and its potential role during acute exacerbation of the studied conditions.

1.2 Acute exacerbation of cardiorespiratory diseases

In this thesis, the study population is patients who presented with acute exacerbation events of cardiorespiratory conditions including chronic obstructive pulmonary disease (COPD), asthma, pneumonia, and heart failure (HF). An overview of each of these conditions with a focus on their acute phases, is provided below, including definitions, prevalence, pathogenesis, and diagnostics.

1.2.1 Definitions, prevalence, and healthcare burden of cardiorespiratory diseases

Acute events of cardiorespiratory conditions, including acute exacerbations of COPD (AECOPD), acute asthma attacks, acute pneumonia, and acute heart failure (AHF), collectively account for a significant rate of morbidity and mortality worldwide. COPD is a chronic lung disease that is characterized by the obstruction of airflow in the lungs. It includes chronic bronchitis (inflammation and narrowing of the airways) and emphysema (the destruction of lung tissue) (3). AECOPD refers to the sudden worsening of COPD symptoms, which necessitates a change in treatment. It can be triggered by respiratory infections, air pollution, exposure to allergens, medication non-compliance, or lifestyle changes. According to the World Health Organization (WHO), COPD is the third leading cause of death globally, accounting for 5% of all deaths worldwide (4). COPD patients with frequent exacerbation suffer a steeper decline in lung function and quality of life and exhibit increased mortality and morbidity rates (5). COPD is a significantly heterogenic condition

among patients, who show differences in clinical presentation, underlying mechanisms, and responsiveness to treatment (6).

Asthma is a chronic respiratory disorder that is characterized by recurrent episodes of symptoms, variable airflow limitations, and underlying airway inflammation. It is a complex disease that is influenced by genetic and environmental factors, and management involves controlling inflammation and bronchial hyperresponsiveness through a combination of medications and the avoidance of triggers. Acute asthma refers to the sudden worsening of asthma symptoms, such as coughing, wheezing, chest tightness, and shortness of breath, due to various triggers, such as exposure to allergens, irritants, viral infections, exercise, or stress (7). According to the WHO, asthma affects approximately 339 million people worldwide (8). Acute asthma can be a life-threatening condition, and mortality rates vary depending on factors such as the severity of the attack, the patient's age, comorbidities, and access to prompt medical care. With appropriate and timely management, the mortality rate for acute asthma is generally low, and most patients recover without complications. However, in some cases, acute asthma can progress rapidly, leading to respiratory failure, cardiac arrest, or other complications that result in death (7).

Pneumonia is an inflammatory infectious condition that affects the lungs and is characterized by the accumulation of fluid and inflammatory cells in the alveoli. It can be caused by various microbial agents and presents with respiratory symptoms. Treatment consists of antimicrobial therapy and supportive care. Pneumonia can range in severity from mild to severe and can also be life-threatening, especially among young children, the elderly, and people with weakened immune systems. Symptoms of pneumonia include

cough, fever, chest pain, and shortness of breath (9). According to the WHO, pneumonia is the single most common infectious cause of death worldwide and is responsible for an estimated 2.6 million deaths annually.

While AHF can be the first presentation of heart disease, it is more commonly seen as decompensation of pre-existing cardiomyopathy or other cardiac conditions, such as hypertension, coronary artery disease, or valvular heart disease, due to the progressive nature of these diseases and the increased workload on the heart. The decompensation of a pre-existing cardiac condition can be triggered by several factors such as infections, arrhythmias, medication non-compliance, dietary choices, or the worsening of comorbidities, such as COPD. Symptoms include fatigue, shortness of breath, swelling in the legs, and difficulty exercising (10, 11). Heart failure is a major public health problem that affects an estimated 64.3 million people worldwide. It is a leading cause of morbidity and mortality, particularly among older adults. The estimated five-year mortality rate for heart failure is approximately 50% (12).

Overall, acute cardiorespiratory conditions are associated with significant morbidity and mortality worldwide. Thus, these conditions present a major healthcare burden in terms of hospitalizations, frequent exacerbations, emergency department visits, the need for ongoing management and treatment, medication expenses, and patients' reduced quality of life. This highlights the importance of both early diagnosis and effective and efficient treatment strategies to reduce the burden these conditions impose on individuals and healthcare systems.

1.2.2 Shared pathogenesis pathways and pathophysiology in cardiorespiratory diseases

Pathogenesis pathways are the sequence of events that occur during the development and progression of a disease. These pathways involve various biological processes, such as metabolism, the activation of signaling pathways, and tissue damage or repair.

Understanding disease pathogenesis is essential for developing biomarkers and therapeutic interventions by detecting key points in the pathway that can be identified then targeted with drugs or other interventions (13-15). Contrary, pathophysiology is the study of the functional changes that arise in the body as a consequence of a disease or disorder. It entails comprehending the underlying mechanisms that are responsible for these changes and their impact on the body's normal functions. This understanding aids healthcare professionals in identifying the changes caused by diseases, predicting their progression, and devising effective treatment strategies to enhance patient outcomes (16). While each of the examined conditions in this thesis, COPD, asthma, pneumonia, and HF, have distinct mechanisms, they share overlapping pathogenesis pathways and pathophysiology traits. The various shared pathways and physiological changes during the development of these cardiorespiratory conditions include inflammation and immune dysfunction, vascular dysfunction, metabolic dysfunction, and pathophysiological mechanisms, such as ventilation heterogeneity (VH).

1.2.2.1 Inflammation and immune dysfunction

1.2.2.1.1 Immune responses: Innate, adaptive, and resolution phases

Inflammation is a complex immune response to tissue damage, infection, or other triggers. It consists of three phases: innate, adaptive, and resolution. The innate phase involves nonspecific immune reactions, the activation of immune cells, and

the release of pro-inflammatory mediators (17, 18). The adaptive phase targets specific antigens and involves lymphocytes, antigen-presenting cells, and the production of antibodies and cytotoxic T cells (19, 20). The resolution phase restores tissue homeostasis, actively terminating inflammation through clearing pathogens, releasing specialized pro-resolving mediators (SPMs), and the actions of regulatory immune cells (21). These phases are coordinated to ensure an effective and controlled inflammatory process.

1.2.2.1.2 Intricate mechanisms in inflammation to resolution

Inflammation and the subsequent resolution phase are dynamic processes that require a balance between pro-inflammatory and pro-resolving mediators (22). Intricate mechanisms are engaged to regulate this process. These mechanisms include the regulation of lipid mediators, immune cells' phenotypic switching and modulation of function, and the release of cytokines.

The first mechanism is the regulation of the lipid mediators involved in inflammation and resolution through different enzymatic pathways, namely, lipoxygenase (LOX), cyclooxygenase (COX), and cytochrome P450 (CYP). Each of these enzymatic pathways produces distinct lipid mediators that can either promote or resolve inflammation, depending on the context and molecules involved (23).

The second mechanism is the phenotypic switching and function modulation of immune cells, such as neutrophils, macrophages, and T cells. Neutrophils, which are important for pathogen clearance, can cause tissue damage if they accumulate

excessively. To resolve inflammation, mechanisms that induce neutrophil apoptosis and clearance by macrophages are activated, inhibiting chemotaxis signals that attract neutrophils (24). Macrophages switching from pro-inflammatory (M1) to anti-inflammatory/pro-resolving (M2) phenotypes. M1 macrophages amplify inflammation, while M2 macrophages promote tissue repair and inflammation resolution (25). T cells, particularly regulatory T cells (Tregs), coordinate immune responses and suppress pro-inflammatory processes, aiding in inflammation resolution (26).

The last mechanism is the release of cytokines; alongside pro-inflammatory cytokines, the release of anti-inflammatory cytokines, such as interleukin-10 (IL-10) and transforming growth factor-beta (TGF- β), helps to regulate and dampen the immune response (27). These molecules act as negative feedback signals, reducing the intensity of inflammation and promoting resolution.

The mechanisms underlying inflammation and its resolution are complex and intertwined. The interplay between immune cells, lipid mediators, and tissue repair processes orchestrates the resolution of inflammation and the restoration of homeostasis. By unraveling these intricate pathways, researchers aim to identify novel biomarkers and develop therapeutic approaches that harness the body's natural resolution mechanisms and mitigate the detrimental effects of chronic inflammation.

1.2.2.1.3 Implications in cardiorespiratory diseases

The inflammation response is a key feature in cardiorespiratory conditions. For instance, the release of pro-inflammatory mediators contributes to airway remodelling, increased mucus production, and obstruction (28). AECOPD and acute asthma can be classified into different phenotypes according to the inflammation process, including the type of immune cells involved and the pattern of cytokine release. COPD exacerbation can be classified as one of four groups based on inflammatory biomarkers: bacterial, viral, eosinophilic predominant, and pauc-inflammatory (exhibiting limited inflammatory changes) (29, 30). Eosinophilia is identified in about 20–30% of AECOPD cases (30). In this category, eosinophils comprise a significant proportion of the inflammatory cells in the lungs and airways. Patients who exhibit this phenotype have a good response to inhaled steroids (31-34). In contrast, airway microbial dysbiosis and infection, which might also trigger exacerbation, represent another phenotype (30, 35, 36). Patients exhibiting this phenotype, particularly those with bacterial infection exacerbation, respond best to antibiotic therapy. In clinical practice, bacterial infection-triggered AECOPD can be described as either an exacerbation with consolidation or pneumonia, but it is generally considered an exacerbation phenotype (37). In acute asthma exacerbations, inflammation is primarily driven by an immune response to allergens or irritants, which leads to the activation of inflammatory cells. The most common acute asthma exacerbation phenotype is eosinophilic asthma, which is characterized by eosinophilia in the airway tissues and the increased production of cytokines such as interleukin-4 (IL-4), interleukin-5 (IL-5), and interleukin -13 (IL-13). Eosinophilic asthma is often associated with allergies and responds well to corticosteroid therapy

or other targeted therapies, such as anti-IL-4 biologics (38, 39). Another phenotype of asthma is neutrophilic asthma, which is characterized by neutrophils in the airway tissues and the increased production of cytokines such as interleukin-8 (IL-8) and tumor necrosis factor-alpha (TNF-alpha)(40). Neutrophilic asthma is less common and may be associated with more severe asthma symptoms, decreased responsiveness to corticosteroids, and a higher risk of exacerbation. Asthma can also present a mixed phenotype of both eosinophilic and neutrophilic inflammation. While eosinophilic asthma may respond well to corticosteroid treatment, neutrophilic asthma may require different medications, such as macrolides or biologics to target specific cytokines (41-44). HF is also influenced by inflammation. In response to various triggers, such as ischemia or infection, the immune system releases pro-inflammatory cytokines and chemokines, which recruit immune cells and promote inflammation in the heart that leads to myocardial damage, impaired contractility, and the development of cardiac dysfunction (45). Advanced heart failure is significantly influenced by unresolved inflammation. Macrophages contribute to cardiac repair by synthesizing lipid mediators that regulate inflammation, thereby avoiding chronic inflammation and supporting cardiac repair. However, various factors can disrupt this resolution process and impair cardiac repair (46-48).

In COPD, asthma, and HF, immune dysfunction is characterized by the limited resolution of inflammation, leading to chronic low-grade inflammation. These limitations can be caused by several factors, such as prolonged exposure to triggering stimuli, impaired immune function, and the presence of comorbidities,

such as cardiovascular disease and diabetes. In addition, the use of certain medications, such as corticosteroids, can suppress the resolution of inflammation, which may lead to chronic inflammation and tissue damage. Furthermore, ageing and lifestyle factors, such as smoking, poor nutrition, and lack of exercise, may also play role. These barriers to the resolution of inflammation can foster the development of chronic cardiorespiratory diseases and increase the risk of disease progression and exacerbation.

In pneumonia, infection is the trigger for the immune response and the initiation of inflammation. However, an unbalanced pro-inflammatory and anti-inflammatory, along with excessive or prolonged inflammation can lead to tissue damage and complications such as empyema, sepsis, or acute respiratory distress (49-51). The severity of pneumonia and its complications are directly related to the degree of immune response. Dysregulated inflammation can occur before, during, and after acute infection in pneumonia, increasing the patient's susceptibility to infectious diseases and raising mortality rates among the elderly. However, studies on the precise mechanisms of the inflammatory response report conflicting results (52).

1.2.2.2 Vascular dysfunction

Vascular dysfunction can manifest in different ways, such as impaired endothelial function, altered vascular tone, or increased vascular permeability, leading to tissue damage and inflammation. In acute exacerbations of COPD and asthma, vascular dysfunction is influenced by chronic airway inflammation. The release of vasoactive mediators, such as histamine and leukotrienes, during inflammation increases pulmonary vascular resistance

that impairs gas exchange and decreases oxygenation. Furthermore, during exacerbations, the escalation in released vasoactive mediators worsens pulmonary vascular resistance and further impairs oxygenation (53). In acute pneumonia, vascular dysfunction is also caused by the dysregulated immune response and pathogen invasion, resulting in systemic inflammation, increased vascular permeability, and organ dysfunction (54, 55). In acute HF, vascular dysfunction is characterized by impaired myocardial perfusion, increased peripheral resistance, and altered neurohormonal regulation, causing cardiac remodeling and impaired heart function. In addition to increased vascular permeability, which results in fluid and protein leakage into the lung tissue, all can contribute to the development of edema and pulmonary congestion (56, 57).

1.2.2.3 Metabolism dysfunction

Metabolism dysfunction is a substantial aspect of the pathogenesis of acute respiratory and cardiovascular diseases, displaying through various pathways such as oxidative stress, impaired energy metabolism, altered glucose metabolism, disturbed lipid metabolism, and amino acid metabolism dysfunction.

1.2.2.3.1 Oxidative stress

Oxidative stress occurs when the production of reactive oxygen species (ROS) exceeds the body's antioxidant defense mechanisms' capacity. As the production of ROS increases, the body's antioxidant defense mechanisms become overwhelmed. This imbalance leads to the accumulation of ROS, which triggers oxidative stress and damages cellular structures such as lipids, proteins, and deoxyribonucleic acid (DNA) (58). There are various situations in which an increase in the production of ROS can lead to oxidative stress. One such scenario is the activation of immune cells,

including neutrophils and macrophages, which release ROS as part of their defense mechanisms against pathogens. However, if these cells are excessively or persistently activated, the production of ROS can become unregulated. In addition, conditions involving ischemia-reperfusion injury can trigger the generation of ROS during the reperfusion phase, leading to oxidative damage. Chronic inflammatory conditions can also cause the accumulation of ROS over time, contributing to oxidative stress. While ROS contribute to normal physiological processes and immune responses, excessive ROS production can have detrimental effects on cellular structures and contribute to the development of various diseases (59).

In AECOPD and acute asthma, oxidative stress contributes to airway remodeling by activating several signaling pathways and transcription factors that promote the proliferation of airway smooth muscle cells, fibroblasts, and epithelial cells (60, 61). While in acute pneumonia, oxidative stress results in lung injury and tissue damage (62). In acute HF, it causes endothelial dysfunction, impaired myocardial contractility, and cardiac remodeling. Strategies to reduce oxidative stress, such as antioxidant supplementation, may have therapeutic benefits in treating these acute diseases (62, 63).

1.2.2.3.2 Impaired energy metabolism

Impaired energy metabolism arises when the cells' ability to produce adenosine triphosphate (ATP) decreases, leading to energy deficiency. This metabolic dysfunction contributes to the development and, potentially, the acute exacerbation of respiratory and cardiovascular diseases. Patients with asthma exhibit energy

metabolism dysregulation in their early lives, which may affect the development of airway epithelial cells and render the airways more susceptible to allergic sensitization (64). An analysis of bronchoalveolar lavage fluid (BALF) in mice exposed to ovalbumin revealed significant metabolic pathway alterations in asthmatic lungs, indicating disruptions in energy metabolism that were characterized by elevated lactate, malate, and creatinine levels and reduced concentrations of carbohydrates (65). In COPD patients, metabolomics analysis provided insights into energy metabolism pathways and profiles, that emphasized the roles anaerobic and low-efficiency energy supply pathways play in lung injury, inflammation, lung ventilatory function, and motion limitations (66). In addition, in HF cases, energy deficiency stems from reduced mitochondrial oxidative capacity, uncoupled glycolysis, and impaired fatty acid oxidation, which decrease cardiac efficiency (67). Furthermore, during acute exacerbations, compromised oxygen supply is common and can further exacerbate energy metabolism dysfunction. This situation can reduce ATP production through oxidative phosphorylation in the mitochondria. Consequently, cells shift towards anaerobic metabolism, leading to the buildup of lactate. The accumulation of lactate impairs cellular function and can result in organ dysfunction.

1.2.2.3.3 Altered glucose metabolism

Acute respiratory and cardiovascular diseases disrupt glucose homeostasis, causing hyperglycemia, insulin resistance, and impaired glucose utilization. Inflammation and oxidative stress, which are characteristic of these conditions, activate stress signaling pathways and worsen insulin resistance, further compromising glucose metabolism. These alterations in glucose metabolism contribute to disease progression and

unfavorable outcomes. Therefore, maintaining glucose homeostasis by focusing on the metabolites associated with glucose metabolism has been introduced as a strategy to manage these diseases effectively.

Individuals with severe COPD exhibit changes in glucose metabolism that result in higher glucose production and faster glucose metabolism via glycolysis and oxidation (68). Furthermore, hyperglycemia is a risk factor for hospital-associated complications and mortality in AECOPD. Therefore, patients with high glucose levels may require nutritional management or insulin treatment during hospitalization (69). Abnormal glucose homeostasis is prevalent in individuals with severe asthma, and in HF, continuous activation of glucose metabolism may lead to decompensation and disease progression (70, 71). Moreover, sugar metabolism is linked to virulence in *Streptococcus pneumoniae*, suggesting new targets for therapeutic drugs based on mathematical models analyzing data associated with sugar metabolism (72).

1.2.2.3.4 Disturbed lipid metabolism

Lipid metabolism disorders widely participate in COPD pathogenesis, leading to the development of inflammation, pulmonary and extrapulmonary clinical heterogeneity, and changes in innate immunity in the lungs and body. Lipid mediators, such as eicosanoids, prostanoids, leukotrienes, and SPMs, regulate inflammation and its resolution in the lungs (73). Additionally, lipid changes are linked to bacterial colonization and infectious exacerbations of COPD. During AECOPD, the levels of some free polyunsaturated fatty acids increase, exhibiting antimicrobial effects, while others, such as arachidonic acid, increase inflammation

(74). In asthmatic patients, abnormal lipid metabolism correlates with disease severity and IgE levels (75). Moreover, abnormal lipid metabolism has been observed in both COVID-19 and non-COVID-19-associated pneumonia in human lungs. Various staining techniques have revealed increased levels of unsaturated fatty acids at inflammation sites compared to healthy lung regions. Additionally, the expression of genes associated with lipid metabolism is decreased in pneumonia cases (76).

1.2.2.3.5 Amino acid metabolism dysfunction

Amino acid metabolism dysfunction is a common feature of cardiorespiratory diseases and their acute exacerbations as the body undergoes a state of stress, which alters amino acid metabolism.

In COPD, studies have shown a decrease in the circulating levels of branched-chain amino acids, which may lead to skeletal muscle wasting (77). In acute asthma, arginine metabolism is altered, decreasing nitric oxide production and increasing airway hyperresponsiveness, as illustrated in the fractional exhaled nitric oxide (FeNO) asthma phenotype (78). In acute pneumonia, amino acid metabolism is altered during the acute phase and persists to the recovery phase of community-acquired pneumonia (CAP), which could differentiate CAP from infection-triggered exacerbations in COPD cases (79). In AHF, alterations in amino acid metabolism have been implicated in the development of cardiac cachexia, which is characterized by muscle wasting and weight loss (80).

1.2.2.4 Pathophysiological mechanisms

Cardiorespiratory diseases exhibit diverse pathophysiological mechanisms that progress during acute status of the disease and result in common clinical manifestations, including the activation of the sympathetic nervous system, airway obstruction, impaired gas exchange, compromised cardiac function, and worsening VH. These manifestations contribute to the complexity and difficulty of diagnosing and treating these diseases.

1.2.2.4.1 Ventilation heterogeneity

1.2.2.4.1.a Overview

VH describes the uneven distribution of airflow into and out of the lungs. Variations in ventilation and gas exchange within the lungs occur naturally due to differences in the lung ventilation units, the complexity of airway tree branching, and the impact of factors including gravity, posture, physical activity, and age (81-83). However, this heterogeneity is relatively small and is considered to be within a normal physiological range. Thus, air flows freely and adequately through the bronchi and bronchioles to reach the alveoli, where oxygen is absorbed into the bloodstream and carbon dioxide is released through the alveoli's capillary membranes. However, pathological changes in the lungs due to disease processes can increase VH, subsequently leading to alveolar ventilation–perfusion ($\dot{V}_A:\dot{Q}$) mismatch, a cause of respiratory failure (84). There are several proposed means by which lung diseases lead to ventilation heterogeneity, including small airway dysfunction, a major contributor to VH, mixed or large airway obstruction, changes in lung compliance, lung hyperinflation, increased mucus production, and alveolar collapse. These mechanisms can act alone or in combination to contribute to VH in the lungs. While much is known about these contributing factors, our understanding of the precise

and comprehensive mechanisms involved in VH is limited, despite the valuable insights that modern technology and computational modelling have provided into this phenomenon. Therefore, VH represents an interesting aspect of respiratory research concerning pathophysiologic progression and the loss of communicating lung units (82), which might not be recognized in routine clinical examinations and could contribute to better clinical decision-making.

1.2.2.4.1.b Measurement modalities

Several methods are used to measure ventilation heterogeneity, including multiple-breath washout (MBW) tests, oscillometry, lung imaging, and poorly communicating fraction (PCF) measures.

MBW techniques are used to evaluate the heterogeneity of ventilation in different zones of the lungs (85). These tests involve having a patient breathe a specific gas mixture and analyzing the exhaled gases to calculate various indices that reflect ventilation heterogeneity. MBW commonly involves a nitrogen (N_2) gas mixture or a trace gas that is not typically present in the lungs, such as sulfur hexafluoride (SF_6) or helium (He). In the first technique, the patient will initially breathe in 100% oxygen to wash out the nitrogen within the lungs, and then breathe the nitrogen-enriched air. The concentration of nitrogen in the exhaled air is measured and the washout curve is generated. In the second technique, the patient breathes the tracer gas mixture, and the concentration of the tracer gas is measured continuously during expiration. The patient then breathes 100% oxygen during the washout phase to wash the tracer gas from the lungs, allowing the washout curve to be generated. In MBW indices, such as the lung clearance index (LCI), the conductive $S(\text{cond})$, and the

acinar $S(\text{acin})$, the ventilation heterogeneity index is calculated from the generated curves. LCI is a measure of the efficiency of gas mixing and clearance from the lungs. $S(\text{cond})$ and $S(\text{acin})$ are determined by models that use specific equations during the slope of phase III of the washout curve and reflect the homogeneity of ventilation in the larger and small airways, respectively (86).

The imaging techniques utilized to assess ventilation include magnetic resonance imaging (MRI) and computed tomography (CT) with computation models. MRI ventilation imaging creates images of inhaled trace gases, such as hyperpolarized helium-3 or xenon-129, as they move through the airways and into the lungs. This technique allows for the visualization of both global and regional ventilation patterns. MRI ventilation imaging is used to identify the location of ventilation abnormalities in patients with respiratory conditions such as asthma and COPD (87). Ventilation SPECT/CT imaging is a diagnostic modality that combines single-photon emission computed tomography (SPECT) and CT to produce high-resolution images of lung ventilation. During the procedure, the patient inhales a radioactive gas, such as xenon or technetium, which is then detected by the SPECT/CT scanner. The resulting images show how well air flows through the patient's lungs. Ventilation SPECT/CT imaging reveals areas of low ventilation with induced bronchoconstriction (88). The indices that quantify VH in these imaging techniques are ventilation defect percentage (VDP), mean lung transit time (MLTT), and lung clearance index (LCI).

PCF, is a measurement employed in pulmonary function testing to assess VH. The PCF value is derived from the ratio of two measurements: total lung capacity (TLC),

obtained through body plethysmography, and alveolar volume (VA), measured via single-breath lung diffusing capacity. PCF utilizes the washout kinetics of inert gases such as helium, sulfur hexafluoride, carbon monoxide, or nitrogen to estimate the ratio of alveolar volume to total lung capacity. In healthy lungs, the concentration of the inert gas decreases smoothly during exhalation, while in diseased lungs with poorly communicating airspaces, the concentration of inert gas decreases more rapidly. This ratio reveals the poorly communicating fraction. PCF is a valuable tool that provides a measure of global and S(acin) VH that correlated positively with MBNW but not with S(cond) (89). In addition, the correlation with VDP using MRI ventilation imaging was generally high, although less correlation was observed in patients with severe COPD (90).

Oscillometry, which includes the impulse oscillation system (IOS) and forced oscillation technique (FOT), measures the mechanical properties of the respiratory system and has been extensively used in studies related to COPD and asthma (91). Studies have found independent relationships between FOT-measured impedance and MRI ventilation heterogeneity measurements (87), while MBW was a more sensitive measure for VH than IOS (92). Oscillometry provides a non-invasive and convenient way to assess the mechanical properties of the respiratory system in various clinical settings.

There is no single “gold standard” method for measuring VH in clinical practice, and the choice of a method depends on the specific research or clinical question and available resources. MBW is considered the most sensitive test for detecting VH, but

requires specialized equipment and expertise and might be difficult for some patients to perform. CT and imaging techniques, such as ventilation SPECT/CT and MRI ventilation imaging, can provide detailed information about the distribution of ventilation within the lungs, but they require exposure to ionizing radiation and the equipment's availability and portability are limited. PCF limitations include the need for multiple maneuvers (time and effort) and expert administration, the inability to provide regional information (conductive or large airways), and the relative lack of studies on sensitivity to subtle changes in VH, especially in the early stages of lung disease. On the other hand, oscillometry offers several advantages, including being safe and convenient for patients of all ages and medical conditions, not requiring a specialized gas mixture, being quick and easy to perform, providing a comprehensive assessment of respiratory resistance and compliance, and being readily available in clinical and research settings, including through portable devices for resource-limited areas. Oscillometry will be described in more detail later in this chapter.

1.2.2.4.1.c Implications in cardio and respiratory diseases

The presence of VH is distinctive in obstructive respiratory conditions and is often studied in the context of asthma and COPD.

In asthma, airway hyperresponsiveness (AHR) in response to various stimuli leads to the narrowing of airways and inflammation and contributes to airway remodeling, which increases airway resistance and alters lung mechanics, especially in peripheral airways (92-94). Studies have shown that VH predicts AHR in patients with asthma regardless of airway inflammation (95). In addition, abnormalities in the lung

periphery play a dominant role in VH and are related to quality of life in asthma patients (87). Moreover, the degree of ventilation heterogeneity varies in asthma with the severity of the disease and is closely related to asthma symptoms and control (88, 91, 96). Furthermore, MRIs used to quantify VH found to be predictive of asthma phenotypes with higher levels of type 2 inflammatory markers and was localized to areas of the lungs with eosinophilia (97).

Meanwhile, in COPD, ventilation heterogeneity is often more pronounced than it is in asthma (89). Several pathologic processes can lead to VH individually or in combination. The first is excess sputum production, which instigates fibrosis and narrows the airway lumen, resulting in airflow limitation. The second is the destruction of alveolar walls and loss of support, which leads to airway collapse and decreased lung elasticity. The third is dynamic hyperinflation, which is a significant cause of dyspnea among COPD patients due to the increased work of breathing and contributes to VH in compromised lungs (98). COPD patients with more severe diseases, as determined by their GOLD grade, had significantly higher (i.e. worse) VH index values (VDP and PCF) (90). In addition, VH determined by abnormalities in the peripheral regions of the lungs was significantly related to quality of life (87). However, while $S(\text{acin})$ was affected in COPD patients compared to healthy smokers, $S(\text{cond})$ was not (99).

In pneumonia, inflammation and infection in lung tissue result in the consolidation of non-aerated areas, which can cause uneven and impaired ventilation. Despite this, few studies have attempted to quantitatively assess VH in patients with

pneumonia. COVID-19 pneumonia was suggested to be accompanied by impaired pulmonary ventilation (100). CT with computation modeling was used to identify regional lung ventilation defects in a COVID-19 patient beyond CT resolution or microvascular thrombosis, which might be due to inflammation. The authors of that study suggested that assessing regional ventilation defects may facilitate the treatment, monitoring, and surveillance of respiratory dysfunction in COVID-19 patients (101).

Although it is commonly observed in respiratory conditions, VH is also a component of cardiovascular disease. Increased pulmonary capillary pressure in heart failure can cause injury to pulmonary capillaries, leading to changes in the lung tissue and vessels such as dilation, congestion, and thickening. The alveolar walls can also be affected, resulting in edema, thickening, and fibrosis. These changes result in excess fluid in the lungs, leading to pulmonary edema and orthopnea. These changes may also occur in the peripheral airways, leading to detectable functional impairments. Studies have shown that heart failure patients have higher lung clearance index and S(cond) values compared to healthy controls, suggesting the presence of peripheral airway pathology and VH in these patients (102).

In summary, ventilation heterogeneity is an important aspect of respiratory physiology. Multiple methods can be used to measure VH; however, no technique is widely used as part of a standard lung function assessment in a variety of clinical settings (103). Despite the existing research, many patients with ventilation heterogeneity, specifically patients with obstructive lung disease, continue to have

poor disease control and quality of life. Further research is needed to study VH in a variety of clinical conditions and settings, such as acute settings in respiratory units and emergency departments and among admitted patients, as well as the implications of VH to better design personalized care plans for these patients.

1.2.3 Microbiological tests and biomarkers

Several biomarkers and microbiological tests have been studied or utilized for phenotyping, diagnostics, and prognostics related to cardiovascular and respiratory conditions and acute exacerbation events. The following sections provide more details about these biomarkers and tests and their limitations.

1.2.3.1 Molecular technique and microbiological tests

1.2.3.1.1 Gram stain and sputum culture

Gram staining and sputum culture are two common laboratory tests used in the diagnosis of respiratory infections. Gram staining is a laboratory technique that involves applying a series of dyes to a sample to identify and classify the bacteria present based on their staining properties. Gram staining offers a quick and relatively inexpensive preliminary assessment of AECOPD and pneumonia. However, it has limited sensitivity, specificity, and ability to identify antibiotic susceptibility. Meanwhile, routine standard sputum cultures involve incubating a sample for a certain period to identify the bacterial or fungal pathogen responsible for infection in pneumonia or exacerbated COPD symptoms, which then informs treatment decisions. Although sputum cultures provide a more definitive identification of the bacteria or fungi causing the infection than Gram staining, they may not reliably identify pathogens, especially when patients have already been exposed to

antibiotics (104). In acute asthma, sputum cultures are less useful as asthma exacerbations are typically triggered by viral infections, such as rhinovirus or respiratory syncytial virus, which cannot be detected by sputum culture.

1.2.3.1.2 Polymerase chain reaction and 16S ribosomal RNA sequencing

Polymerase chain reaction (PCR) is a molecular biology technique that detects the presence of DNA or RNA from pathogens in a patient's sample. PCR can detect a wide range of pathogens, including bacteria, viruses, and fungi. In the context of acute cardiorespiratory events, PCR is used to detect the presence of pathogens that caused the infection in pneumonia or triggered acute exacerbations in COPD (e.g., *Haemophilus influenzae*, *Streptococcus pneumoniae*, and *Moraxella catarrhalis*) or caused the sepsis associated with AHF (e.g., *Staphylococcus aureus*, *Streptococcus pneumoniae*, and *Escherichia coli*). PCR is particularly useful for detecting viral infections as it provides a rapid, sensitive method for detecting the common triggering pathogens in acute asthma exacerbations (e.g., rhinoviruses, influenza and parainfluenza viruses, and coronaviruses). PCR's advantages include its ability to detect a wider range of pathogens, high sensitivity, and rapid turnaround time. However, it requires specialized equipment and expertise, incurs higher costs comparing to sputum cultures, and can be oversensitive as any DNA contamination may be misinterpreted (105, 106). For 16S ribosomal RNA (16S rRNA) sequencing, PCR is used to amplify the 16S rRNA gene, which all bacterial species carry. The amplified 16S rRNA gene is then sequenced to identify the bacterial species in the sample. It is not currently a routine test in clinical practice; however, it is becoming more common in research and some specialized clinical settings. This technique is

particularly useful in identifying bacterial infections in samples with negative sputum culture results when antibiotics have been administered (107-109) as it shows high sensitivity for identifying bacterial infections in AECOPD (106).

1.2.3.2 Common clinical biomarkers

Several biomarkers have been established in routine clinical practice in the context of acute cardiorespiratory diseases. These markers can provide valuable information for the diagnosis, severity assessment, and management of AECOPD, acute asthma, pneumonia, and AHF. However, these biomarkers should always be used and interpreted in the context of the patient's clinical presentation and overall medical history. Below is an overview of common biomarkers.

1.2.3.2.1 C-reactive protein and high-sensitivity C-reactive protein

C-reactive protein (CRP) is an acute-phase protein that the liver produces in response to the inflammation caused by inflammatory cytokines released in response to acute infections, autoimmune disorders, trauma, or other conditions. Therefore, CRP is widely used to monitor inflammatory status (110). CRP is commonly used as a marker of inflammation and infection in patients with AECOPD and pneumonia as CRP levels elevates due to the presence of bacterial or viral infections, which exacerbate inflammation in the lungs. CRP levels help distinguish bacterial from viral infections, as bacterial infections typically result in higher CRP levels, though this effect is not specific to bacterial infections (111). Butler et al.'s review that looked at the role of CRP as a biomarker to direct antibiotic administration. They concluded that the use of CRP reduced antibiotic prescriptions among patients with AECOPD (112). High-sensitivity C-reactive protein (hs-CRP) is a

more sensitive test that measures lower levels of CRP in the blood. In asthma cases, hs-CRP elevated levels differentiated asthmatic patients from healthy subjects and correlated with asthma severity, disease control, and treatment response (113). Elevated hs-CRP levels were also observed particularly during acute exacerbations and have been suggested as a useful tool to monitor inflammation, which causes the release of cytokines that stimulate CRP production in the liver (114). In addition, hs-CRP is typically measured in cases of cardiovascular disease; elevated levels were identified in AHF, and persistent higher levels after 30 days of hospital discharge were associated with a higher mortality rate (115).

1.2.3.2 Serum procalcitonin

Serum procalcitonin (PCT) is a protein that consists of amino acids which is normally produced by thyroid medulla C-cells. Under inflammatory stimulation, PCT is produced in several different parts of the body by other cell types, elevating its levels in blood serum. Thus, it has been suggested as a general indicator of bacterial infection (116). However, the ability of PCT to differentiate between bacterial and other mediators of inflammation (viral and noninfectious causes) in AECOPD and pneumonia to reduce antibiotic administration remains controversial (117-121).

1.2.3.3 Blood eosinophils and serum immunoglobulin E

Elevated blood eosinophil levels (eosinophilia) commonly occur in individuals with eosinophilic asthma and other allergic diseases. When the immune system responds to allergens or triggers, it increases the recruitment and activation of eosinophils. Eosinophils release inflammatory mediators and cytotoxic substances, thus

contributing to tissue damage and exacerbating inflammation. Serum immunoglobulin E (IgE) antibodies, produced by B cells, recognize and bind to allergens. These antibodies then bind to receptors on mast cells and basophils, triggering a cascade of immune responses that release chemicals that cause inflammation, vasodilation, bronchoconstriction, and allergy symptoms. Although eosinophils do not directly produce IgE, they contribute to the immune response associated with IgE-mediated allergies and promote IgE production by B-cells. The measurement of serum IgE levels serves as a biomarker for allergic diseases.

Elevated blood eosinophil counts are not typically observed in pneumonia or acute HF. However, asthma patients often exhibit elevated blood eosinophil levels, which are associated with increased bronchial hyperreactivity (122). In acute asthma, elevated blood eosinophil counts indicate an allergic component to the disease and help inform clinical decisions. Eosinophilia has been identified as a potential predictor of severe asthma exacerbation, suggesting a higher risk of experiencing such episodes. Therefore, identifying eosinophilia presents an opportunity for proactive intervention to prevent future exacerbations (123). Monoclonal antibodies against immunoglobulin E (IgE) or interleukin (IL)-5 can be used as add-on treatments for severe uncontrolled asthma. Treatment decisions should take into account the underlying biological mechanisms of the disease to anticipate patient responses, such as IgE playing a role in early allergic asthma inflammation and eosinophilia resulting from the overall process (124). In certain individuals with COPD, the presence of eosinophilic inflammation is linked to the release of proinflammatory mediators. Studies suggest an increased probability of reducing

exacerbations through inhaled corticosteroid (ICS) therapy in COPD that is associated with eosinophilia. Additionally, interleukin-5 (IL-5), a cytokine that regulates and produces eosinophils, is responsible for their growth, differentiation, activation, and survival. Treatments targeted to IL-5 have shown promise in addressing the eosinophilic phenotype of COPD (125). Furthermore, a study reported the potential involvement of IgE in certain subgroups of COPD. The authors suggested conducting clinical trials with antibodies targeting the IgE pathway, particularly for patients who have frequent exacerbations and elevated serum IgE levels; such trials could provide further insights into the therapeutic implications of these findings (126).

1.2.3.2.4 Fractional exhaled nitric oxide

Fractional exhaled nitric oxide (FeNO) is a non-invasive test that measures the amount of nitric oxide in a patient's exhaled breath as an indicator of airway inflammation. While FeNO is not part of the diagnostic tools for pneumonia, AECOPD, or acute HF, as these conditions are not associated with elevated levels of nitric oxide in the airways, it is a useful test for the diagnosis and management of acute asthma. Elevated FeNO levels are typically seen in patients with eosinophilic asthma and are associated with inflammation and AHR (127). Eosinophilic asthma is often triggered by allergens, such as pollen, dust mites, and pet dander. FeNO levels and total IgE are positively correlated, as are peripheral blood eosinophils and FeNO (128). FeNO levels help to guide treatment decisions. For example, patients with high FeNO levels may benefit from inhaled corticosteroids to reduce inflammation and improve asthma symptoms (129).

1.2.3.2.5 B-type natriuretic peptide and N-terminal pro-BNP

While B-type natriuretic peptide (BNP) and N-terminal pro-BNP (NT-proBNP) testing is not typically used in the diagnosis or management of pneumonia, AECOPD, or acute asthma, it is a valuable tool in the diagnosis and management of AHF. BNP is a hormone that is primarily released by the heart in response to increased pressure and stretching of the heart muscle; thus,, it is most commonly used as a diagnostic and prognostic tool for heart failure. NT-proBNP is a precursor molecule of BNP and is released into the bloodstream in response to the same conditions as BNP.

However, NT-proBNP has a longer half-life in the bloodstream, which makes it a more stable biomarker. Both tests are highly sensitive and can effectively rule out the presence of heart failure. Using these tests in emergency departments can potentially reduce hospital stays. Economically, incorporating BNP and NT-proBNP testing to rule out suspected heart failure increased costs in ED settings but resulted in savings in community care (130).

1.2.3.2.6 Creatinine and blood urea nitrogen

Creatinine and serum blood urea nitrogen (BUN) are laboratory tests that are commonly used while evaluating AHF to assess kidney function, which can be impaired due to reduced cardiac output and poor perfusion and is associated with worse outcomes (131).

In AECOPD, acute asthma, and pneumonia, these biomarkers are not routinely measured. However, in severe cases, these tests may be ordered to assess kidney

function, particularly in hospitalized patients who are receiving intravenous fluids or medications that may affect kidney function.

In conclusion, the biomarkers discussed are valuable tools for investigating various cardiorespiratory conditions; however, their utility is constrained by some limitations. Table (1-1) summarizes these challenges.

Table 1-1 Common biomarkers of cardiorespiratory conditions and their limitations

Biomarker	Applications and limitations
CRP and hs-CRP	Non-specific marker of inflammation; helps distinguish bacterial from viral infections but is not definitive. Lacks specificity to particular conditions (e.g., COPD vs. pneumonia).
PCT	Suggested as an indicator of bacterial infection, but reducing antibiotic administration remains controversial. Not specific to a particular condition.
Blood eosinophils/IgE	Limited relevance beyond the eosinophilic asthma phenotype and allergic diseases.
FeNO	Limited relevance beyond the eosinophilic asthma phenotype.
BNP and Pro-BNP	Primarily applicable for the diagnosis and management of AHF.
Creatinine and BUN	Used to evaluate kidney function in AHF; not routinely used in other respiratory conditions. Occurs in severe cases and hospitalized patients.

CRP and hs-CRP: C-reactive protein and high-sensitivity C-reactive protein. PCT: Procalcitonin. IgE: Immunoglobulin E. FeNO: Fractional exhaled nitric oxide
 BNP and Pro-BNP: B-type natriuretic peptide and pro-brain natriuretic peptide. Creatinine and BUN: Creatinine and blood urea nitrogen.

1.2.3.3 Lipid mediators: Pro-inflammatory and specialized pro-resolving mediators

Lipid mediators, such as eicosanoids, platelet-activating factor (PAF), endocannabinoids, sphingolipids, and lysophospholipids, are crucial for various biological processes. They contribute to inflammation, blood clotting, immune responses, pain regulation, cell signaling, apoptosis, and more. An abnormal lipid profile is associated with several health conditions. Therefore, assessing lipid mediators can provide valuable insights into the underlying pathology of various cardiorespiratory conditions and they might be useful as biomarkers for patient stratification and prognoses. However, their clinical value in various acute settings remains unclear and requires further investigation.

Eicosanoids are lipid mediators that can be broadly categorized as pro-inflammatory, anti-inflammatory, and pro-resolving mediators based on their biological effects. Pro-inflammatory lipid mediators are involved in the initiation and amplification of inflammation. These molecules promote vasodilation, increase vascular permeability, and increase the recruitment of immune cells to the site of injury or infection. Anti-inflammatory lipid mediators, on the other hand, limit inflammation and promote tissue repair by reducing the recruitment of immune cells, promoting the clearance of apoptotic cells and debris, and enhancing tissue repair processes. Pro-resolving lipid mediators are a subclass of anti-inflammatory lipid mediators that specifically promote the resolution of inflammation. These molecules are synthesized during the resolution phase of inflammation and help to restore tissue homeostasis. Overall, the balance of pro-inflammatory, anti-inflammatory, and pro-resolving lipid mediators is critical for maintaining tissue homeostasis and preventing chronic inflammation (132, 133).

Pro-inflammatory lipid mediators, including leukotrienes and prostaglandins, are involved in disease pathogenesis and are potential biomarkers for the presence, severity, and clinical outcomes of acute cardiorespiratory diseases. Leukotrienes and prostaglandins are involved in several key aspects of the pathophysiology of respiratory and cardiovascular diseases as they promote inflammation, oxidative stress, vasoconstriction, bronchoconstriction, and increased mucus production. They promote the recruitment of inflammatory cells and enhance their activation and survival (134). Leukotrienes are potent chemoattractants of neutrophils and eosinophils, while prostaglandins can promote the recruitment of mast cells and T lymphocytes. One of the most important leukotrienes in asthma is leukotriene E4 (LTE4). Significantly elevated levels of LTE4 were present in the urine of patients with acute asthma compared to stable asthmatics and their levels correlate positively with blood eosinophilia (135, 136). Another study reported elevated levels of LTE4 in the plasma of AECOPD patients (137). Leukotriene B4 (LTB4), a potent chemoattractant for neutrophils, was found to be elevated in the sputum of patients with asthma (138) and AECOPD; these levels gradually recovered after treatment. Prostaglandins, such as prostaglandin D2 (PGD2) and prostaglandin E2 (PGE2), have also been implicated in acute asthma. Increased levels of PGD2 have been reported in asthma patients, and higher PGD2 levels are associated with asthma severity and asthma exacerbations (139, 140). In addition, increased levels of PGE2 in the sputum of COPD patients are associated with increased symptoms and exacerbations (141). Several medications used to treat acute asthma and AECOPD target the leukotriene and prostaglandin pathways. For example, leukotriene receptor antagonists, such as montelukast and zafirlukast, positively altered the markers of inflammation (142). Corticosteroids can also inhibit the production of both leukotrienes and prostaglandins

(143). Leukotrienes and prostaglandins lipid mediators have also been implicated in the pathophysiology of AHF and pneumonia. Measuring the levels of LTB4 and thromboxane B2 (TXB2) could be valuable in identifying cardiac-related chest events due to myocardial infarction (MI), a common cause of HF (144). PGE2 is a key mediator of the inflammatory process. However, its role in heart failure is complex and controversial. PGE2 contributed to myocardial dysfunction by reducing myocardial contractility and inducing the apoptosis of cardiac myocytes in a study of mouse models (145). In pneumonia cases, leukotrienes and other lipid mediators are thought to promote inflammation, oxidative stress, and vascular permeability, particularly in the context of acute respiratory distress syndrome (ARDS) (146); while pneumonia is not the only cause of ARDS, it is a common cause.

The involvement of pro-inflammatory lipid mediators like leukotrienes and prostaglandins in the pathogenesis of acute cardiorespiratory diseases signifies their potential utility as biomarkers for disease severity and clinical outcomes. Table 1-2 presents a summary of the discussed biomarkers for each condition.

Table 1-2 Pro-inflammatory biomarkers across cardiorespiratory diseases

Biomarker	COPD	Asthma	HF	Pneumonia
LTE4	Elevated in the plasma during exacerbations	Elevated in the urine of acute asthma patients; correlates with blood eosinophilia		Contribute to inflammation, oxidative stress, and vascular permeability, particularly when the disease progresses to ARDS
LTB4	Elevated during exacerbations, but recovers post-treatment	Elevated in the sputum	Valuable in identifying cardiac-related chest events	
PGD2	Associated with increased	Elevated levels associated with asthma severity		

	symptoms and exacerbations	and exacerbations		
PGE2	Associated with increased symptoms and exacerbations		Contributes to myocardial dysfunction	
TXB2			Valuable in identifying cardiac-related chest events	

LTE4: Leukotriene E4. LTB4: Leukotriene B4. PGD2: Prostaglandin D2. PGE2: Prostaglandin E2. TXB2: Thromboxane B2

Specialized pro-resolving mediators (SPMs) are endogenous lipid mediators that are synthesized during the resolution phase of inflammation to promote the resolution of inflammation and help tissues return to homeostasis. SPMs act on immune cells, endothelial cells, and other cells to dampen inflammation, assist in tissue repair, and stimulate the clearance of apoptotic cells and debris. SPMs promote macrophage phagocytosis, reduce neutrophil infiltration, and inhibit pro-inflammatory cytokine production. They are mainly produced from omega-3 essential fatty acids and classified into families of mediators, including lipoxins, resolvins, protectins, and maresins (Table 1-3). New SPM molecules are constantly being discovered and characterized.

Table 1-3 Families and specific molecules of specialized pro-resolving mediators (SPMs)

SPM family	SPM molecules
Resolvins	Resolvin D1 (RvD1), resolvin D2 (RvD2), resolvin D3 (RvD3), resolvin D4 (RvD4), resolvin D5 (RvD5), resolvin E1 (RvE1), resolvin E2 (RvE2), and resolvin E3 (RvE3)
Protectins	Protectin D1 (PD1), protectin D2 (PD2), and protectin DX (PDX)
Maresins	Maresin 1 (MaR1) and maresin 2 (MaR2)

Lipoxins	Lipoxin A4 (LXA4) and lipoxin B4 (LXB4)
Electrophilic nitro-fatty acids (NO₂-Fas)	Nitro-oleic acid (NO ₂ -OA), nitro-linoleic acid (NO ₂ -LA), and nitro-arachidonic acid (NO ₂ -AA)
Others (Leukotrienes, prostaglandins*)	<p>LTB₄ can induce the production of lipoxins through the upregulation of 5-lipoxygenase and 15-lipoxygenase enzymes.</p> <p>Pro-resolving prostaglandins (PGE₂, PGD₂, PG_{2a}) work in concert with SPMs such as resolvins and protectins to promote inflammation resolution and tissue repair and may stimulate the production of these other lipid mediators.</p>

* Leukotrienes and prostaglandins are generally considered pro-inflammatory mediators (147, 148). However, both have also been shown to have anti-inflammatory and pro-resolving properties under certain conditions. These pro-resolving effects are generally thought to be secondary to their pro-inflammatory effects. LTB₄ can exert pro-resolving effects by inducing the production of lipoxins, which promote the resolution of inflammation (149). Prostaglandin PGE₂ has exhibited pro-resolving effects in several models of inflammation, including the enhancement of the macrophage phagocytosis of apoptotic neutrophils and the promotion of tissue repair (150).

Recent studies have investigated SPMs as potential biomarkers in various acute respiratory and cardiovascular conditions. In COPD, the RvD1 levels were associated with reduced AECOPD recovery (151). LXA4 levels were also significantly lower in the induced sputum of patients with COPD compared to healthy controls (152, 153). This may contribute to the continuation of inflammation in COPD in which the production of leukotrienes fails to shift towards the production of lipoxins due to disruptions in the metabolism of arachidonic acid (153). Overall, these studies suggest that SPMs may play a role in the pathophysiology of AECOPD and may function as biomarkers or therapeutic targets. In asthma, the levels of SPMs including RvD1, RvD2, and MaR1 were decreased in the serum of patients with acute asthma compared to that of stable asthmatics and healthy controls and were associated with increased severity of asthma exacerbations and impaired lung function. These findings

suggest that targeting the SPM pathway may provide a novel therapeutic approach for treating asthma and reducing airway inflammation (154). In pneumonia (*E. coli* and *P. aeruginosa*), lipid mediators such as RvD1 promoted the resolution of the pathogen in an animal experiment (155). Similarly, lipoxins and protectins limited pathogen replication, delayed bacterial invasion, and decreased inflammation, ultimately lowering patients' mortality rate (156). Moreover, in COVID-19 patients, those with severe pneumonia had significantly different levels of pro-resolving lipid mediators compared to those with mild or moderate pneumonia and the control group. This finding suggests that SPMs may contribute to the development and progression of severe pneumonia (157). Chronic heart failure (CHF) patients had reduced levels of RvD1, which were linked to weakened leukocyte production of lipids and an impaired T-cell response to the anti-inflammatory effects of RvDs, suggesting impaired signaling in the pro-resolving pathway (158). The exogenous administration of RvD1 in mice after myocardial infarction showed the potential to reduce cardiorenal syndrome in acute and chronic heart failure by promoting the resolution of inflammation, increasing reparative macrophages, limiting edema, and attenuating renal inflammation (159). Additionally, the precursors to SPMs, such as arachidonic acid and eicosapentaenoic acid, predict cardiac events, including HF (160, 161).

Overall, the literature indicates that SPMs play crucial roles in the regulation of inflammation and its resolution, implying their utility as biomarkers in acute respiratory and cardiovascular conditions. Yet, few studies have investigated an extended panel of these biomarkers and compared their levels across different cardiorespiratory conditions. Further research into the role of SPMs in these conditions using several sample types, such as sputum samples, which are an indirect, readily available, non-invasive lung sampling

method, is warranted to fully elucidate their role in cardiorespiratory diseases during the chronic and acute phases and identify novel biomarkers and their potential use as therapeutic targets. Table 1-4 summarizes the roles of SPMs in acute cardiorespiratory conditions.

Table 1-4 SPMs in acute cardiorespiratory conditions

Condition	SPMs investigated	Findings and implications
COPD	RvD1, LXA4	RvD1 is associated with reduced AECOPD recovery. LXA4 is lower in the sputum of COPD patients and aligned with ongoing inflammation.
Asthma	RvD1, RvD2, MaR1	All are decreased in the serum of acute patients and related to disease severity and impaired lung function.
Pneumonia	RvD1, LXs, SPM profiles	RvD1 may promote pathogen resolution. LXs limit pathogen replication and decrease inflammation. Severe pneumonia cases showed different SPM levels than mild to moderate cases and controls, indicating their involvement in disease progression.
HF	RvD1, SPM precursors	Decreased are levels associated with weakened leukocyte production and impaired T-cell response. Exogenous RvD1 reduced cardiorenal syndrome. Precursors (arachidonic acid and eicosatetraenoic acid) predicted cardiac events.

RvD1: Resolvin D1. RvD2: Resolvin D2. MaR1: Maresin 1. LXA4: Lipoxin A4. LXs: Lipoxins. SPMs: Specialized pro-resolving mediators.

1.3 Metabolomics

1.3.1 Metabolomics contributes to advances in medical practice

The human body conducts various metabolic processes, including glycolysis, protein and lipid metabolism, gluconeogenesis, immune cell metabolism, inflammation, and detoxification, among others. These processes are intricately interconnected and regulated to maintain homeostasis and ensure optimal bodily function. Metabolomics is the study of the small molecules (metabolites) that are produced or altered by the metabolic processes within cells, tissues, or organisms (162). Metabolomics has made significant contributions to modern medical science, enabling advancements in precision medicine, disease diagnosis and prognosis, drug discovery, nutritional assessment, and microbiome research.

Metabolomics is utilized to advance medicine precision by identifying biomarkers based on the unique metabolic profiles and signatures that are characteristic of specific diseases or their subgroups. Identifying these biomarkers contributes to disease diagnosis, monitoring, and evaluating the response to therapy (163). In addition, stratifying patients helps guide the creation of personalized therapies (162, 163). In therapeutic investigations, metabolomics can be used to identify novel targets for drug discovery by detecting dysregulated metabolic pathways that are associated with exacerbations or disease severity. It also involves evaluating the efficacy and toxicity of new drugs on metabolic pathways. Furthermore, in nutritional assessment, metabolomics provides information regarding an individual's nutritional status and the metabolic deficiencies that can contribute to disease, such as biomarkers of vitamin and mineral deficiencies and evaluating the effects of dietary interventions on metabolic pathways (164). Furthermore, in

microbiome research, metabolomics can reflect the metabolic interactions between the host and the gut microbiome, which have important implications for human health. For example, metabolomics can be used to identify the microbial metabolites that are associated with disease and evaluate the effects of prebiotics, probiotics, and dietary interventions on the gut microbiome and host metabolism (165).

Overall, advances in metabolomics can revolutionize medical practice by providing new insights into the pathophysiology of disease, facilitating early diagnosis and personalized therapy, and improving drug discovery and nutritional assessment.

1.3.2 Current technology

The technologies that are currently utilized in the study of metabolites and metabolic pathways include mass spectrometry (MS), nuclear magnetic resonance (NMR), high-throughput screening (HTS), imaging mass spectrometry (IMS), and bioinformatics.

MS is a powerful analytical platform that is widely used in metabolomics. It involves ionizing metabolites through electron ionization (EI), electrospray ionization (ESI), or matrix-assisted laser desorption/ionization (MALDI). The ionized metabolites are then separated based on their mass-to-charge ratio. The resulting mass spectrum is used to detect and quantify metabolites by analyzing their characteristic fragmentation patterns. MS can be coupled with various separation techniques, such as liquid chromatography (LC), gas chromatography (GC), or capillary electrophoresis (CE). These combinations enhance the technique's sensitivity and specificity by improving the resolution and separation of metabolites before detection and quantification. LC–MS and GC–MS are commonly used

techniques in metabolomics research. LC–MS is suitable for analyzing polar and nonpolar metabolites, such as amino acids and lipids, while GC–MS is typically used for volatile and thermally stable metabolites, such as organic acids and sugars. LC–MS encompasses a range of mass spectrometry techniques used in combination with liquid chromatography, including quadrupole–time of flight (Q–TOF) MS, ion trap mass spectrometry (IT–MS), triple quadrupole mass spectrometry (TQ–MS), and orbitrap mass spectrometry (OT–MS). MS offers several advantages for metabolomics research, including high sensitivity and specificity, the simultaneous identification and quantification of multiple metabolites, and the ability to identify unknown metabolites via their fragmentation patterns. However, MS has some limitations, such as the need for careful sample preparation to avoid contamination, potential ion suppression and matrix effects, and the requirement of specialized expertise and equipment. Overall, MS is a valuable analytical technique driving advances in our understanding of metabolism and disease.

NMR spectroscopy is another widely used technique in metabolomics. It involves subjecting metabolites to a strong magnetic field and measuring their absorption and emission of radiofrequency energy. This provides information about the chemical structure and molecular dynamics of metabolites and enables quantitative and qualitative analysis. HTS enables the rapid screening of many compounds or samples for metabolites of interest. It typically involves the use of robotic systems to prepare and analyze samples and can be employed for both targeted and untargeted metabolomics. IMS enables the spatially resolved analysis of metabolites in tissue samples. It involves coupling MS with a microscope, allowing metabolites to be visualized and localized within tissues.

Bioinformatics is essential in metabolomics research, it provides computational methods and tools for analyzing and interpreting the large, complex datasets obtained from these analysis platforms. Bioinformatics tools are used for data processing, statistical analysis, pathway analysis, and the identification of disease biomarkers and potential drug targets. In combination, these methods and technologies have greatly advanced the field of metabolomics.

1.3.3 Biological Samples Used in Metabolomics Studies

Different biological samples can be used to study metabolites and metabolic pathways, such as blood (serum and plasma), urine, tissue, saliva, sputum, cerebrospinal fluid (CSF), and breath. Each sample type has advantages and disadvantages; these are summarized in Table 1-5. Choosing the appropriate sample type for a given research question is crucial, in addition to high-quality collection techniques to ensure accurate and meaningful results. Samples should be collected in sterile containers and immediately refrigerated or frozen after collection to prevent the degradation of the metabolites; they should be transported in dry ice to maintain the integrity of the metabolites. Patient information, such as age, sex, smoking status, and any medications being taken, must also be recorded as these factors can influence the metabolites present in the samples.

Table 1-5 Comparison of sample types for metabolomics analysis

	Feasibility and collection	Specifications
Blood (plasma and serum)	Accessible, commonly used, minimally invasive (fingerstick or venipuncture)	Wide range of metabolites that can provide insights into systemic metabolic processes.

Urine	Accessible, commonly used, non-invasive, and relatively easy to process	Wide range of metabolites that can provide insights into systemic metabolic processes.
Tissue	Requires biopsy or surgical resection	Metabolites in specific organs or tissues, such as liver, muscle, brain, and tumor tissues.
Saliva	Accessible, non-invasive, easy to collect	Often utilized in studies of oral health.
Sputum	Non-invasive by asking the patient to cough up sputum; however, collection can be challenging	Wide range of metabolites, particularly in studies of respiratory diseases (e.g., studying SPMs in sputum).
Cerebrospinal fluid	Requires lumbar puncture	Metabolites can provide insights into brain metabolism and function.
Bronchoalveolar lavage fluid	Requires bronchoscope inserted into lungs and saline instilled and aspirated to collect lining fluid, airway mucus, and immune cells for processing and downstream analyses	Bronchoscopy is generally safe and samples provide valuable information about metabolic changes in response to disease or treatment, although complications such as bleeding, infection, and bronchospasm can occur and samples may be contaminated.
Breath (VOCs)	Non-invasive with breath collection devices; however, many factors contribute to sample collection and VOC recovery.	Used to study volatile organic compounds (VOCs) that are produced by metabolic processes.

1.3.4 Plasma metabolomic biomarkers in acute cardiorespiratory diseases

1.3.4.1 Profiling systemic metabolic changes: The value of plasma analysis in metabolomics studies

Cardiovascular and respiratory diseases have systemic manifestations. Therefore, the plasma and serum are commonly profiled as they provide valuable information about the systemic metabolic changes associated with these diseases. Direct lung sampling of lung through biopsy or bronchoscopy carries risks and is an invasive procedure. However, indirect methods, such as sampling expectorated or induced sputum or analyzing exhaled breath, have drawbacks as well, including variability in sample composition, contamination, limited representation of specific lung regions, incomplete analyte coverage, and discomfort or inconvenience during sample collection. These limitations explicate the preference for plasma and serum profiling in metabolomics studies as relatively reliable approaches to assessing the systemic metabolic changes associated with cardiorespiratory diseases. Advances in mass spectrometry and other analytical technologies have enabled the high-throughput analysis of plasma metabolites, allowing for the simultaneous analysis of a diverse range of metabolites, including small molecules and proteins (166).

1.3.4.2 Plasma metabolomic biomarkers and pathways in cardiorespiratory conditions

Metabolomics studies of plasma have identified several potential biomarkers for acute cardiorespiratory conditions, including AECOPD, acute asthma, pneumonia, and acute HF. A scoping review by Godbole et al. of studies investigating the metabolome of COPD patients described specific findings related to plasma in COPD patients. AECOPD patients' plasma exhibited elevated levels of amino acids and fatty acids, including glutamic acid, lysine, and

arachidonic acid, compared to stable COPD patients. Furthermore, increased levels of various amino acids, including lactate, pyruvate, alanine, leucine, isoleucine, valine, phenylalanine, tyrosine, methionine, and acylcarnitines, were observed in the plasma of COPD patients compared to healthy controls. In contrast, decreased levels of certain amino acids, including glutamate, arginine, and lysine, were noted in the plasma of COPD patients compared to healthy controls. The authors discussed how these plasma metabolites could participate in key mechanisms of the pathogenesis of COPD and the exacerbation of the disease. For example, elevated levels of arachidonic acid, a type of fatty acid, in the plasma of AECOPD patients when compared to stable COPD patients and healthy controls could contribute to airway inflammation and mucus production. Similarly, the increased levels of lactate, pyruvate, and other metabolites may indicate increased oxidative stress and inflammation, while decreased levels of certain amino acids, such as arginine and lysine, may impair immune function and increase oxidative stress (167).

In the context of asthma, the plasma metabolome distinguished individuals with asthma from healthy individuals and suggested the activation of immune and inflammatory pathways. Several metabolites were significantly different in asthma patients, including higher levels of taurine, lathosterol, bile acids (taurocholate and glycodeoxycholate), nicotinamide, and adenosine-5-phosphate. Among asthmatic patients, those with severe asthma and high levels of FeNO exhibited specific metabolic changes indicating distinct subtypes within the asthma population (168).

Likewise, systemic metabolic alterations in plasma metabolites might reveal different aetiologies of pneumonia and acute HF by reflecting the host metabolism, immune

responses, and host energy during pneumonia, as well as the host metabolism and oxidative stress in cardiac cells during acute HF. The levels of amino acids, including alanine, arginine, asparagine, citrulline, glutamine, glycine, histidine, lysine, methionine, serine, threonine, and tryptophan, were notably reduced in the CAP group, which included cases caused by *Streptococcus pneumoniae*, *Haemophilus influenzae*, *Staphylococcus aureus*, *Klebsiella pneumoniae*, and other bacteria on the day of hospitalization compared to the control group (169). Different metabolic alterations, such as changes in fatty acids, can also distinguish pneumonia groups, such as those caused by H1N1 . Additionally, COVID-19 pneumonia patients exhibit a distinct plasma metabolic profile compared to individuals with bacterial culture-positive pneumonia (170-172). Furthermore, lipid-based plasma metabolites have predictive value for outcomes and disease severity in pneumonia cases (173).

The plasma metabolome provides insights into metabolic pathways in heart failure cases, including arginine metabolism, nitric oxide regulation, and energy utilization. Biomarkers such as aminoterminal pro-B-type natriuretic peptide (NT-proBNP) and endogenous arginine are positively associated with left ventricular (LV) filling pressures and linked to adverse cardiovascular events. Elevated levels of long-chain acylcarnitines (LCACs) in the failing myocardium are associated with lower peak VO_2 and an increased risk of mortality, hospitalization, and cardiovascular events. Additionally, a metabolic shift was observed in failing myocytes, which favor glucose over fatty acids (174), furthermore, increased levels of certain metabolites, such as glutamate, glutamine, sphingomyelin (SM), and ceramides, were associated with worse clinical outcomes in patients with AHF (175).

Cardiorespiratory diseases can present with similar clinical pictures. AECOPD and acute HF in specific have significant overlap in clinical presentation, with dyspnea, wheezing, cough, and edema being common symptoms in both conditions. The shared clinical presentation of AECOPD and acute HF can make distinguishing between these conditions challenging. Thus, misdiagnosis is common due to the overlapping symptoms and demographics. During acute exacerbations, diagnostic testing may return similar and nonspecific findings, causing diagnostic challenges. The shared risk factors of these diseases, such as health behaviors, environment, socioeconomic status, and respiratory viral infections, contribute to the risk of both COPD and HF exacerbation (176, 177). Limited work has been done on metabolomic biomarkers across healthy individuals and those with AHF and AECOPD in general and specifically using the plasma metabolome. One study analysed serum and urine via metabolic profiling and found that patients with respiratory failure due to AECOPD, CHF, and pneumonia were distinct from stable COPD patients. The metabolic profile did not reveal a definitive global metabolic signature of AECOPD, but potential markers, such as glycine, formate, histidine, citrate, glutamate, proline, and creatine phosphate, were identified. The metabolites citrate, furoylglycine, 3-hydroxymandelate, niacinamide, and nicotinamide N-oxide occurred at lower levels in patients with respiratory failure (178). The differences in the studied populations and variations in studies designs and analytical methods make it challenging to compare results across different studies. Therefore, while there is some promising preliminary evidence that examined HF from AECOPD, further work utilizing different sample types, including plasma samples, and larger sample sizes with validation in independent cohorts is needed to fully understand the metabolome's clinical utility. Table 1-6 summarizes the various biomarkers that have been investigated in the plasma samples of patients with COPD, asthma, HF, or pneumonia.

Table 1-6 Plasma metabolites investigated in patients with COPD, asthma, HF, or pneumonia

Conditions	Findings regarding the plasma metabolite investigated
COPD	<p>Increased lactate, pyruvate, and various amino acids were found in COPD plasma compared to that of healthy individuals.</p> <p>Elevated levels of amino acids (glutamic acid, lysine) and fatty acids (arachidonic acid) occurred during exacerbations.</p>
Asthma	<p>Plasma metabolome profiles distinguished asthmatic from healthy individuals.</p> <p>Higher levels of taurine, lathosterol, bile acids, nicotinamide, and adenosine-5-phosphate were present in asthmatic plasma.</p> <p>Specific metabolic changes were identified in severe asthma subtypes.</p>
Pneumonia	<p>Reduced amino acid levels (alanine, arginine, etc.) occurred in CAP-related pneumonia.</p> <p>Distinct metabolic profiles were identified for different pneumonia causes, including COVID-19.</p>
HF	<p>Plasma metabolome profiles provided insights into metabolic pathways in HF (arginine metabolism, nitric oxide regulation, and energy utilization).</p> <p>Elevated LCAC was linked to the mortality risk.</p> <p>Heightened glutamate, glutamine, sphingomyelin (SM), and ceramide levels were associated with worse clinical outcomes.</p>

1.3.5 Breathomics and VOCs

1.3.5.1 Unveiling the potential of VOCs for clinical utilization

VOCs are a diverse group of chemicals that include man-made substances (e.g., those resulting from industrial processes), naturally occurring substances (e.g., those from plants and microorganisms), and biological substances (e.g., substances produced by the processes

of the human body) (179, 180). VOCs' chemical composition can vary widely, but they typically have a low boiling point and can easily evaporate into the air. VOCs can be classified into different groups according to their chemical structure and properties, such as alkanes, alkenes, alcohols, ketones, esters, terpenes, etc. (181).

In the human body, the production and release of VOCs in the breath can be influenced by a wide range of factors, including metabolic and biochemical processes, inflammation, oxidative stress, the breakdown of drugs or toxins, and microbiota activity. In diseased states, alterations in these factors can change the types and quantities of VOCs produced, which may be detected through breath analysis. The identification and quantification of these specific VOC changes in the breath can provide valuable insights into the underlying pathophysiology. Thus, by identifying VOC signatures and understanding the mechanisms underlying the production of these VOCs, researchers may be able to identify biomarkers for the diagnosis and monitoring of disease and novel therapeutic targets for disease prevention and treatment (182).

Breathomics is an emerging field of metabolomic research that focuses on the analysis of the VOCs in exhaled breath. Breath analysis approaches broadly offer non-invasive, cost-effective, rapid disease diagnosis (183). Breath analysis is promising for detecting diseases at an early stage, improving treatment success and patient outcomes; for instance, breath analysis has been used to identify early-stage lung cancer with high accuracy, which improves survival rates (184). In addition, recent advances in technology have introduced portable and miniaturized breath analysis devices for use in various locations, clinical settings, and remote locations. For example, a breath analyzer has been developed and

tested for the remote monitoring of COPD patients who require non-invasive ventilation at home (185). Overall, breath analysis technology could potentially transform the field of personalized medicine. Thus, breathomics is a promising research area that could revolutionize the way we approach disease diagnosis and monitoring, as well as our understanding of disease pathophysiology, with the potential to significantly affect healthcare.

1.3.5.2 VOCs from exhaled breath: Collection to data analysis

Studying VOCs in breathomics research involves several aspects; the initial phase is breath sample collection and preparation; the samples are then assessed with various analytical techniques, and, finally, data from the analysis are processed with statistical and bioinformatics tools to identify patterns and specific VOCs associated with different diseases. The interpretation of the results usually requires expertise in both analytical chemistry and clinical medicine (183). In terms of analytical techniques, some of the most commonly used systems for the detection and quantification of VOCs in breath samples include GC–MS, proton transfer reaction–mass spectrometry (PTR–MS), selected ion flow tube–mass spectrometry (SIFT–MS), and electronic nose (E-nose) technology. GC–MS is considered the gold standard technique for VOC analysis due to its high sensitivity, specificity, and ability to identify a wide range of VOCs. PTR–MS and SIFT–MS are both sensitive, real-time techniques that offer the rapid detection and quantification of VOCs. E-nose technology, on the other hand, uses an array of non-specific chemical sensors and a pattern recognition engine to detect and identify VOC patterns in breath samples (186, 187).

Prior to the analysis phase, breath samples are typically collected using non-invasive methods, such as with a breath collection bag, sorbent tubes, or solid-phase microextraction (SPME) fibers. Breath bags are made of materials such as Tedlar, which is inert and does not react with VOCs in breath.; conversely, breath collection tubes are coated with a substance that absorbs VOCs. In both methods, the breath can be collected by exhaling directly or via a mouthpiece or mask into the tube or bag. Breath bags and tubes can also be attached to other specialized devices, including spirometry devices and breath collection devices. In spirometer-based devices, the subject breathes into a mouthpiece connected to a spirometer, and the exhaled breath is directed into a collection bag or tube. Breath collection devices, e.g., the respiration collector for in vitro analysis (ReCIVA) breath sampler, are used to collect breath samples from individuals and store them for later analysis utilizing sorbent tubes, bags, or other methods to capture the exhaled breath.

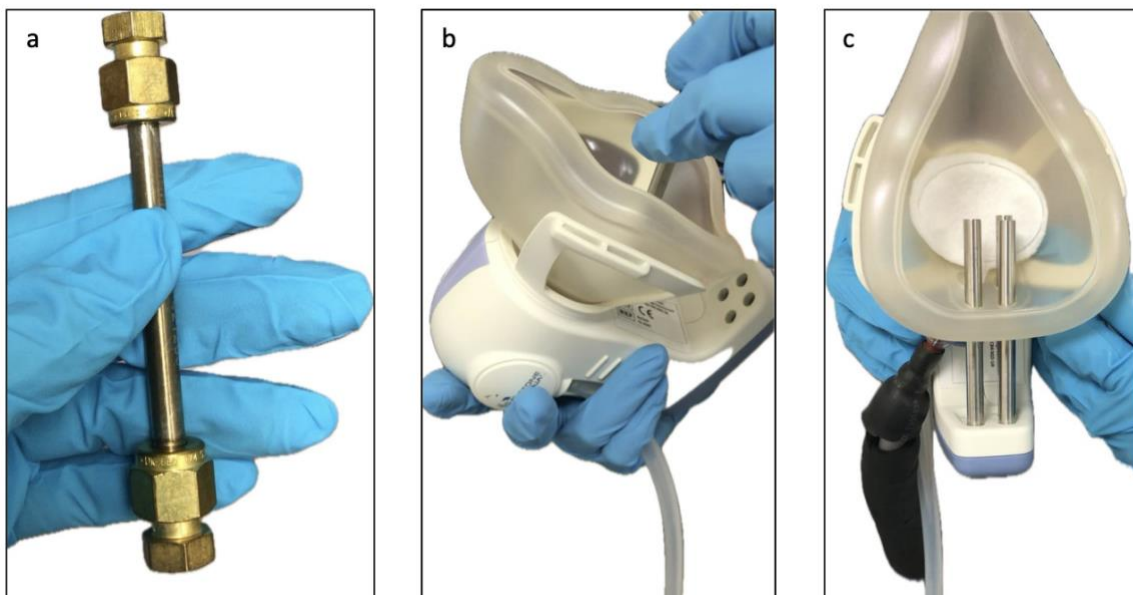


Figure 1-1 ReCIVA breath sampler device utilizing sorbent tubes

(a) Sorbent tubes conditioned, sealed, and ready to use. (b) Loading the sorbent tubes into the ReCIVA device. (c) ReCIVA device prepared for VOC collection. Respiratory testing laboratory, Department of Respiratory Science, NIHR Leicester Biomedical Research Centre (Respiratory).

Another breath collection method involves having the patient breathe directly into the inlet of a breath biopsy device via a mouthpiece or a mask. Breath biopsy devices are designed to collect and analyze the collected breath samples for the presence of biomarkers or other disease indicators; thus, a breath biopsy device encompasses more than just the collection phase. These include E-nose devices, online breath analyzers, and real-time sampling instruments. These instruments use technologies such as PTR-MS or cavity ring-down spectroscopy (CRDS) to detect the VOCs in the breath.

Each method has advantages and limitations. Exhaling directly into a mouthpiece of the analyzing instrument is a quick and easy collection method, but may not be suitable for all subjects or to collect VOCs from a large breath volume. Breath collection bags can hold a larger breath sample and may be more convenient for some subjects, but the bags can be prone to contamination and may not preserve the breath sample for long periods. Sorbent tubes and SPME fibers effectively collect the VOCs in the breath but require specialized equipment for preparation and analysis. The choice of breath collection device depends on the specific application and analytical techniques available for metabolomics analysis. Careful consideration should be given to factors such as the specific research question and the type of VOCs of interest, sample size, the sensitivity and specificity of the analytical techniques, and the feasibility of collecting breath samples from the study population (188). In addition, several measures can be taken to overcome the limitations of each breath collection method; researchers can also use a combination of methods to increase the accuracy and reliability of their results. Furthermore, the proper training of study

participants, following best practices for sample collection, and careful collection, storage, and transportation procedures can help minimize the risk of contamination and ensure the preservation of the breath sample for accurate analysis. Finally, using quality control measures, such as internal standards and blank samples, can help identify and correct for analytical errors or instrument drift. Access to the appropriate instrumentation and expertise is important to apply these methods (189, 190).

1.3.5.3 Challenges and considerations in breathomics research and VOC composition:

Toward clinical applications

The challenges associated with breathomics research have been the reasons why it has not widely applied clinically. Despite the potential advantages of breath analysis, several obstacles remain to be overcome, including the lack of standardization in sampling and analysis methods, the identification and quantification of biomarkers, and the need for larger studies to validate the diagnostic accuracy and clinical utility of breath analysis in different diseases (187, 191). In addition, several other challenges are related to the collection methods, the nature of VOCs, and their composition in the air. The literature discusses several aspects of these challenges, including the variability in VOC profiles due to confounding demographic elements, such as diet, age, sex, medications, and smoking (192). Another challenge is the difficulty in distinguishing between disease-related VOCs and non-disease-specific VOCs. Third, VOC composition can be influenced by external factors, including environmental conditions and the dynamics of air movement or the air exchange rate (193, 194). Finally, the physical characteristics of the conduit through which the VOCs are transported may affect the results. In the engineering field, factors such as diameter and length significantly affect the design of pipelines for transporting fluids and gases, including

VOCs. When VOCs move between locations, pipeline diameter, flow rates, and turbulence play vital roles in VOC dispersion and emission (195). This is also potentially relevant in the context of breathomics studies in humans for endogenous VOCs, which are the products of metabolic processes in tissues, diffuse from the capillaries into the alveoli, and are exhaled during expiration through the airways. Conversely, exogenous VOCs originate from the surrounding environment and are transported through the upper airways via the air stream.

Breath metabolomics biomarkers have been explored for the diagnosis and monitoring of several diseases, including asthma and COPD (196). Ibrahim et al. identified a set of 101 VOC biomarkers of acute breathlessness in exhaled breath samples. The study found that the levels of these VOCs were significantly different between patients with acute cardiorespiratory breathlessness (including acute asthma, AECOPD, AHF, and pneumonia cases) and healthy controls. The authors suggested that these VOCs could serve as diagnostic biomarkers for acute cardiorespiratory breathlessness and that future studies could further investigate the use of exhaled breath analysis for this purpose (197). With this promising growth in utilizing breathomics VOC biomarkers in the context of cardiorespiratory diseases, the potential effects of physiological and mechanical pulmonary changes on the physical composition of breath VOCs must be addressed. Other studies have investigated the effects of basic respiratory mechanics on breath collection for VOC analysis. For example, one study showed that changes in breathing patterns, such as flow rate, can affect the concentration of some VOCs, specifically hydrogen peroxide, in the exhaled breath of healthy and asthmatic patients; due to the flow dependency the authors suggested that the production of this VOC occurs within the airways (198). However, to our knowledge, no studies have yet been published investigating the effects of underlying lung

mechanics and VH on the collection of breath samples for VOC analysis. The studies above did not specifically focus on VH in patients presenting with acute events. However, these results highlight the importance of standardizing breath collection protocols to ensure accurate and reliable results. Therefore, further studies are needed in patients with acute events to uncover the Impact of Ventilation Heterogeneity on VOC movement, emission, and recovery in breath samples.

Overall, breath metabolomics is an emerging field with great potential for clinical applications. However, more research is needed to establish the reliability and validity of breath metabolomics in various disease contexts and to develop standardized protocols for breath sample collection and analysis.

1.4 Oscillometry

1.4.1 Respiratory mechanics: Understanding pressure gradients, resistance, and compliance in the respiratory system

Gas flows through a tube due to the pressure gradient along the tube from the inlet to the outlet. The same principle applies to the respiratory system during ventilation, where bulk movement of air occurs between the external environment and the alveoli. When the respiratory muscles contract during inhalation, they generate force that decreases the intrapleural pressure and increases lung volume. This creates a pressure gradient between the intra-alveolar pressure and the atmospheric pressure, causing air to rush into the lungs. During exhalation, the respiratory muscles relax, and the elastic recoil of the lungs and chest wall decreases lung volume and increases intrapulmonary pressure, which becomes greater than atmospheric pressure. This pressure gradient allows air to flow out of the lungs. Throughout the breathing cycle, the intrapleural pressure remains slightly negative relative to the intrapulmonary pressure, which provides the necessary transpulmonary pressure gradient for lung expansion. These pressure changes are crucial for proper gas exchange in the lungs and various respiratory controls regulate these mechanisms (199). The mechanical characteristics of the respiratory system affect this process during cyclic breathing, as two opposing forces impede lung inflation. The first is elastic resistance, which is measured when there is no gas flow. The work performed to overcome elastic resistance is stored as a source of energy during passive expiration. The second is frictional resistance (respiratory system resistance, or R_{rs}), a non-elastic resistance measured during gas flow where the energy used is dissipated as heat and lost (200).

Elastic resistance consists of the resistive force of surface tension at the alveolar interface to lung inflation and the elasticity of the lungs and chest wall. The lungs' functional tissue and the chest wall both have elastic properties that resist changes in shape. The chest wall naturally recoils outward, while the lungs recoil inward, resulting in balanced opposing forces that contribute to maintaining intrapleural pressure (201). When the driving force, the activation of the inspiratory muscles, is removed at the end of inspiration during cyclic breathing, the lung and chest wall tend to return to their resting position, leading to passive exhalation. Changes in elasticity due to pathology alter this equilibrium, affecting functional residual capacity (FRC). In emphysema, for example, lung elasticity decreases, allowing outward thoracic recoil to predominate and lung equilibrium to occur at a larger volume, increasing the FRC (202). The relationship between pressure, volume, and elasticity is expressed by the formula

$$E = \Delta P \text{ (cm H}_2\text{O or kPa)} / \Delta V \text{ (L or ml)}$$

Where each unit of pressure applied to the lung causes a unit increase in lung volume.

Compliance, the reciprocal of elastance, measures the ease of stretchability and is expressed as

$$C = \Delta V \text{ (L or ml)} / \Delta P \text{ (cm H}_2\text{O or kPa)}$$

Therefore, when compliance increases (a measure of distensibility), elastance decreases (a measure of resistance). The total compliance comprises both lung compliance and chest wall compliance. Lung compliance is the change in lung volume per change in transpulmonary pressure (the pressure difference between the alveoli and the pleural space), while chest wall compliance is the change in thoracic cage volume per change in transthoracic pressure (the pressure difference between the ambient air and the pleural space). In clinical settings, compliance is categorized as static or dynamic. Static compliance

(C_{st}) is measured when there is no gas flow or resistance and reflects the elastic properties of the respiratory system (lungs and chest wall). Dynamic compliance (C_{dyn}) is measured during gas flow and reflects both the elasticity of the respiratory system and its resistance to airflow (i.e., airway resistance). The difference between dynamic and static compliance (C_{dyn} – C_{st}) represents the extent of airway resistance present in the respiratory system. Dynamic compliance is often more convenient to measure in clinical settings, and it is obtained during the short-term static status at the end of inspiration during tidal breathing (200, 203, 204).

The second opposing force to lung inflation is respiratory system resistance (R_{rs}). It comprises three components: airway resistance, tissue viscous resistance, and inertance. Tissue viscous resistance is a minor contributor that arises from the frictional resistance of the displacement of tissues in the lungs, thorax, and abdominal contents. Inertance, on the other hand, is primarily significant at high frequencies and is associated with gas and tissue (lungs, thorax) as objects that must offer resistance to the change in their state of motion due to flow and volume changes during ventilation, according to Newton's laws of physics (205). Airway resistance (R_{aw}) is the main component of R_{rs}, accounting for about 80% of the total resistance. It is the frictional resistance of airflow in the airways and is defined as the change in transpulmonary pressure required to produce a unit flow of gas through the airways of the lung (200). The mathematical relationship between pressure, resistance, and flow is described by the formula

$$R = \Delta P \text{ (cm H}_2\text{O or kPa)} / \dot{V} \text{ (L or ml/min)}$$

where R represents resistance, ΔP represents the pressure difference (expressed in cm H₂O or kPa), and \dot{V} represents the flow rate (expressed in L or ml/min).

Factors that dominate R_{aw} include flow and its contributors, such as respiratory rate and flow type (laminar or turbulent) in addition to airway properties, i.e., length and diameter.

Turbulent flow in the airway is chaotic and irregular, with random movement and mixing of air molecules. It occurs when air velocity exceeds a threshold, increasing resistance. Laminar flow, conversely, is smooth and streamlined, with parallel movement of air molecules. It has low turbulence and resistance, enabling efficient airflow in the airway. Olson et al. (1970) provided a theoretical analysis of the pressure changes in the human airway, indicating that turbulent airflow is expected in the high-velocity upper airways, while laminar flow predominates in the bronchial tree. The pressure–flow relationship shows that at lower flow rates, flow increases proportionally to the pressure gradient. However, once the flow rate exceeds a certain threshold, further increases in the pressure gradient only modestly affect flow improvement (206). In laminar flow, the airway radius significantly influences resistance. Mathematically, when the airway diameter is halved, the required pressure must increase significantly to maintain flow, as demonstrated by the Hagen–Poiseuille equation. Therefore, the patient must exert significantly more effort to sustain airflow through the airways. The continuous branching of airways results in smaller individual diameters, but the significant increase in the number of airways offsets the decrease in individual diameters, which makes the small airway resistance (or small airway dysfunction) difficult to measure as many small airways must be obstructed first to cause changes in the measured resistance or contribute to symptoms and difficulty breathing (204, 207, 208). Resistance in the airways is also affected by lung volume. At low volumes, the airways are narrower, increasing resistance. This occurs during expiration or partial deflation. Reduced lung volume reduces radial traction on airway walls, increasing their collapsibility and resistance.

Conversely, higher lung volumes expand the airways, reducing resistance. This happens during inspiration or full inflation, maintaining airway patency. Lung elasticity also plays a role, influencing airway caliber and resistance. As lung volume changes, so does airway resistance (209, 210).

The function of the respiratory system is determined with both of its mechanical properties, i.e., the elastic properties and frictional resistance, by applying a simple equation of motion (211, 212) as follows

$$FRS = F_{el} + F_{Raw} + F_{inertia}$$

where forces in the respiratory system (FRS) comprise the forces of elasticity (F_{el}), raw airway resistance (F_{Raw}), and inertia ($F_{inertia}$).

Since the pressure generated by the muscles imposes the force, the equation of motion can be expressed as

$$P = P_{el} + P_{Raw} + P_{inertia}$$

where P represents the pressure in the respiratory system, P_{el} represents the elastic recoil pressure of the system, P_{Raw} represents the pressure required to overcome the resistance of the airways, and $P_{inertia}$ represents the pressure needed to overcome the inertia of the respiratory system. This can be written in terms of the more easily measurable variables (pressure, volume, compliance, and resistance), omitting the term for inertial force since it is typically negligible at lower frequencies, as

$$P_t = (V \cdot 1/C) + (\dot{V} \cdot R)$$

where P_t represents the total pressure in the respiratory system, V represents the volume of air moved, $1/C$ represents the compliance (the reciprocal of elastance or stiffness) of the respiratory system, and R represents the resistance of the airways.

1.4.2 Oscillometry and respiratory impedance

1.4.2.1 Concept and measurements

Oscillometry is a non-invasive technique for measuring respiratory impedance (Z_{rs}), which is a measure of the opposition presented by the respiratory system to the flow of gas induced by an acoustic pressure applied to the system and is a combination of resistance and reactance to airflow (213). Oscillometry works by superimposing external pressure oscillations on spontaneous breathing using a loudspeaker or piston that delivers pressure waves with small amplitudes and measures the resulting flow by pneumotachograph. Then, the value of Z_{rs} as a function of the elastic (reactive) and resistive loads on the respiratory system can be mathematically modeled with a sinusoidal function. The phase angle between pressure and flow around a complex plane indicates the relative magnitudes of airway resistance and compliance (214, 215). The oscillometry equation modifies the original equation of motion for the respiratory system to account for the oscillatory nature of the airflow and pressure waves generated by sound waves. The modified equation expresses respiratory impedance (Z) as the sum of resistance (R) and reactance (X), where R represents the pressure required to overcome the frictional resistance to airflow and X reflects the energy storage and dissipation properties of lung tissue and airways. Z_{rs} is projected as the spectral complex ratio of oscillatory pressure and flow (frequency domain f) and can be expressed as

$$Z_{rs}(f) = R_{rs}(f) + iX_{rs}(f)$$

On the complex plane, R_{rs} is the real part and corresponds to the frictional resistance in the airways, and X_{rs} is the imaginary part and represents the elastic and inertance values of the respiratory system. Moreover, by superimposing a range of frequencies (usually 5 to 30 Hz) in the signal return flow, Oscillometry measure the mechanical characteristics of the central and peripheral airways. At higher frequencies, the airflow travels shorter distances, thus, it primarily interacts with the larger central airways, such as the trachea and bronchi, reflecting their mechanical properties. As the frequency decreases, the airflow penetrates deeper into the respiratory system, reaching the smaller, peripheral airways, including the bronchioles and alveoli. By analyzing the frequency-dependent changes in respiratory impedance, oscillometry helps elucidate the mechanical properties and heterogeneity within the system.

Common measurements generated in the oscillometry resistance curve are the resistance at frequencies of 5 Hz (R_5) and 19 Hz (R_{19}) and the resistance at 5 Hz minus the resistance at 19 Hz ($R_5 - R_{19}$). The R_5 encompasses all airways and reflects the overall assessment of airway tree resistance. The R_{19} specifically assesses the resistance of the proximal airways, i.e., the larger central airways, such as the trachea and bronchi. The $R_5 - R_{19}$ is a calculated value that indicates the presence of inhomogeneities across the respiratory system. In other words, the $R_5 - R_{19}$ helps identify variations in resistance between the larger central airways and the smaller peripheral airways. Any significant difference between R_5 and R_{19} suggests potential dysfunction or irregularities in the small airways. Other common measurements in the oscillometry reactance curve, which provides insights into the elastic properties of the respiratory system, include the X_5 , a measure of lung stiffness that reflects the lungs' resistance to expansion during breathing. As X_5 decreases (becomes more negative) it

indicates less compliance and more elastic recoil or stiffness at the peripheral airways, indicating potential abnormalities in the lung parenchyma, e.g., interstitial fibrosis or small airway obstruction. The area under the reactance curve (AX) is limited to the portion of the reactance curve that lies below the x-axis ($y < 0$). The AX captures the overall reactance of the respiratory system within a specific frequency range, typically between 5Hz and the resonant frequency (F_{res}). It encompasses the entire area under the reactance curve, representing the capacitance elastic properties of the lung. Finally, the F_{res} is another important parameter obtained from the reactance curve. It indicates the balance between the elastic and inertial forces in the respiratory system. Specifically, it represents the frequency at which the reactance equals zero, indicating the transition point from predominant elastic properties to predominant inertial properties. In pulmonary conditions characterized by either obstructive or restrictive patterns, the value of F_{res} is elevated beyond the normal range. This phenomenon can be attributed to the increased negativity of reactance at low frequencies that occurs in both types of diseases (216).

1.4.2.2 Current technologies

Two technologies are currently available for measuring respiratory impedance, both capable of signaling energy at multiple frequencies but applying different methods of forcing pressure. An impulse oscillometry system (IOS) uses short pulses of pressure generated by a loudspeaker to deliver vibrations to the air column at a fixed frequency (217). The forced oscillation technique (FOT) uses a continuous oscillatory signal generated by a loudspeaker to force sine wave properties upon the respiratory system during tidal breathing. Some devices can deliver both impulse and sine waves. While both techniques measure impedance, they are not entirely interchangeable. For example, the reactance measured by

IOS and FOT may not be directly comparable (218). Therefore, interpreting and comparing measurements across the two techniques should be done cautiously. Major commercial oscillation clinical testing devices for oscillometry measurements include TremoFlo, iOS, Pulmonscan, MostGraph, Resmon Pro, and Quark i2m.

1.4.2.3 Interpreting results

In healthy lungs, respiratory impedance is influenced by various factors, including the subject's demographics. Age affects impedance as lung function naturally declines with increasing age (94). The age dependence of ventilation heterogeneity in normal lungs has not been conclusively defined, although some studies have found that age affects certain respiratory impedance indices in the study population (219). Gender differences also play a role, as men typically have larger lung volumes and airways than women, which can affect impedance measurements (220). Additionally, factors such as body size and composition, including height, weight, and body mass index, can alter respiratory function by affecting lung size and thoracic dimensions (221); some studies suggest using height and BMI as independent variables, rather than the conventional approach of height and weight (222). Ethnicity may also contribute to variations in impedance measurements due to genetic and anatomical differences across ethnic backgrounds (222-225). Furthermore, smoking history can significantly affect impedance, as smoking can compromise lung health and alter impedance measurements. Smoking affects the elastic properties of the lungs, as evidenced by lower baseline values and greater decreases in post-methacholine challenge reactance values in smokers compared to nonsmokers (226). These subject demographic factors should be considered as part of the comprehensive assessment of respiratory impedance to better understand lung function and identify potential abnormalities. When selecting

reference values for respiratory impedance measurements, several important factors should be considered to ensure their appropriateness for the study population. Firstly, the technique used for impedance measurements, such as FOT or IOS, needs to be carefully evaluated, as the reference values for these techniques are not necessarily interchangeable. Secondly, reference values that are specifically tailored to the age group being studied are necessary given the developmental changes and variations in respiratory impedance that occur across different age ranges. Moreover, researchers should consider the frequency ranges at which impedance is reported and ensure that they align with the selected measurement technique and objectives of the study. Lastly, adherence to the standard procedures recommended for the selected technique is essential, such as applying pressure at the mouth and following the guidelines provided by the European Respiratory Society (ERS), which suggest holding the subject's cheeks during measurements. By considering these factors, researchers can make informed choices and select reference values that align with their study population and requirements. Dekel et al. conducted a review in which they assessed 34 studies that calculated reference equations, providing valuable insights into the existing literature on this topic (227).

1.4.2.4 Potential and limitations

Oscillometry has both advantages and limitations; it is a non-invasive, user-friendly technology that utilizes passive maneuvers that do not require patient cooperation, making it feasible for use with children, the elderly, and individuals experiencing exacerbations or with disabilities (215, 224, 225, 228, 229). This is because oscillometry uses an external signal, such as small-amplitude oscillations, to ensure linearity and employs the return flow measurements to investigate the mechanical properties of the lung. In contrast, spirometry

relies on specific breathing maneuvers to generate the return measurements of lung functions. While there is limited data on aerosol generation, oscillometry measurements during quiet tidal breathing may reduce the risk of exposure to pathogens and induced cough compared to forced expiratory maneuvers (230). Because of these advantages, oscillation techniques have become preferable over spirometry in recent years, and we can expect FOT to be more widely used in different clinical scenarios. However, there are variations in the estimated predicted values of healthy controls within the literature (227), in addition to the limitations in differentiating between pathologies as several conditions may produce similar patterns of measured impedance (231).

1.4.3 Clinical implications

Oscillometry is a valuable tool in clinical practice for various purposes related to identifying abnormalities, disease progression and severity, disease control, response to treatment, and quality of life (232, 233).

Firstly, oscillometry is demonstrably useful in differentiating healthy individuals from other disease including those with asthma, COPD, and interstitial lung disease (ILD) (234).

Moreover, during bronchoprovocation testing, an increase in R5, Fres, and AX, along with a decrease in X5, has been observed, indicating the sensitivity of IOS to detect bronchial hyperreactivity. X5 was proposed as a more sensitive indicator of hyperreactivity than FEV1 (235). Notably, these changes are sensitive even at lower doses of methacholine (236). In addition, the IOS parameters show a strong correlation with traditional pulmonary function parameters (237), including a particularly robust association with reactance parameters (232). Interestingly, IOS has shown sensitivity in identifying abnormalities in subjects with

symptoms of COPD but normal spirometry (238) and in smokers with normal spirometry (239), which highlights its potential superiority for detecting subtle changes and, therefore, early detection of pulmonary function abnormalities (240).

Furthermore, oscillometry provides insights into disease progression and severity. For example, parameters such as R5, Fres, and X5 are significantly associated with COPD severity (241). Furthermore, in patients with moderate to severe persistent asthma, R5-R20 and AX were closely correlated with asthma control, as determined by the Asthma Control Questionnaire (ACQ) (242). In terms of disease control, studies suggest that changes in X5 over time may serve as a prognostic indicator for respiratory diseases (243). Increased R5 values are commonly observed during exacerbations (237). Moreover, impedance values over time can distinguish frequent exacerbators from less frequent exacerbators in asthma patients (244), and baseline IOS parameters such as R5, R5-R20, and AX could predict a loss of disease control in asthma patients (245). In terms of treatment response, IOS offers sensitive parameters to detect the bronchodilation response (246, 247).

Oscillometry has proven valuable in clinical practice and has been used to identify abnormalities, assess disease progression and severity, evaluate disease control, monitor treatment response, and assess quality of life, especially in cases of asthma and COPD. Nevertheless, the utilization of this technology in acute clinical settings and across various exacerbations of breathlessness diseases is yet to be explored.

1.5 Thesis

1.5.1 Introduction summary

Overall, acute cardiorespiratory conditions, including AECOPD, acute asthma, acute HF, and pneumonia, are associated with significant morbidity and mortality worldwide. Therefore, these conditions are associated with a significant healthcare burden, including hospitalizations, frequent exacerbations, emergency department visits, the need for ongoing management and treatment, medication expenses, and reduced quality of life for patients. This highlights the importance of effective management to reduce the burden of these conditions on both individuals and healthcare systems. The effective management of these conditions entails a comprehensive approach that starts with the early identification of the acute underlying medical conditions to optimize treatment strategies and provide timely interventions to manage acute exacerbations.

While the current biomarkers are useful for diagnosing and managing these conditions, some limitations are associated with their use in clinical practice. The first limitation is that biomarkers are not always specific to a single condition. For example, elevated levels of CRP and procalcitonin occur in both AECOPD and pneumonia, making it challenging to differentiate between these two conditions solely according to biomarker levels.

Additionally, biomarkers' sensitivity and specificity can vary depending on the severity and stage of a disease, as well as individual patient factors, such as comorbidities and medication use. Some biomarkers have limited availability or are expensive, which limits their routine use in clinical practice. Another limitation is that the current biomarkers may not always capture the full complexity of the underlying disease processes. For example, while biomarkers such as IL-6 and IL-8 can provide insights into the inflammatory response

in AECOPD, they may not fully capture the heterogeneity of the disease or the effects of other factors, such as viral infections or air pollution exposure.

The limitations of the current biomarkers reinforce the need to explore further biomarkers that can differentiate among these acute conditions and provide insights into targeted treatment strategies. Understanding pathogenesis pathways is essential to developing new biomarkers by detecting key points in the pathway that can be identified as disease signatures and targeted with drugs or other interventions. Acute cardiorespiratory conditions share several pathogenesis including metabolism dysfunctions, immune dysfunction, and changes in physiological mechanisms that result in ventilation heterogeneity. Therefore, metabolomics and pulmonary function testing studies can contribute substantially to the current knowledge in the field.

In the context of metabolomics, we identified two knowledge gaps throughout the introduction. First, there has been limited work undertaken on the metabolomic plasma biomarkers that differentiate AHF from AECOPD. Those that exist used relatively small sample sizes and have not been validated in independent cohorts. In addition, considerable heterogeneity exists in the studied patient populations, and the study designs and analytical methods vary, making it difficult to compare results across different studies. Therefore, while there is some promising preliminary evidence for metabolomic plasma biomarkers that can differentiate acute HF from AECOPD, more research using more diverse cohorts and rigorous validation is needed to fully understand their clinical utility. Second, because of the growing recognition of the inflammation component in cardiorespiratory conditions, SPM studies in the context of respiratory diseases have gained more interest. In recent

years, studies have described the activation process of inflammation resolution by SPMs after acute inflammation. Despite the promising established work that holds significant potential in terms of new treatment development, little to no work has been performed to define an extended SPM panel for sputum samples taken during acute events of cardiorespiratory conditions.

In the context of pulmonary function testing, FOT has been proposed as an alternative non-invasive modality to assess lung function and has become increasingly attractive due to its ease of use. FOT involves effort-independent, simple tidal breathing maneuvers that require minimal patient cooperation. The balance of advantages between oscillation technique and spirometry has shifted in recent years, and we can expect FOT to be more widely used for patients in both acute and stable states. However, its utility in acute cases of a variety of cardiorespiratory diseases has not yet been elucidated.

1.5.2 Hypotheses and aims

This thesis primarily aims to investigate further biomarkers (metabolomics and physiological) in patients with acute cardiorespiratory diseases.

We hypothesize that:

1. The application of plasma metabolomic profiling in clinical settings is sensitive and specific in distinguishing acute exacerbations of COPD from acute HF and healthy individuals. Our case-control study design will provide an overview of metabolomics signatures and their biomarker scores for differentiating AECOPD and HF.

2. Handheld FOT measurements (I) can be feasibly obtained from patients experiencing acute exacerbations of chronic diseases (asthma, COPD, heart failure), as well as those with new-onset respiratory illness (pneumonia), and (II) are capable of distinguishing and characterizing cardiorespiratory exacerbation events from healthy control individuals. (III) changes in lung mechanics affect the composition of the VOCs recovered in the breath. Two case-control projects utilizing EMBER data will investigate underlying VH using FOT; then, will explore the association between VOC biomarkers collected from alveoli-enrich breath in patients with acute cardiorespiratory diseases and the FOT measurements of lung impedance.
3. SPMs will demonstrate distinct compositions and patterns in acute exacerbations of chronic or new-onset respiratory disease, potentially serving as clinical biomarkers for diagnosis and prognosis. We predict that the SPM profiles of sputum samples from patients with chronic respiratory diseases, such as asthma or COPD, will show unfavorable changes after acute exacerbations compared to control samples. Additionally, we anticipate that the SPM profiles of these patients, who experience chronic inflammation, will not return to homeostasis post-recovery, suggesting dysfunctional SPM regulation. Furthermore, we anticipate that the SPM profiles of patients with new-onset respiratory illnesses, such as pneumonia, will differ from the healthy control samples.

Chapter 2 Methods

2.1 Overview

In this section, I provide an overview of the research method conducted in this thesis, which involved the utilization of different data sources and collaboration with various departments and teams to achieve the aim of exploring additional biomarkers, including metabolomics and physiological measures, in patients with acute cardiorespiratory diseases.

2.2 Integration of data and leveraging resources through the EMBER project

The East Midlands Breathomics Pathology Node, referred to as the EMBER project, played a pivotal role in shaping this thesis, in which I am immensely proud to acknowledge its invaluable contribution. This was an ESPRC/MRC-funded molecular pathology node that initially ran from 2015 to 2019, with analysis extended until 2024. The EMBER team's comprehensive study protocol encompassed a wide range of critical components, including clinical assessments, sputum collection, lung function measurements, blood sampling, and clinical observations. Their meticulous planning and the clinical team's dedication were instrumental in collecting high-quality data (including secondary data for further analysis) and samples (including samples feeding EMBER biobank to support future studies) which laid the foundation for this thesis. In our research, we employed a combination of both secondary data analysis and primary data generation to comprehensively investigate our study objectives.

The secondary data analysis utilized the EMBER study's oscillometry measurement data in addition to the published VOC data as valuable resources to explore lung mechanisms and their associations with volatile organic compounds. Additionally, we undertook primary data generation through two projects, including a collaborative effort between the respiratory science and cardiovascular departments. The collaborative project focused on plasma metabolomic profiling, for which blood samples from the EMBER biobank were utilized. Moreover, to expand our investigation, I obtained sputum samples from the EMBER biobank and independently conducted the subsequent experimental process, ensuring meticulous control over the experiment and data quality.

Throughout my analysis of the EMBER data and samples, I maintained close communication with the EMBER team to ensure my understanding and adherence to the applied protocols. This collaborative effort facilitated a uniquely comprehensive exploration of the underlying factors and biomarkers associated with acute cardiorespiratory conditions. I extend my heartfelt gratitude to each member of the EMBER team for their exceptional work and willingness to collaborate, which significantly enhanced the scientific rigor and depth of this research. This collaborative endeavor underscores the importance of pooling resources and expertise, specifically during the difficult time of the COVID-19 pandemic, to maintain research advances and attaining meaningful insights that improve our comprehension of acute cardiorespiratory conditions.

2.3 Participants

Study participants were recruited within the EMBER project to investigate acute cardiorespiratory conditions that resulted in acute hospital admission. The primary clinical diagnoses included acute asthma, exacerbation of COPD, acute heart failure, and pneumonia. A control group of healthy individuals with no prior history of asthma, COPD, or heart failure and who had not been admitted to the hospital with community-acquired pneumonia within 6 weeks of the baseline study visit was also recruited. The case definitions for the included conditions are: Acute heart failure is characterized by a clinical diagnosis and a prototypical response to treatment. Community-acquired pneumonia is defined by the presence of new radiological consolidation that shows responsiveness to treatment per the British Thoracic Society (BTS) Guidelines. The exacerbation of asthma and COPD was defined by clinical diagnosis corroborated by objective evidence based on historical or prospective measurement and requiring an acute change in treatment, such as antibiotics, oral corticosteroids, or intensified bronchodilator therapy.

This thesis represents a comprehensive and interconnected exploration of acute cardiorespiratory conditions. The study cohorts were examined based on one total population derived from EMBER recruits. The total sample size is $n = 436$, consisting of 81 healthy individuals, 94 individuals with asthma (87 with acute exacerbation and 7 in a stable state), 118 individuals with COPD (109 with acute exacerbation and 9 in a stable state), 72 individuals with AHF, and 71 individuals with pneumonia. These participants formed the core group for defining sub-cohorts in our studies, fostering a cohesive and integrated research framework.

In this thesis, I conducted analyses on four sub-cohorts:

- 1) Plasma metabolomic analysis was conducted in a sub-cohort of 54 individuals, including 14 healthy individuals, 20 individuals with AECOPD, and 20 individuals with AHF (Chapter 3).
- 2) A sub-cohort of 310 participants was selected to elucidate lung mechanics using FOT and consisted of 47 healthy individuals, 80 individuals with acute asthma, 75 individuals with AECOPD, 46 individuals with AHF, and 62 individuals with pneumonia (Chapter 4).
- 3) A sub-cohort of 208 individuals, including 35 healthy individuals, 52 individuals with acute asthma, 48 individuals with AECOPD, 37 individuals with AHF, and 36 individuals with pneumonia was selected to explore the correlation between lung mechanics and VOCs (Chapter 5).
- 4) Finally, SPM analysis of sputum samples was performed on a sub-cohort of 141 individuals, including 22 healthy individuals, 37 individuals with acute asthma, 45 individuals with AECOPD, and 37 individuals with pneumonia (Figure 2-1).

This multi-faceted study design demonstrated a comprehensive and integrated examination of acute cardiorespiratory conditions within a single large-scale study.

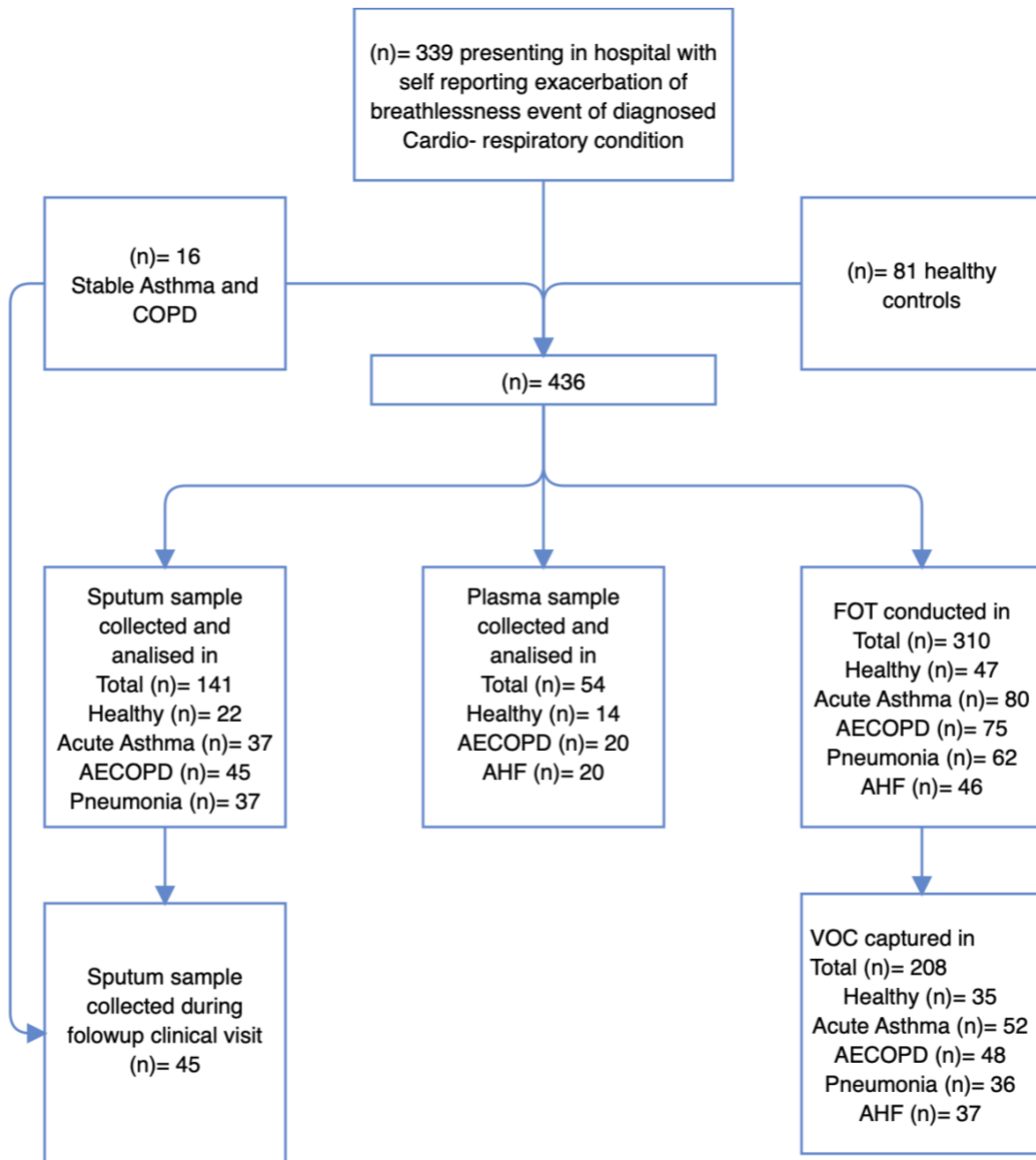


Figure 2-1 Total study population and sub-cohorts

2.4 Lab analysis platforms and equipment

In this section, the various machinery, tools, and resources utilized in the study for comprehensive metabolite biomarker assessment and pathophysiology assessment are described. These components enabled accurate, efficient data acquisition and analysis.

2.4.1 Mass spectrometry platforms

In line with the established guidelines and best practices, both targeted and non-targeted metabolomic analyses were applied utilizing the MS platform. I employed gas chromatography–gas chromatography mass spectrometry (GC–GC MS) data for breath analysis (Chapter 5) and liquid chromatography (LC–MS, including TQ–MS and Q–TOF) for plasma metabolite analysis (Chapter 3) and sputum analysis (Chapter 6). This involved meticulous instrument setup, sample preparation, chromatographic condition control, mass spectrometry parameter definition, data acquisition and analysis, quality control measures, and instrument maintenance to ensure the reliability and integrity of the resulting MS data.

2.4.1.1 MS instruments

In three independent laboratories, GC–GC MS and LC–MS analyses were conducted to facilitate the separation and identification of compounds for targeted analysis (sputum) and profiling for non-targeted analysis (plasma and breath).

In chromatography (gas or liquid), the sample is introduced into a column where the compounds separate by their affinity for the stationary phase of the column. In gas chromatography, the sample is vaporized and injected into the column as a gas. The inlet,

where the sample is introduced, is maintained at a higher temperature than the ambient temperature to ensure that the compounds are in the gas phase when they are introduced. The compounds then travel through the column, which is also heated, and separate based on their interactions with the stationary phase inside the column (Figure 2-2). In liquid chromatography, the sample is dissolved or suspended in a liquid solvent and injected into the column. The compounds in the sample then interact with the stationary phase in the column and separate as they move through the column according to their affinity for the stationary phase.

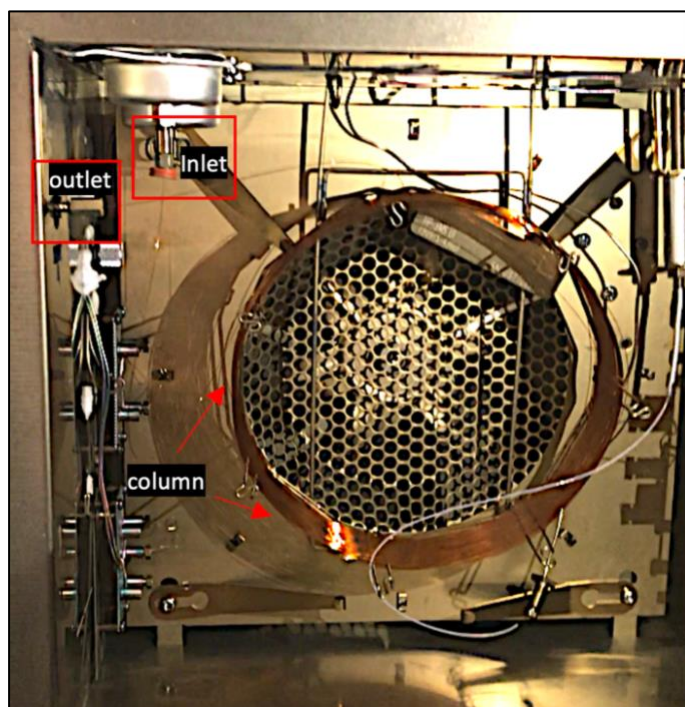


Figure 2-2 Gas chromatography oven at the chemistry laboratories of the University of Leicester

The untargeted analysis of breath samples was conducted in the chemistry laboratories of the University of Leicester, led by Dr. Wilde and Dr. Cordell. The analysis involved the utilization of thermal desorption (TD) in conjunction with comprehensive two-dimensional

gas chromatography (GCxGC) employing dual flame ionization detection (FID) and MS to detect and characterize the compounds in the samples. This approach enables the untargeted analysis and comprehensive profiling of breath samples. The two-dimensional separation that GCxGC provides enhances peak capacity and resolution, allowing for the identification of complex mixtures of volatile compounds in the breath. The dual FID and MS techniques provide complementary information, with FID offering quantification capabilities and MS providing structural information through mass fragmentation patterns for the in-depth exploration of the breath metabolome (Figure 2-3).

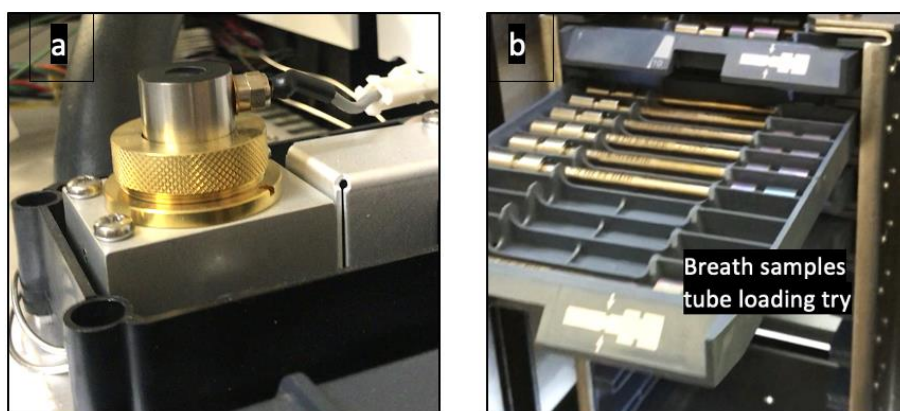


Figure 2-3 Components of the comprehensive GCxGC MS system

(a) The dual flame ionization detection unit; (b) UNITY universal thermal desorption unit for sorbent tubes at the chemistry laboratories of the University of Leicester

Meanwhile, the Q-TOF MS plasma analyses were performed in the Cardiovascular Biomedical Research Unit (LCBRU) at Glenfield Hospital in collaboration with the respiratory department under the expertise of Dr. Zubair Israr. In Q-TOF MS instruments, the electrospray ionization (ESI) method is employed to generate ions from the analytes in the sample. These ions are then introduced into the mass analyzer, which consists of quadrupole and time-of-flight components. The quadrupole selectively filters the ions based

on their mass-to-charge ratio (m/z), allowing only ions within a specific mass range to pass through. The filtered ions are then accelerated into the time-of-flight analyzer, where their flight times are precisely measured to determine their m/z values. This high resolution and accurate mass measurement capability of Q-TOF MS makes it well-suited for non-targeted analysis and the comprehensive profiling of plasma samples.

Sputum lipid mediator data were generated using TQ-MS combined with a chromatography system. The analysis was conducted in collaboration with Dr. Donald JL Jones's laboratory at the MultiOmics Facility in the Hodgkin Building. I also received valuable training from Dr. Rajinder Singh, who assisted with equipment calibration, performance checks, and solvent preparation. My active involvement in the experimental process involved all sample preparation pre-MS injection; loading, initiating, and monitoring the sampling process; retrieving and reviewing peak areas and results; and generating the data matrix. The combination of TQ-MS with a liquid chromatography system is suitable for targeted sputum analysis due to its specific and selective detection capabilities. This setup utilizes a high-performance liquid chromatography technique to separate the compounds in the sputum sample based on their chemical properties. The separated compounds are then introduced into the triple quadrupole mass spectrometer, which consists of three quadrupole mass analyzers (Figure 2-4). The first quadrupole acts as a filter and selectively allows specific precursor ions to pass through based on their mass-to-charge ratio (m/z). These selected precursor ions undergo collision-induced dissociation (CID) in the second quadrupole, which generates product ions. Finally, the third quadrupole detects and quantifies the specific product ions of interest, providing high sensitivity and specificity for the targeted analysis.

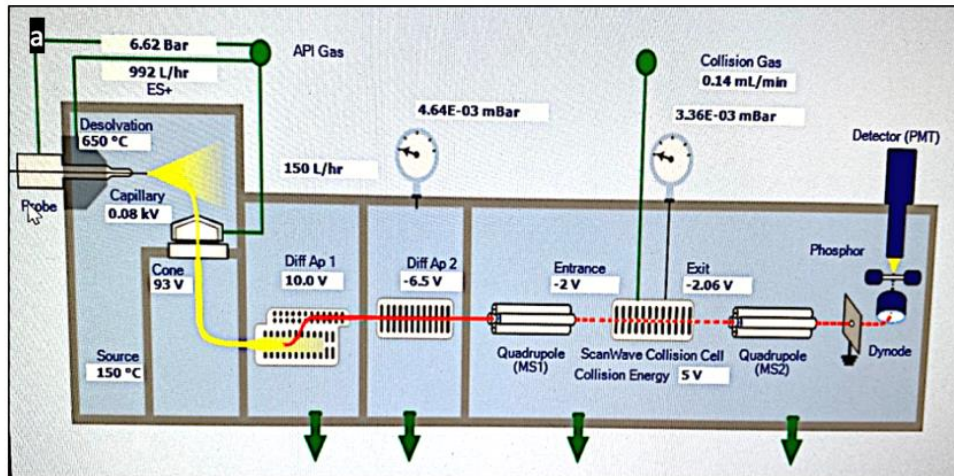


Figure 2-4 Components of the LC–electrospray ionization tandem MS system

(a) Xevo TQ-XS triple quadrupole mass spectrometry components (screenshot of the infographic provided by the equipment software); (b) Sample manager unit with solutions A, B, and C, containing the solvents and reagents used in the analysis process; (c) Liquid chromatography system (ACQUITY UPLC I-Class PLUS System) in the laboratory at the MultiOmic facility in the Hodgkin Building

2.4.1.2 MS output parameters

To analyze the sputum, plasma, and breath samples, several parameters were examined to characterize the compounds of interest, providing valuable insights into their properties and behavior during both the targeted and untargeted analyses.

For targeted analysis, the neutral mass and mass-to-charge ratio (m/z) are crucial factors for identifying and characterizing specific compounds. Comparing these parameters with known standards allows the presence of the targeted analytes in the samples to be determined.

The retention time is also pivotal in the targeted analysis, providing a reference for identifying and quantifying the compounds of interest. Furthermore, the chromatographic peak width was assessed to ensure the proper separation and resolution of the targeted analytes and enhance the accuracy of the analysis (Figure 2-5).

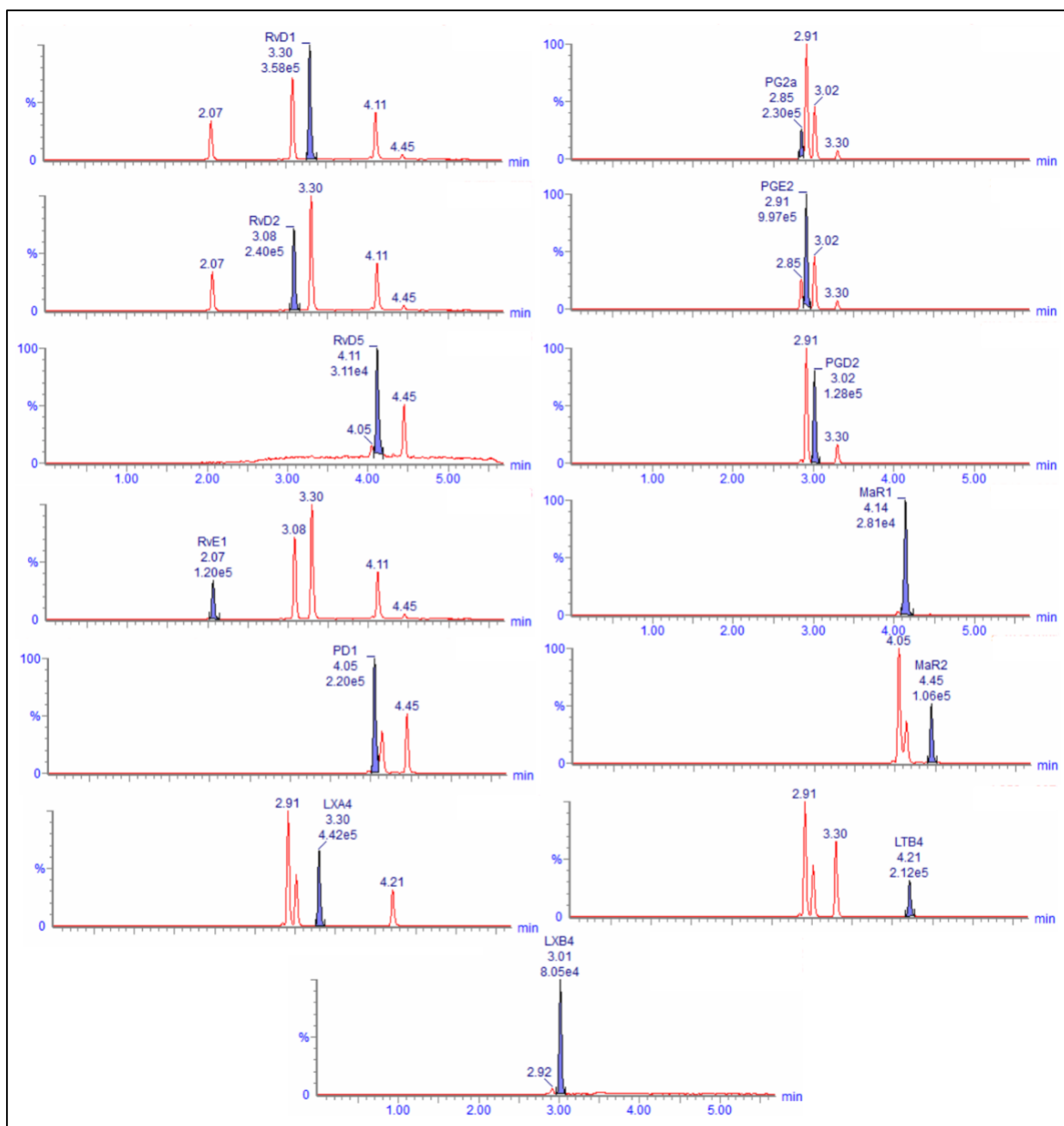


Figure 2-5 Chromatograms of the examined targeted SPMs within the lipidomic standards mix

Chromatograms showing retention time and chromatographic peak area, height, and width, Waters MassLynx Software

For the untargeted analysis, the neutral mass and mass-to-charge ratio (m/z) were employed to discover and profile a wide range of compounds present in the samples utilizing online metabolomic database. By examining these parameters across the entire mass range, we identified known, unknown, and unexpected compounds and gained a comprehensive understanding of the sample composition.

Regardless of the analysis approach, the minimum coefficient of variation between injections (%) served as a valuable parameter for assessing the precision and reproducibility of the analysis. This parameter affirmed the reliability of the measurements, ensuring consistent and accurate results.

2.4.1.3 Automated extraction and drying for sample preparation prior to MS

To overcome the challenges associated with handling sputum samples containing specialized pro-resolving lipid mediators (SPMs), which are highly sensitive and prone to oxidation, specialized equipment was employed in this study. Specifically, an automated evaporator and extraction systems were used. Other common laboratory machinery used included a centrifuge, microcentrifuge (Figure 2-8), scales, and analytical instruments (Figure 2-9).

The automated nitrogen evaporator system employed in this work, which allowed the efficient evaporation of low-volume samples, featured several key components. The system includes a sample holder tray for secure sample placement during evaporation that accommodates various tube sizes. A nitrogen cylinder enables the controlled evaporation of solvents. The system also incorporates flow distribution lines that regulate the distribution

and movement of the nitrogen gas, ensuring uniform evaporation across the sample holder tray. The temperature was controlled by filling the water tank, which has temperature control capabilities, to precisely adjust the evaporation temperature, ensuring optimal drying conditions.

The system's intuitive interface facilitated the programming of the drying parameters, including temperature, airflow, and duration. These parameters were set and saved as method settings for each phase of the sample drying process in the software. This feature ensured reproducibility and consistency in subsequent runs. In addition, a ventilation hose was connected to a fume hood to effectively remove the fumes and vapors generated during the evaporation process, maintaining a safe working environment (Figure 2-6).



Figure 2-6 The automated nitrogen evaporator system, TurboVap® LV system

(a) Water tank capacity in the TurboVap® LV system; (b) Overhead view of the automated solvent evaporation system showing the interface screen, the sample tray holder, and flow distribution pipelines; (c) Utilizing the proper ventilation system by connecting the system to a fume hood system at the biology laboratory in the Maurice Shock Building of the University of Leicester

For extraction, an automated system was also utilized. This system consisted of a pressure controller, a sample cartridge holder, a waste container, a collecting tubes holder, and a control unit. The pressure controller precisely controlled the extraction pressure applied to the cartridges, ensuring consistent extraction conditions for each sample. The sample cartridge holder accommodated solid-phase extraction cartridges. The waste container served as a designated receptacle for the discarded solvents and waste materials generated during the extraction process. In addition, a collection tube holder provided a convenient

secure location for the collection tubes used to hold the extracted analytes. Furthermore, the control unit facilitated the easy programming of extraction protocols as pressure parameters were meticulously fine-tuned for each agent and extraction face (Figure 2-7).

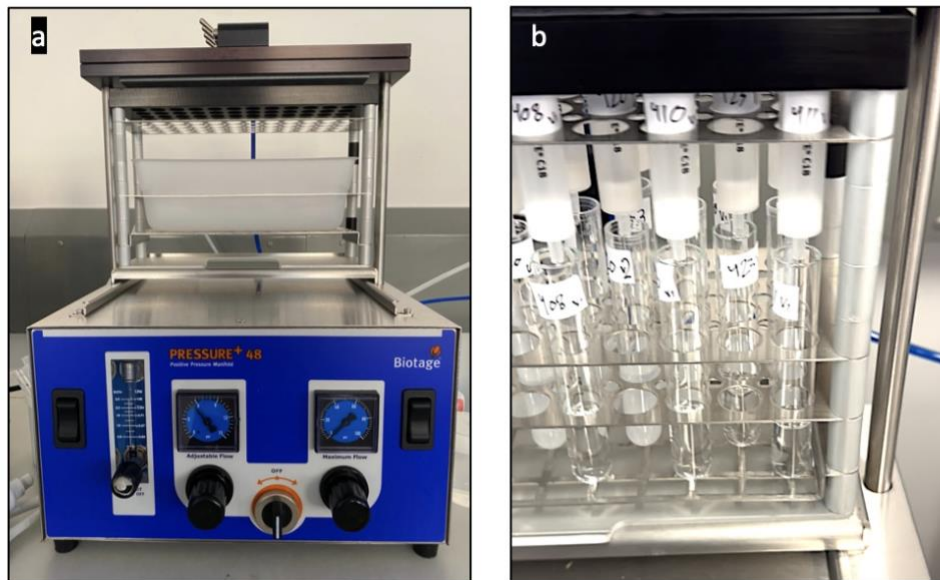


Figure 2-7 Automated extraction system, Biotage® PRESSURE+

(a) Front view of the system and its control unit; (b) Loaded cartridge holder and collection tube holder at the biology laboratory in the Maurice Shock Building of the University of Leicester

To maximize the SPM recovery rates from the samples, a rigorous optimization process was undertaken. By systematically adjusting and evaluating various extraction conditions, including flow rate, temperature, time, and pressure, we sought to attain the highest possible SPM recovery rates. The integration of these components and advanced systems in our study enabled efficient and reliable sample preparation by minimizing human error and ensuring the consistent processing of the sputum samples.



Figure 2-8 Laboratory centrifuges

(a) The Sanyo MSE Micro Centaur microcentrifuge, a compact and versatile instrument utilized for rapid and efficient centrifugation of small-volume samples; (b) The Beckman Allegra X-22R centrifuge utilized for the separation of samples, which accommodates various tube sizes and has a large capacity, in the biology laboratory in the Maurice Shock Building at the University of Leicester.

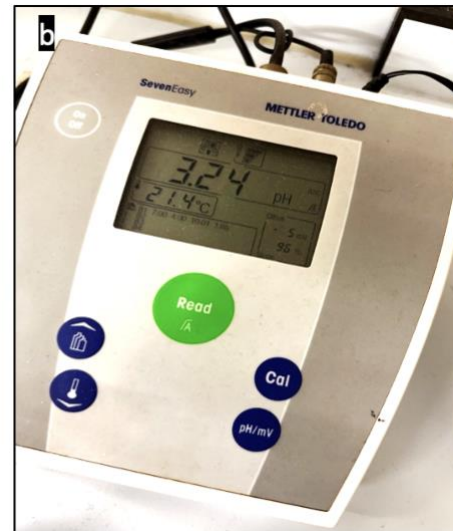


Figure 2-9 Laboratory PH meter

(a) The precision pin high-quality sensor of the Mettler Toledo pH Seven Easy system for pH measurement; (b) The interface unit of the Mettler Toledo pH Seven Easy system, which displays measurements and allows navigation and control of the system

2.4.1.4 Levels of chemical identification

In this study, metabolite identification follows the four levels of chemical identification defined by the Metabolic Standards Initiatives (MSI) (248).

- Level 1 – Identified metabolites: For this level of identification, at least two orthogonal properties of the examined metabolites are compared with chemical reference standards of equivalent structures.
- Level 2 – Putatively annotated compounds: At this identification level, the physicochemical properties of the studied metabolites are searched in metabolomics libraries and databases. No additional experiments are conducted to match the annotated compounds to chemical reference standards.
- Level 3 – Putatively characterized compound classes: For this level of identification, the studied metabolites are compared to those of known classes of organic compounds that share the same physicochemical properties. As in level 2, matching to a chemical reference standard is not applied at this level.
- Level 4 – Unknown compounds: At this identification level, compounds are differentiated and quantified using spectral technologies.

Within our projects, chemical identification reporting was conducted at different levels for various sample types. For plasma samples, we achieved level 2 and 3 identifications. For the VOC analysis, researchers adhered to level 1 and 2 identifications guidelines as outlined in the publication. For the targeted analysis of sputum samples, we also implemented level 1 identification approach, allowing us to confidently identify and report on the specific targeted components in the samples.

2.4.2 Handheld FOT

The TremoFlo THORASYS device utilized for our FOT sub-cohort comprises several essential components designed to take accurate respiratory measurements. The device includes a handheld unit and the TremoFlo THORASYS software application. These were set to capture representations of respiratory mechanics over multiple breath cycles and average them in an adult population.

The FOT measurements were performed by the EMBER clinical team using the handheld unit, which features an ergonomic design with a built-in pressure transducer, mouthpiece slot, and a handle that ensures stability and provides a comfortable grip during the test.

The TremoFlo THORASYS software version (10.34.32) provided a real-time visualization of respiratory parameters, waveforms, and calculated the impedance parameters according to the adult population mode (WAVEFORM AOS 5-37 H2 analysis mode). It was the primary interface for interacting with the TremoFlo device, which employs return flows and pressures to automate mathematical formulas that calculate resistance and reactance for data processing, eliminating the need for manual calculations. The software offers customizable settings, allowing us to specify the displayed measurements of interest for our study (Table 1.1). The software's intuitive interface and powerful analysis tools allowed me to effectively explore and interpret the FOT measurements acquired by EMBER clinical team. The majority of my interactions with the TremoFlo system during this project involved utilizing the software on a computer workstation to visualize, revise, and interpret the raw

data. One notable feature of the software is the inclusion of reference values for adults, which aided in the interpretation of the FOT results. By default, the software incorporates the adult Oostveen et al. (2013) reference values, which apply to individuals aged 18–80 years, weighing 43–128 kg and with heights of 1.47–1.97 m. Additionally, the software provides the option to select Brown et. al (2010) as a secondary reference, with values that are suitable for individuals aged 18–92 years, without height or weight restrictions, and with no smoking history or a history of 0 packyears. As these default reference values did not accurately represent our study’s healthy population, custom reference values were generated that were specific to our participant cohort. However, for the purpose of comparison and visualization, the Oostveen references within the software were extracted.

Table 2-1 Software parameters reported for patients, which were used to generate the study data matrix

Parameter	Definition
R5 cmH2O.s/L R11 cmH2O.s/L R13 cmH2O.s/L R17 cmH2O.s/L R19 cmH2O.s/L R23 cmH2O.s/L R29 cmH2O.s/L R31 cmH2O.s/L R37 cmH2O.s/L	The measurement of resistance in the respiratory system, expressed in units of centimeters of water per second per liter. This provides information about the resistive component of the impedance encountered during oscillatory airflow in the respiratory system, particularly at the specified frequency.
X5 cmH2O.s/L X11 cmH2O.s/L X13 cmH2O.s/L X17 cmH2O.s/L X19 cmH2O.s/L X23 cmH2O.s/L X29 cmH2O.s/L X31 cmH2O.s/L X37 cmH2O.s/L	The measurement of reactance in the respiratory system, expressed in units of centimeters of water per second per liter. It provides information about the elastic properties component of the impedance encountered during oscillatory airflow at the specified frequency.
COH5 COH11 COH13 COH17 COH19 COH123	Coherence at the specified Hz, which measures the correlation between the pressure and flow signals at a specific frequency during respiratory measurements. Values range from 0 to 1, with higher values indicating stronger coherence or correlation between the pressure and flow signals, suggesting more reliable measurements.

COH129 COH31 COH37	
AX cmH ₂ O/L	A combination of the reactance (A) and the pressure–volume relationship (X) to describe respiratory characteristics at the resonant frequency. The resonant frequency is the frequency at which the reactance component of the impedance is at its minimum value or crosses the zero axis. It represents the frequency at which the respiratory system’s elastic and inertial properties are in balance.
VT L	Tidal volume measured in liters, a fundamental parameter that represents the volume of air inspired or expired during a normal breath.
R5-19 cmH ₂ O.s/L	The difference between the resistance values at frequencies of 5 Hz and 19 Hz, expressed in centimeters of water pressure per second per liter of airflow.
Reference	Predefined values established by Oostveen et al. (2013) that provide a normative range for a given subject’s demographic characteristics.
M1 M2 M3 M4	The value of the specific measured respiratory parameter obtained from the first, second, third, and fourth repeated measurements performed during the test session.
Test average	The average value of the specific measured respiratory parameter obtained from the multiple measurements performed during the test session.
SD	The measure of the variability from the multiple measurements performed during the test session. It provides information about how much individual values deviate from the average.
CV%	The coefficient of variation, a relative measure of the variation in a parameter, expressed as a percentage. It is calculated by dividing the standard deviation by the mean and multiplying by 100.
Z score	A statistical measure that indicates how many standard deviations a particular value is from the mean of a reference population.
Abs.diff	Absolute difference, which represents the absolute numerical difference between two values or measurements. It can be used to evaluate the magnitude of the difference between observed and expected values.
% Pred.	The percentage of a measured value compared to a predicted value based on the reference data.

2.5 Statistical methods

2.5.1 Software utilized for statistical analysis and visual representation

Software tools were employed for data analysis, statistical analysis, and the generation of analytical graphs. Prism 9, a widely recognized software package, was selected for its robust statistical capabilities and user-friendly interface. R Studio, a powerful programming environment, was employed to conduct various statistical analyses, which allowed the customized and in-depth exploration of the data. The combination of Prism 9 and R Studio provided a comprehensive framework for the rigorous statistical evaluation and

interpretation of our findings. Moreover, to enhance the visual presentation of the results, Biorender, a specialized software for scientific graphics, was utilized to create figures panels and aesthetically appealing and informative graphs. The integration of these software tools facilitated accurate data analysis, sophisticated statistical modeling, and the production of visually compelling figures, enhancing the overall scientific rigor and communicative impact of this research.

2.5.2 High-dimensional data

In this study, advanced statistical methods were essential for achieving the specific objective of differentiating studied conditions through non-targeted metabolomic analysis. While conventional techniques, such as principal component analysis (PCA), are commonly used for data reduction, in this study, topological data analysis (TDA) was specifically chosen as the primary approach to visualize high-dimensional metabolite data. TDA offers distinct advantages over PCA in the context of metabolomic analysis. Unlike PCA, which aims to capture the majority of the variance in the data by reducing it to its principal components, TDA retains the entire set of metabolites. This comprehensive approach enabled a more thorough exploration of the metabolomic landscape, facilitating a detailed assessment of the discriminatory potentials of all metabolites collectively. For the implementation of TDA, Matthew Richardson, an expert in advanced statistical methods, provided valuable expertise.

2.5.3 Regression models

Various regression models were employed in this study to analyze the relationships between dependent variables and one or more independent variables. The regression

models used included simple linear regression, multiple linear regression, logistic regression (self-performed), and elastic net regression (supported by Matthew Richardson).

Elastic net regression, a combination of the LASSO and ridge regression methods, was employed to extract a list of features from the compounds identified in the mass spectrometry output which demonstrated the best discrimination between the studied groups. This model was chosen due to the exceptionally large number of predictors, the compounds, compared to the sample size, as it addresses the issue of potentially inaccurate correlations that can occur in such cases. By utilizing cross-validation, elastic net regression identified consistently stable predictor subsets and estimated coefficients simultaneously, thus providing more reliable statistically significant features.

Linear regression was utilized to examine the relationship between forced oscillation technique (FOT) measures and the length of hospital stay. Through multiple linear regression models, we investigated how FOT influenced the recovered VOCs while considering disease status and smoking status as covariates.

In addition, logistic regression models were employed to analyze binary or categorical outcome variables. For example, in this study, the logistic regression analysis was used to determine whether FOT measurements influenced the probability of hospital readmission. Logistic regression was also used to assess the association of combined plasma biomarker scores and routine blood clinical biomarkers with the likelihood of disease diagnosis.

In addition, regression models were applied to generate reference normative values of FOT measures for subjects' demographic parameters. The model development process involved scanning the data for missing values and outliers, including both outcome variable data (FOT measures) and predictor variable data, such as age, weight, gender, BMI, and height. Next, we created a scatterplot of all of the data to visualize the relationship between targeted and predictor variables (Figure 2-10).

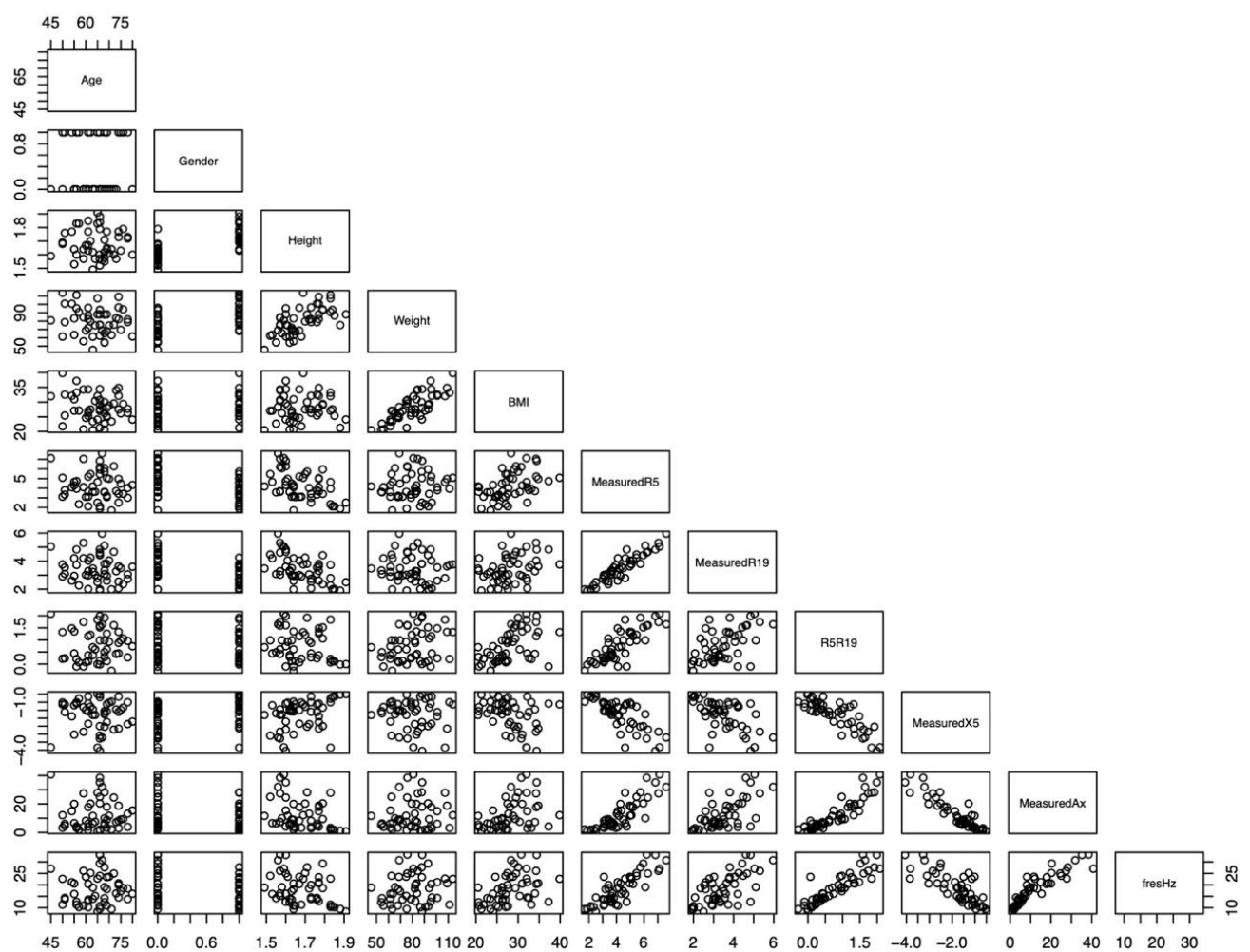


Figure 2-10 Scatterplot of FOT data to visualize the relationship between variables

This multi-panel scatterplot reveals several key observations regarding the relationships between various variables and the targeted variable (FOT data). Firstly, the relationship between age and the targeted variable appears nonlinear or random. Secondly, a low to moderate linear relationship between height and FOT data is evident. Thirdly, a moderate linear relationship between BMI and FOT data is indicated. Finally, weight shows a strong correlation with BMI, while height and BMI exhibit a weaker correlation. These findings were considered when developing the models from the study data.

The regression models were then built progressively, starting with simple linear regression and advancing to multiple linear regression. A forward selection method was used for the multiple linear regression, in which the variables explaining the most variability were sequentially added based on the adjusted R-squared of the preceding simple linear regression. The improvement in the adjusted R-squared values between models was evaluated with ANOVA tests to determine statistical significance. The models' assumptions were examined through diagnostic plots (Figure 2-11) and statistical tests (Table 2-2). These included testing the linearity, checking for the independence of errors using the Durbin–Watson test (which concludes that errors are uncorrelated if the p -value is >0.05), assessing the normal distribution of errors using the Shapiro–Wilk test (which states that errors are normally distributed if the p -value is >0.05), and evaluating the constant variance of errors. Multicollinearity between predictors was assessed with the variance inflation factor, in which a value less than 5 is considered indicative of the absence of multicollinearity. Figure 2-12 provides a summary of the model development process in generating the reference normative values.

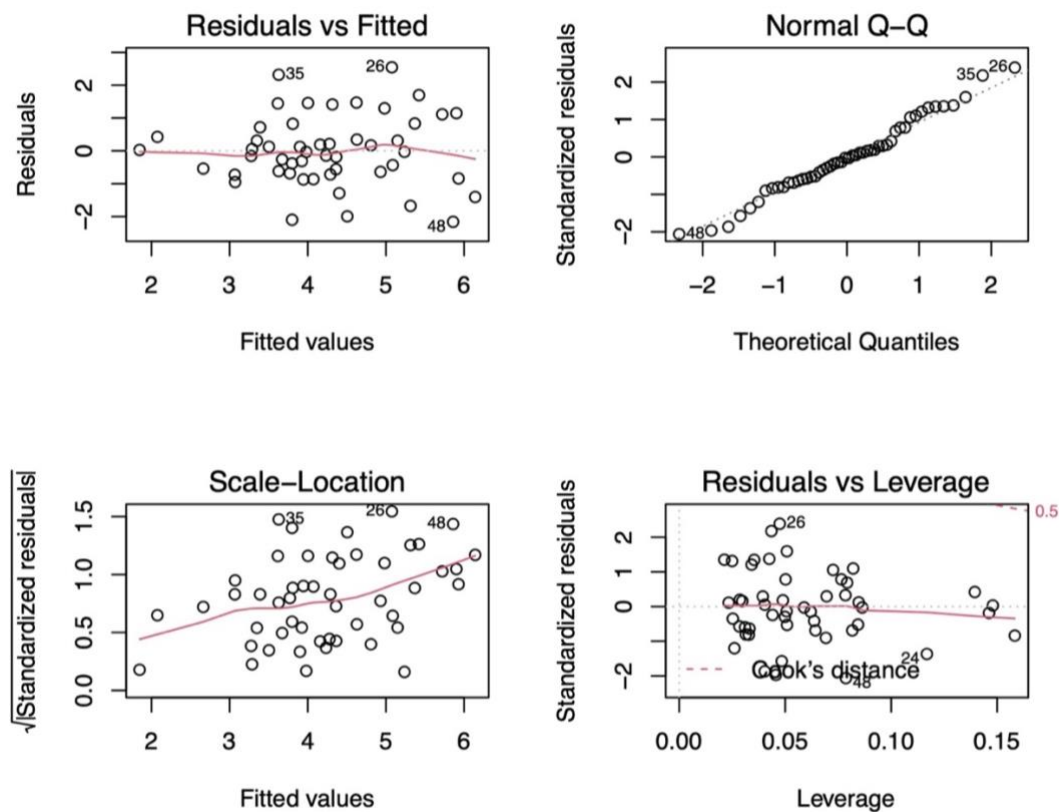


Figure 2-11 Diagnostic plots of reference values' models

Diagnostic plot of the model ($R5 \sim \text{Height} + \text{BMI}$). The red lines in the residuals vs. fitted residuals plot are approximately horizontal and linear at 0, which indicates that the linearity assumption holds well as the residuals are scattered evenly and randomly above and below the line at values between 3 and -3. No pattern or correlation was observed, indicating that errors are independent with equal variance. The Q-Q plot also affirms that residual errors are normally distributed.

Table 2-2 Statistical tests to examine the model ($R5 \sim \text{Height} + \text{BMI}$) according to the of multiple linear regression assumptions.

Using the Durbin–Watson test to detect the effects of autocorrelation			
Lag	Autocorrelation	D–W statistic	<i>p</i> -value
1	0.1317925	1.722528	0.294
As the <i>p</i> -value is >0.05 , Hence, we may accept the null hypothesis that the errors are uncorrelated.			
Checking multicollinearity between height and BMI considering the variance inflation factor			
Height	1.00059	The variance inflation factors for height and BMI are less than 5; therefore, there is no multicollinearity between predictors.	
BMI	1.00059		

Checking normality assumption of the model residuals using the Shapiro–Wilk test	
--	--

W	0.98106
<i>p</i> -value	0.5972

Normality holds as the <i>p</i> -value is >0.05.
--

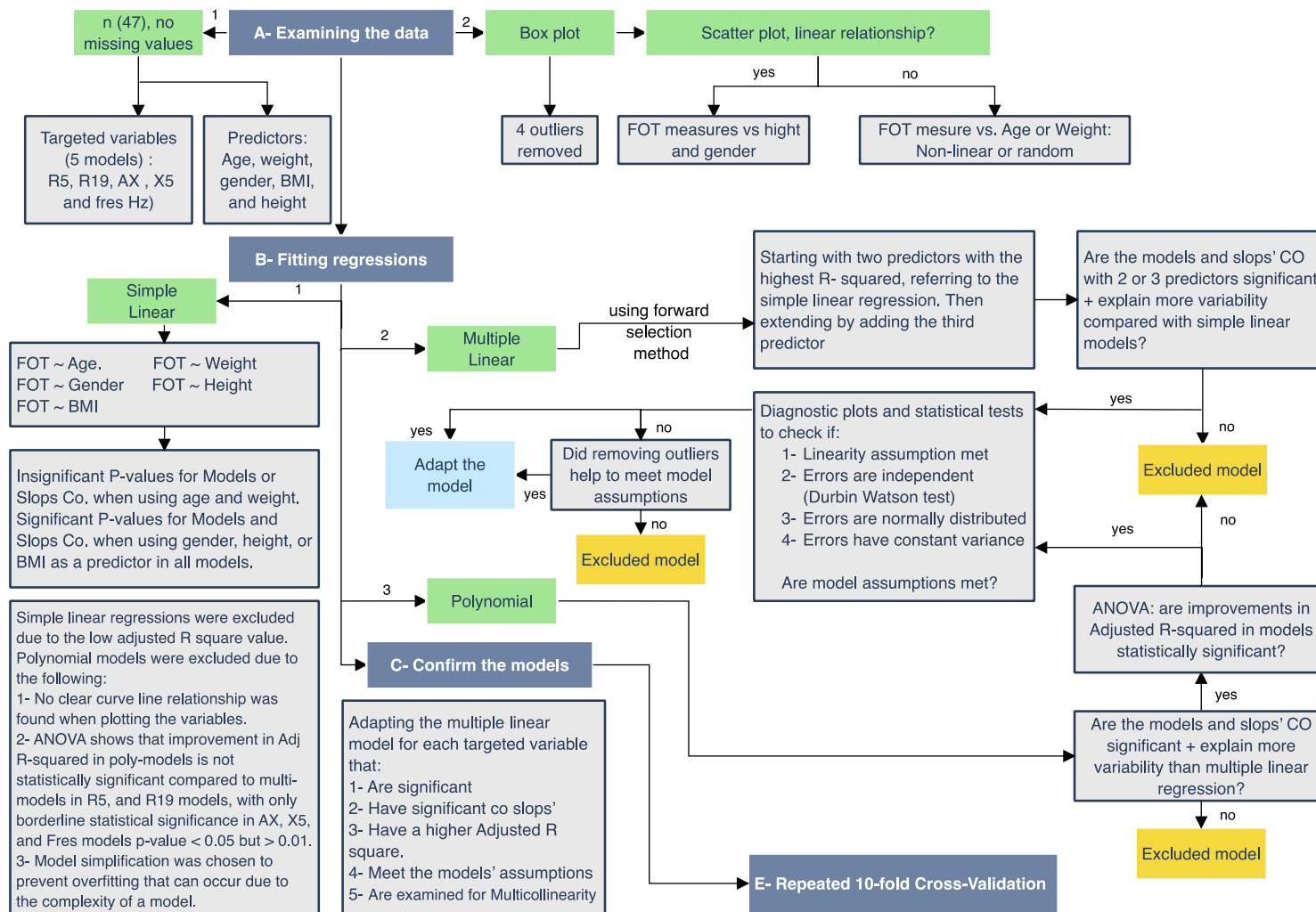


Figure 2-12 Summary of the model development process

2.5.4 ROC curve and its performance measures

For the statistical analysis utilized in this thesis, receiver operating characteristic (ROC) curves were employed to assess the performance of the diagnostic tests and evaluate the discriminatory power of different biomarkers among specific conditions.

The first set of ROC curves was generated with the Prism software's built-in ROC analysis tool. This analysis focused on evaluating the performance of AECOPD scores in differentiating between AECOPD and non-COPD cases. In the second set of ROC curves, logistic regression was utilized to explore the relationship between the plasma metabolite biomarker scores and routine laboratory tests. This analysis aimed to investigate the added value of the biomarker scores in predicting the outcome of interest. Multiple variables were considered predictors in the logistic regression model, allowing for a comprehensive assessment of their impact. The estimated probabilities from the model were used to generate ROC curves that provided a visual representation of the model's performance. The area under the ROC curve (AUC) values were calculated to quantify the overall discriminating power of different conditions.

The ROC curve plots sensitivity against 1-specificity at various score cutoff points. The AUC values were calculated to quantify the model's overall accuracy when discriminating between different conditions. The interpretation of the ROC curves involved selecting an optimal cutoff point that balanced sensitivity and specificity, which occurred in the upper-left corner of the plot.

2.5.5 Association and correlation coefficient

We employed Spearman's rank correlation coefficient, which is particularly suitable for nonparametric data distribution, to assess the relationship between the FOT and sputum data with established blood biomarkers and clinical observations, such as oxygen saturations (SpO₂), respiratory rate (RR), modified early warning system (MEWS), blood eosinophils, CRP, BNP, breathlessness, and wheeze visual analog scale (VAS) scores. This approach allowed us to examine both the magnitude and direction of the associations, providing insights into the variables' interdependencies.

2.5.6 Standard descriptive and statistical tests

Throughout this project, various standard statistical tests were applied to gain a comprehensive understanding of the data. Descriptive statistics, including the mean, standard deviation, median, and proportions (%), were utilized to summarize the clinical characteristic tables and the characteristics of the investigated variables.

To assess the differences between groups, a one-way ANOVA was employed for parametric data, while the Kruskal–Wallis test was used for nonparametric data. These tests allowed for the comparison of means and medians, respectively, across multiple groups, providing insights into potential differences between groups. The Wilcoxon rank-sum test, also known as the Mann–Whitney U test, was used to compare the medians of nonparametric data in two independent groups, acute and stable/recovery states within the disease group. For the post-hoc analysis, Tukey's multiple comparisons test was applied to perform multiple pairwise comparisons, allowing for the identification of specific within-group differences. Dunn's test was utilized as a nonparametric alternative for the post-hoc analysis.

A chi-squared test was utilized to examine proportions and categorical variables, enabling the assessment of associations and dependencies among the study variables. Additionally, various graphical tools, such as normal Q–Q plots, histograms, skewness, and kurtosis were employed to assess the data's distributional properties.

Chapter 3 Studies; Blood Plasma Metabolome Signatures Differentiate Acute Exacerbations of COPD and Decompensated Heart Failure in Hospitalized Patients

3.1 Abstract

Introduction: Prompt recognition and management are critical to improve outcomes and reduce mortality rates in patients who are hospitalized with exacerbations of cardiovascular and respiratory conditions, such as heart failure and COPD. However, the clinical presentation of these conditions, including symptoms and clinical signs, can be similar and may delay treatment or result in incorrect diagnoses. We conducted plasma metabolomic profiling in hospitalized patients who presented with either an acute exacerbation of COPD (AECOPD) or decompensated heart failure (AHF).

Methods: Plasma samples from individuals with AECOPD (n = 20) and AHF (n = 20), as well as healthy volunteers (n = 14), were examined. The samples were obtained from hospitalized patients within 24 hours of admission (Leicester, UK). Plasma metabolomic profiles were generated by performing a nontargeted metabolomic analysis using mass spectrometry (MS) technology. Topological data analysis (TDA) and elastic net regression were used to investigate the statistical data and propose the compounds that best distinguished the three groups.

Results: Mass spectral output differentiated and quantified 2,193 compounds. Metabolite biomarker scores were calculated for 19 significant metabolites and suggested a sensitivity and specificity of $\geq 70\%$ for biomarkers that differentiated COPD from non-COPD (HF and healthy) individuals. The scores that differentiated HF from non-HF (COPD and healthy) cases indicated a sensitivity and specificity of $\geq 88\%$.

Conclusion: Changes in shared metabolomic profiles can be identified and quantified by studying comers with acute exacerbations of COPD and HF and comparing the results to those of healthy volunteers. The data suggest acute exacerbation plasma metabolite signatures that are sensitive and specific to AECOPD and AHF.

3.2 Introduction

Acute cardiology and respiratory diseases are the leading causes of morbidity and mortality worldwide, including in the United Kingdom (UK); AHF and AECOPD are among the main causes of the acute decompensation of chronic disease. COPD affects around 1.2 million people in the UK, and exacerbations of COPD are the second-most frequent cause of emergency hospital admissions (249), representing about 12.5% of all emergency room admissions in the UK (250). Both AHF and AECOPD carry a significant risk of mortality. Data from the National Heart Failure Audit showed that the in-hospital mortality rate for HF was around 9% in 2021–2022 (251), while the National COPD Audit revealed a 90-day mortality rate of 12% for AECOPD (252).

The prompt recognition and management of these conditions are critical to improve outcomes and reduce mortality rates. Whilst COPD and HF are distinct conditions, they share various physiological pathways (57, 208, 253-256). During acute events, similarities also arise in both conditions due to the impact of inflammation, hypoxia, and changes in the autonomic nervous system (257-259). These shared pathways may contribute to the increased cardiovascular risk seen in patients with COPD, the respiratory symptoms seen in patients with HF, and the overlapping symptoms (176).

The current diagnostic approaches depend heavily on patients' clinical presentation, but this method lacks specificity as patients in both conditions may present with increasing dyspnea, chest discomfort with clinical signs of wheezing, and infiltrates on chest X-rays. Some biomarkers help with the diagnosis and management of these conditions. NT-proBNP levels tend to be much higher in HF cases than in COPD, whereas CRP and leukocytosis tend to be

higher in COPD cases than in HF. Pulmonary function tests can also help differentiate between the two conditions, but these are difficult to perform during acute events as they require patient cooperation and effort, and echocardiographs can be difficult to interpret in acute care settings.

Metabolomics, the study of small molecules and their interactions within biological samples, can directly reflect the underlying biochemical processes, potentially providing techniques for biomarker identification (162). To date, little information on the metabolomes of hospitalized patients with AECOPD or AHF exists, and none compares plasma profiles between the two conditions.

In this study, we hypothesize that the application of plasma metabolomic profiling in clinical settings is sensitive and specific to acute exacerbations of breathlessness, specifically differentiating acute exacerbations of COPD from acute HF and healthy conditions. This study design presents an overview of the metabolomics signature profiles of AECOPD and HF, two conditions with potentially overlapping or coexisting metabolomic pathways.

3.3 Methods

3.3.1 Study design and participants

We compared the plasma data of 54 subjects; 20 hospitalised with AECOPD, 20 hospitalised with AHF, and 14 healthy volunteers. Samples were taken as part of an exploratory outcome from the East Midlands Breathomics Pathology Node (EMBER project) conducted in Leicester, UK (1, 260). For subjects with AECOPD and AHF, samples were collected within the first 24 hours of hospitalization. The inclusion criteria were acute breathlessness with a physician diagnosis of asthma, COPD, pneumonia, or HF. For this analysis, only patients with COPD or HF were included. Healthy controls were defined as subjects with no breathlessness who had not been diagnosed with asthma, COPD, or heart failure and had not been admitted to the hospital due to community-acquired pneumonia for at least six weeks prior to the study visit. Details of the EMBER study design, condition diagnostics, and inclusion criteria are available in the published EMBER study protocol by Ibrahim et al. (1).

Ethical approval was granted for the main EMBER project by the National Research Ethics Service Committee East Midlands (REC number: 16/LO/1747). Integrated Research Approval System (IRAS) 19899.

3.3.2 Instrumentation and sample processing

Plasma samples were processed in the Cardiovascular Biomedical Research Unit (LCBRU) at Glenfield Hospital by Dr. Zubair Israr, an expert in mass spectrometry techniques. First, 150 μ l of cold methanol was added to 50 μ l of plasma sample and centrifuged at 23,238 g for 5 mins. The supernatant was then transferred to a glass vial and analysed. Quality control (QC) samples were prepared by pooling 20 μ l of each plasma sample and adding cold

methanol at a volume ratio of 1:3 (i.e., for 1 ml of plasma, we added 3 ml of cold methanol) to the tube. The samples were investigated with quadrupole–time of flight mass spectrometry (Q–TOF MS) using the Waters UPLC–Synapt G2 system (WATER Corporation). Samples were injected in duplicate and in a random sequence. Fourteen quality control samples were utilised in the analysis workflow. Eight initial QC injections were made, and then a single QC injection was made after every 10 sample injections. Details of the LC–MS parameters are presented in Table 3-1. We used Progenesis QI software to perform the pre-processing of the raw data; automatic normalisation was performed to correct systematic experimental and sample loading variations when running samples. The automatic processing also included lock mass calibration, peak alignment, and peak picking.

Table 3-1 LC–MS parameters utilized in the analysis workflow

LC-MS parameters	
Mobile phase A	Water + 0.1% formic acid (FA)
Mobile phase B	Acetonitrile (ACN) + 0.1% FA
Seal wash	Water + ACN (1:1) + 0.1% FA
Column	50°C, C18
For C18	100% A to 100% B, curve 6, over 10 mins. Then 2 mins equilibration at 0.5ml/min
Injection volume	5µl
For positive ionization mode with lock mass	Leucine enkephalin
Number of injections	Each sample was injected twice at random.
Scan time	0.2 s
Scan mode	Centroid
Scan window	50–1200 m/z
Mode	+ve mode
Capillary voltage (kV)	3.0
Sample cone (V)	40
Extraction cone (V)	5
Source temperature (°C)	110

3.3.3 Statistical analysis

A combination of statistical methods was used for the data analysis. Topological data analysis (TDA) with the supervised tool linear discriminant analysis (LDA) lens was used to provide an overall visualizing for high dimensional data (261). To prepare the data for the TDA, features that are constant across all subjects were removed. Then, log transform data was applied, and the following parameters were specified: Metric Euclidean, number of hypercubes = 20, percentage overlap = 70%.

Moreover, as samples were analyzed in duplicates (two injections), persistent homology (PH) was applied, which showed that the injection A and injection B data were topologically equivalent (262). In addition, the dimensional reduction algorithm uniform manifold approximation and projection (UMAP) was used to study each data point and its relative proximate. This allowed the similarities and dissimilarities of features in dataset A injections and dataset B injections to be visualised. The plot showed that both datasets A and B were randomly spread with no batch effects. Thus, we can conclude that there were no fundamental differences between datasets, and the average of both injections was used in subsequent analyses (extracting significant features and calculating biomarkers).

The second technique used was penalized regression with elastic net penalty α between 1 and 0 (to target the smallest error while maintaining a practical number of features). This was used to extract the list of unique features from the total compounds that best discriminated between the three groups (263). Cross-validation was then applied with true class labels and randomly shuffled labels to assess the models' performance. Features with a non-zero regression coefficient that appeared 80 times or more over the 100 runs were

selected. To generate the scores for each selected feature, we used the average regression coefficient over the 100 runs (264).

Third, using the feature list and elastic net regression output, we calculated the biomarker score of the significant compounds from each approach by utilizing the slope formula

$$Y = a + b \cdot X$$

where Y is the dependent variable (biomarker score), X is the independent variable (actual compound concentration in a subject), b is the slope of the line (the compound coefficient), and a is the intercept (from the elastic net regression output). Biomarker scores were then calculated for the extracted compounds list from the elastic net regression using the cumulative sum of the calculated linear regression of each featured compound listed for the studied condition (COPD or HF) per all subjects (n_{1-54}).

3.4 Results

3.4.1 Baseline characteristics

Demographics and baseline characteristics are provided in Table 3-2 for the three groups. The groups were matched for age and gender ($p = 0.274$ and $p = 0.520$, respectively). BNP values were highest in the AHF group (AHF 653 ± 716 vs. AECOPD 67 ± 59 , $p = 0.015$), but no difference was seen in CRP. The blood troponin levels among the three groups showed an increasing trend from healthy individuals to those with COPD and a further elevation with HF patients. However, despite the conceivable clinical significance, the p -values were not statistically significant, potentially due to the sample size or the considerable variability within the groups, as the standard deviation shows.

Table 3-2 Cohort clinical characteristics

	Healthy	COPD	Heart failure	p -value
Total (n)	14	20	20	
Age (yr) [†]	66 ±6	69 ±5	66 ±6	0.274
Gender* (Male)	11 (79%)	14 (70%)	17 (85%)	0.520
VAS of breathlessness (mm) [†]	3 ±4	77 ±17	71 ±13	0.000
BNP (pg/ml) [†]	34 ±28	67 ±59	653 ±716	0.015
Blood troponin T (ng/L) ^{^†}	2.62 ±2.82	22.51 ±37.96	90.63 ±211.44	0.084
Blood eosinophils count x 10 ⁹ /L [†]	0.14 ± 0.05	0.27 ±0.29	0.19 ±0.11	0.205
CRP (mg/L) ^{^†}	2.95 ±1.01	24.83 ±35.51	35.83 ±68.77	0.068
30-day readmission	N/A	4 (20%)	4 (20%)	N/A
60-day readmission	N/A	5 (25%)	4 (20%)	N/A

Antibiotics prior to admission**	N/A	8 (40%)	0	0.003
Steroids prior to admission**	N/A	8 (40%)	1 (5%)	0.019

VAS: Visual analog scale

Values are shown as frequencies and percentages, or as a mean and standard deviation. Statistical analyses were performed with *chi-squared test, †ANOVA test, or **Fisher's exact test. ^Values that fell below the range of the lower limit of detection of the examined biomarker were assigned a value of half that lower limit of detection level.

3.4.2 High-dimensional data visualization

A total of 2,193 compounds were identified in the samples, of which 1,005 were non-constant features across the three groups and subjected to statistical analysis. For the TDA, a supervised method using LDA showed that healthy, HF, and COPD appear to cluster in broadly separate regions of the graph. This indicated that subjects from the same group tended to present data that clustered in nodes close to each other, suggesting that they shared similar metabolite characteristics. Consequently, AECOPD patients, AHF patients, and healthy controls could be distinguished from each other (Figure 3-1).

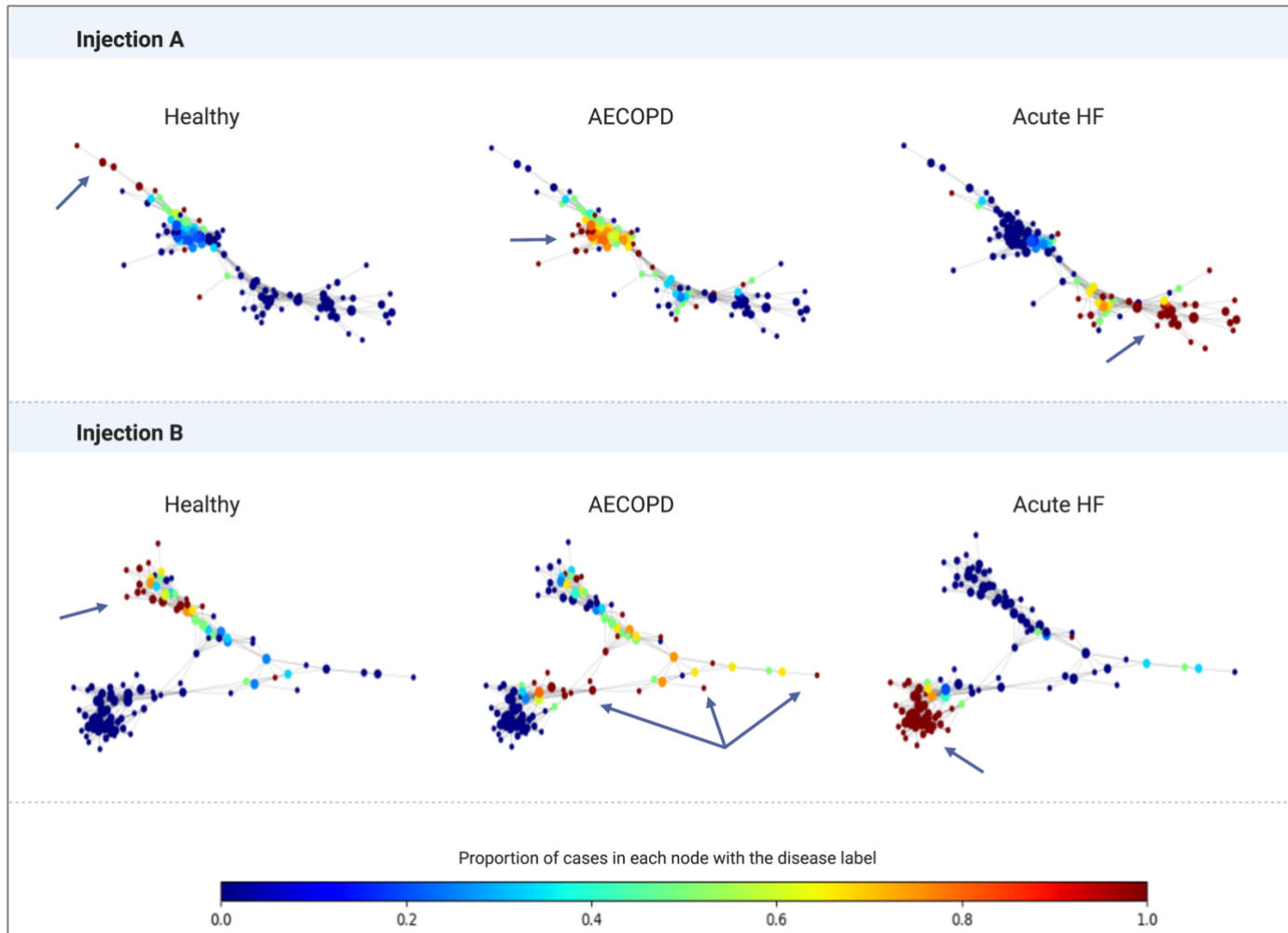


Figure 3-1 TDA visualization of plasma metabolomics across the AECOPD, AHF, and healthy control groups.

Nodes in the graph represent the metabolomic compounds computed within the subjects' plasma samples. Node color represents the probability that subjects in a given node belong to the indicated group. Net connections represent the similarities or differences in the studied metabolomic data between the nodes; the nodes of subjects with similar metabolites are physically close and vice versa.

3.4.3 Significant plasma biomarkers

Significant features were extracted from the 1,005 identified compounds via penalized regression with elastic net regression. In total, 9 unique features associated with AECOPD and 10 associated with AHF were identified as significant. For model validation, 15-fold cross-validation was applied.

The biomarker scores for distinguishing AECOPD from AHF and healthy individuals and for distinguishing AHF from AECOPD and healthy individuals are summarized in Table 3-3.

Table 3-3 Biomarker score summary

	AECOPD biomarker scores			Acute HF biomarker scores		
	AECOPD	Non-COPD		Acute HF	Non-HF	
		Acute HF	Healthy		AECOPD	Healthy
Mean	1010	-173.2	-1148	-1701	-5710	-8058
Std. D	1392	1367	676.5	908.7	3275	3569
Std. E	311.3	305.6	180.8	203.2	732.3	953.8
Lower 95% CI	358.5	-812.9	-1538	-2126	-7243	-10119
Upper 95% CI	1662	466.4	-756.9	-1276	-4178	-5998
Median	655.2	138	-1043.4	-1432.1	-5894	-6443.4
p-value	<0.0001			<0.0001		

Table 3-3 shows a significant difference ($p < 0.0001$) in the plasma biomarker scores calculated from the extracted unique features associated with AECOPD when comparing AECOPD, AHF, and healthy volunteers. This suggests that the biomarker scores based on these 9 unique significant features could distinguish individuals with COPD from non-COPD patients in the study population. Similarly, the biomarker scores based on the 10 unique significant features associated with AHF were significantly different ($p < 0.0001$) in individuals with AHF compared to non-HF patients. Tukey's multiple comparisons test confirmed the significant differences in both the AECOPD plasma biomarker scores and the

AHF biomarker scores, affirming that they distinguished the labeled group associated with the unique features from the other two groups studied.

ANOVA testing of the plasma biomarker scores across the groups reflected the statistical significance ($p < 0.0001$) of both the AECOPD plasma biomarker scores and the AHF biomarker scores. The results of Tukey's multiple comparisons test are presented in Figure 3-2.

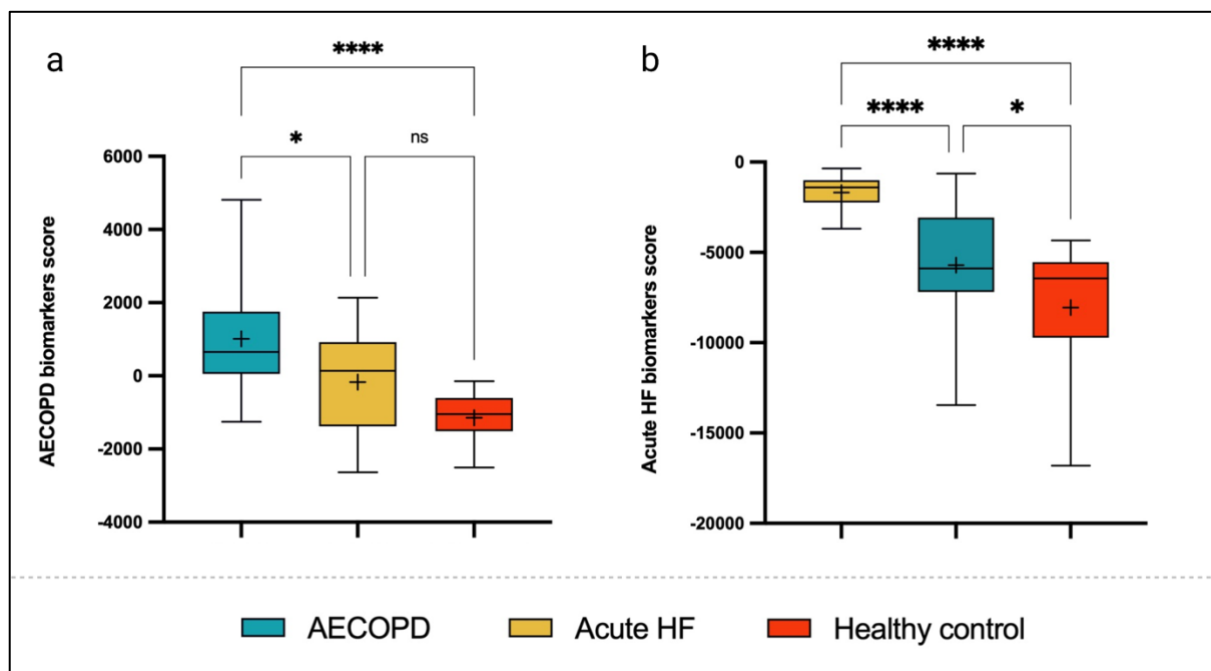


Figure 3-2 AECOPD and AHF plasma biomarker score box plots

ANOVA and Tukey's multiple comparisons test were applied, and the statistical significance of the plasma biomarker scores in differentiating the three groups is indicated as * $p < 0.05$, ** $p < 0.01$, *** $p < 0.001$, and **** $p < 0.0001$.

The AECOPD plasma biomarker score demonstrated an AUC of 0.80 with a sensitivity and specificity of 0.75 and 0.70, respectively, when predicting AECOPD cases from healthy and AHF individuals; an AUC of 0.96 with a sensitivity and specificity of 0.90 and 0.92, respectively, when distinguishing AECOPD patients from healthy individuals; and an AUC of

0.69 with a sensitivity and specificity of 0.70 and 0.55, respectively, when predicting AECOPD cases from AHF cases. Meanwhile, the AHF plasma biomarker score demonstrated an AUC of 0.93 with a sensitivity and specificity of 0.90 and 0.88, respectively, when distinguishing AHF cases from healthy and AECOPD individuals; an AUC of 1.0 when distinguishing AHF cases from healthy individuals; and an AUC of 0.89 with a sensitivity and specificity of 0.85 each when distinguishing AHF from AECOPD. ROC curve of the biomarker scores is presented in Figure 3-3. The AUC, sensitivity, and specificity for the ROC curve based on optimal cutoffs are summarized in Table 3-4.

Table 3-4 Sensitivity, specificity, negative, and positive predictive values of biomarker scores

	Sensitivity	Specificity	PPV	NPV	LR+
AECOPD biomarker scores					
AECOPD vs. AHF and healthy control	0.75 [0.53 to 0.88]	0.70 [0.53 to 0.83]	0.59	0.83	2.50
AECOPD vs. healthy control	0.90 [0.69 to 0.98]	0.92 [0.68 to .99]	0.94	0.87	12.60
AECOPD vs. AHF	0.70 [0.48 to 0.85]	0.55 [0.34 to 0.74]	0.68	0.57	1.55
AHF biomarker scores					
AHF vs. AECOPD and healthy control	0.90 [0.69 to 0.98]	0.88 [0.73 to 0.95]	.81	.94	7.65
AHF vs. healthy control	1.0 [0.83 to 1.0]	1.0 [0.78 to 1.0]	1.0	1.0	NA
AHF vs. AECOPD	0.85 [0.63 to 0.94]	0.85 [0.63 to 0.94]	0.89	0.8	5.66

ROC curve analyses were applied to evaluate plasma biomarkers' potential to enhance the diagnostic performance of the current blood biomarkers, CRP and BNP, in differentiating AECOPD and AHF cases, respectively, from non-AECOPD and non-AHF individuals. For AECOPD, the combination of plasma biomarkers with CRP demonstrated a significantly higher AUC (0.83, 95% CI: 0.71–0.94) compared to CRP alone (AUC=0.64, 95% CI: 0.48–0.80).

Similarly, for AHF, the combination of plasma biomarkers with BNP exhibited a remarkably higher AUC (0.97, 95% CI: 0.93–1.0) compared to BNP alone (AUC=0.88, 95% CI: 0.77–1.0) (Figure 3-4).

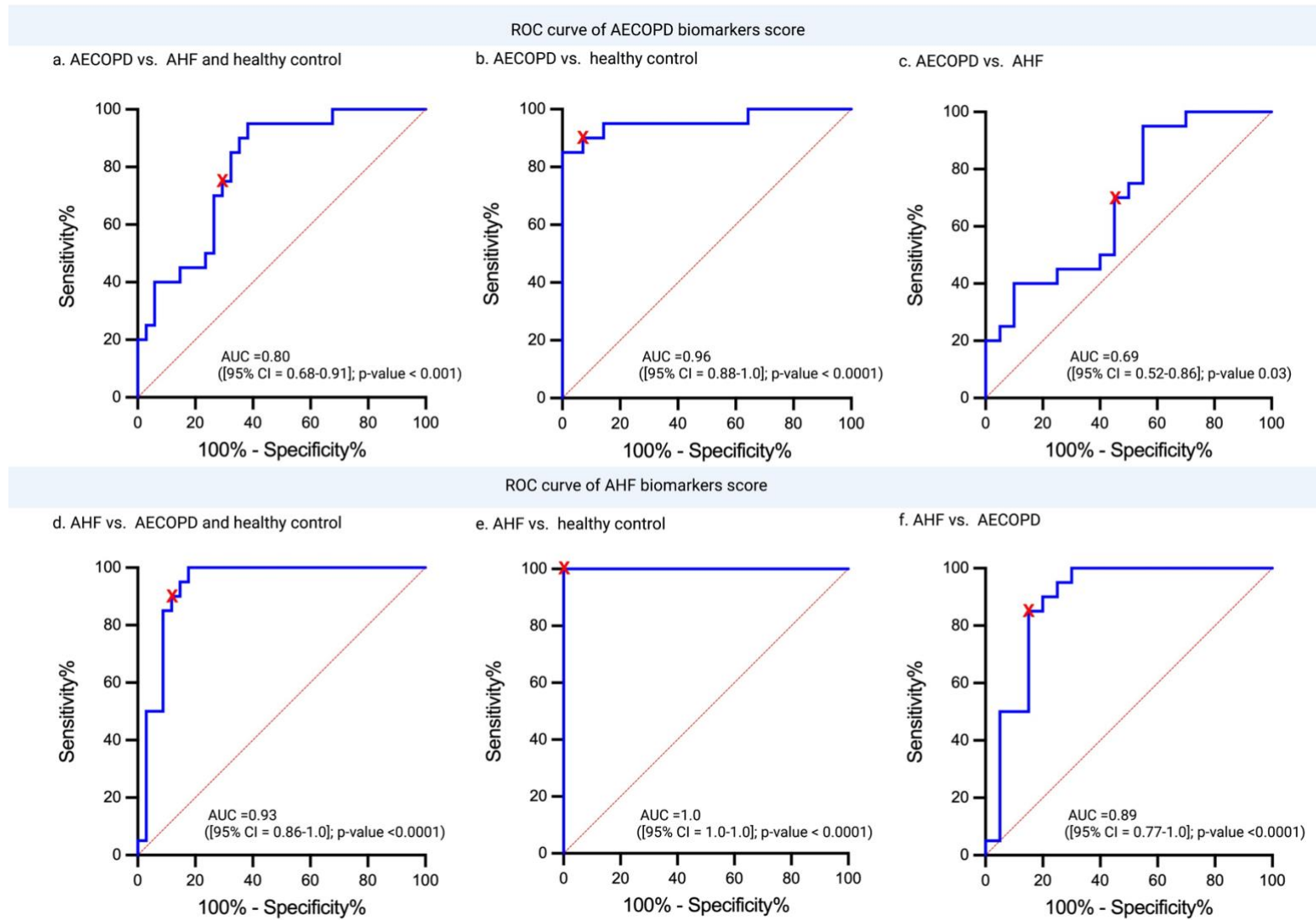


Figure 3-3 Receiver operating characteristics (ROC) curve analysis and area under the curve (AUC) for plasma metabolomic biomarker scores

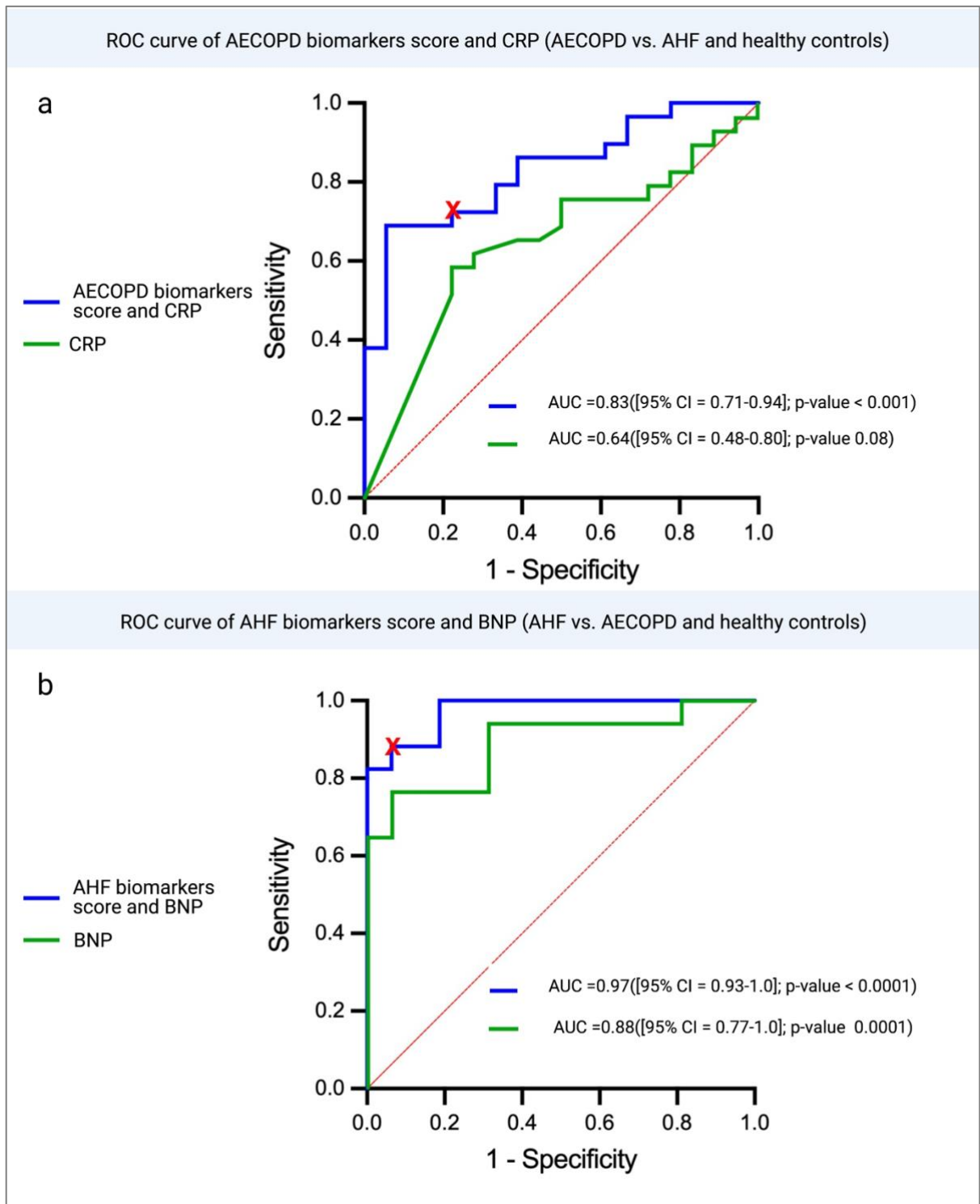


Figure 3-4 Receiver operating characteristics (ROC) curve analysis and area under the curve (AUC) for plasma metabolomic biomarker scores and clinical blood biomarkers

3.4.4 Classifying the significant compounds

Online libraries and the Human Metabolome Database (HMDB) were searched to determine putative metabolite identities for the significant compounds; in this study, we achieved level two MIS chemical identification. The total putative compounds were then grouped based on their chemical taxonomy (biochemical classes). The majority of the AECOPD biomarkers were glycolipids and the majority the AHF biomarkers were glycerophospholipids. A summary of the metabolites' chemical taxonomy is provided in Figure 3-5.

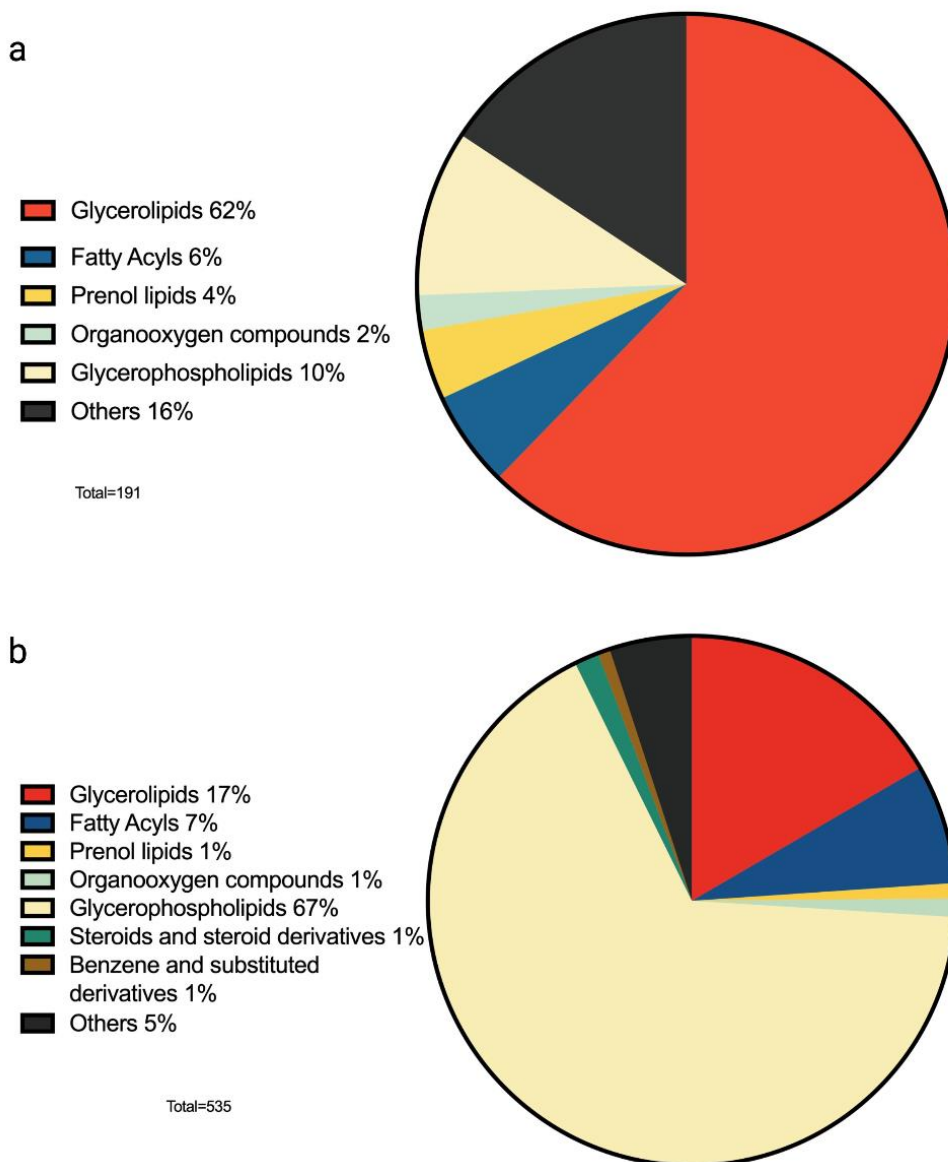


Figure 3-5 Proportions of the chemical classes of the putative metabolites extracted

- (a) Extracted features for AECOPD and (b) extracted features for AHF. Atomic mass (m) to charge (z) expressed as the m/z value of each molecular ion of interest was searched in the Human Metabolome Database (HMDB) (<https://hmdb.ca/spectra/ms/search>) (265). The search was performed in the database under LC–MS using the following settings: tolerance of 0.05 Da, Ion Mode positive, adduct type Unknown. After generating the putative identification list, ppm <10 was used as a cutoff point (a measure of the accuracy of the experimental mass compared to the theoretical mass) to narrow the suggested putative identification list for the feature compounds (266).

3.5 Discussion

In this study, we examined the plasma profiles of patients admitted to the hospital with acute breathlessness to identify either an exacerbation of AECOPD or decompensated heart failure. We used LC–Q–TOF–MS to identify metabolites that could differentiate the study conditions and were additive to the diagnostic ability of the existing biomarkers.

We used TDA to show distinct clusters of metabolites in AHF, healthy control, and AECOPD participants. Both the healthy controls and the AHF populations were closely grouped.

While the AECOPD population also formed a distinct cluster, it was slightly more dispersed.

This was echoed in the metabolite ROC curves, where AHF was well-differentiated from all separate and combined groups, but the AECOPD metabolite profile less accurately differentiated AECOPD from AHF.

Using the metabolites identified, we were able to derive biomarker scores that could differentiate AECOPD and AHF and were additive to existing blood biomarkers (BNP and CRP). This study's findings illuminate the diagnostic performance of CRP and BNP, two commonly used blood biomarkers, in specific respiratory and cardiovascular conditions. The ROC curve analysis revealed that CRP alone had a moderate discriminatory ability between the AECOPD and non-AECOPD individuals in the study population, while BNP exhibited good diagnostic accuracy in distinguishing AHF and non-AHF individuals. However, the addition of plasma biomarkers to these blood biomarkers significantly enhanced their diagnostic performance. Plasma biomarkers combined with CRP resulted in more accurate discrimination between AECOPD and non-AECOPD individuals. Similarly, combining plasma

biomarkers with BNP substantially enhanced the differentiation of AHF from non-AHF individuals. The significant improvement in the AUC for the combined plasma biomarkers and CRP or BNP affirms that these biomarkers provide additional, relevant data. These findings highlight the potential of plasma biomarkers to augment the diagnostic value of the established blood biomarkers. By integrating information from both, clinicians can make more accurate and informed decisions.

Regarding the chemical classes of the identified compounds, it all fall within the superclass of lipids. The identified lipid classes were glycerophospholipids, prenol lipids, glycerolipids, and fatty acyls (267). These findings are consistent with those reported previously in the literature as lipid metabolic dysfunction has previously been recognized in pulmonary diseases (268-270), as well as cardiovascular diseases (271-273). This study contributed to current knowledge by showing that the metabolite disturbance, when examined during the exacerbation of breathlessness and even in two conditions that share metabolic pathways, presents distinct, disease-specific patterns compared to both other conditions and healthy individuals.

Differentiating COPD from HF based on metabolic plasma biomarkers can be challenging as these conditions share some common mechanisms and metabolic pathways (274). The COPD physiological pathway includes but is not limited to vascular permeability, high IL-6, surfactant dysfunction, mitochondrial dysfunction, and oxidative stress. These changes are associated with metabolomics biomarkers and metabolite changes in COPD patients (275). The same physiological pathways are also commonly recognized in HF studies (57, 253-256). Therefore, metabolomics studies in these two populations can help not only in identifying

biomarkers but also in understanding their shared metabolic pathways. Some of the suggested metabolic plasma biomarkers may help to differentiate between these conditions. The COPD plasma biomarkers — adiponectin, leptin, and branched-chain amino acids (BCAAs) — are associated with increased disease severity and mortality in patients with COPD. The HF plasma biomarkers include glucose, free fatty acids (FFAs), and lactate; elevated levels of these markers have been associated with increased mortality and worse outcomes in patients with HF.

This study does have some limitations. First, the small sample size posed challenges in achieving statistical significance, potentially masking clinically meaningful differences, as observed in the troponin level analysis among the groups (Table 3-2). Conversely, a very large set of variables can yield statistically significant differences that lack clinical relevance. Hence, reliance on *p*-values alone invites caution when considering both the statistical and clinical significance of the results. This necessitates a balanced approach to acknowledge the limitations and ensure comprehensive interpretation. In the statistical analysis, we applied a penalized regression model to extract the significant metabolite features. The applied regression models were then fitted with true class labels and randomly shuffled labels 500 times to assess the models' accuracy; in which cross-validation was also used to estimate the regression coefficient. However, this method may be subject to overfitting and, therefore, requires external validation in a separate cohort. Second, we divided participants into groups based on their primary diagnosis. Whilst the participants were not known to have overlapping diagnoses, we might have missed sub-clinical or undiagnosed diseases (e.g., coexisting heart failure in COPD). Certainly, the results in the COPD population are less definite than those in the AHF population, which may suggest some similar metabolic

processes. Thirdly, we achieved level 2 MIS chemical identification, which suggests a list of “compound notations” rather than one “confirmed identification” for each feature. To achieve level one MIS identification, where one metabolite is confirmed as the identity of the studied feature, an advanced laboratory experiment that compares each of the proposed putative metabolites with a matching standard is needed.

In summary, we were able to identify distinct plasma metabolites that differentiated AHF and exacerbations of COPD in the hospital setting compared with both healthy controls and the other condition. Using these metabolites, we were able to develop a biomarker score that improved diagnostic accuracy over traditional biomarkers, although this score needs external validation. Finally, we were able to identify the likely chemical classes of these metabolites, which predominantly belonged to lipid groups.

Chapter 4 Studies; Forced Oscillometry Technique (FOT) to Assess Ventilation Heterogeneity (VH) During Hospital Admission for Acute Cardiorespiratory Illness

4.1 Abstract

Introduction: Hospitalisation due to exacerbations of cardiorespiratory disease results in reduced lung function and increased airway obstruction. However, traditional measures of lung function require maximal effort, which is difficult for patients to exert when they are unwell (e.g., FEV₁) and may focus on larger airways away from the major part of airways disease (e.g., peak flow). We aimed to measure whole-airway function using the forced oscillometry technique (FOT) in patients during exacerbations of cardiorespiratory illness compared to healthy controls.

Methods: In this study, 310 participants underwent assessment, of which 263 were admitted to hospital with acute cardio-respiratory illness (asthma (n=80), COPD (n=75), heart failure (n=46) and pneumonia (n=62)) and 47 healthy individuals were included. Participants underwent handheld FOT measurements within the first 24 hours of admission.

Results: FOT measurement was feasible for all patients (n = 310, 100%). There was a significant difference in both absolute and percent predicted measures of lung mechanics ($p < 0.05$ for all measures), with significantly worse lung mechanics found in COPD cases. The measures of resistance and reactance were worse in those that were more breathless ($p < 0.0001$), had more wheeze ($p < 0.001$), and had low oxygen saturation ($p < 0.001$). No difference was seen based on early warning score nor blood biomarkers (eosinophil count, C reactive protein, and brain natriuretic peptide) and lung mechanics did not predict length of hospital stay or hospital readmission.

Conclusion: In conclusion, handheld FOT can be feasibly deployed in acute care settings to obtain information on respiratory mechanics. It demonstrates significant differences in ventilation heterogeneity between individuals experiencing acute breathlessness and healthy volunteers.

4.2 Introduction

Hospitalization due to a cardiorespiratory condition represents a large proportion of unplanned emergency medical admissions. These are commonly due to the of chronic conditions, such as asthma, chronic obstructive pulmonary disease (COPD), or decompensated heart failure, but may also be due to new acute illnesses, such as pneumonia (276, 277).

While the systemic severity of a cardiorespiratory illness can be measured through early warning scores and blood biomarkers, no tests are routinely used to directly measure airway function in acute clinical settings. Symptoms (i.e., dyspnea), oxygen saturation, and respiratory rate are collected and act as surrogate markers of function. Traditional measures of airway function, used in the stable state, like forced expiratory volume in one second (FEV₁), are difficult to implement in an acute setting and are less accurate as maximal tests are difficult when patients are breathless and fatigued (278). While peak flow is used to measure lung function in acute asthma, it is a poor measure that provides a measure of more central airways, whereas it is the smaller airways that are more likely to be predominantly affected (279).

FOT measures the mechanics of the respiratory system during tidal breathing. It is able to detect both small airway disease (SAD) and ventilation heterogeneity (VH) (87, 280, 281). The technique, therefore, lends itself to potential use in the acute care setting, where passive ventilation and measures of whole lung mechanics may be beneficial (282). Despite being described more than 60 years ago by DuBois et al. (213), studies of FOT during acute severe exacerbations of airway disease or in other acute cardiorespiratory conditions are limited, in part as until recently FOT required highly specialized equipment fixed in a

dedicated space. However, more recent FOT devices are now portable, allowing bedside measures to be taken (282).

In this study, we describe the feasibility and measures of handheld FOT within 24 hours of patients admitted to the hospital with acute cardiorespiratory illness due to exacerbations of their chronic disease (asthma, COPD, or heart failure), or new respiratory illness (pneumonia). We compared these measures across the disease groups to a cohort of healthy volunteers, along with symptoms, blood biomarkers, and clinical parameters.

4.3 Methods

4.3.1 Study design and participants

This was a prospective cohort study of patients admitted to the hospital with self-reported acute breathlessness and a primary clinical diagnosis of one of; exacerbation of asthma, exacerbation of COPD, decompensated heart failure, or pneumonia.

Participants were prospectively recruited between May 2017 and December 2018 as part of the Exhaled Breath Metabolomic Biomarkers in the Acutely Breathless Patient (EMBER) study (1, 260), for which FOT was collected as a predetermined secondary outcome.

Informed written consent was obtained and measures, including FOT, were taken within 24 hours of hospital admission. Age-matched healthy controls with no history of cardiorespiratory illness were also recruited. Full details of the protocol and inclusion and exclusion criteria have previously been published (1). The study was approved by the National Research Ethics Service Committee (16/LO/1747).

4.3.2 Forced oscillation technique

Participants performed handheld FOT measurements using the TremoFlo airway oscillometry device (Thorasys, Canada), in line with ATS/ERS consensus (283, 284). The FOT device was calibrated daily using standardised volume and resistance. FOT was performed with participants sitting up and holding their heads in a neutral or slightly extended position. Participants were instructed to form a tight seal around the mouthpiece and to firmly use both hands to suppress their cheeks to minimise airway shunting. Nose clips were worn during the procedure. Pressure oscillations were initiated and subjects were instructed to

breathe quietly at the FRC level. A total of three technically acceptable measurements were performed.

4.3.3 FOT parameters and normative values

Several oscillometry measurements of lung mechanics were collected in this study. For the resistance component of respiratory impedance, we measured resistance at 5 Hz (R5), at 19 Hz (R19), and the resistance at 5 Hz minus the resistance at 19 Hz (R5-R19). These measurements, respectively, indicate the resistance in the whole respiratory system, the proximal airways, and the small airways plus the ventilation inhomogeneities of the system. For the reactance component of respiratory impedance, we collected data on the reactance at 5 Hz (X5) and the area under the reactance curve (AX), which are both measurements of the elastic properties, lung stiffness, and ventilation heterogeneity. Moreover, we reported the resonant frequency (Fres), at which inertance and elastance are balanced and the impedance is entirely explained by the resistance.

Oscillometry measurements of lung mechanics are influenced by the subject's unique characteristics (including age, gender, height, weight, and BMI) (81, 285, 286). Several studies have published reference equations for the percent predicted value to correct value for these factors using oscillometry techniques. However, considerable variation exists between cohorts; therefore, the reference normal values should be generated from the equation that best matches both the characteristics of the target population and the selected measurement techniques (227). We generated predicted values equations based on the recruited healthy control group to best match the population of interest (Table 4-1). A comparison of the healthy subjects included for reference value calculation in this study

versus those in published reference equations by Oostveen et al. (287) is presented in Table 4-2.

Table 4-1 Demographics and baseline oscillometry data for the healthy subjects included for reference value calculations

Total (43)	Min	Max	1st Qu	Median	Mean	3rd Qu
Sex (Male, n (%))	22 (51.2%)					
Age (years)	50	80	60.50	66	65.35	70.50
Height (m)	1.49	1.91	1.62	1.68	1.69	1.77
Weight (kg)	45.0	111.1	66.6	78.9	78.5	88.00
BMI (kg/m²)	20.5	34.8	24.7	27.1	27.3	29.8
Measured R5	1.70	7.05	3.11	3.70	3.94	4.64
Measured R19	1.90	5.31	2.67	3.10	3.27	3.77
Measured R5-R19	-0.28	2.92	0.21	0.49	0.67	1.02
Measured X5	-3.85	-0.49	-2.04	-1.50	-1.63	-1.05
Measured AX	0.84	28.22	3.89	7.53	10.26	15.20
Measured Fres (Hz)	8.37	29.27	12.62	16.11	17.04	20.93

Table 4-2 Comparison of reference values: Current study vs. Oostveen et al.

	Current study	In Oostveen et al.
Total	43	368
Age (years)	65.35 ±(7.76)	49 ±17
Sex (Male, n (%))	22 (51.2%)	(49%)
Height (m)	1.69 ±(0.11)	1.71 ±(0.9)
Weight (kg)	78.55 ±(15.78)	n/a
BMI (kg/m²)	27.29 ±(3.87)	25.5 ±3.94
Model specifications	<p>Multiple linear regression was employed.</p> <p>Height and BMI were included as predictors, but age did not show significance as predictor in any of the models.</p> <p>FOT was utilised and conducyed in a single center.</p>	<p>Mixed model analysis was employed.</p> <p>Age, height, and weight were included as predictors. But BMI did not show significance as predictor in any of the models.</p> <p>Age, although was non significant in some of the models , but was not excluded for the sake of consistency.</p> <p>FOT and IOS techniques were utilized, incorporating three commercial and two custom-made FOT devices across five centers</p>

4.3.4 Statistical analysis

Baseline characteristics, FOT measures between disease groups, and across clinical and blood biomarkers at baseline were compared using one-way analysis of variance (ANOVA) and Kruskal–Wallis tests for parametric and non-parametric data, respectively. A post-hoc Dunn’s test was applied for multiple comparisons. Chi-squared tests were used for categorical data. Spearman’s rho was used to calculate correlation coefficients. Linear

regression and logistic regression were used to assess measures of FOT and length of hospital stay and hospital readmission, respectively.

For the FOT normative values, linear regression models were used to adjust for subjects' height and body mass index (BMI) as predictors of each FOT measure (Tables 4-3 and 4-5).

The effects of age, weight, gender, height, and BMI were examined initially as independent variables in the regression models; subsequently, age, gender, and weight were excluded as they were insignificant in the model (Table 4-3).

Table 4-3 Univariate analysis using linear regression for each measure

Predictor	Age		
(Rrs) or (Xrs)	Beta coefficient	95% CI	p-value
R5	0.006	[-0.044, 0.056]	0.806
R19	-0.008	[-0.042, 0.026]	0.637
AX	0.130	[-0.197, 0.457]	0.427
X5	-0.011	[-0.042, 0.020]	0.490
Fres	0.108	[-0.116, 0.332]	0.338
Predictor	Gender (Male)		
(Rrs) or (Xrs)	Beta coefficient	95% CI	p-value
R5	-0.644	NA	0.089
R19	-0.719	NA	0.004
AX	-1.558	NA	0.536
X5	0.316	NA	0.184
Fres	-1.126	NA	0.516
Predictor	Weight		
(Rrs) or (Xrs)	Beta coefficient	95% CI	p-value
R5	0.003	[-0.022, 0.027]	0.824
R19	-0.009	[-0.025, 0.007]	0.273
AX	0.098	[-0.061, 0.257]	0.220
X5	-0.006	[-0.021, 0.009]	0.433
Fres	0.059	[-0.051, 0.169]	0.286
Predictor	Height		
(Rrs) or (Xrs)	Beta coefficient	95% CI	p-value
R5	-4.645	[-8.036, -1.254]	0.008
R19	-4.043	[-6.211, -1.875]	<0.001
AX	-16.82	[-40.331, 6.684]	0.156
X5	2.102	[-0.101, 4.304]	0.060
Fres	-12.838	[-28.942, 3.267]	0.115
Predictor	BMI		

(Rrs) or (Xrs)	Beta coefficient	95% CI	p-value
R5	0.126	[0.032, 0.219]	0.009
R19	0.043	[-0.024, 0.110]	0.204
AX	0.963	[0.375, 1.550]	0.001
X5	-0.081	[-0.138, -0.023]	0.007
Fres	0.649	[0.241, 1.056]	0.002

Age and weight were not related to the measured FOT parameter in all models of this group of subjects, while gender, height, and BMI were significant and, therefore, were included in the subsequent multivariate analysis.

Table 4-4 Multivariate linear regression for normative values

Predictors		Gender, Height, and BMI		
(Rrs) or (Xrs)	Factor	Beta coefficient	95% CI	p-value
R5	Gender	-0.135	NA	0.790
	Height	-5.049	[-9.800, -0.297]	0.037
	BMI	0.153	[0.067, 0.238]	<0.001
R19	Gender	-0.339	NA	0.336
	Height	-3.202	[-6.485, 0.081]	0.055
	BMI	0.069	[0.009, 0.128]	0.023
AX	Gender	0.077	NA	0.982
	Height	-23.384	[-56.099, 9.332]	0.156
	BMI	1.064	[0.473, 1.655]	<0.001
X5	Gender	0.196	NA	0.559
	Height	1.951	[-1.174, 5.076]	0.214
	BMI	-0.096	[-0.153, -0.040]	0.001
Fres	Gender	0.470	NA	0.844
	Height	-18.791	[-41.250, 3.667]	0.098
	BMI	0.7163	[0.310, 1.121]	<0.001
Predictors		Height and BMI		
R5	Height	-5.532	[-8.541, -2.523]	<0.001
	BMI	0.150	[0.067, 0.232]	<0.001
R19	Height	-4.414	[-6.516 -2.311]	<0.001
	BMI	0.063	[0.005, 0.120]	0.033
AX	Height	-23.110	[-43.811, -2.408]	0.029
	BMI	1.066	[0.497, 1.634]	<0.001
X5	Height	2.649	[0.663, 4.635]	0.010
	BMI	-0.093	[-0.147, -0.038]	0.001
Fres	Height	-17.114	[-31.332, -2.896]	0.019
	BMI	0.725	[0.334, 1.115]	<0.001

Table 4-5 Final prediction equations for normal values of FOT measures

y	β_0	B1	B2	RSE
R5	9.190	-5.532	0.150	1.012
R19	9.016	-4.413	0.063	0.706
AX	20.261	-23.110	1.066	6.959

X5	-3.573	2.649	-0.093	0.667
Fres	26.196	-17.114	0.725	4.780

$y = \beta_0 + \beta_1 * \text{Height} + \beta_2 * \text{BMI}$. Height (m); BMI (kg/m²); Height range: 1.49–1.91 m; BMI range: 20.5–34.8 kg/m². The residual standard error (RSE) was reported from the regression model. The percentage predicted value (% pred) was then estimated as the subject measured/subject predicted value*100 for the total population (310 individuals across the healthy and disease groups).

4.4 Results

4.4.1 Feasibility of FOT in acute settings

FOT was attempted in 310/386 (80.3%) participants from the EMBER study; the device was not available for the 76 participants with whom FOT measurement was not attempted. In total, 310 (100%) participants with whom FOT was attempted were successful in providing data to the ERS/ATS standard. No adverse events were noted during or after the FOT maneuver.

4.4.2 Baseline characteristics

263/310 (84.8%) participants were admitted to the hospital with self-reported acute breathlessness due to an exacerbation of asthma (n=80), AE COPD (n=75), AHF (n=46), or pneumonia (n=62). The presented dyspnoea, measured using a visual analog score, was similar across all disease groups and significantly higher than healthy controls ($p < 0.001$). Participants with asthma were younger and more likely to be female than those in other groups. Patients with COPD were more likely to be current smokers than those in other groups, and BMI was highest in the asthma and heart failure groups. Clinical observations and laboratory blood results are presented in Table 4-6.

Table 4-6 Cohort clinical characteristics

	Healthy	Asthma	COPD	Pneumonia	Heart failure	p-value
Total (n)	47	80	75	62	46	
Demographics						
Age (years)	63.1 ±12.1	41.7 ±17.5	68.9 ±8.3	59.0 ±16.9	72.4 ±10.42	<0.001
Male Sex, n (%)	25 (49%)	33 (41%)	45 (60%)	30 (48%)	32 (70%)	0.021
Height (m)	1.69 ±0.11	1.67 ±0.11	1.67 ±0.09	1.69 ±0.09	1.70 ±0.11	0.457
Weight (kg)	79.3 ±16.0	86.7 ±25.5	74.9 ±22.4	81.6 ±21.7	91.4 ±26.2	0.001
BMI (kg/m²)	27.6 ±4.2	31.0 ±9.1	26.7 ±7.4	28.8 ±7.79	31.2 ±7.2	0.001
Current smoker	0 (0%)	21 (26%)	33 (44%)	13 (21%)	6 (13%)	<0.001
Clinical observations[†]						
Temperature, °C	36.2 ±0.4	36.9 ±0.6	36.8 ±0.52	37.3 ±0.8	36.6 ±0.4	<0.001
Heart rate (beats/min)	66 ±14	98 ±18	92 ±18	93 ±16	80 ±15	<0.001
Respiratory rate (breaths/min)	13.5 ±2.9	20.8 ±3.2	21.9 ±9.5	21.3 ±10.3	20.2 ±3.8	<0.001
Oxygen saturation (%)	98 ±1	96 ±2	94 ±3	95 ±4	97 ±2	<0.001
Systolic blood pressure (mmHg)	134 ±18	134 ±19	133 ±21	128 ±20	126 ±21	0.103
MEWS	1 ±1	2 ±2	3 ±3	2 ±2	2 ±2	<0.001
Dyspnea measures						
MRC score	1.0 (1.0–1.0)	5.0 (4.0–5.0)	5.0 (4.0–5.0)	5.0 (3.0–5.0)	5.0 (4.0–5.0)	0.039
Breathlessness VAS score (mm)	3.48 ±(5.33)	69.76 ±(21.76)	69.53 ±(18.63)	67.7 ±(22.5)	68.8 ±(18.2)	<0.001
Wheeze VAS score (mm)	2.98 ±(5.27)	65.72 ±(23.10)	59.28 ±(28.15)	43.62 ±(33)	30.02 ±(29.5)	<0.001
Laboratory						
Eosinophil count, x10⁹/L	0.14 (0.09–0.21)	0.17 (0.06–0.40)	0.14 (0.06–0.30)	0.10 (0.05–0.14)	0.12 (0.07–0.22)	<0.001
Brain natriuretic peptide (ng/l)	15.0 (18.2–40.7)	20.2 (7.7–39.7)	50.5 (25.1–92.4)	12.5 (25.6–122.5)	520.8 (175.4–1051.5)	<0.001
C-reactive protein (mg/L)	2.5 (2.5–2.5)	8.0 (2.5–20.0)	12.0 (2.5–25.75)	149.0 (84.0–252.0)	13.0 (2.5–24.0)	<0.001

Data are expressed as mean ±standard deviation, median (interquartile range), or proportion (%). BMI: Body mass index. VAS: a 100mm visual analog scale. MEWS: Modified early warning score. MRC score: Medical Research Council Dyspnoea scale

4.4.3 Measures of lung mechanics during acute illness

All measures of lung mechanics using FOT were significantly higher in participants hospitalised with breathlessness than in healthy volunteers irrespective of aetiology (Table 4-7). The only measure in which no significant difference was seen between healthy volunteers and heart failure patients was R19 (Figure 4-1, panel b). The greatest differences compared with healthy volunteers were seen in R5-R19, X5, and AX (Figure 4-1, panels c, d, and e). Patients with acute exacerbations of COPD also had significantly higher abnormal lung mechanics (R5, R5-R19, X5, AX, and Fres) than patients with other acute conditions (Figure 4-1).

Table 4-7 Measures of FOT in healthy controls and acutely unwell patients with different cardiorespiratory conditions.

	Healthy	Asthma	COPD	Pneumonia	Heart failure	<i>p</i> -value
Total (n)	47	80	75	62	46	
R5 (kPa.s.L⁻¹)	3.70 (3.115–4.810)	5.28 (3.84–7.16)	5.61 (4.62–7.85)	5.11 (4.077–6.910)	5.44 (4.84–6.978)	<0.001
R19 (kPa.s.L⁻¹)	3.10 (2.690–3.785)	3.85 (3.067–5.008)	3.62 (2.89–5.135)	3.82 (3.038–4.612)	3.81 (2.895–5.418)	0.014
R5-R19 (kPa.s.L⁻¹)	0.61 (0.215–1.135)	1.23 (0.46–2.16)	2.14 (1.49–2.715)	1.35 (0.815–2.237)	1.81 (1.32–2.28)	<0.001
X5	-1.48 (-2.045–-1.050)	-2.61 (-3.893–-1.448)	-5.08 (-7.285–-3.275)	-2.68 (-4.838–(1.750)	-4.04 (-7.15–-2.627)	<0.001
AX (Kpa/L)	7.53 (3.895–15.200)	20.45 (8.828–46.828)	55.25 (33.03–85.08)	25.27 (13.18–54.87)	37.35 (27.12–64.07)	<0.001
Fres (Hz)	23.00 (12.62–21.91)	40.50 (16.63–28.78)	37.00 (27.18–33.21)	31.50 (21.92–30.47)	23.50 (23.67–29.55)	<0.001

Results are reported as median (interquartile range).

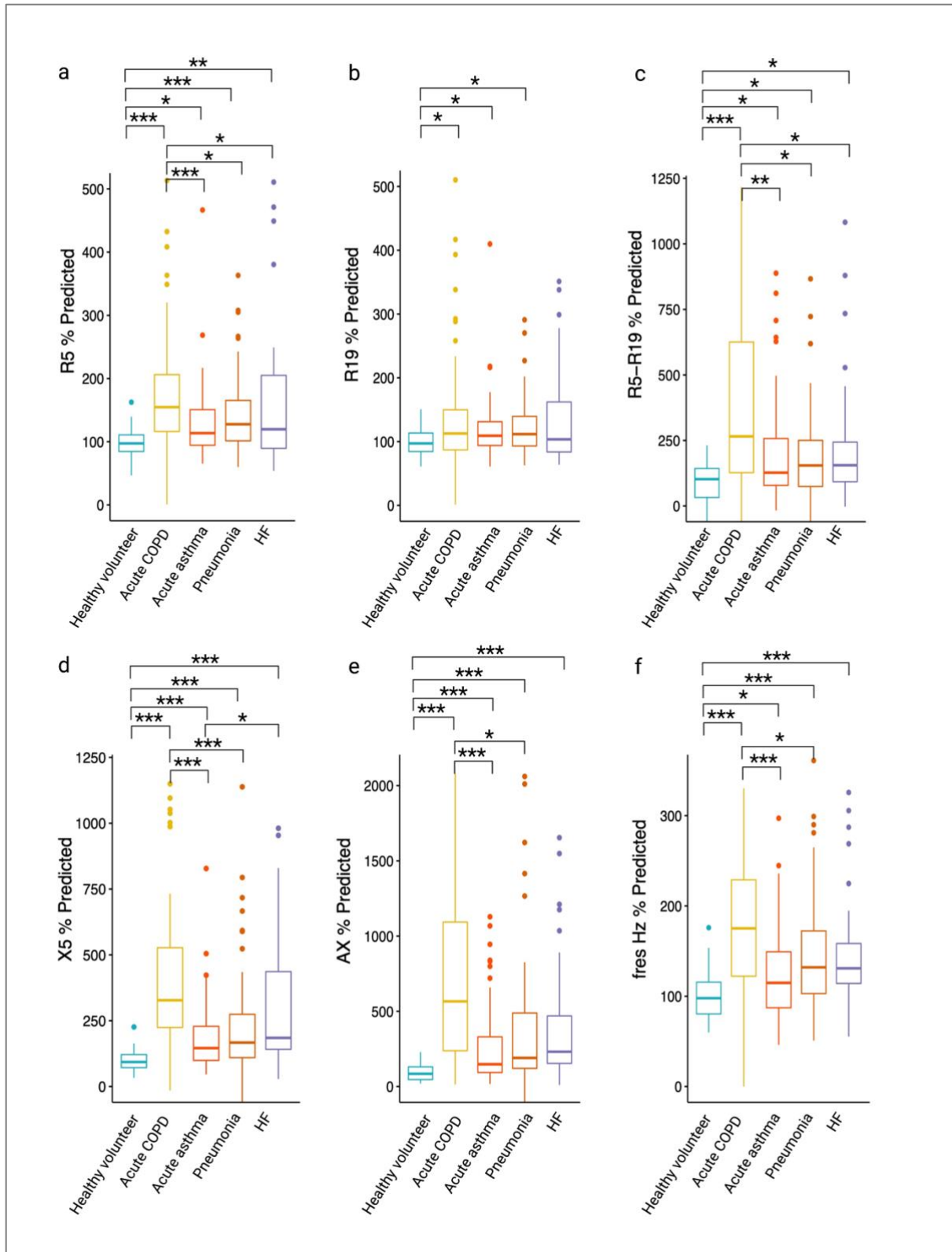


Figure 4-1 Box and whiskers plots of % predicted measures of lung mechanics across healthy volunteers and acutely unwell in COPD, asthma, pneumonia, and heart failure patients.

(a) R5 % predicted; (b) R19 % predicted; (c) R5-R19 % predicted; (d) X5 % predicted; (e) AX % predicted; (f) Fres % predicted. * $p < 0.01$, ** $p < 0.001$, *** $p < 0.0001$. Bold lines represent medians; boxes, IQR; whiskers, minimum and maximum range; and dots, individual outliers.

4.4.4 Association between lung mechanics, clinical parameters, and blood biomarkers

FOT measures were compared with symptoms (breathlessness and wheeze) and routinely collected clinical parameters used to monitor the respiratory system; SpO₂, RR, and MEWS. These measures were either poorly or not significantly correlated with FOT measures (Table 4-8). SpO₂ and Fres had the highest correlation coefficient (-0.35, $p < 0.001$).

The measures of lung mechanics were significantly different with increasing breathlessness and wheeze (Figure 4-2 and Table 4-9). Similarly, worse lung mechanics were seen in hypoxemic patients (SpO₂ <92%) (Figure 4-3, panels a and d, and Table 4-9). There were significant differences between lung mechanics and RR, with a reverse in the FOT patterns specifically in patients with a respiratory rate of >30 breaths per minute (Figure 4-3, panels b and e). In addition, no difference was seen in FOT measures based on the MEWS, blood eosinophil count, CRP, or NT-proBNP (Figure 4-4 and Table 4-9).

Table 4-8 Correlation coefficients between FOT and symptoms, clinical parameters, and blood biomarkers

	SpO ₂		Respiratory rate		MEWS	
	Coefficient	<i>p</i> -value	Coefficient	<i>p</i> -value	Coefficient	<i>p</i> -value
R5 (kPa.s.L⁻¹)	-0.24	<0.001	0.	0.006	0.04	0.489
R19 (kPa.s.L⁻¹)	-0.	0.087	0.	0.195	0.04	0.542
R5-R19 (kPa.s.L⁻¹)	-0.29	<0.001	0.2	<0.001	0.05	0.428
X5	0.29	<0.001	-0.26	<0.001	-0.04	0.493
AX (KPa/L)	-0.32	<0.001	0.26	<0.001	0.07	0.250
Fres (Hz)	-0.35	<0.001	0.23	<0.001	0.11	0.081

	Blood eosinophil count		CRP		BNP	
	Coefficient	<i>p</i> -value	Coefficient	<i>p</i> -value	Coefficient	<i>p</i> -value
R5 (kPa.s.L⁻¹)	-0.12	0.038	0.18	0.001	0.18	0.062
R19 (kPa.s.L⁻¹)	-0.12	0.039	0.11	0.071	0.03	0.610
R5-R19 (kPa.s.L⁻¹)	-0.08	0.179	0.22	<0.001	0.16	0.009
X5	0.11	0.048	-0.21	<0.001	-0.18	0.003
AX (KPa/L)	-0.08	0.153	0.23	<0.001	0.20	0.001
Fres (Hz)	0.04	0.489	0.26	<0.001	0.21	0.002

	Breathlessness VAS score (mm)		Wheeze VAS score (mm)	
	Coefficient	p-value	Coefficient	p-value
R5 (kPa.s.L ⁻¹)	0.22	<0.001	0.21	<0.001
R19 (kPa.s.L ⁻¹)	0.	0.036	0.	0.039
R5-R19 (kPa.s.L ⁻¹)	0.26	<0.001	0.26	<0.001
X5	-0.28	<0.001	-0.25	<0.001
AX (KPa/L)	0.33	<0.001	0.29	<0.001
Fres (Hz)	0.35	<0.001	0.31	<0.001

Table 4-9 Measures of FOT across symptoms, clinical parameters, and blood biomarkers

Oxygen saturation (%)						
Total (n)	R5 (kPa.s.L ⁻¹)	R19 (kPa.s.L ⁻¹)	R5-R19 (kPa.s.L ⁻¹)	X5	Ax (KPa/L)	Fres (Hz)
Oxygen saturation (%)						
<92% n (12)	6.125 4.405– 8.652	3.775 3.015–5.350	2.020 1.170- 3.695	-5.975 (-7.338)- (-2.828)	49.45 (29.19- 73.31)	30.41 (25.23- 32.77)
92–96% n (126)	5.430 4.105– 7.415	3.710 2.905– 4.902	1.675 1.062- 2.445	-3.385 (-5.582)- (-2.312)	34.53 (17.70 - 59.60)	26.50 (20.66- 31.38)
>96 n (119)	4.650 3.590– 5.835	3.430 2.965–4.210	1.210 0.310- 1.885	-2.270 (-3.895)- (-1.425)	20.00 (6.545- 36.120)	22.48 (14.43- 27.63)
p-value	0.004	0.380	<0.001	<0.001	<0.001	<0.001
Respiratory rate (breaths/min)						
<21 n (217)	5.000 (3.710– 6.910)	3.620 (2.900– 4.710)	1.470 (0.610- 2.220)	-2.900 (-5.090)- (-1.480)	26.600 (9.057- 51.633)	24.20 (16.46- 29.55)
21–29 n (80)	5.395 (4.285– 7.095)	3.715 (2.978– 4.730)	1.725 (1.073- 2.550)	-3.595 (-6.130)- (-2.285)	40.02 19.68- 70.33	27.64 (22.34- 32.48)
30+ n (6)	3.945 (3.570– 5.678)	3.585 (3.098– 5.093)	0.4500 (0.150- 0.8175)	-1.305 (-2.930)- (-1.165)	9.110 5.117- 19.275	15.30 (12.51- 22.37)
p-value	0.194	0.888	0.012	0.027	0.004	0.001
Modified early warning score						
0-2 n (182)	5.060 (3.710– 6.765)	3.580 (2.905– 4.665)	1.5350 (0.5675- 2.2125)	-2.840 (-4.957)- (-1.528)	26.58 (10.26 - 50.50)	24.12 (17.10- 29.36)
3 n (28)	4.770 (3.395– 5.822)	3.120 (2.572– 4.030)	1.440 (0.665- 2.180)	-3.190 (-3.825)- (-1.675)	29.36 (9.73- 44.07)	27.35 (17.34- 32.11)
>3 n (55)	5.390 (4.130– 7.505)	3.650 (3.035– 5.310)	1.400 (0.855- 2.520)	-3.430 (-5.69–) - (-1.900)	31.96 (16.30- 66.64)	25.02 (19.97- 32.59)
P value	0.130	0.034	0.731	0.494	0.350	0.105
Eosinophil count, x10⁹/L						

<0.30 × 109/L N (245)	5.130 (3.920– 7.340)	3.740 (2.950– 5.000)	1.520 (0.700– 2.480)	-3.000 (-6.06–) (-1.620)	30.19 (11.72– 65.79)	24.71 (18.14– 30.62)
≥0.30 × 109/L n (56)	5.005 (3.748– 6.037)	3.430 (2.915– 4.185)	1.345 (0.825– 1.883)	-3.095 (-3.975– (-1.502)	27.79 (13.13– 43.65)	24.23 (17.57– 29.32)
p-value	0.149	0.151	0.246	0.258	0.305	0.953
Brain natriuretic peptide (ng/l)						
<400 (ng/L) n (221)	5.090 (3.870– 6.980)	3.590 (2.940– 4.680)	1.480 (0.660– 2.330)	-2.990 (-5.530– (-1.560)	27.61 (11.70– 58.78)	24.36 (17.12– 30.41)
≥400 (ng/L) n (34)	5.690 (4.853– 6.825)	4.065 (3.265– 5.447)	1.6250 (0.9475– 2.1800)	-4.045 (-7.537– (-2.400)	36.50 (23.01– 73.62)	26.56 (23.30– 32.59)
p-value	0.210	0.233	0.604	0.019	0.076	0.026
C-reactive protein (mg/L)						
<40 (mg/L) n (217)	5.090 (3.710– 6.840)	3.510 (2.940– 4.870)	1.470 (0.640– 2.300)	-3.020 (-5.600– -1.510)	29.34 (10.06– 58.04)	24.03 (17.16– 30.01)
≥40 (mg/L) n (77)	5.14 (4.07–7.35)	3.810 (2.970– 4.650)	1.640 (0.830– 2.770)	-3.28 (-5.90– -1.84)	32.52 (13.86– 59.08)	25.77 (18.58– 30.63)
p-value	0.440	0.715	0.254	0.334	0.329	0.319
Breathlessness VAS score (mm)						
0–25	4.020 (3.365– 5.275)	3.280 (2.775– 3.935)	0.7400 (0.240– 1.500)	-1.580 (-2.515– -1.135)	8.79 (3.99– 20.10)	17.83 (12.84– 23.16)
26–50	5.350 (3.650– 7.140)	3.530 (2.970– 4.870)	1.470 (0.820– 2.220)	-3.630 (-5.020– -1.840)	33.06 (15.58– 66.82)	23.84 (22.43– 31.29)
51–75	5.600 (4.525– 7.308)	3.845 (3.112– 5.025)	1.770 (0.975– 2.607)	-3.385 (-5.582– -2.030)	33.02 (17.74– 55.14)	26.51 (19.50– 31.05)
76–100	5.290 (4.110– 7.395)	3.810 (2.870– 4.930)	1.660 (1.015– 2.490)	-3.670 (-6.505– -2.340)	40.74 (19.68– 70.11)	26.83 (22.00– 31.99)
p-value	<0.001	0.010	<0.001	<0.001	<0.001	<0.001
Wheeze VAS score (mm)						
0–25	4.830 (3.610– 6.090)	3.560 (2.940– 4.250)	1.210 (0.420– 1.840)	-2.370 (-3.850– -1.300)	20.0 (6.57– 38.41)	22.53 (13.95– 26.91)
26–50	5.040 (4.120– 7.060)	3.530 (2.895– 4.830)	1.470 (0.935– 2.245)	-2.610 (-5.975– -2.025)	31.39 (14.93– 58.62)	25.91 (18.69– 30.28)
51–75	5.140 (4.120– 7.555)	3.430 (3.050– 4.895)	1.700 (1.130– 2.585)	-3.580 (-6.635– -2.085)	34.53 (19.32– 62.70)	26.37 (20.07– 31.56)
76–100	5.555 (4.460– 7.440)	3.935 (3.010– 4.995)	1.775 (0.980– 2.635)	-3.720 (-5.860– -2.062)	41.03 (18.88– 73.52)	27.01 (22.18– 32.00)
p-value	0.016	0.354	<0.001	<0.001	<0.001	<0.001

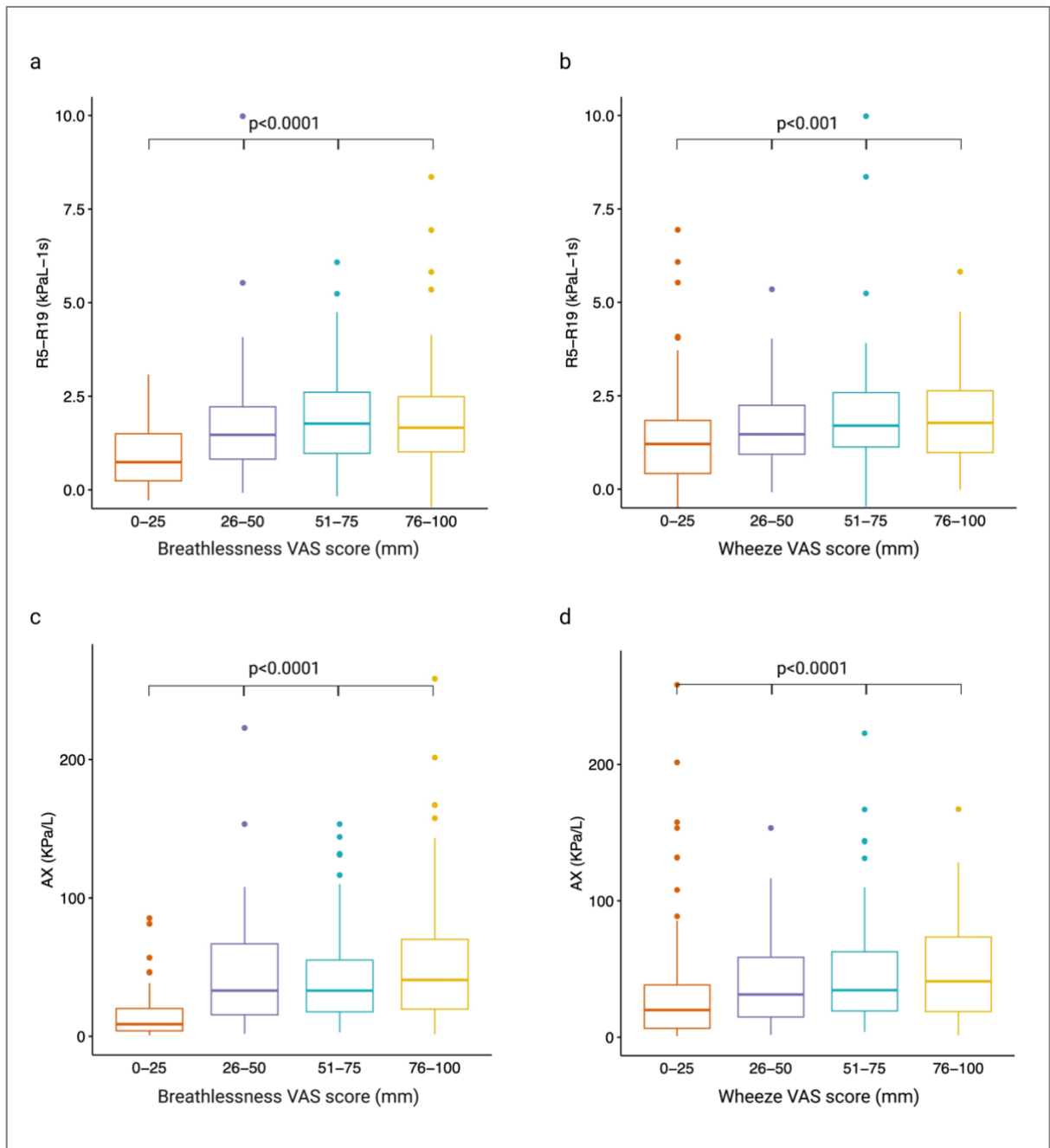


Figure 4-2 Box and whiskers plots of selected lung mechanics across breathlessness and wheeze scores

Lung mechanics represented by resistance and reactance comparing breathlessness and wheeze scores measured using visual analog scale (VAS), where higher scores represent worse symptoms. (a) R5-R19 across breathlessness scores; (b) R5-R19 across wheeze scores; (c) AX across breathlessness scores; (d) AX across wheeze scores.

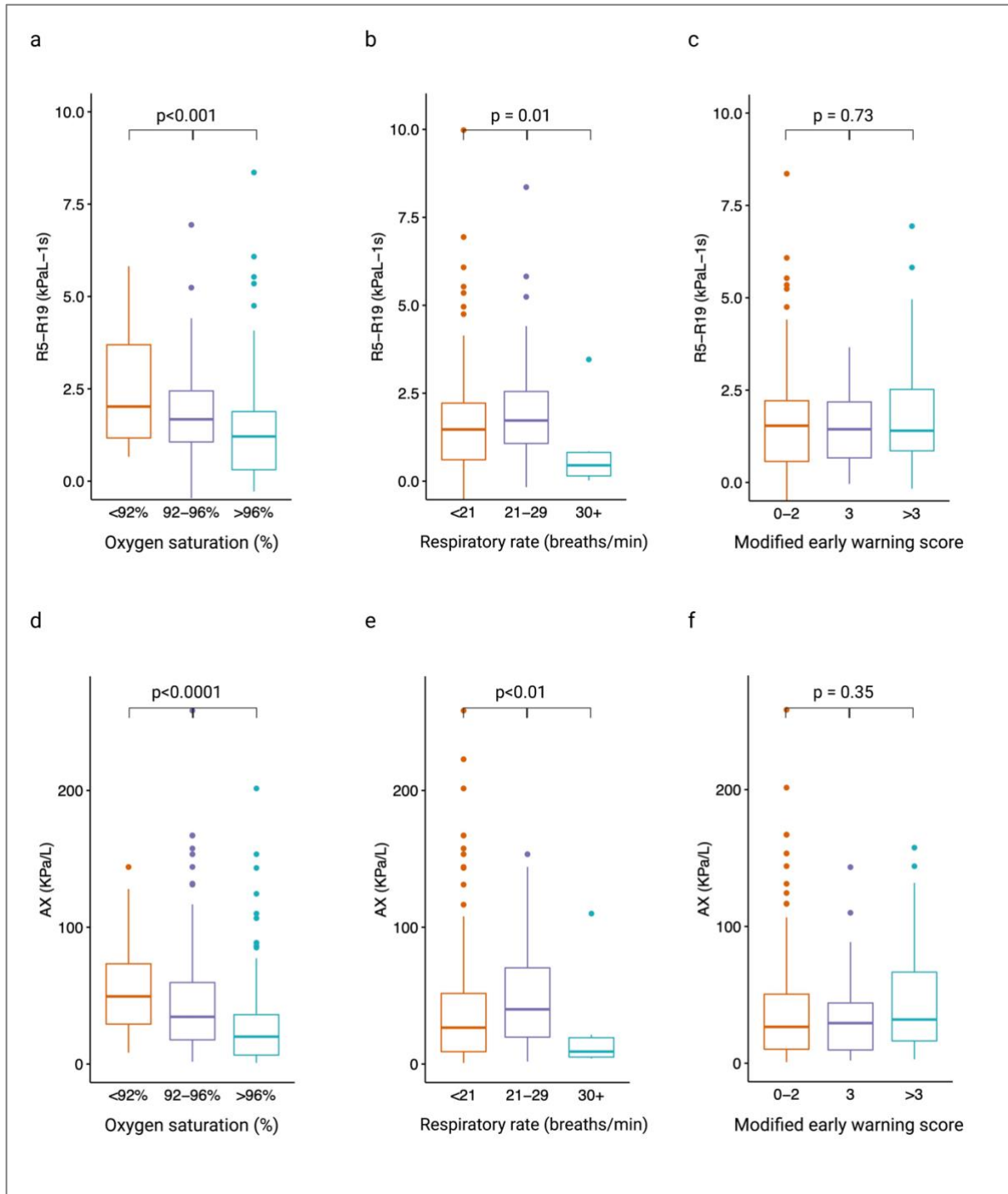


Figure 4-3 Box and whiskers plots of selected lung mechanics and clinical parameters

Selected lung mechanics representing resistance and reactance comparing oxygen saturation (SpO_2), respiratory rate, and modified early warning score (MEWS). (a) R5-R19 across SpO_2 ; (b) R5-R19 across respiratory rates; (c) R5-R19 across MEWS scores; (d) AX across SpO_2 ; (e) AX across respiratory rates; (f) AX across MEWS scores.

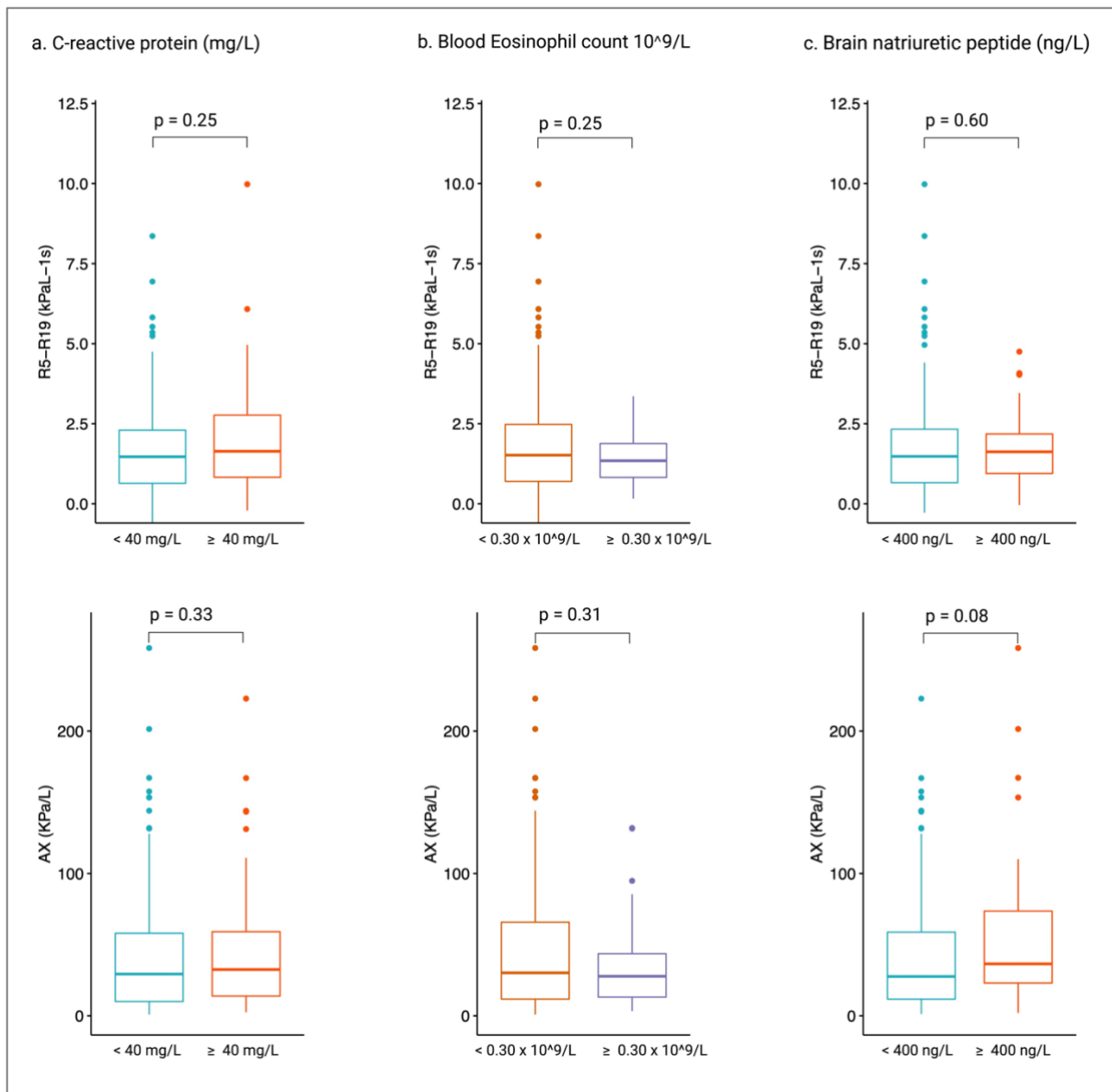


Figure 4-4 Box and whiskers plots of selected lung mechanics and blood biomarkers

Selected lung mechanics representing resistance and reactance comparing blood biomarker levels. (a) R5-19 and AX across CRP levels; (b) R5-R19 and AX across blood eosinophil counts; (c) R5-R19 and AX across BNP levels.

4.4.5 Lung mechanics and healthcare utilization

FOT at the time of hospital admission did not predict the length of hospital stay, nor hospital readmissions at 30 or 90 days ($p > 0.05$ for all measures of FOT and outcomes; data not shown).

4.5 Discussion

In this prospective observational study of patients hospitalised with acute breathlessness due to COPD, asthma, pneumonia, or heart failure, we demonstrated that lung mechanics measured using FOT are abnormal in all parameters compared to healthy individuals. These measures are most abnormal in those patients with acute exacerbations of COPD compared to exacerbations of asthma, pneumonia, and heart failure. We also showed that lung mechanics are related to symptoms of breathlessness and wheeze, as well as oxygen saturation. This supports the use of FOT in acute care settings as a direct measure of lung mechanics and a potential clinical tool.

We observed differences in acute breathlessness according to measures of both resistance and reactance. This would suggest that abnormalities in acute care settings occur in both the small airways and lung elasticity and are not specific to one aspect of lung mechanics. Similarly, changes in both resistance and reactance were similar across different aetiologies of breathlessness, despite their different underlying pathophysiologies. This is unsurprising as the cardiorespiratory diseases in this cohort cause lung infiltrates irrespective of aetiology. This means that FOT is unlikely to be useful for diagnosing the aetiology of dyspnoea; however, it could be used to monitor the respiratory system independent of cause.

Worse respiratory symptoms and low oxygen saturation were associated with abnormal measures of FOT. This was anticipated, as abnormal FOT results reflect compromised lung mechanics, which in turn might contribute to ventilation/perfusion (V/Q) mismatch, physiological shunting, and increased work of breathing. Conditions with increased airway resistance or reduced lung compliance can increase the effort required from the respiratory

muscles to move air in and out of the lungs, increasing energy expenditure and oxygen consumption. If the lungs cannot adequately meet this increased demand, irrespective of the underlying pathophysiology causing compromised respiratory function, decreased oxygen saturation levels in the blood (hypoxemia) may result. V/Q mismatch occurs when ventilation and perfusion in different areas of the lungs are mismatched, which leads to impaired gas exchange. Increased airway resistance can limit airflow to certain regions of the lungs, further contributing to V/Q mismatch, while reduced lung compliance can make moving air in and out of the lungs more difficult. Therefore, the same respiratory driving pressure will result in lower minute ventilation compared to a normal lung. In other words, the lung will achieve a reduced air exchange rate compared to blood flow, resulting in less efficient gas exchange and increasing physiological shunting, decreasing the oxygen saturation levels in the blood leaving the lungs. The presence of more negative values of X5 (indicating lower elastance) and higher values of R5-R19 or AX during acute exacerbations of respiratory conditions can be attributed to a combination of factors, such as mucus plugging, airway closure, and bronchoconstriction. These exacerbations are often accompanied by elevated levels of lung extracellular water (pulmonary edema) in patients with heart failure. These changes in oscillometry indices may be suggestive of a V/Q mismatch, indicating impaired matching of airflow and blood flow within the lungs; however, it is important to note that FOT primarily assesses oscillatory airflow and tissue mechanics. Therefore, while FOT can provide valuable insights into respiratory function, the resulting measures should be interpreted in the context of oscillatory airflow, tissue mechanics, and their reflection of ventilation heterogeneity, rather than considering them measures of the entire spectrum of V/Q matching.

Moreover, the clinical correlations were poor, meaning that FOT may provide additional information beyond clinical observation, i.e., an indication of compromised respiratory function that may not be apparent through clinical examination but is reflected by airway resistance, lung compliance, and ventilation homogeneity. Thus, FOT can offer insights to healthcare providers into the underlying dysfunctions associated with these respiratory mechanisms, such as V/Q mismatch, physiological shunting, and the increased work of breathing, that may not be readily apparent through clinical observation. This additional information can potentially help to develop more targeted treatment plans and optimize patient care, including site of monitoring (e.g., respiratory support or high-dependency units).

Surprisingly, a respiratory rate of greater than 30 was associated with lower measures of FOT. An increased respiratory rate is known to be a marker of disease severity, and, therefore, we expected to see worse in FOT measures with a high respiratory rate.

However, the observations of patients with respiratory rates over 30 may reflect inaccuracies in FOT measurements taken at higher rates, when tidal volume is less likely to be achieved. Severe tachypnoea (above 30 breaths per minute in this case) is typically characterized by shallow breathing with decreased depth and force; therefore, reduced airflow turbulence at lower frequencies may occur, as well as decreased tidal volume, minute ventilation, and lung overdistention, leading to drop in the measured resistive and reactive components of respiratory impedance. This observation should be validated for FOT to be used clinically in acute care settings, as the measures may underestimate poor lung mechanics in this case.

This is the first study to investigate FOT across multiple cardiorespiratory conditions in the acute hospital setting. A small number of studies have looked at individual conditions in hospital settings, such as COPD (288, 289) and asthma (228), mostly in the pediatric population. The existing studies have consistently shown that FOT measures are feasible in the acutely unwell patients, though none have explored differences in clinical parameters. One other study compared COPD and heart failure cases and, similar to our findings, noted worse lung mechanics in patients with COPD (289).

This study investigated FOT measures of respiratory impedance taken at the time of acute admission to the hospital; however, it did not look at recovery during the acute phase. The feasibility and speed of FOT measurement means that regular monitoring would be feasible to accurately track clinical recovery and indicate when hospital discharge is safe, much like peak flow in asthma guidelines. Future, prospective studies of this possibility would be of interest.

Moreover, in this study, we have identified changes in both resistance and reactance that distinguished the acute exacerbation groups from the healthy group using traditional respiratory impedance measurements (Z_{rs}). However, these changes were similar across cases with different exacerbation causes. Traditional oscillometry primarily focuses on the frequency dependence of respiratory impedance. Z_{rs} is averaged over multiple cycles, which fails to capture certain respiratory occurrences, such as dynamic changes in lung compliance, variations in bronchial airway resistance at different lung volumes, and changes in airway resistance in response to variations in the airflow rate or magnitude during breathing. Recent advancements in oscillometry have introduced new modalities and

measures, including intra-breath measures of respiratory impedance and airway impedance entropy, to overcome these limitations. Intra-breath measures of Zrs involve analysing changes in respiratory impedance within each breath. To do so, impedance values are captured at a high temporal resolution throughout the breathing cycle, providing detailed information about the dynamic behaviour of the respiratory system. On the other hand, airway impedance entropy is a derived measure that quantifies the complexity and unpredictability of the airway impedance signal via a mathematical calculation that reflects variability and irregularity in impedance patterns (290, 291). These measures offer a more comprehensive understanding of respiratory mechanics. Consequently, future studies should employ these techniques to investigate potential biomarkers that can differentiate between different conditions or serve as indicators of early exacerbation recovery and response to intervention.

The limitations of this study include that FOT data were not the primary outcome of the study, though they were prespecified outcome measures. As discussed above, FOT measures were only taken at the time of admission and not longitudinally. The largest limitations of the use of FOT are the interpersonal variability of the measure and that accurate normative values in this population do not exist. However, projects to generate these values are currently underway and would allow future standardised studies.

In summary, measures of lung mechanics using FOT are feasible across patients admitted to the hospital with breathlessness due to cardiorespiratory conditions. They are significantly different from healthy controls, with the worst measures seen in COPD cases. FOT is related

to measures of symptoms and respiratory failure and offers a direct measure of lung mechanics.

Chapter 5 Studies; Do Lung Mechanics Affect the Volatile Organic Compound Composition in the Breath of Patients with Cardiorespiratory Breathlessness?

5.1 Abstract

Introduction: Breathomics is a growing area in the metabolomics field that shows promise as a conventional non-invasive biomarker, which can be integrated into point-of-care devices. However, the current ways of capturing volatile organic compounds (VOCs) in the breath do not account for differences in lung mechanics. We sought to provide insight into the impact of the underlying pathophysiology components of small airway dysfunction and ventilation heterogeneity during acute hospital admission for cardiorespiratory disease on 101 breath VOCs.

Methods: A total of 208 adult patients with self-reported acute breathlessness who had both VOCs captured (ReCIVA) and underwent handheld FOT measurements within the first 24 hours of admission were included in the analysis.

Results: The resistive airflow heterogeneity in the lung did not affect the VOC function group peak area. However, tissue compliance in the lung periphery (measured using AX) seems to affect the recovery of selected VOCs; notably, O-VOCs, S-VOCs, and N-VOCs.

Conclusion: Recovered VOCs may be impacted by ventilation heterogeneity. Future breathomics studies of conditions that alter lung mechanics may need to account for this.

5.2 Introduction

Breathomics, the study of the molecular composition of exhaled breath, has gained significant interest in recent years as a potential tool for disease diagnosis, monitoring, and treatment. Breathomics is based on the idea that the VOCs present in the exhaled breath can provide information about a person's health status (292). There are several advantages to using VOC biomarkers as a diagnostic tool. First, breath samples are non-invasive and easy to collect, making them more attractive option than blood or tissue samples, as well as direct bio-sampling from the airways (293). Second, VOCs can be detected with sensitive analytical techniques, such as mass spectrometry and gas chromatography, which can provide a wealth of information about a person's health status (186). Third, breathomics could potentially be used to diagnose a wide range of diseases, including lung cancer, asthma, and chronic obstructive pulmonary disease (COPD) (196). A key challenge in the metabolomics field is that disease status is not the only element that correlates with the VOC levels in exhaled breath. Several factors have been introduced that affect the concentration and composition of breath VOCs and, therefore, affect the accuracy of these biomarkers as a diagnostic tool. These factors include diet, smoking, environment, age, and gender (192). For example, consuming alcohol can increase the concentration of ethanol in exhaled breath. Smoking and environmental pollution can introduce a range of VOCs that make identifying the specific VOCs associated with disease more challenging. Age and gender can also affect the composition of the exhaled breath, as hormonal and metabolic changes can alter VOC concentration.

Air exchange rates and the airflow patterns within a space in general are known to significantly affect particulate movement within a ventilated space (294, 295). However, the

significance of lung mechanics changes on the VOCs recovered from the breath has not yet been investigated. Healthy lungs exhibit uniform ventilation, making this less of a problem. However, in patients with cardiorespiratory conditions, for example, an acute event of respiratory disease, the lung mechanics are disrupted, leading to the uneven distribution of pressure gradients, ventilation heterogeneity, and impaired gas and air exchange.

Breathomics is a relatively new field, and much research is needed to fully understand its potential as a diagnostic tool. Therefore, in this study, we utilized pulmonary function testing to assess lung physiology across diseased and healthy participants to link ventilation heterogeneity to breathomics. We evaluated two measurements of the resistive and reactive components of lung mechanics measured by the FOT against 101 potential VOC biomarkers in the exhaled breath of patients with acute exacerbations of cardiopulmonary conditions. As particle properties, such as size and density, can contribute to particle movement within a ventilated space, the VOCs in this study were categorized into ten sets based on their functional groups, which determine their chemical and physical properties, including their volatility and toxicity, and influence their behavior, including their solubility and reactivity.

5.3 Methods

5.3.1 Study design and participants

The EMBER project (The East Midlands Breathomic Pathology Node) is a prospective study of patients admitted with self-reported acute breathlessness of cardiorespiratory diseases (1, 197). Participants were prospectively recruited between May 2017 and December 2018, for which FOT measures were collected as a predetermined secondary outcome. Informed written consent was obtained and measurements, including FOT, were performed within 24 hours of hospital admission. Healthy controls were also recruited. Full details of the protocol and inclusion and exclusion criteria have previously been published (1). The study was approved by the National Research Ethics Service Committee (16/LO/1747). In this study, we examined a subset ($n = 208$) of subjects from the total cohort who completed both breath sampling for breath VOC biomarkers and FOT measures of lung mechanics.

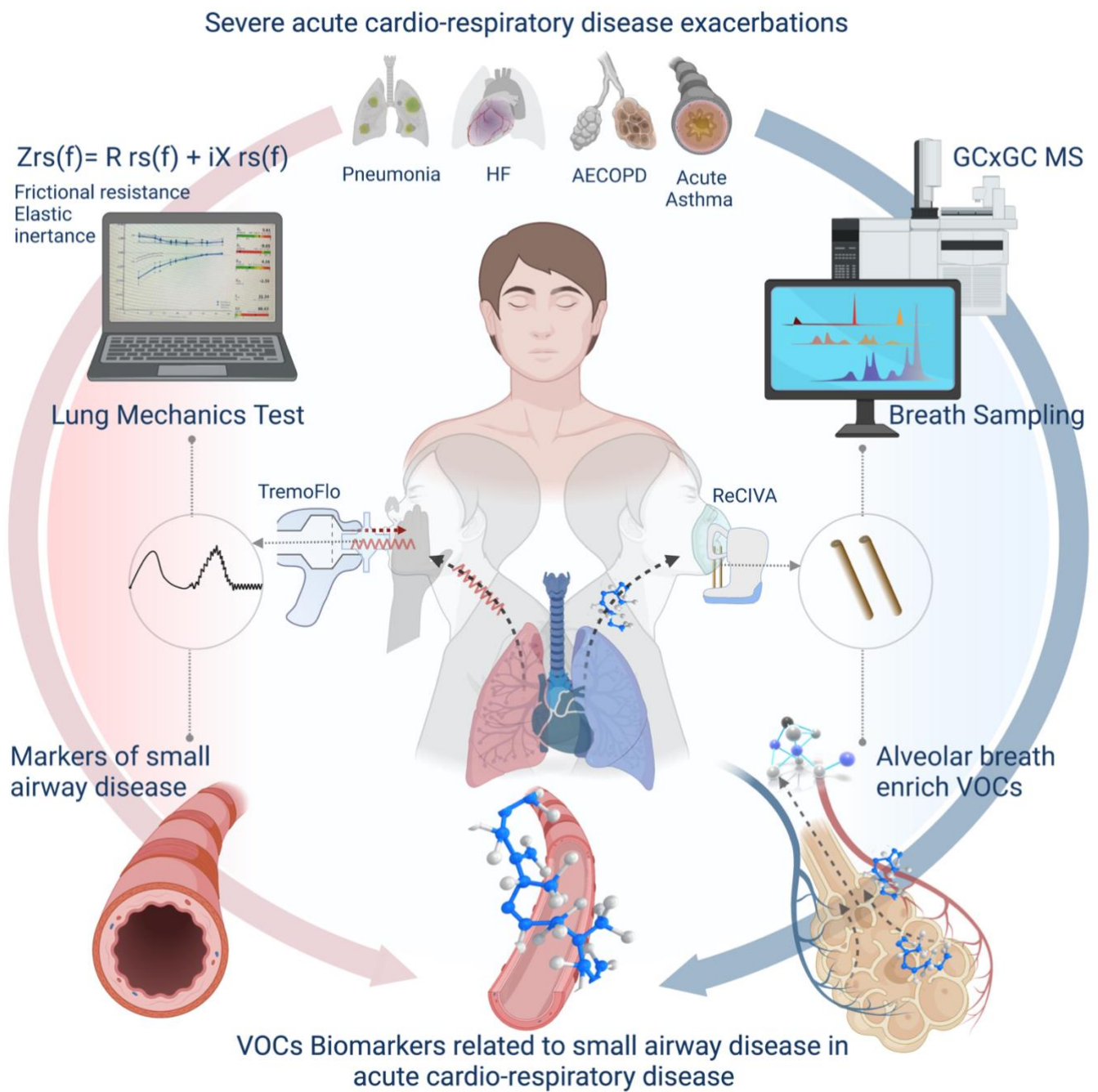


Figure 5-1 Abstract illustration of the study workflow

This study utilised FOT to differentiate acute disease (n = 173) from health (n = 35). The study was feasibly conducted using a TremoFlo device that measures respiratory impedance by superimposing external pressure oscillations using a loudspeaker. This technology delivers information that identifies and characterises central and peripheral lung mechanics using multiple frequencies (5 and 19 Hz, in this study).

5.3.2 Exhaled breath VOCs

Breath samples were collected using a commercially available breath sampler (RECIVA, Owlstone, Cambridge, UK). Breath samples, air samples, and clean air were collected on thermal desorption tubes and stored. The samples were processed with comprehensive two-dimensional gas chromatography–mass spectrometry GC×GC–MS in the chemistry laboratories at the University of Leicester, as described by Wilde et al. (2). Integrated peak areas were generated following an automated metabolomics pipeline (296). In this study, we investigated 101 VOCs previously identified in the EMBER cohort as significantly predictive of acute breathlessness (197). These 101 VOCs were assigned to ten groups based on their functional groups, grouping together those with similar physical and chemical properties. (Figure 5-2).

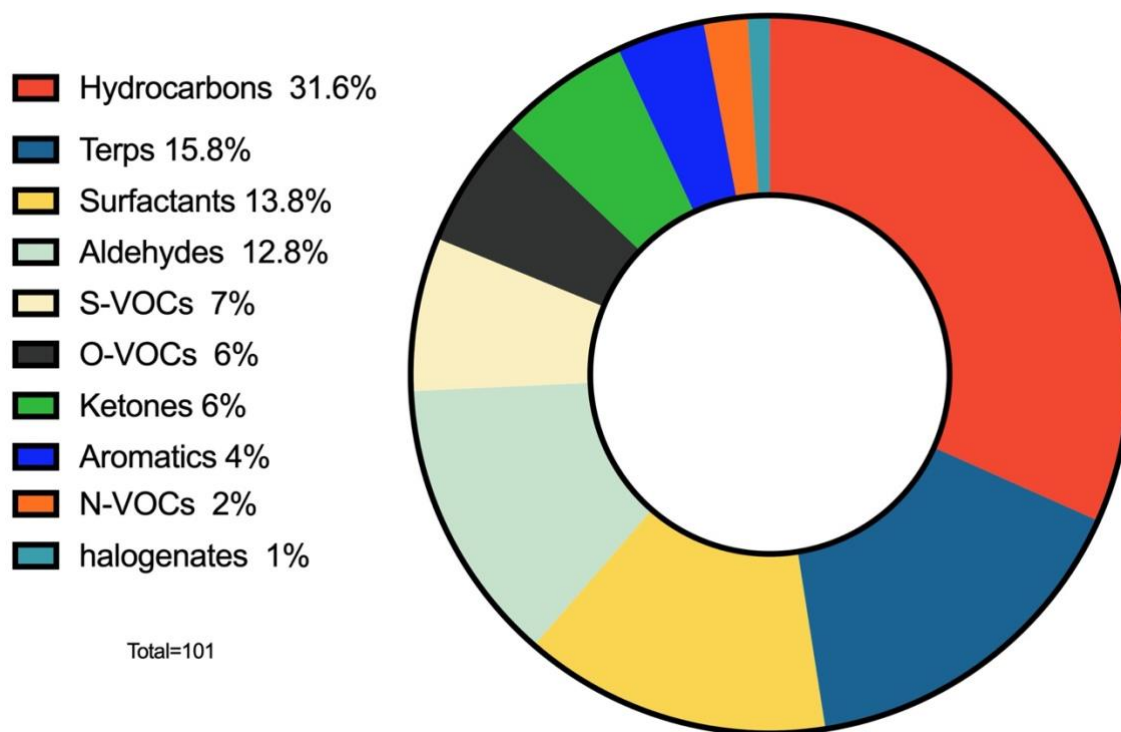


Figure 5-2 VOCs categorized according to their functional groups

5.3.3 Forced oscillation technique (FOT)

Measurements and normative values were calculated as described in Chapters 2 and 4.

5.3.4 Statistical methods

A single measure of resistance and reactance was used from FOT. Small airway resistance was measured using R5-R19 %predicted (a marker of both small airway resistance and ventilation heterogeneity) and the area under the reactance (AX) %predicted (a marker of elastic properties and ventilation heterogeneity).

Multiple linear regression models were used to examine the correlation of FOT on the VOC recovered peak area, with disease status (acute vs healthy) and smoking status (reported as packs per year) as covariates because the extracted set of VOCs in this study was associated with the exacerbation of breathlessness in acute cardiorespiratory diseases (197).

5.4 Results

5.4.1 Clinical characteristics

In total, 208 participants were included, of whom 173 patients were hospitalised for acute breathlessness (acute asthma (n=52), acute COPD (n=48), acute heart failure (n=37), or pneumonia (n=36)). 35 healthy volunteers with no history of cardiorespiratory illness were recruited as controls. The demographics were generally similar across the participants in the breathless and healthy group, other than smoking status and BMI. Clinical observations (vital signs) were significantly higher in the disease groups, except for systolic blood pressure (Table 5-1). As described in more detail in Chapter 4, FOT measures demonstrated significantly abnormal deviations in acute patients compared to healthy controls (Table 4-7).

Table 5-1 Cohort clinical characteristics

	Healthy	Acute breathlessness				p-value
		Asthma	COPD	Pneumonia	Heart failure	
Total (n) 208	35	173				
		52	48	36	37	
Demographics						
Age (years)	61.5 ±13.3	58.5 ±19.06				0.26
		40.7 ±17.9	69.5 ±8.5	56.3 ±16.9	71.4 ±10.8	<0.001
Sex (male, n (%))	19 (54.3%)	90 (52%)				0.854
		20 (38%)	27 (56%)	17 (47%)	26 (70%)	0.049
Height (m)	1.70±0.11	1.68 ±0.10				0.44
		1.67 ±0.11	1.67 ±0.09	1.69 ±0.09	1.70 ±0.11	0.37
Weight (kg)	80.9±16.2	84.6 ±25.4				0.27
		88.4 ±26.4	76.0 ±25.0	82.6 ±22.4	92.5 ±24.4	0.01
BMI (kg/m²)	28.0 ±4.4	29.9 ±8.2				0.05
		31.8 ±9.2	27.1 ±7.9	28.9 ±7.4	31.6 ±6.9	0.007
Current smoker	0 (0%)	45 (26%)				0.05
		13 (25%)	19 (39.5%)	9 (25%)	4 (11%)	<0.001
Clinical observations						
Temperature (°C)	36.2 ±0.3	36.8 ±0.6				<0.001
		36.8 ±0.6	36.8 ±0.6	37.2 ±0.8	36.6 ±0.4	<0.001
Heart rate (beats/min)	68 ±10	92 ±17				<0.001
		100 ±16	93 ±16	92 ±16	79 ±15	<0.001
Respiratory rate (breaths/min)	13 ±2	21 ±7				<0.001
		21 ±4	23 ±12	20 ±5	19 ±2	<0.001
Oxygen saturation (%)	97.8 ±1.4	95.5 ±3.1				<0.001
		96.2 ±2.6	94.1 ±3.1	95.0 ±4.4	96.4 ±1.9	<0.001
Systolic blood pressure (mmHg)	131 ±15	132 ±20				0.76
		135 ±19	133 ±21	131 ±21	128 ±22	0.5
MEWS	1 ±1	2 ±2				<0.001
		3 ±2	3 ±3	2 ±2	1 ±2	<0.001
Lung mechanics						
R5-R19 (kPa.s.L⁻¹)	0.62 (0.22–1.24)	1.780 (0.980–2.470)				<0.001
		1.33 (0.46–2.08)	2.22 (1.57–2.69)	1.35 (0.65–2.67)	1.80 (1.29–2.19)	<0.001
R5-R19 %predicted	89.98 (30.40–144.64)	167.0 (97.2–325.9)				<0.001
		113.94 (78.6–252.0)	303.89 (174.5–827.5)	172.23 (92.31–259.87)	144.47 (90.84–215.50)	<0.001
AX (KPa/L)	7.53 (3.30–16.70)	35.85 (17.61–66.26)				<0.001
		20.67 (8.33–46.90)	56.59 (36.38–86.01)	26.33 (12.84–59.38)	33.99 (26.77–58.47)	<0.001
AX %predicted	79.11	258.5 (122.2–658.3)				<0.001

	(44.08– 142.71)	128.99 (81.98– 294.44)	595.99 (350.2– 1037.6)	258.54 (127.94– 677.30)	228.49 (132.9– 399.5)	<0.001
--	--------------------	------------------------------	------------------------------	-------------------------------	-----------------------------	--------

Data are expressed as mean and standard deviation, median and interquartile range, or proportion (%). One-way analysis of variance was used for parametric data. A two-sided unpaired t-test was used for parametric data when testing two groups. Pearson's chi-squared test was used for proportions and categorical variables. MEWS: Modified early warning score.

5.4.2 VOCs vs FOT

When modeling FOT measures as predictors of VOC sets based on functional groups via linear regression, the results suggest that heterogeneity in resistance to airflow (R5-R19 %predicted) in the lungs does not affect VOC functional group peak area, which is proportionally related to compound recovery. However, tissue compliance in the lung periphery (AX %predicted) seems to affect the recovery of selected VOCs; O-VOCs, S-VOCs, and N-VOCs (Table 5-2 and Figure 5-3).

Table 5-2 Multivariate linear regression for VOC sets and FOT

Functional group	Beta coefficient	95% CI	p-value
R5-R19 %predicted			
Ketones	2.979e-06	[-1.364e-05, 1.960e-05]	0.724
Hydrocarbons	1.317e-05	[-4.615e-05, 7.250e-05]	0.662
Terps	1.016e-05	[-2.997e-05, 5.028e-05]	0.618
Aldehydes	-1.060e-05	[-3.779e-05, 1.658e-05]	0.443
Surfactants	4.812e-06	[-2.258e-05, 3.220e-05]	0.729
O_VOCs	-3.998e-06	[-1.677e-05, 8.779e-06]	0.538
S_VOCs	5.284e-06	[-1.450e-05, 2.507e-05]	0.599
Halogenates	-1.302e-08	[-3.206e-06, 3.180e-06]	0.994
Aromatics	3.673e-06	[-6.686e-06, 1.403e-05]	0.485
N_VOCs	4.654e-06	[-2.154e-06, 1.146e-05]	0.179
AX %predicted			
Ketones	-0.0001058	[-0.0003, 0.0001]	0.347
Hydrocarbons	-1.446e-04	[-0.0009, 0.0006]	0.719
Terps	-0.0001182	[-0.0006, 0.0004]	0.664
Aldehydes	-0.0002617	[-0.0006, 9.993e-05]	0.155
Surfactants	-0.0001402	[-0.0005, 0.0002]	0.450
O_VOCs	-1.779e-04	[-0.0003, -9.038e-06]	0.039 *
S_VOCs	-0.0003096	[-0.0005, -4.891e-05]	0.020 *

Halogenates	-2.290e-05	[6.541e-05, 1.961e-05]	0.289
Aromatics	-2.154e-05	[-0.0001, 0.0001]	0.759
N_VOCs	-1.077e-04	[-0.0001, -1.766e-05]	0.019 *

Formula = VOCs by functional group ~ FOT measure %predicted values + Breathless vs no breathless + smoking as packs per years

* $p < 0.05$, ** $p < 0.001$, *** $p < 0.000$.

Referring to Ibrahim et al., a total of 14 VOCs were classified within these three sets of functional groups (197). Two VOCs were identified in N-VOCs, seven in S-VOCs, and 5 in O-VOCs. The chemical assignments of these VOCs are presented in Table 5-3.

Table 5-3 Chemical assignment of significant features

Compound	CAS	HMD
Nitrogen-containing VOCs		
4-cyanocyclohexene	100-45-8	
Methenamine	100-97-0	HMDB0029598
Sulfur-containing VOCs		
3-methyl thiophene	616-44-4	HMDB0033119
Dimethyl sulfide	75-18-3	HMDB0002303
Allyl methyl sulfide	10152-76-8	HMDB0031653
Carbonyl sulfide	463-58-1	
1-(methylthio)-1- propene	10152-77-9	HMDB0059843
1- methylthio-propane	3877-15-4	HMDB0061871
Unknown (C4 thio-containing)		
Oxygen-containing VOCs		
Ethyl acetate	141-78-6	HMDB0031217
Tetrahydrofuran	109-99-9	HMDB0000246
1,4-dioxane	123-91-1	
2-methyl-1,3- dioxolane	497-26-7	
1,3- dioxolane	646-06-0	

<https://hmdb.ca/metabolites>

<https://commonchemistry.cas.org>

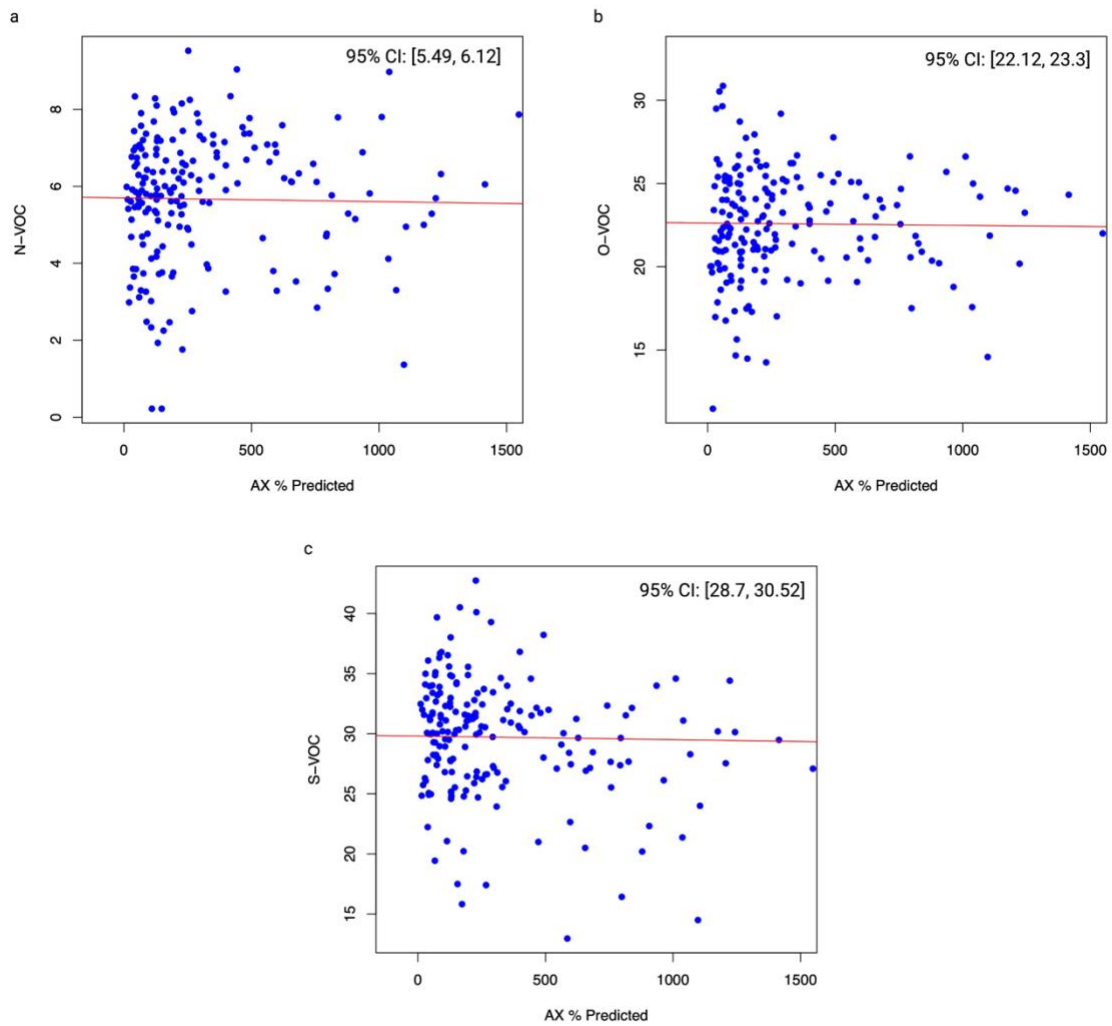


Figure 5-3 Scatter plots with regression lines and 95% CI for significant VOCs' functional groups vs AX %predicted values for subjects' height and BMI

The y-axis indicates the sum of the compounds' transformed batch-corrected peak areas within the labeled functional group; two compounds were N-VOCs, seven were S-VOCs, and five were O-VOCs.

5.5 Discussion and conclusions

In this study, we demonstrated that some groups of VOCs are influenced by ventilation heterogeneity as measured by oscillometry in patients admitted to the hospital with breathlessness secondary to cardio-respiratory illness. These observations were seen in three specific functional VOC groups and abnormal measures of reactance. This suggests that abnormal lung mechanics may affect VOCS, and potentially require to be accounted for in the field of breathomics.

The study population was acutely breathless due to cardiorespiratory illness, which frequently results in poor ventilation heterogeneity. The study's findings, presented in the previous chapter, emphasize the clinical significance of using FOT measurements to assess respiratory mechanics and ventilation heterogeneity in patients with acute cardiorespiratory conditions. In COPD exacerbations, FOT may indicate ventilation heterogeneity due to regional narrowed airways, reduced lung elasticity, and impaired airflow dynamics. Similarly, in acute asthma exacerbations, FOT may reflect ventilation heterogeneity caused by bronchial constriction, inflammation, and airway remodeling. In pneumonia, FOT abnormalities may suggest increased airway resistance and ventilation heterogeneity related to airway inflammation and lung consolidation. Lastly, in acute heart failure (HF), FOT measurements may reveal increased airway resistance and altered ventilation heterogeneity related to pulmonary congestion and fluid accumulation in the lungs. These findings highlight the utility of FOT as a valuable tool for evaluating respiratory health in various respiratory conditions. In this study, we aimed to observe the effects of altered lung mechanics and ventilation heterogeneity on breath VOC composition among

patients who present with breathlessness due to acute cardiorespiratory exacerbation events.

We identified three functional groups that were affected by changes in respiratory reactance: nitrogen-containing VOCs (N-VOCs), sulfur-containing VOCs (S-VOCs), and other oxygen-containing VOCs (O-VOCs). Nitrogen-containing, sulfur-containing, and oxygen-containing VOCs share commonalities, including volatility, chemical reactivity, acting air pollutants and sources of emissions, and their potential health effects. These VOCs are known for their ability to easily vaporize, and they can participate in various chemical reactions and atmospheric processes. In general, N-VOCs, S-VOCs, and O-VOCs can be endogenous (naturally produced in the human body as metabolic byproducts or through biochemical processes), meaning they can serve as biomarkers for physiological and pathological processes. For example, nitrogen-containing VOCs, such as amines, can be generated during protein metabolism and by gut microbial activity (297), while sulfur-containing VOCs, such as hydrogen sulfide and dimethyl sulfide, can be produced by bacteria during the digestion of sulfur-containing compounds in food (298). Oxygen-containing VOCs, such as acetone, can be metabolic byproducts during carbohydrate metabolism (299). These endogenous VOCs can be released through the breath, sweat, and other bodily excretions. Additionally, N-VOCs, S-VOCs, and O-VOCs can also originate from exogenous sources (such as the environment via agricultural, industrial, or vehicle emissions, food, medications, and other exposures) and be introduced into the body. VOCs from exogenous sources can be detected in various cellular compartments or organelles due to their distribution, metabolism, or interaction with cellular components. Their detection in biological samples can provide information about environmental contaminants, exposure

levels, diet, and other information associated with health risks or disease processes.

Endogenous and exogenous VOCs are both important components of health and disease biomarkers.

An overview of the compounds' disposition, allowing them to be classified within these three sets of functional groups obtained by referencing the Human Metabolome Database (HMDB) and relevant scientific literature. The compounds included in the N-VOC group are not commonly detected in human breath or other biospecimens and are not typically studied in relation to respiratory and cardiovascular diseases. However, these compounds may be utilized to synthesize other chemicals. Trace amounts of methenamine or its metabolic byproducts may be present in the breath due to external sources, such as medicines, diet, environmental factors, or other exposures.

The compounds in the S-VOC group are found in cellular substructure locations, such as extracellular zones and the cytoplasm. These compounds have been analysed in various biospecimens, including breath samples; allyl methyl sulfide has been studied in asthma patients and 1-methylthio-propane in healthy subjects (300, 301). These compounds have also been investigated in other biospecimens, such as feces, blood, urine, cerebrospinal fluid (CSF), breast milk, and saliva, in healthy subjects as well as in subjects with conditions such as nonalcoholic fatty liver disease, ulcerative colitis, and Crohn's disease (302-304).

The compounds in the O-VOC group are commonly found in food and beverages and are used as solvents in various industrial processes, such as the production of coatings, adhesives, and pharmaceuticals. Due to their extensive industrial use and occurrence in

various foods, this compound is a common exposure contaminant that may be detected in human biofluids. Overall, these compounds have relatively low toxicity profiles and are generally considered safe for use in industrial applications, except for 1,4-dioxane, which has been classified as a probable human carcinogen (305, 306). These compounds are also found in cellular substructures and biospecimens, including blood, feces, saliva, and urine, in the context of several conditions, including breast cancer and celiac disease (307, 308).

When considering each compound and its potential sources (endogenous or exogenous), it is speculative to make definitive conclusions. Further research is needed to fully understand the potential sources, fate, and implications of VOC compounds in exhaled breath.

Determining the origins of VOCs in breath samples has long been a challenging issue in breathomics studies. On one hand, endogenous and exogenous compounds are difficult to differentiate. On the other hand, it is also difficult to obtain certainty regarding the source of the VOCs within exhaled breath samples e.g., the VOCs in collection tubes can come from environmental contamination (exogenous origins), systemic VOCs passed through the blood circulating through the lungs, or VOC release in the respiratory system (systemic and pulmonary VOCs can be endogenous or introduced to the body from external sources, including diet or medication). This uncertainty arises from the complexity of the dynamic processes involved in the gas exchange between the lungs and the blood and between the blood and the body's tissues during respiration. Factors such as gas diffusion, blood flow, and ventilation, which are regulated by various physiological mechanisms and can be influenced by multiple variables, make the overall process intricate and challenging to fully understand and characterize. Regardless of the interpretation of the VOCs origin in this study, this observation is evidence that the statistical model and study design resulted in a

proposed set of features that are affected by the heterogeneous washout of VOCs as a result of ventilation heterogeneity.

The implications of ventilation heterogeneity on VOC washout and recovery in breath samples can be explained by several dynamics. The first is a reduction in alveolar sampling in certain areas of the lung with gas trapping and decreasing total lung capacity. The second is an increase in the sampling rate of the dead space beyond the VH-affected area. Although the breath sample collection methods are designed to collect the samples in the late expiratory phase to enrich alveolar sampling, however, in the context of physiological abnormalities that increase the measurement of physiological dead space, ventilation heterogeneity has been identified as a key pathophysiological mechanism (309). Therefore, VOCs from the trachea, conducting airway, mouth, or environment may tend to increase in concentration due to the recirculation of air from beyond the dead space. Furthermore, the physical and chemical properties of certain VOCs can affect emission and increase their retention in specific areas of the respiratory system; i.e., some VOCs' properties may make them more likely to be trapped in certain regions. For example, VOCs with higher molecular weights or lower volatility may be more prone to accumulating in specific areas of underlying abnormalities in the respiratory system.

It's critical to acknowledge that these hypotheses about VOC differences in various respiratory areas need to be validated through further research and modeling. The interplay between gas trapping, ventilation, VOCs' physical and chemical properties, and their sources in the respiratory system is complex and requires further investigation to fully understand the mechanisms underlying the observed differences in VOC levels. We call for an ongoing

need to standardise the measurement of VOCs for clinical practice and to validate this theory in the laboratory with mathematical models and a virtual lung structure. Experiments should be conducted on the healthy structure, and then homogenous or heterogenous bronchoconstriction should be imposed. Two methodologies are proposed to test the impact of VH on VOC concentration. The first is by spiking the model with known VOCs at different levels of the system (lower and upper airways, mouth) to represent systemic and pulmonary (endogenous or exogenous) VOC origins and collect VOCs during tidal breathing over a predetermined period while accounting for carrier gas diffusion. The second methodology is to examine the washout and recirculation of identified environmental (exogenous) VOCs and measure their standard dynamics density to define the kinetics of washout during different VH patterns and constrictions over a predetermined period.

This study's potential limitations include the statistical model used, which may be subject to overfitting. In overfitting, a model may perform well on the data it was trained on, but may not generalize well to new data. In this study, including disease status and smoking index in the statistical model may increase the risk of overfitting; although these variables may be strongly associated with VOC levels, they are not necessarily the only factors affecting VOC concentrations. On the other hand, not including other potential confounding factors, such as age and gender, from the statistical model could also limit the generalizability of this study. Age and gender were proposed as factors that influence VOC profiles (310), and their exclusion from the model may have caused incomplete or biased results. Considering and accounting for potential confounding variables in the analysis is important to ensure that the observed associations between VOC levels and other factors are accurate. Furthermore, it is crucial to note that the findings of this study are based on observational data, which can

only generate hypotheses and associations but cannot establish causality or definitive conclusions. Observational studies are prone to bias, and unmeasured or unknown factors may confound the results. Therefore, the findings of this study should be interpreted with caution and validated in further research using controlled laboratory models or interventional studies to establish causality and confirm the observed associations. In addition, the sample size and characteristics of the study population may limit the generalizability of the results, the findings may not be applicable to broader populations. While this study identified lung compliance, reflected by AX %predicted ($p < 0.05$), as a significant predictor of VOCs in exhaled breath within the three groups, the lack of an obvious slope in the regression line suggests that the effect size or practical significance of this relationship may be limited (Figure 5-3). Therefore, caution should be exercised when interpreting the significance of the results for specific compounds and the practical implications. Additional factors, potential confounders, and the study's limitations must be considered when interpreting the findings. Further research with larger and more diverse samples may be needed to better examine the relationship between AX %predicted and VOC recovery and enhance the generalizability of the results.

In summary, this study found that ventilation heterogeneity, as measured by oscillometry, influenced functional groups of VOCs in patients with breathlessness due to cardiorespiratory illness. Three specific functional groups of VOCs, nitrogen-containing VOCs, sulfur-containing VOCs, and other oxygen-containing VOCs, were affected by changes in respiratory reactance. The study's limitations include its limited certainty in determining the origins of the VOCs in the breath samples, the potential for overfitting or the omission of relevant confounding factors in the statistical model, its reliance on observational data,

and the need for further validation with laboratory models or interventional studies.

Despite these limitations, the findings highlight the need for ongoing studies to understand the role that the measurement of VOCs in clinical practice may play and validate this study's findings through laboratory simulations and mathematical models of known VOCs to examine the washout and recirculation rates related to changes in ventilation mechanics.

Chapter 6 Studies; Assessment of Specialized Pro-resolving Lipid Mediators (SPMs) in Asthma, COPD, and Pneumonia Patients through Hospital Admission, Acute Exacerbation, and Recovery

6.1 Abstract

Introduction: Following an acute inflammation event, the resolution of inflammation is initiated with a specific action mechanism to actively clear the inflammatory components, naturally resolving the inflammation. Specialized pro-resolving lipid mediators (SPMs) play a significant role in the resolution process. SPM dysfunction contributes to the persistence and progression of inflammatory processes, leading to the development of chronic inflammation. We aimed to investigate the composition and patterns of SPMs in respiratory disease. By enhancing the understanding of the regulation of SPMs during acute events with chronic and new-onset inflammation conditions, we sought to uncover their potential implications as clinical biomarkers for disease diagnosis and prognosis.

Methods: In this study, a solid-phase extraction (SPE) protocol for targeted LC–MS analysis utilizing triple quadrupole mass spectrometry was optimized, and a panel of 13 SPMs was quantified during the acute phase post-exacerbation into the recovery phase in the sputum samples of patients presenting with acute asthma (n=37), AECOPD (n=45), and pneumonia (n=37) and a healthy control group (n=22).

Results: Significant differences were observed in PGE2 levels among the studied groups ($p = 0.006$), and the post-hoc analysis revealed that AECOPD patients had significantly higher PGE2 levels compared to acute asthma patients ($p \leq 0.01$) and healthy subjects ($p \leq 0.001$). Pneumonia subjects had significantly higher PGE2 levels compared to healthy individuals ($p = 0.03$). In the stable cohorts, no significant differences in PGE2 levels were observed. The correlation analysis showed associations between PGE2 levels and clinical parameters.

Eosinophil count exhibited a significant negative correlation with PGE2 level (coefficient = -0.21, $p < 0.05$), while a significant positive correlation was found between neutrophil count and PGE2 level (coefficient = 0.24, $p < 0.05$).

Conclusions: PGE2 level variations between the studied groups suggest their potential use as biomarkers for distinguishing between healthy and diseased subjects, with AECOPD exhibiting the highest median PGE2 levels. The correlation analysis revealed associations between PGE2 levels and eosinophil and neutrophil counts, emphasizing the intricate interaction between SPMs and the immune cell populations participating in the inflammatory response.

6.2 Introduction

Inflammation is the natural protective biological response to tissue injury and infection (e.g., trauma, wounds, bacterial or viral infection, allergies). Previously, it was widely believed that the resolution of inflammation occurred passively, with the assumption that all infiltrated cells and residual debris from the inflammatory process resolved over time. However, recent studies have revealed that this perception was inaccurate. It is now known that the resolution of inflammation is an active process that occurs following acute inflammation. This process is distinct from the anti-inflammatory response mechanism that blocks and inhibits the triggered inflammatory response (311-315).

Specialized pro-resolving lipid mediators (SPMs) are the biological compounds that actively drive the resolution process by directing leukocyte actions, promoting the resolution of acute inflammation, reducing pro-inflammatory signals, stimulating tissue repair mechanisms, and promoting the transition of immune cells from pro-inflammatory to pro-resolving phenotypes (316). Four groups of SPMs have been defined based on their chemical structures: resolvins, protectins, maresins, and lipoxins. These are biosynthesized and regulated as byproducts of breaking down omega-3 and omega-6 fatty acids in leukocyte-rich exudates (311, 317-322). Because of these compounds' different molecular structures and stereochemical and physical properties, their chromatographic behaviour can be defined and used to identify or quantify them to explore their role in human physiology and disease. These known families of SPMs were identified by the Serhan group, which conducted much of the seminal work in SPM detection and identification (323).

SPMs can be detected systemically, as well as in various biological samples and tissues. The majority of the research into SPM detection and quantification has been performed to study the immune system. SPMs increase when the inflammatory process initiates. They then peak and resolve over time until the inflammation is resolved at the tissue level, returning the tissue to homeostasis. Subsequent studies have examined SPMs' roles in different diseases, particularly those characterized by a degree of chronic inflammation. In such conditions, the inflammation never completely resolves to a state of hemostasis, causing a tissue-specific low grade of unresolved, persistent inflammation that leads to a dysfunctional tissue phenotype.

Inflammation is key in the pathogenesis of COPD and asthma and triggered by various factors. Both COPD and asthma are characterized by chronic inflammation, persistent symptoms, ongoing lung damage, and exacerbation events. On the other hand, pneumonia is an inflammatory respiratory disease caused by infection. The timely resolution of inflammation is crucial for the healing of lung tissue in pneumonia cases as impaired resolution might lead to chronic inflammatory foci, where sites in the lungs have persistent inflammation despite addressing or resolving the initial cause of symptoms (324).

Because of the growing recognition of the chronic inflammatory component within respiratory conditions, SPM studies in the context of respiratory diseases have garnered more interest. Yang et al. conducted a review that investigated SPMs and their mechanisms in pulmonary diseases including tuberculosis, asthma, COPD, cystic fibrosis, pneumonia and bronchopulmonary dysplasia, and ALI/ARDS (325). In that review, studies that examined SPMs in serum, sputum, bronchoalveolar lavage fluid, and the exhaled breath of asthma

patients demonstrated a correlation between LXA4 and asthma severity, oxidative stress, lung function, hyperresponsiveness, mucous epithelial metaplasia, and the resolution of inflammation (326-328). Other experiments in animal models of asthma affirmed the effect of LXA4 on allergic pulmonary inflammation, airway endothelial cell repair, and maintaining the homeostasis of airway endothelial cells (329). Studies have also examined the roles of Mar1 and PD1 within the airways in impeding the proliferation of eosinophils, T lymphocytes, and the production of inflammatory factors (133, 330). An additional study utilized a self-limited allergic airway inflammation model and suggested that RvE1 supports the resolution of inflammation in allergic pulmonary conditions (331). Meanwhile, COPD studies have shown that RvD1 and LX levels are decreased in COPD patients' serum, sputum, and exhaled breath samples (332-334). Two studies reported RvD1's role in reducing neutrophils and cells stimulated by smoking to reduce inflammation, oxidative stress, and cell death (333, 335). Studies have also suggested that resolvins might be important in controlling COPD exacerbations triggered by smoking by promoting macrophage recruitment and the activation of type M2 macrophages, thus promoting the resolution of the inflammatory response (333, 336, 337). In pneumonia, the review described how SPMs, such as PD1, RvD1, and LXs, played roles in various infections observed in animal model studies. (325). *Streptococcus pneumoniae* infection was associated with reduced levels of eicosapentaenoic acid-derived resolvins (e-series resolvins) and lipoxins (338). In *Pseudomonas aeruginosa* pneumonia, RvD1 expression is decreased, but exogenous RvD1 and exogenous aspirin-triggered resolvin D1 (AT-RvD1) both inhibit inflammatory pathways, reducing macrophage activation and inflammatory factors in both in vitro and in vivo studies (155, 339, 340). AT-RvD1 also can reverse the inflammatory environment triggered by *Haemophilus influenzae* infection (324). In viral infections, such as H1N1, the precursor to

lipid mediators, 17-HDHA, increases anti-viral antibodies, potentially enhancing the immune response (341). The omega-3 polyunsaturated fatty acid (PUFA)-derived lipid mediator PD1 demonstrated promising result as a potential treatment for inhibiting H5N1 virus separation (342). These findings highlight the significance of lipid mediators in infection-related inflammation and tissue repair. Yang et al.'s review sheds light on the significant correlation between SPMs and the underlying pathogenesis of respiratory inflammatory conditions. Consequently, a promising avenue for future research entails the development of biomarkers and investigation of potential pharmacological interventions or methods to enhance the natural production of SPMs, such as targeting signaling responses and modulating the activity of key immune cells, including neutrophils, eosinophils, NETosis, and macrophages, to restore host homeostasis and thereby make valuable contributions in the management of these diseases.

Despite the promising established work that holds potential in term of possible new treatment strategies, minimal work has been done to describe a larger panel of SPMs in sputum samples taken during acute events and in stable status of asthma, COPD, and pneumonia individually, with no work has been done across the three conditions. In light of this, we sought to quantify a larger panel of SPMs in sputum samples, describing a panel of 13 SPMs measured via targeted LC–MS/MS analysis to compare acute asthma, acute COPD and healthy volunteers, as well as quantify SPMs post-recovery in the acute populations. We hypothesize that there will be (1) SPM profiles that are unfavorable following an acute exacerbation of asthma, COPD, or pneumonia compared to healthy controls and (2) a dysfunctional SPM profile in our patient populations that does not return to homeostasis post-recovery.

6.3 Methods

This study employed specific sample selection, preparation, and analysis methods, summarised in Figure 6-1.

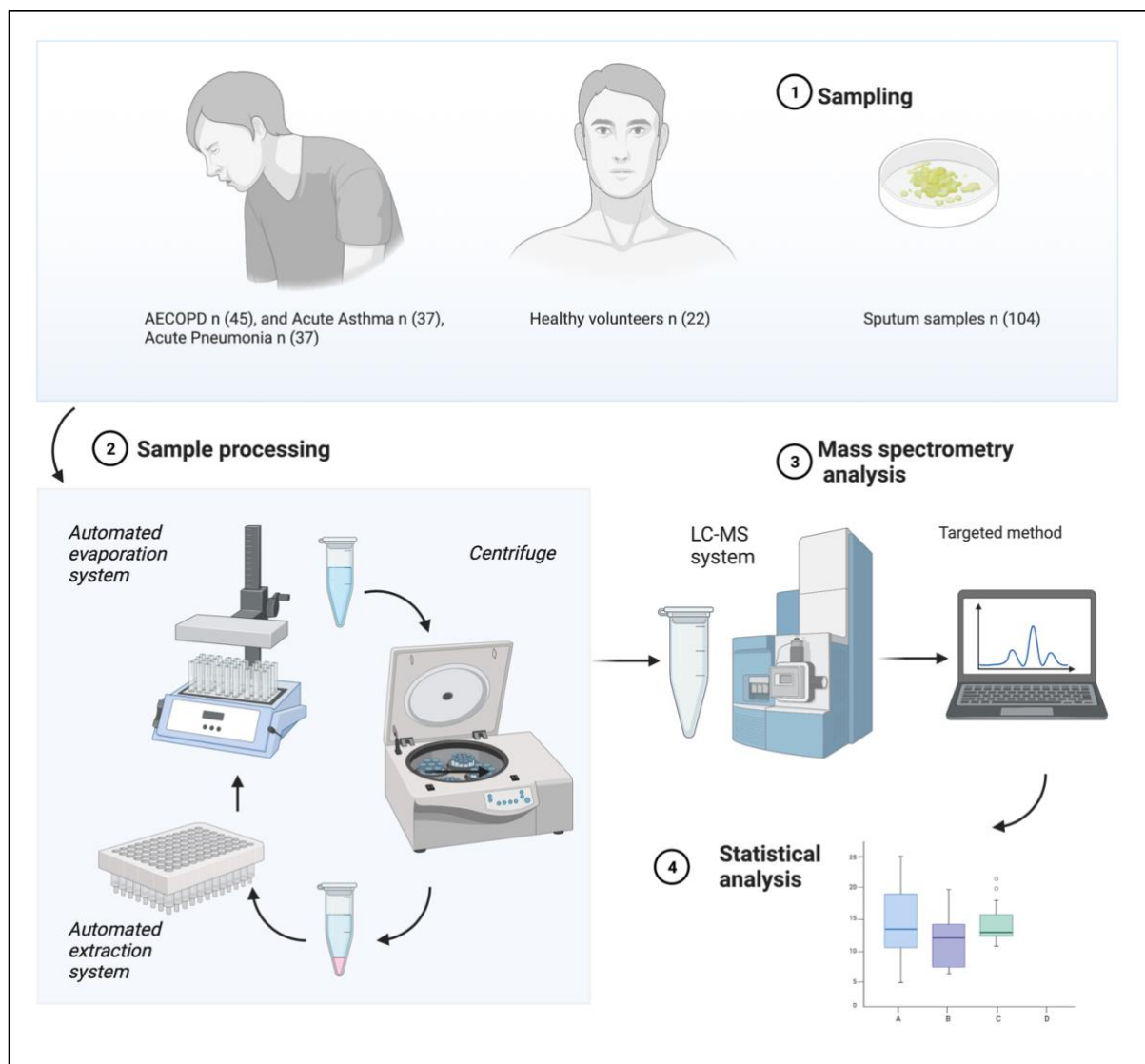


Figure 6-1 Illustration of the study process; sample collection, preparation, and analysis

(1) Sputum samples were collected from patients admitted to the hospital with acute asthma, exacerbations of COPD, or pneumonia within 24 hours of admittance. (2) The SPE protocol was employed, incorporating an automated evaporator and extraction system. (3) The LC-MS analysis was optimized using automated software for targeted analysis by applying peak selection criteria to generate data. (4) A standard statistical analysis was performed to report the study results.

6.3.1 Study design and participants

This is a prospective study of patients admitted to the hospital with a primary clinical diagnosis of acute asthma, exacerbation of COPD, or pneumonia between May 2017 and December 2018 as part of the Exhaled Breath Metabolomic Biomarkers in the Acutely Breathless Patient (EMBER) study (1, 260). The sputum samples utilized in the study were originally collected as part of the EMBER study protocol and stored in a biological bank to be examined in future research. Informed written consent was obtained from participants, including for the collection of sputum samples within 24 hours of hospital admission. Participants were also invited to attend a stable-state follow-up visit once they had clinically recovered from their hospital admission, at least six weeks following their discharge. A control group methodology was applied; healthy individuals with no history of prior cardiorespiratory illness were recruited as controls. Full details of the protocol and inclusion and exclusion criteria have previously been published (1). The study was approved by the National Research Ethics Service Committee (16/LO/1747). The process of subject inclusion and exclusion is outlined in the chart below. Figures 6-2 and 6-3 represent the criteria used to determine the participants included in each cohort of the study's sample selection process.

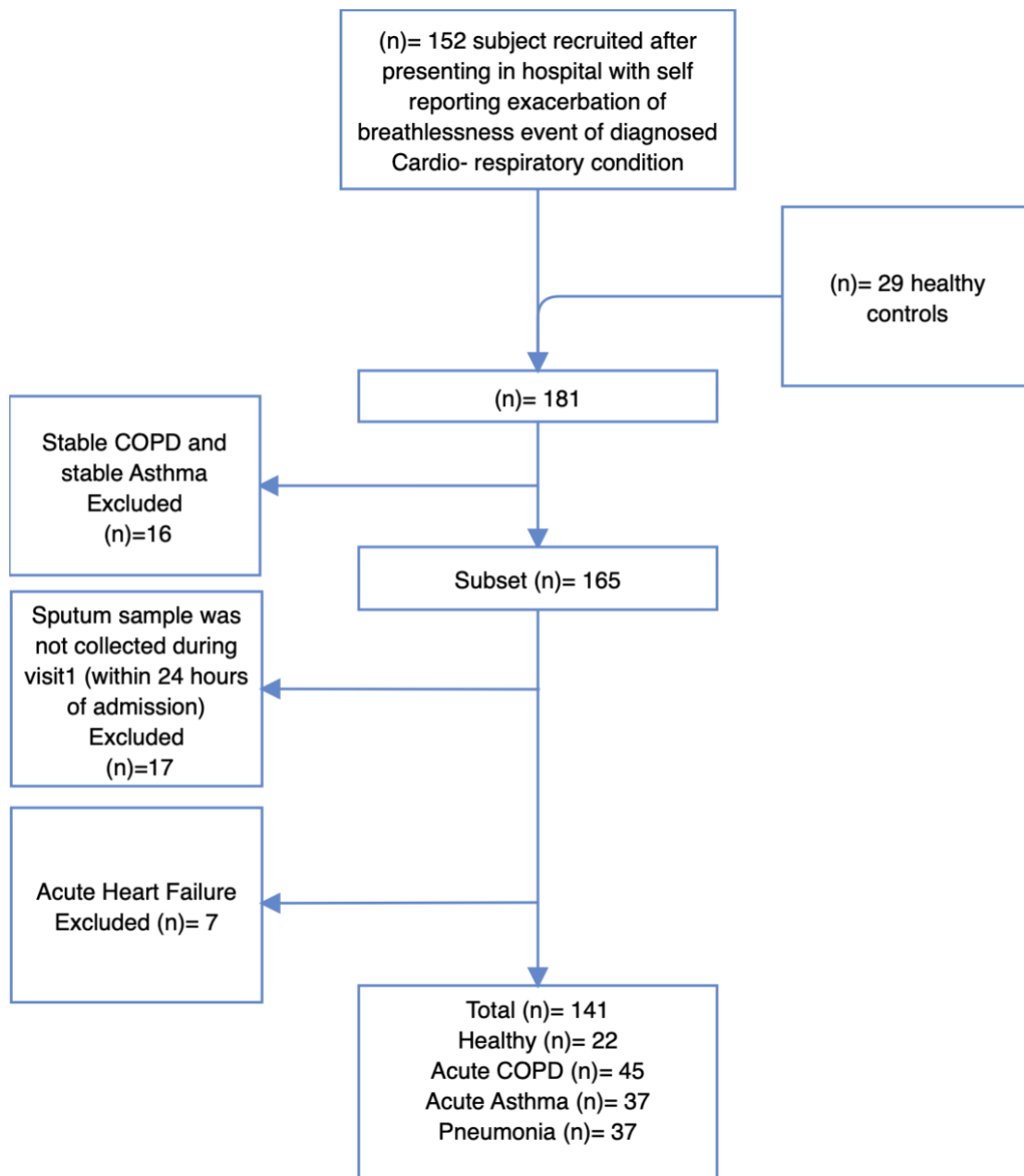


Figure 6-2 Summary of sample selection and inclusion/exclusion criteria for the acute cohort of the study

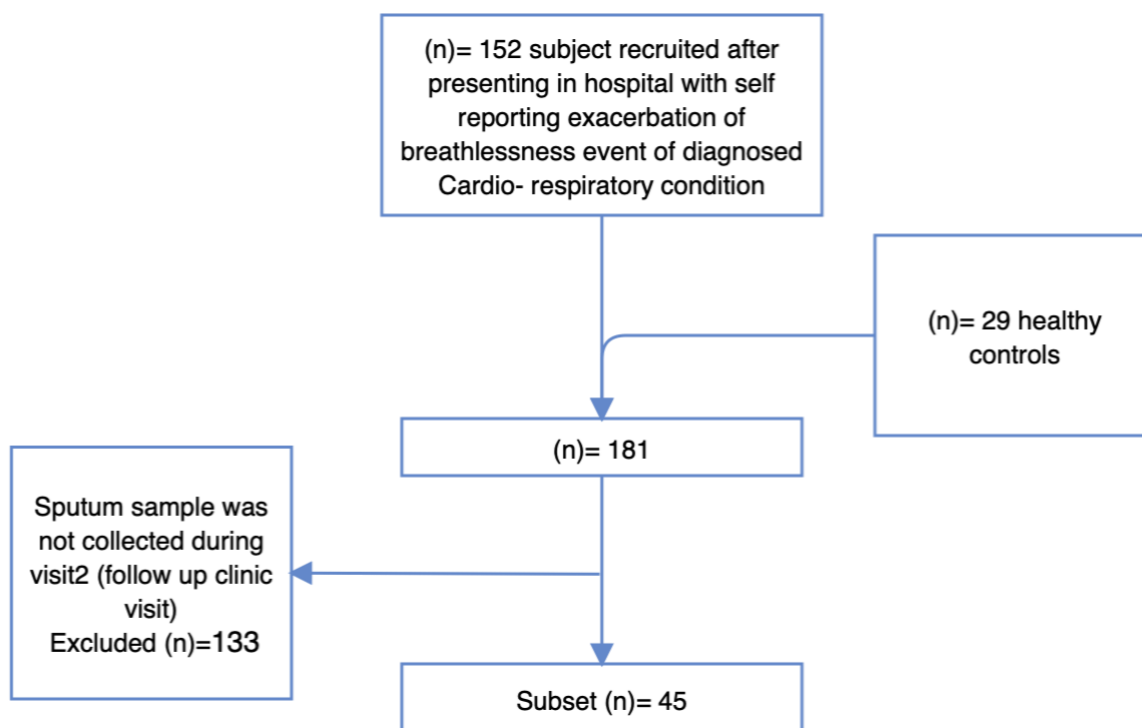


Figure 6-3 Summary of sample selection and inclusion/exclusion criteria for the stable cohort of the study

6.3.2 Solid-phase extraction and sample preparation for SPM detection

In this study, we optimized the samples for tandem liquid chromatography–mass spectrometry (LC–MS/MS) analysis for the detection of 13 compounds in the SPM family. Solid-phase extraction (SPE) was applied to filter the sample from the proteins and large lipids while maintaining the small lipid compounds of interest. This filtration process decreases the background noise in the mass spectrometry results, generating a cleaner signal for detecting the SPMs. The methodology and applied protocol were carefully adjusted and developed to align with the study settings, including sample storage,

preparation, and analysis, with a focus on sputum samples. Factors like proper storage at -80°C, sample volume, and safe handling techniques were considered to optimize the analysis. Compatibility with the laboratory equipment, especially the mass spectrometry instrument, was also accounted for, and experimental runs were performed to enhance parameters such as sensitivity and detection limits to achieve the highest possible recovery rate via optimal extraction techniques, solvent selection, and sample handling. Moreover, through experimentation with standards, the recovery rate of SPMs during the analysis process was further optimized. process. These included assessing the recovery rate when running the samples immediately after preparation versus next day frozen prepared samples, comparing manual methods to automated equipment methods, testing different drying techniques such as using larger TurboVap tubes or smaller 1 ml tubes, and evaluating the recovery rate when using different volumes of agents (e.g., 3 ml versus 5 ml of hexane). Furthermore, we examined the effect of the water level in the TurboVap, by comparing the results when using a full tank (where water touches the tube walls) or a low water level (where water does not touch the tube walls). These meticulous tests and comparisons allowed us to refine the protocol to ensure that the methodology yielded reliable, accurate results when analyzing SPMs in the sputum samples. By continuously refining the protocol and exploring different approaches, we were able to achieve an average recovery rate of 53% (MaR1) to 85% (RvE1).

All samples were initially spiked with a known amount of the internal standard (20 µL of LTB4-d4 at 0.5 pmol/µL diluted in 40% MeOH to 60% H₂O) to ensure accurate, precise measurements of the target analyte. The internal standard is used for calibration, allowing any variations in sample preparation, extraction efficiency, and instrument response to be

normalized. Its presence in the samples allows the concentration or relative abundance of the SPMs of interest to be determined and enables accurate calculation of their levels in the samples. Column-based methodologies (Isolute® C18 500mg/6ml, Biotage, Sweden) were used in the SPE sample processing. Proteins were precipitated via incubation in ice-cold methanol for 45 minutes at -20°C before centrifugation. The columns were conditioned with 3 ml of iced methanol before running samples through them to establish a stable baseline, remove impurities, ensure solvent compatibility, wet the stationary phase, and remove air bubbles. They were then washed with 6 ml of nanopure water to remove any residual methanol in the column, further stabilize the baseline, and remove any remaining impurities or contaminants that could interfere with the separation and detection of analytes. Furthermore, 20 µL formic acid (HCOOH) mixed with 90 ml nanopure water was utilised as a solvent medium when running the samples through the isolate columns. In aqueous solutions, HCOOH dissociates to release hydrogen ions (H⁺) and formate ions (HCOO⁻), exhibiting its acidic properties. The targeted pH level of 3.0 to 3.5 was assessed using a pH meter (Mettler Toledo SevenEasy, Mettler-Toledo International Inc). Adjusting the pH enhanced the extraction efficiency of the target compounds. The acidified water helped promote analyte ionization and improved their retention in the C18 stationary phase of the column. In addition, 5 ml of hexane was used to bind and pull the larger lipids through the column filter. Hexane is a nonpolar organic compound that has a strong affinity for lipids, particularly those with larger molecular sizes. When a sample mixture containing lipids is passed through the column, hexane selectively interacts with the larger lipids, forming complexes with or solvating them and effectively pulling them out of the sample matrix. Then, 9 ml of methyl formate was used to unlock the column filters to collect the isolated sample. Methyl formate disrupts the interactions between the analytes and the stationary

phase of the column, allowing the analytes to be released and collected as the eluent flows through. For efficient, consistent sample drying, an automated nitrogen evaporator system was utilized (TurboVap[®], Biotage AB, Sweden). To enhance the efficiency and speed of sample processing through the columns, an automated extraction system (Biotage[®] PRESSURE+, Biotage AB, Sweden) was used to allow for precise control of pressure and flow, reduce manual handling, and increase the reproducibility of the sample preparation workflows. The LC–MS targeted analysis was performed immediately after sample preparation whenever possible. Table 6-1 presents a detailed description of the SPE protocol utilizing equipment such as a centrifuge, pH meter, automated evaporator, and automated extraction system. The table presents equipment-specific settings, durations, pressure levels, flow rates, and volumes, offering a thorough overview of the SPE protocol used in this study.

Table 6-1 Comprehensive description of the solid-phase extraction (SPE) protocol and parameters for the automated evaporator and automated extraction system

Solid-phase extraction and sample preparation: Machinery method	
1	Mix 4 ml ice-cold methanol with approximately 1 ml weighted sample, label, and place in fridge for 45 min. Then, pre-set centrifuge to 4°C. Set timer and wait.
2	Arrange samples balanced on both sides in the centrifuge, using balancing samples if needed, and set RCF to 2000 for 10 minutes.
3	Prepare columns (isolate c 18) by running 3 ml of iced methanol, followed by 6 ml of pure water. Settings for automated extraction system: Conditioning with 3 ml of iced methanol: 2 psi Washing with 6 ml of pure water: 10 psi
4	Move samples to a new TurboVap Pyrex tube, leaving solid protein behind, and label.
5	Transfer samples to TurboVap drying system to evaporate methanol until less than 1 ml of sample remained (targeting 0.5 ml remaining). Settings: TurboVap water tank level 5.5 L Temperature: 37°C Flow: 1.2 L/min Time/flow: at 10 min, increase the flow to 1.6 L/min Time/flow: at 20 min, increase the flow to 1.8 L/min Time/flow: at 30 min, increase the flow to 2 L/min Approximate finish time: 45 min*
6	Place samples and set RCF to 2000 for 10 minutes (temperature preset to 4°C).
7	Mix 20 µL of formic acid with 90 ml of pure water to target pH of 3.0 to 3.5.
8	Add 5 ml of acidified water to each sample, mix, and run through columns immediately at a slow rate. Then, wash residual acid with 6 ml of pure water. Settings for automated extraction system: Loading sample using acidified water: 2 psi Washing with 6 ml pure water: 10 psi
9	Run 5 ml of hexane through column. Setting for automated extraction system: Washing with 5 ml hexane: 1 psi
10	Run 9 ml of methyl formate through column and use a collection tube to collect isolated sample. Setting for automated extraction system: Eluting with methyl formate: 0.5 psi
11	Dry samples with nitrogen gas using TurboVap system until <1ml remains (ideally around 0.5 ml) Settings: TurboVap water tank level: 5.5 L Temperature: 37°C Flow: 0.5 L/min Time/flow: at 4 min, increase the flow to 0.8 L/min Time/flow: at 8 min, increase the flow to 1.0 L/min Approximate finish time: 10 min*

	<p>When < 1ml remains, rinse inner tube walls with 1 ml of methyl formate, then resume the flow. Temperature: 37°C Flow: 1.2 L/min Approximate finish time: 5 min*</p> <p>When <1ml remains, rinse inner tube walls with 1 ml of ice-cold methanol, then resume the flow. Temperature: 37°C Flow: 1.2 L/min Approximate finish time: 5 min*</p>
12	<p>When <1ml remains, transfer sample to 1-ml tubes and label. Customise TurboVap system with size-appropriate tube tray. Settings: Temperature: 37°C Flow: 0.8 L/min Time/flow: after 10 min, increase the flow to 1.0 L/min Time/flow: at 20 min, increase the flow to 1.2 L/min Approximate finish time: 50 min*</p>
13	<p>When solvent is evaporated and sample is completely dry, add 20 µL of methanol/water (40:60). The 40% MeOH suspension solution is optimised for liquid chromatography; higher MeOH content in the suspension solution risks eluting the study compounds in the solvent front rather than retaining them on the column.</p>
14	<p>Mix sample, then place it in the Micro Centaur centrifuge device (balance samples as needed). Settings: Time: 1 min Speed: 10x 1000 rpm</p>
15	<p>Transfer supernatant to LC–MS vials (Waters, 12x32 mm glass screw neck vial) without dislodging precipitate. Remove any air bubbles. The sample is ready for LC–MS/MS analysis.</p>
	<p>To maintain the sample’s low temperature during preparation, ice was used consistently. *Finish times varied depending on the tank water level and nitrogen cylinder pressure (inversely proportional).</p>

6.3.3 LC–MS targeted analysis

The ACQUITY UPLC I-Class PLUS chromatography system was utilized. The LC-MS system used was the Xevo TQ-XS Triple Quadrupole Mass Spectrometry. To ensure accurate quantification and comparison, a standard control of lipidomic standards mix and an internal standard, LTB4-d4, were run in the mass spectrometry instrument before and after

analysing the samples each day. This was done to establish a baseline and validate the analytical method, ensuring the reliable measurement of SPM levels in the samples and allowing for proper interpretation of the results. The standards used are detailed in Table 6-2.

Table 6-2 Lipidomic standards and internal standard, including concentrations and volumes utilized for method validation of the LC–MS analysis.

	Lipidomics	Concentration	Volume used
Standard control	Resolvins (RvE1, RvD1, RvD2, RvD5) Leukotriene B4 (LTB4) Lipoxins (LXB4, LXA4) Prostaglandins (PGE2, PGD2, PG2a) Maresins (MaR2, MaR1) Protectin D1 (PD1)	Diluted in 40% MeOH to 60% H ₂ O at a concentration of 0.5pmol/μL for each compound	20 μL
Internal standard	Deuterated form of leukotriene B4 (LTB4-d4)	Diluted in 40% MeOH to 60% H ₂ O at a concentration of 0.5 pmol/μL	20 μL

When the solvent had evaporated and the sample was completely dry, 20 μL of methanol/water (40:60) was added. The 40% MeOH suspension solution had been optimised for liquid chromatography. Three injection runs were made with each sample (2μL each). The targeted methods were selected for the 13 SPM panels based on Colas et al. (323). Waters MassLynx Software and the TargetLynx application manager were used to process results and generate the data matrix. A detailed description of the parameters is

given in Table 6-3.

Table 6-3 MS parameters, software, and targeted methods for data generation

LC-MS targeted analysis																													
1	<p>Start by loading samples into the ACQUITY UPLC I-Class PLUS chromatography system https://www.waters.com/waters/en_GB/UPLC-inlet-to-MS-with-the-best-dispersion/nav.htm?cid=134613317&icid=lg-othr_00099&locale=en_GB</p> <p>First, three solvents (blanks) are loaded, then three standards, then the samples, and finally, three standards again to ensure that there is no change in the retention time. The following LC-MS parameters were applied for the analysis:</p> <table border="1" style="margin-left: auto; margin-right: auto;"> <tbody> <tr> <td>Mobile phase A</td> <td>0.1% formic acid</td> </tr> <tr> <td>Mobile phase B</td> <td>Acetonitrile plus 0.1% formic acid</td> </tr> <tr> <td>Seal wash</td> <td>10% methanol/water</td> </tr> <tr> <td>Purge wash</td> <td>0.1% formic acid</td> </tr> <tr> <td>Sample manager/needle wash</td> <td>Acetonitrile plus 0.1% formic acid</td> </tr> <tr> <td>Column</td> <td>Premier peptide BEH C18, 300A, 1.7µm, 2.1 times 50mm (from Waters Ltd.)</td> </tr> <tr> <td>Dwell time</td> <td>0.008 seconds</td> </tr> <tr> <td>Capillary voltage (kV)</td> <td>0.5</td> </tr> <tr> <td>Sample cone (V)</td> <td>35</td> </tr> <tr> <td>Electrospray ionization mode</td> <td>Negative</td> </tr> <tr> <td>Source temperature (°C)</td> <td>150</td> </tr> <tr> <td>Desolvation temperature (°C)</td> <td>600</td> </tr> <tr> <td>Cone gas (L/hour)</td> <td>150</td> </tr> <tr> <td>Desolvation gas (L/hour)</td> <td>1000</td> </tr> </tbody> </table>	Mobile phase A	0.1% formic acid	Mobile phase B	Acetonitrile plus 0.1% formic acid	Seal wash	10% methanol/water	Purge wash	0.1% formic acid	Sample manager/needle wash	Acetonitrile plus 0.1% formic acid	Column	Premier peptide BEH C18, 300A, 1.7µm, 2.1 times 50mm (from Waters Ltd.)	Dwell time	0.008 seconds	Capillary voltage (kV)	0.5	Sample cone (V)	35	Electrospray ionization mode	Negative	Source temperature (°C)	150	Desolvation temperature (°C)	600	Cone gas (L/hour)	150	Desolvation gas (L/hour)	1000
Mobile phase A	0.1% formic acid																												
Mobile phase B	Acetonitrile plus 0.1% formic acid																												
Seal wash	10% methanol/water																												
Purge wash	0.1% formic acid																												
Sample manager/needle wash	Acetonitrile plus 0.1% formic acid																												
Column	Premier peptide BEH C18, 300A, 1.7µm, 2.1 times 50mm (from Waters Ltd.)																												
Dwell time	0.008 seconds																												
Capillary voltage (kV)	0.5																												
Sample cone (V)	35																												
Electrospray ionization mode	Negative																												
Source temperature (°C)	150																												
Desolvation temperature (°C)	600																												
Cone gas (L/hour)	150																												
Desolvation gas (L/hour)	1000																												
2	Create files and name the standards and samples with the date and the name of the user.																												
3	<p>Check gas system pressure, flow rate, columns, and dissolvents before running the samples. The Xevo TQ-XS Triple Quadrupole Mass Spectrometry system was used. https://www.waters.com/waters/en_GB/Xevo-TQ-XS-Triple-Quadrupole-Mass-Spectrometry/nav.htm?locale=en_GB&cid=134889751</p>																												
4	Targeted methods setup for the 13 SPM panels, using Waters MassLynx Software and the TargetLynx application manager to process results and generate the data matrix.																												

Compound name	Parent (m/z)	Daughter (m/z)	Dwell (s)	Cone (v)	Collision (eV)
RvE1	349.2000	107.4000 195.2000	0.009	25	17
RvD2	375.4000	141.2000 175.3000	0.009	25	17
RvD1	375.3000	141.1000 215.4000	0.009	25	17
RvD5	359.2000	199.3000 279.3000	0.009	25	20
LTB4	335.4000	195.3000 317.4000	0.009	25	18
LXA4	351.4000	115.2000 217.4000	0.009	25	17
LXB4	351.2000	221.2000 271.3000	0.009	25	17
PGD2	351.2000	189.3000 271.4000	0.009	25	20
PGE2	351.4000	189.3000 271.4000	0.009	25	20
PG2a	353.2000	193.3000 247.4000	0.009	25	27
MaR2	359.3000	147.3000 232.3000	0.009	25	19
MaR1	359.4000	113.2000 228.3000	0.009	25	19
PD1	359.3000	153.3000 206.3000	0.009	25	19

RvE1 Resolvin E1 (5*S*,12*R*,18*R*-trihydroxy-ei- cosa-6*Z*,8*E*,10*E*,14*Z*,16*E*-pentaenoic acid)

RvD2 Resolvin D2 (7*S*,16*R*,17*S*-trihydroxy- docosa-4*Z*,8*E*,10*Z*,12*E*,14*E*,19*Z*- hexaenoic acid)

RvD1 Resolvin D1 (7*S*,8*R*,17*S*-trihydroxy-do- cosa-4*Z*,9*E*,11*E*,13*Z*,15*E*,19*Z*- hexaenoic acid)

RvD5 Resolvin D5 (7*S*,17*S*-dihydroxy-docosa- 4*Z*,8*E*,10*Z*,13*Z*,15*E*,19*Z*-hexaenoic acid)

LTB4 Leukotriene B4 (5*S*, 12*R*-dihydroxy-ei- cosa-6*Z*, 8*E*,10*E*,14*Z*-tetraenoic acid)

LXA4 Lipoxin A4 (5*S*,6*R*,15*S*)-Trihydroxy-7,9,13-trans-11-cis-eicosatetraenoic acid

LXB4 Lipoxin B4 (5*S*,14*R*,6*E*,8*Z*,10*E*,12*E*,15*S*)-5,14,15-Trihydroxy-6,8,10,12- eicosatetraenoic acid

PGD2 Prostaglandin D2 (11-oxo-9α, 15*S*-dihy- droxy-prosta-5*Z*, 13*E*-dien-1-oic acid)

PGE2 Prostaglandin E2 (9-oxo-11α,15*S*-dihy- droxy-prosta-5*Z*,13*E*-dien-1-oic acid)

PG2a Prostaglandin 2 alpha

MaR2 Maresin 2

MaR1 Maresin 1 (7*R*,14*S*-dihydroxy-docosa- 4*Z*,8*E*,10*E*,12*Z*,16*Z*,19*Z*-hexaenoic acid)

	PD1 Protectin D1 (10 <i>R</i> ,17 <i>S</i> -dihydroxy-docosa- 4 <i>Z</i> ,7 <i>Z</i> ,11 <i>E</i> ,13 <i>E</i> ,15 <i>Z</i> ,19 <i>Z</i> -hexaenoic acid), also known as 190 europrotection D1 (NPD1)
5	Start the analysis, and set system to automatically shut off after running all loaded samples, preventing solvents from drying.
6	Open results software and load results. Reflect on results and graphs: A- The retention time between standards and injections should be consistent. B- Study graph peaks for each of the 13 metabolite panels in the sample; there should be two matching peaks, where one is the identifier (quantifier) ion that the peak area (used to calculate the recovery concentration) is based on, and the second is the qualifier that, when compared against the quantifier, confirms that the measured peak is the correct analyte.
7	Create results matrix file.

The following criteria were adapted for compound peak detection and interpretation. First, all of the detected quantifier peaks (automated via software or detected manually) were included regardless of amplitude. Second, each of the detected quantifier peaks had to match a corresponding qualifier peak, otherwise, they were considered artifact noise. In addition, peaks observed in one injection but not in the two duplicate injections were considered artifacts. Between-injections and sample run retention time (RT) variations of ± 0.02 min were considered reasonable.

6.3.4 Statistical analysis

First, the peak areas of the targeted compounds were corrected for the sample weight and the percent recovery of the internal standard per sample. Then, the baseline characteristics, peak areas of the targeted compounds, and clinical and blood biomarkers at baseline were compared between groups using a one-way analysis of variance (ANOVA) and the Kruskal–Wallis test for parametric and non-parametric data, respectively. The Wilcoxon rank-sum test was used for the analysis comparing acute and stable states.

6.4 Results

6.4.1 Clinical characteristics

Baseline characteristics were assessed across four groups: healthy (n = 22), acute asthma (n = 37), AECOPD (n = 45), and pneumonia (n = 37) (Table 6-3). Significant age differences were observed across groups ($p < 0.0001$), with the AECOPD group having the highest mean age (70.44 years) and the acute asthma group having the lowest (46.76 years). Temperature, heart rate, respiratory rate, and oxygen saturation differed significantly ($p < 0.0001$) among the groups as well. Pneumonia patients exhibited the highest mean temperature, while acute asthma patients showed a higher mean heart rate, respiratory rate, and blood pressure. AECOPD patients had lower mean oxygen saturation levels. Dyspnea measures (breathlessness and wheeze VAS scores), and laboratory results (eosinophil count, C-reactive protein level, white blood cell (WBC), lymphocyte, and neutrophil counts) also showed significant differences among the healthy and diseased groups. Furthermore, there were slight differences in steroid use ($p = 0.01$) but no significant differences in antibiotic use ($p = 0.65$) among the diseased groups.

Table 6-4 Clinical characteristics of the study population

	Healthy	Acute asthma	AECOPD	Pneumonia	p-value
Total (141)	22	37	45	37	
Demographics					
Age, years	63.55 ±(8.53)	46.76 ± (18.66)	70.44 ±(7.72)	60.41 ±(16.05)	<0.0001
Sex (male, n (%))	12 (54.54%)	18 (47.36%)	31 (68.88%)	21 (56.75%)	0.30
Clinical observations†					
Temperature (°C)	36.17 ±(0.41)	36.75 ±(0.47)	36.79 ±(0.48)	37.21 ±(0.70)	<0.0001
Heart rate (beats/min)	66.55 ±(8.63)	97.73 ±(17.32)	92.48 ±(17.10)	92.64 ±(15.83)	<0.0001
Respiratory rate (breaths/min)	14.10 ± (3.55)	21.05 ±(2.95)	20.56 ± (2.50)	19.69 ±(2.75)	<0.0001
Oxygen saturation (%)	97.45 ±(1.50)	96.34 ±(2.33)	94.00 ± (3.02)	95.17 ±(2.65)	<0.0001
Systolic blood pressure (mmHg)	136.95 ±(19.86)	135.11 ±(18.93)	133.91 ±(23.82)	126.64 ±(16.58)	0.18
Dyspnea measures					
MRC score	NA	5.0 (4.0 -5.0)	5.0 (4.0 -5.0)	5.0 (3.0 -5.0)	0.49
Breathlessness VAS score (mm)	3.68 ±(6.87)	69.58 ±(23.55)	66.20 ±(20.44)	64.00 ±(25.03)	<0.0001
Wheeze VAS score (mm)	2.41 ±(3.57)	63.81 ±(26.58)	57.20 ±(29.08)	46.43 ±(33.17)	<0.0001
Laboratory (blood)					
Eosinophils (x10⁹/L)	0.17 (0.13-0.29)	0.18 (0.057-0.383)	0.145 (0.09 - 0.31)	0.085 (0.035 - 0.130)	0.005
C-reactive protein (mg/L)	2.5 (2.5 - 2.5)	10.50 (2.5 -43.75)	15.0 (2.5 – 35.0)	186.5 (80.0 -249.2)	<0.0001
WBCs (x10⁹/L)	5.91 ±(1.50)	10.73 ±(2.96)	10.89 ±(3.74)	14.38 ± (6.45)	<0.0001
Lymphocytes (x10⁹/L)	1.78 ±(0.52)	1.69 ±(0.80)	1.39 ±(0.89)	1.04 ±(0.45)	0.001
Neutrophils (x10⁹/L)	3.30 ±(0.97)	7.94 ±(3.08)	8.16 ±(3.89)	12.34 ±(6.44)	<0.0001
Medication use two weeks before admission					
Steroids	NA	13 (34.21%)	17 (35.41%)	4	0.01204
Antibiotics	NA	15 (39.47%)	16 (33.33%)	11	0.65

Data are expressed as mean ±standard deviation, median (interquartile range), or proportion (%). VAS: a 100mm visual analog scale. MRC score: Medical Research Council dyspnoea scale

6.4.2 SPMs during acute events of inflammatory respiratory diseases

In terms of compound detectability, our study investigated 13 SPMs in sputum samples from patients with acute asthma, AECOPD, and pneumonia. We found that some SPMs, such as LTB₄, PGD₂, PGE₂, and PG2a, exhibited distinct peaks and were easily detected in 60% to 93% of the samples. However, other SPMs, such as RvD₂, RvD₅, LXA₄, LXB₄, and PD1, had distinguishable peaks but were detected in 14% to 42% of the samples. The peaks for RvE₁, RvD₁, MaR₂, and MaR₁ were mostly undistinguishable and were detected in only 5% or less of the samples. These variations in detection and distinguishability may be due to the inherent challenges of studying lipid mediators in sputum samples, as certain species are more resistant or sensitive to degradation, and interference during analysis, impacting their detectability.

In terms of differentiating the studied groups (Table 6-4), RvE₁, RvD₅, LXA₄, MaR₂, and MaR₁ were not detected in the samples from healthy subjects. Among the studied groups, no statistically significant differences were observed for RvD₂, RvD₁, RvD₅, LXA₄, LXB₄, LTB₄, PGD₂, PG2a, and PD1. However, significant differences were found for PGE₂ between the studied groups (p -values = 0.006). These findings suggest that these SPMs may play a role in distinguishing between healthy and diseased subjects. Dunn's multiple comparison test was conducted as a post-hoc analysis to compare specific groups (Figure 6-4). AECOPD patients showed significantly higher PGE₂ levels when compared to acute asthma patients ($Z = 2.36$, $p_{\text{unadj}} = 0.01$) and healthy subjects ($Z = 3.26$, $p_{\text{unadj}} = 0.001$). Pneumonia subjects had significantly higher PGE₂ levels when compared to healthy individuals ($Z = -2.16$, $p_{\text{unadj}} = 0.03$). No significant differences were observed between acute asthma and

healthy subjects, acute asthma and pneumonia subjects, or AECOPD and pneumonia subjects. These findings indicate that PGE2 levels vary among the groups and are highest in AECOPD subjects.

Table 6-5 SPMs across acute illness of respiratory disease patients and healthy controls

	Healthy	Acute asthma	Acute COPD	Pneumonia	p-value
Total (n) 141	22	37	45	37	
RvE1 n (7) 5%	ND	522.8 (404.7–659.5) N = 3	2132.0 (1389.2– 2669.8) n = 3	6979 n = 1	0.31
RvD2 n (26) 18%	8031 (6311–9018) n = 3	4046 (2559–11180) n = 10	2915.8 (1332.4– 8920.4) n = 10	6443 (5046–11907) n = 3	0.48
RvD1 n (2) 1%	331.8 n = 1	4798 n = 1	ND	ND	0.31
RvD5 n (28) 20%	ND	8625 (7404–16106) n = 17	3385.9 (907.9–5646.8) n = 7	2682.8 (1606.0– 8794.3) n = 4	0.07
LTB4 n (113) 80%	47856 (20915–98083) n = 15	26719 (15214–44490) n = 28	29034 (13576–40710) n = 38	18336 (12488–32321) n = 32	0.17
LXA4 n (20) 14%	ND	9672 (4859–25208) n = 5	6689.5 (3369.5– 25665.5) n = 8	9263 (5287–35251) n = 7	0.68
LXB4 n (59) 42%	9616 (5508–24512) n = 3	16774 (7375–23150) n = 17	9410 (5075–18633) n = 25	28040 (4991–43473) n = 14	0.40
PGD2 n (85) 60%	11377 (10949–13070) n = 6	22417 (13776–52374) n = 27	19487 (10377–45818) n = 28	18311 (10261–37512) n = 24	0.15
PGE2 n (131) 93%	39647 (26303–76121) n = 19	60277 (32575– 131185) n = 34	106766 (60247– 276374) n = 43	93388 (45265– 216776) n = 35	0.006
PG2a n (112) 79%	7904 (6064–11140) n = (13)	15080 (9842–28457) n = 33	11994 (6229–27073) n = 38	14889 (7317–25588) n = 28	0.23
MaR2 n (3) 2%	ND	1019.7 (728.7–1310.6) n = 2	1341 n = 1	ND	1

MaR1 n (4) 3%	ND	2554.3 (1428.8– 4277.4) n = 4	ND	ND	NA
PD1 n (56) 40%	5659 (3884–10973) n = 7	5020.8 (2670.3– 9550.0) n = 27	3839 (2304–8100) n = 13	9014 (2545–13354) n = 9	0.49

Data are presented as peak area (no units or arbitrary units), reflecting the relative abundance or quantity of the analyte. Peak area proportionally correlates with the compound's concentration. The Kruskal–Wallis chi-squared test was used; data are expressed as median (interquartile range). Values adjusted to account for IS recovery rate and sample weight.

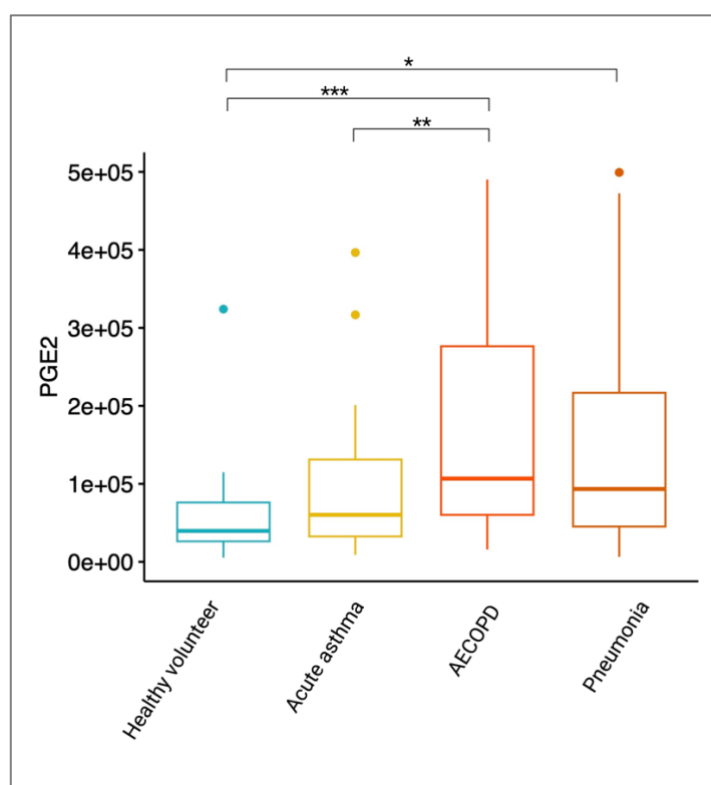


Figure 6-4 PGE2 reported peak area across healthy controls and AECOPD, acute asthma, and pneumonia patients

Box and whiskers plot of PGE2 peak area across healthy volunteers and acutely ill respiratory condition groups. Peak area (no units or arbitrary units), reflects the relative abundance of the analyte. Peak area proportionally correlates with the compound's concentration. Differences between groups were evaluated with the Kruskal–Wallis test, and across groups with the post-hoc Dunn's test for multiple-group comparisons. * $p \leq 0.05$, ** $p \leq 0.01$, *** $p < 0.001$. Bold lines represent medians; boxes, IQR; whiskers, minimum and maximum range; and dots, individual outliers.

6.4.3 Associations between PGE2 and clinical parameters in acute illness of respiratory disease

To further explore the association of PGE2 with clinical parameters, we conducted a correlation analysis between PGE2 levels and various laboratory test results. The correlation analysis revealed intriguing results (Table 6-6). Eosinophil count exhibited a significant negative correlation with PGE2 level (coefficient = -0.21, $p < 0.05$), indicating a potential inverse relationship. C-reactive protein (CRP) levels and WBC count showed non-significant positive correlations with PGE2. In addition, a non-significant negative correlation was observed between lymphocyte count and PGE2. In contrast, a significant positive correlation was found between neutrophil count and PGE2 level (coefficient = 0.24, $p < 0.05$), suggesting a potential link with neutrophil activation (Figure 6-5).

Table 6-6 Correlation analysis between PGE2 Levels and clinical parameters

	Coefficient	p-value
Eosinophil count ($\times 10^9/L$)	-0.21	<0.05*
C-reactive protein (mg/L)	0.11	0.23
WBCs ($\times 10^9/L$)	0.17	0.06
Lymphocytes ($\times 10^9/L$)	-0.17	0.07
Neutrophils ($\times 10^9/L$)	0.24	<0.05*

Correlation coefficients between PGE2 and blood biomarkers were investigated applying Spearman's correlation coefficient.

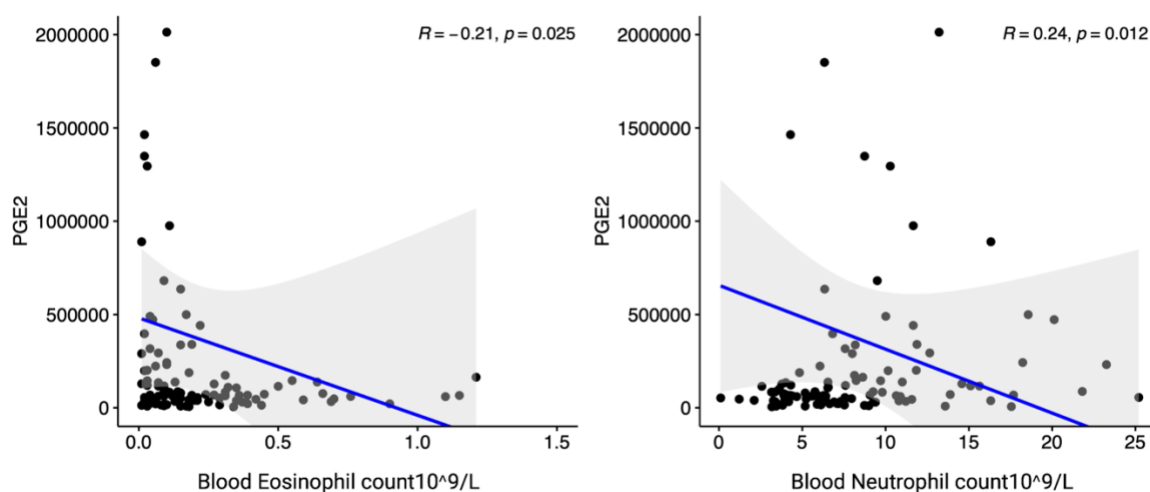


Figure 6-5 Scatterplots of PGE2 association with blood immune cell counts

Scatterplots with regression lines and 95% CI for PGE2 and blood immune cell counts. The y-axis represents the compound adjusted peak area of PGE2 levels in sputum samples.

6.4.4 SPMs during stable cardiorespiratory disease

In terms of compound detectability, the stable and acute cohorts (not paired data), resulted in similar patterns. In the stable cohort, SPMs LTB₄, PGD₂, PGE₂, and PG2a also exhibited higher detection rates, ranging from approximately 51.1% to 91.1%. Conversely, RvE1, RvD₂, RvD₅, LXA₄, LXB₄, and PD1 were detected at lower rates, varying from around 7% to 40%. Furthermore, compounds such as RvD₁, MaR₂, and MaR₁ were mostly undetected, with detection rates of 2% to 0%. Moreover, among the SPMs analyzed, the most notable finding was the non-significant difference in PGE₂ levels between the groups in the stable cohorts compared to those in the acute cohort. While other SPMs showed varying levels and trends across the different groups (see Table 6-7), no significant differences were observed between the acute status groups' measurements and the stable status groups' (Table 6-8).

Table 6-7 SPMs across stable and recovered respiratory illness patients and healthy controls

	Healthy	Asthma	COPD	Pneumonia	p-value
Total (48)	14	8	18	5	
RvE1 n (4)	446.4 (389.5–503.2) n = 2	2092 (1943– 2241) n = 2	ND	ND	0.12
RvD2 n (4)	1785 n = 1	ND	3003 (2319–3485) n = 3	ND	0.65
RvD1 n (1)	ND	2441 n = 1	ND	ND	NA
RvD5 n (5)	5213 (3899–6527) n = 2	23982 n = 1	2246 n = 1	ND	0.25
LTB4 n (34)	31018 (11298–36418) n = 13	10751 (7877–41472) n = 7	11165.7 (4514.0– 25193.3) n = 11	22994 (12336–37533) n = 3	0.58
LXA4 n (3)	2812 n = 1	ND	13429 (13106–13753) n = 2	ND	0.22
LXB4 n (18)	10409 (7665–14836) n = 6	4401 (2867–16829) n = 3	16881 (11925–23656) n = 6	23674 n = 1	0.39
PGD2 n (23)	24955 (15872– 36174) n = 6	15318 (8950–23480) n = 5	31787 (9258– 59470) n = 9	62274 (60856– 63693) n = 2	0.39
PGE2 n (41)	89511 (40299– 108332) n = 11	28758 (19598–79916) n = 7	131268 (56520– 220090) n = 16	220614 (10963– 256502) n = 5	0.33
PG2a n (33)	9575 (5859–14162) n = 13	5506 (4932–9000) n = 5	8141 (5980–21581) n = 12	36270 (27216–45325) n = 2	0.23
MaR2 n ()	ND	ND	ND	ND	NA
MaR1 n ()	ND	ND	ND	ND	NA
PD1 n (12)	4698 (2703–7571) n = 4	8061 n = 1	3601.1 (2012.5– 8282.6) n = 7	ND	0.75

Data are reported as peak area (no unit or arbitrary units) and significance was assessed with the Kruskal-Wallis chi-squared test. Data are expressed as median (interquartile range).

Table 6-8 SPMs across acute and stable respiratory disease groups and healthy controls

Healthy			
	Visit 1	Visit 2	p-value
Total (n)	22	14	
RvE1	ND	446.4 (389.5–503.2), n = 2	NA
RvD2	8031 (6311–9018), n = 3	1785, n = 1	1
RvD1	331.8, n = 1	ND	NA
RvD5	ND	5213 (3899–6527), n = 2	NA
LTB4	47856 (20915–98083), n = 15	31018 (11298–36418), n = 13	0.02
LXA4	ND	2812, n = 1	NA
LXB4	9616 (5508–24512), n = 3	10409 (7665–14836), n = 6	0.42
PGD2	11377 (10949–13070), n = 6	24955 (15872–36174) n = 6	0.57
PGE2	39647 (26303–76121), n = 19	89511 (40299–108332), n = 11	0.92
PG2a	7904 (6064–11140), n = 13	9575 (5859–14162), n = 13	0.70
MaR2	ND	ND	NA
MaR1	ND	ND	NA
PD1	5659 (3884–10973), n = 7	4698 (2703–7571), n = 4	0.8
Asthma			
	Acute	Stable	
Total (n)	37	8	
RvE1	522.8 (404.7–659.5), n = 3	2092 (1943–2241), n = 2	NA
RvD2	4046 (2559–11180), n = 10	ND	NA
RvD1	4798, n = 1	2441, n = 1	NA
RvD5	8625 (7404–16106), n = 17	23982, n = 1	0.66
LTB4	26719 (15214–44490), n = 28	10751 (7877–41472), n = 7	0.04
LXA4	9672 (4859–25208), n = 5	ND	NA
LXB4	16774 (7375–23150), n = 17	4401 (2867–16829), n = 3	0.8
PGD2	22417 (13776–52374), n = 27	15318 (8950–23480), n = 5	0.55
PGE2	60277 (32575–131185), n = 34	28758 (19598–79916), n = 7	0.10
PG2a	15080 (9842–28457), n = 33	5506 (4932–9000), n = 5	0.54
MaR2	1019.7 (728.7–1310.6), n = 2	ND	NA
MaR1	2554.3 (1428.8–4277.4), n = 4	ND	NA
PD1	5020.8 (2670.3–9550.0), n = 27	8061, n = 1	1
COPD			
	Acute	Stable	
Total (n)	45	18	
RvE1	2132.0 (1389.2–2669.8), n = 3	ND	NA
RvD2	2915.8 (1332.4–8920.4), n = 10	3003 (2319–3485), n = 3	0.4
RvD1	ND	ND	NA
RvD5	3385.9 (907.9–5646.8), n = 7	2246, n = 1	1
LTB4	29034 (13576–40710), n = 38	11165.7 (4514.0–25193.3), n = 11	0.60
LXA4	6689.5 (3369.5–25665.5), n = 8	13429 (13106–13753), n = 2	1
LXB4	9410 (5075–18633), n = 25	16881 (11925–23656), n = 6	1
PGD2	19487 (10377–45818), n = 28	31787 (9258–59470), n = 9	0.16
PGE2	106766 (60247–276374) n = 43	131268 (56520–220090), n = 16	0.78
PG2a	11994 (6229–27073) n = 38	8141 (5980–21581), n = 12	0.24

MaR2	1341, n = 1	ND	NA
MaR1	ND	ND	NA
PD1	3839 (2304–8100), n = 13	3601.1 (2012.5–8282.6), n = 7	0.83
Pneumonia			
	Acute	Stable	
Total (n)	37	5	
RvE1	6979, n = 1	ND	NA
RvD2	6443 (5046–11907), n = 3	ND	NA
RvD1	ND	ND	NA
RvD5	2682.8 (1606.0–8794.3), n = 4	ND	NA
LTB4	18336 (12488–32321), n = 32	22994 (12336–37533), n = 3	0.62
LXA4	9263 (5287–35251), n = 7	ND	NA
LXB4	28040 (4991–43473), n = 14	23674, n = 1	1
PGD2	18311 (10261–37512), n = 24	62274 (60856–63693), n = 2	0.8
PGE2	93388 (45265–216776), n = 35	220614 (10963–256502), n = 5	0.73
PG2a	14889 (7317–25588), n = 28	36270 (27216–45325), n = 2	0.8
MaR2	ND	ND	NA
MaR1	ND	ND	NA
PD1	9014 (2545–13354), n = 9	ND	NA

Data are presented as peak area (no units or arbitrary units). The Wilcoxon rank-sum test was used to compare groups. Data are expressed as median (interquartile range).

6.5 Conclusions and discussion

To our knowledge, this is the first study to report this intensive panel of SPMs across three acute respiratory conditions in sputum samples. The results of our study shed light on the varying levels of SPMs in acute events and exacerbations of acute asthma, AECOPD, and pneumonia. Our findings provide valuable insights into the potential use of SPMs as biomarkers and therapeutic targets in the treatment of these conditions.

First, we observed the profiles of 13 SPMs in sputum samples from patients with acute asthma, AECOPD, and pneumonia compared to healthy controls. Notably, we found that PGE2 levels were significantly different between the groups; they were significantly higher in patients with AECOPD compared to acute asthma patients and healthy subjects. This finding suggests that PGE2 could potentially serve as a biomarker to differentiate the two

obstructive inflammatory conditions (COPD and asthma) during acute exacerbations. On the other hand, no significant difference in PGE2 level was observed between AECOPD and pneumonia cases, and pneumonia cases, like AECOPD cases, shared significantly elevated levels compared to healthy controls. This might be explained by the etiological overlap between pneumonia and COPD, both of which involve airway microbial dysbiosis and infection exacerbation phenotypes (30, 35, 36) as infections trigger exacerbation events. Furthermore, when comparing the stable and acute cohorts, we observed similar SPM detection rate patterns. However, there were no significant differences in the levels of PGE2 between the groups in the stable cohorts, in contrast to those in the acute cohort. This suggests that the dysregulation of PGE2 observed during acute exacerbations may change during the stable phase of respiratory diseases. Further longitudinal studies are needed to explore dynamic changes in PGE2 levels and their implications for disease progression and resolution.

Our results are consistent with the current literature on asthma, COPD, and pneumonia, in which elevated PGE2 levels have been reported. Increased PGE2 levels in asthma patients were associated with disease severity and exacerbations (139, 140), while higher levels in COPD patients are linked to increased symptoms and exacerbations (141). Limited studies have investigated PGE2 in pneumonia; however, in an animal-model study, mice were infected with *Mycobacterium tuberculosis* to study the kinetics of PGE2 production and its role in the pathogenesis of pulmonary tuberculosis. The study reported elevated PGE2 levels during the late phase of pulmonary tuberculosis infection; specifically, it was four-fold higher than in the early phase of infection (343). Another study described increased PGE2 levels in mice with induced lung fibrosis and *Streptococcus pneumoniae*-exacerbated lung

fibrosis (344).

The role of PGE2 in the inflammatory process is complex and its pro-inflammatory role has been described intensively in the literature (147). However, recent evidence suggests that prostanoids, including PGE2, also play an important role in the resolution of inflammation and the restoration of homeostasis. PGE2 stimulates the production of enzymes that are involved in generating pro-resolving lipid mediators, facilitating the shift toward a pro-resolving profile (345). In addition, it has pro-resolving effects in promoting macrophage phagocytosis and tissue repair (150). This highlights prostanoids' multifaceted role in both promoting inflammation and facilitating its resolution. In the context of our observational study, the increased levels of PGE2 might contribute to both its pro-inflammatory and resolution of inflammation roles. Our study also revealed interesting correlations between PGE2 levels and clinical parameters. Eosinophil count exhibited a significant negative correlation with PGE2 level, suggesting a potential inverse relationship. Conversely, neutrophil count showed a significant positive correlation with PGE2 level, indicating a potential association with neutrophil activation. These findings highlight the complex interplay between SPMs and the immune cell populations involved in the inflammatory response, warranting further investigation into their specific roles and interactions.

In contrast to PGE2 levels, we did not observe significant differences in the levels of other SPMs, such as RvD2, RvD1, RvD5, LXA4, LXB4, LTB4, PGD2, PG2a, and PD1, among the studied groups, which could be attributed to the limited sample size and detection rate variations. However, alternations in patterns might provide insight into SPMs' roles in acute and stable states of the studied diseases. During the acute phase, we found that LTB4 levels

were consistently lower in all disease groups than in the healthy group. This relatively low level of LTB₄ was also observed in the stable/recovery cohort, indicating its potential role in the pathogenesis of these conditions. Furthermore, when comparing the stable phase to the acute phase within each disease group, we found that LTB₄ levels were further decreased in stable asthma and stable COPD compared to acute asthma and AECOPD, while they tended to normalize in recovered pneumonia patients. Conversely, PGD₂, PGE₂, and PG2a levels were higher in all disease groups during the acute phase compared to the healthy group, suggesting their involvement in the inflammatory response associated with the studied diseases. Upon recovery from pneumonia, the levels of PGD₂, PGE₂, and PG2a were higher than those in both the healthy group and the acute cohort, even after the acute symptoms resolved. The same pattern held in stable COPD for PGD₂ and PGE₂ levels. In stable asthma, however, PGD₂, PGE₂, and PG2a occurred at lower levels than in the healthy group (Table 6-9). These patterns demonstrate the complexity of prostaglandins as key mediators of the inflammatory process, operating as pro-inflammatory mediators (147) with pro-resolving properties under certain conditions. Although these pro-resolving effects are generally thought to be secondary to their pro-inflammatory effects, PGE₂'s pro-resolving effects have been demonstrated in several models of inflammation, including its enhancement of the macrophage phagocytosis of apoptotic neutrophils and promotion of tissue repair (150). Variations in prostaglandin levels might function as biomarkers of asthma severity and exacerbations or inflammatory foci in COPD or post-pneumonia cases, but further research is needed to confirm this association.

Table 6-9 Visual comparison of SPM patterns in acute and stable phases of respiratory diseases using control group methodology

	Asthma		COPD		Pneumonia	
	Acute	Stable	Acute	Stable	Acute	Stable
LTB4						
LXB4						
PGD2						
PGE2						
PG2a						

- Arrows compare the median level of the compound in diseased subjects to healthy subjects.
 - ↑ Higher levels than in healthy subjects
 - ↓ Lower levels than in healthy subjects
- Dot size compares the median level of the compound in the same disease group during the acute and stable/recovery phases.
 -   higher levels in the acute cohort than in the stable cohort
 -   higher levels in the stable cohort than in the acute cohort

Moreover, in our population, a comparison of the disease groups showed a statistically significant difference in the prior use of steroids ($p = 0.01$), but no significant difference in antibiotic use. Reflecting on the direct impact of the significant difference in prior steroid use on the recovered SPM levels from each disease group is challenging given the limited literature on the topic. Regarding steroids, a published study suggests a connection between corticosteroid use and the effects of SPMs on IgE production. This finding aligns with the reduced responsiveness of B cells to SPM treatment that was observed in asthma patients taking oral steroids in this study (346). It implies that steroid use in asthma patients may affect SPM levels and their effectiveness in regulating inflammation and immune responses. However, to better understand the effects of steroids and antibiotics on SPM levels and activity, future observational studies could compare SPM levels in individuals

using steroids or antibiotics with those who are not within each disease group (asthma, COPD, pneumonia). and then compare these groups to healthy individuals. In vivo and in vitro studies can also provide insights into the potential interactions between these drugs and SPMs in the context of inflammation and immune modulation.

Despite the valuable insights provided by our study, its limitations should be acknowledged. First, the sample size in each group was relatively small, which may limit the generalizability of our findings. Larger cohorts are needed to validate our results and explore potential subgroup differences. Additionally, the detectability and precision of certain SPMs proved challenging, highlighting the need for precise analytical methods and delicate sample-handling techniques. A standard control analysis of the lipidomic standards mix was performed before and after analysing the sputum samples (Table 6-10). The morning standard run (which occurred after turning on the instrument) typically returned lower concentrations and higher coefficients of variation (CV) than subsequent runs, after analysing each batch of 20 samples. This observation may be attributed to improved signal detection capabilities as the device stabilised and optimised its performance over time. Importantly, the results demonstrated consistent retention times throughout the analysis period. This consistency indicates the stability and reliability of the analytical method over time. Furthermore, analysing the standards after each batch of 20 samples exhibited CV values ranging from 20% to 30% for most compounds, indicating moderate variability. This level of CV is generally considered acceptable in many cases, although it indicates some level of variability in the measurements or estimates. However, for MaR1 and PD1, the CV values were 39% and 32%, respectively, exceeding the threshold of 30%. This higher CV suggests greater variability and lower precision in the measurements for these particular

SPMs and indicates that the amount of variation in the results may affect their reliability or comparability. These findings underscore the significance of incorporating quality control measures, including standards and assessments of the results' CV to guarantee the precise and dependable quantification of SPM levels. Considering the hurdles involved in preserving the integrity of these compounds during sample preparation and detection, as well as the potentially potent effects of even minor variations in their levels on their biological impact within the body, maintaining rigorous measurement practices are crucial for the accurate interpretation of the results of future analyses.

Table 6-10 Control analysis of lipidomic standards mix: Pre- and post-analysis performance

	*Pre-patch std mix	Coefficient	*Post- patch std mix	Coefficient	RT	Coefficient
RvE1	67733.2 ±26638.3	39.3	104548.7 ±20996.5	20.0	2.05 ±0.008	0.4
RvD2	111039.8 ±49516.7	44.5	175690.2 ±43491.7	24.7	3.07 ±0.009	0.3
RvD1	154904.4 ±64986.07	41.9	237509 ±65746.0	27.6	3.28 ±0.009	0.2
RvD5	42915.6 ±17021.3	39.6	68688.9 ±20928.1	30.4	4.10 ±0.009	0.2
LTB4	63231.8 ±27270.9	43.1	104413.5 ±31303.5	29.9	4.19 ±0.008	0.2
LXA4	167127.4 ±56568.8	33.8	272154.5 ±82216.6	30.2	3.28 ±0.011	0.3
LXB4	143407.6 ±58397.3	40.7	212940.6 ±54791.6	25.7	3.00 ±0.013	0.4
PGD2	296288.8 ±118156	39.8	427398 ±120093.3	28.0	3.01 ±0.016	0.5
PGE2	605362.5 ±253899.2	41.9	865267.5 ±256252.7	29.6	2.89 ±0.008	0.3
PG2a	152081.7 ±68247.9	44.8	208016.6 ±55740.26	26.7	2.83 ±0.009	0.3
MaR2	22778.7 ±9422	41.3	38594.4 ±11918.1	30.8	4.43 ±0.009	0.2
MaR1	22209.2 ±11016.63	49.6	34024 ±13474.36	39.6	4.133 ±0.011	0.2
PD1	63079.6 ±24515.1	38.8	99456 ±32163.4	32.3	4.033 ±0.010	0.2

* Data are presented as peak area (no units or arbitrary units); data are expressed as mean \pm standard deviation. RT (retention time).

In conclusion, our study contributes to the growing body of evidence supporting the role of SPMs in the pathogenesis of respiratory diseases. We observed distinct profiles and patterns of SPMs in sputum samples from patients with asthma, COPD, and pneumonia. PGE2 levels were significantly different among the study groups, indicating its potential as a biomarker and linked to blood measurements. However, further research is needed to elucidate the specific roles and interactions of SPMs in respiratory diseases and to explore their therapeutic potential using optimised detection methods in a study with a greater sample size.

Chapter 7 Discussion, Conclusions, and Future Work

7.1 Overview of thesis

By meticulously examining carefully selected sub-cohorts within the EMBER population, this research showcases a diligent and resourceful approach to unraveling the complexities of acute cardiorespiratory conditions. The aim of this thesis was to investigate metabolomics and physiological biomarkers in patients with acute cardiorespiratory diseases. I have reported four observational studies that address the core aim of this thesis (Figure 1). These investigations were carried out during a challenging period marked by the COVID-19 pandemic, with its inherent limitations, restrictions, and obstacles. This comprehensive and interconnected approach I adopted, conducted under the constraints of limited resources, emphasizes the significance and resilience of the research. It stands as a testament of determination to advance scientific knowledge, even in the face of adversity. This thesis highlights my commitment to contributing to the scientific community and patient care during a time when clinical research resources were predominantly focused on COVID-19-related studies.

Evaluation of Acute Cardiorespiratory Disease: Integrating Metabolite-wide Analysis and Lung Mechanics Pathophysiology

Aim

The overarching objective of this thesis is to explore biomarkers, encompassing metabolomics and physiological measures, in individuals with acute cardiorespiratory disease.

Studies

(I) Blood Plasma Metabolome Signatures Differentiates AECOPD and Decompensated Heart Failure in Hospitalised Patients

In our untargeted plasma metabolomic analysis, involving a (20) individuals with AECOPD, (20) AHF, and (14) healthy volunteers, we hypothesized that our approach would accurately differentiating and identifying these groups. The results obtained from biomarker scores calculated for total 19 significant metabolites revealed a promising sensitivity and specificity of $\geq 70\%$ in distinguishing between individuals in three groups

(II) Assessment of SPMs in Asthma, AECOPD, and pneumonia Patients through Hospital Admission, Acute Exacerbation & Recovery

SPM dysfunction contribute to chronic inflammation. We analyzed 13 SPMs in 119 sputum samples from patients with asthma, AECOPD, and pneumonia and compare it to 22 healthy controls to evaluate resolution post-exacerbation. PGE2 levels differed between groups, potentially serving as biomarkers to distinguish healthy and diseased individuals. AECOPD exhibited the highest median PGE2 levels. Associations were found between PGE2 levels and eosinophil count (negative correlation) and neutrophil count (positive correlation).

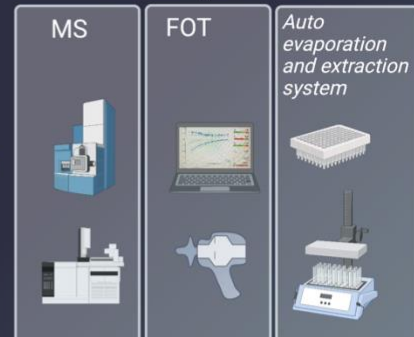
(III) FOT to Assess VH During Hospital Admission for Acute Cardio-Respiratory Illness

We assessed airway function using FOT in 263 patients with acute cardio-respiratory illness (asthma, COPD, heart failure, and pneumonia) and 47 healthy individuals. Measurements were feasible in all patients (n=310). Significant differences in lung mechanics were observed between the patient groups and healthy controls, with COPD patients having the worst lung mechanics ($p < 0.05$ for all measures). Resistance and reactance were worse ($p < 0.001$) in patients with more breathlessness, wheezing, and low oxygen saturation

Sub-Study: Do Lung mechanics affect Volatile Organic Compounds composition in breath in patients with cardio-respiratory breathlessness?

A sub-cohort of 208 who had both VOCs captured and FOT measurements, results showed that tissue compliance in the lung periphery (AX) seems to affect the recovery of selected VOCs; O-VOCs, S-VOCs, and N-VOCs.

Machinery and Tech



Biological Samples

Plasma Breath Sputum



All samples acquired from subjects recruited into EMBER Study within twenty-four hours of admission to Glenfield Hospital, Leicester, presenting with acute exacerbation of an established underlying cardio-respiratory disease

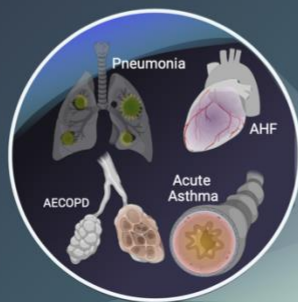


Figure 7-1 Evaluation of acute cardiorespiratory disease: Integrating metabolite-wide analysis and lung mechanics pathophysiology

7.2 Results chapters

The results chapters of this thesis unveiling the culmination of several studies and a compelling research journey, characterized by its inclusive exploration and noteworthy findings.

In Chapter 3, my research began by delving into plasma metabolomics as a convenient sample type, employing an untargeted approach with a smaller cohort. I learned how to navigate high-dimensional data and applied different statistical approaches to gain insights into the metabolomic profiles associated with acute disease conditions. In that study, I found that a panel of 19 significant metabolites could effectively differentiate between acute exacerbations of chronic obstructive pulmonary disease (AECOPD) and decompensated heart failure (AHF) when compared to healthy controls. The metabolite profiles exhibited distinct patterns for each condition, with some overlap observed in the COPD population. The biomarker scores derived from these metabolites improved the accuracy in distinguishing AECOPD and AHF compared to commonly used blood biomarkers, such as B-type natriuretic peptide (BNP) and C-reactive protein (CRP). Specifically, the sensitivity and specificity of the biomarker scores were equal to or greater than 70% for differentiating COPD from non-COPD individuals and equal to or greater than 88% for differentiating AHF from non-AHF individuals. The identified metabolites primarily belonged to lipid classes and included glycerophospholipids, prenol lipids, glycerolipids, and fatty acyls. These findings align with existing research highlighting the role of lipid metabolic dysfunction in both respiratory and cardiovascular diseases.

Simultaneously, amidst the peak of pandemic restrictions, I capitalized on my previous expertise in lung function tests and respiratory physiology by conducting the study presented in Chapter 4 and examined lung mechanics in acute patients with COPD, asthma, pneumonia, or heart failure. The forced oscillation technique (FOT) employed to assess lung mechanics revealed significant differences in both absolute and percent-predicted measures of lung mechanics between acute care patients and healthy volunteers. COPD patients showed the most pronounced lung mechanics abnormalities compared to individuals with asthma, pneumonia, or heart failure exacerbations. Measures of resistance and reactance, reflecting airway resistance and lung elasticity, were worse in patients with greater breathlessness and wheezing and lower oxygen saturation levels. However, no significant differences were observed based on early warning scores or blood biomarkers, such as eosinophil count, CRP, or BNP. In addition, the measures of lung mechanics did not predict the length of hospital stay or hospital readmission.

Building upon the promising results from the FOT study and the acquired expertise in metabolomics, I embarked on the third study, discussed in Chapter 5, to examine the impact of ventilation heterogeneity on breath VOCs. I found that alterations in respiratory reactance were associated with changes in three VOC functional groups. Acknowledging the study limitations and the challenges of determining the origin of VOCs in breath samples, ventilation heterogeneity was suggested as a possible contributing factor, impacting the sampling of VOCs.

As pandemic restrictions gradually eased, my interest in exploring metabolomics deepened. Equipped with knowledge from the previous studies, I was ready to embark on laboratory research. Chapter 6 discusses this study, which focused on specialized pro-resolving lipid

mediators (SPMs) in acute asthma, AECOPD, and pneumonia cases. Significant differences in PGE2 levels were found among the studied groups, indicating its potential utility as a biomarker, and AECOPD patients showed the most pronounced increase. However, no significant differences in PGE2 levels were observed between the groups in the stable cohort. The study analysis also revealed correlations between PGE2 levels and some blood biomarkers, specifically, eosinophil and neutrophil counts. These findings highlight the complex interplay between SPMs and immune cells during the inflammatory response.

7.3 Converging insights: Implications for field advancement and clinical applications

Acute cardiorespiratory conditions, such as AECOPD, acute asthma, acute HF, and pneumonia, impose a significant healthcare burden globally, leading to hospitalizations, frequent exacerbations, and reduced quality of life for patients. Beginning with the fundamental requirements of a supreme biomarker for examining these conditions, such a diagnostic tool must have specific characteristics to be effective in clinical practice. Ideally, a biomarker should demonstrate high sensitivity and specificity. Moreover, it should be practical to measure, enabling rapid and cost-effective assessment. Robust biomarkers require well-established normative values and references for reliable comparisons. In addition, they should be sufficiently repeatable to ensure consistent, accurate measurement in diverse settings. This comprehensive set of characteristics in a single biomarker could significantly advance diagnostic precision and patient care. Unfortunately, the current landscape of clinical biomarkers often entails limitations, such as inadequate sensitivity or specificity or impracticality for rapid assessments when examining patients with acute exacerbations of cardiorespiratory diseases. As I recognized these limitations

that underscore the need for advancements in the field, I designed studies intended to bridge these gaps. The studies aim to seek effective biomarkers through in-depth metabolomic and lung mechanics, focusing on potential biomarkers present during acute events of cardiorespiratory conditions. Our research findings have important implications for advancing our understanding of the physiological and pathogenetic components of these conditions and contributing to the development of biomarkers. Both results will help improve patient care and address the substantial healthcare burden these conditions impose globally. By integrating the knowledge gained from these converging insights, we could transform diagnostic approaches and treatment strategies and potentially improve the mortality rates associated with acute cardiorespiratory conditions—goals that emphasize the importance of advancing the field and implementing these findings in clinical practice.

First, the recognition of ventilation heterogeneity (VH) as a common characteristic across various acute cardiorespiratory conditions highlights its clinical significance. VH is associated with airway hyperresponsiveness, inflammation, and airway remodeling, all elements of altered lung mechanics. The presence of VH exacerbates disease symptoms, contributes to disease progression, and influences treatment response. By incorporating VH assessments, such as using portable forced oscillation technique (FOT) devices, clinicians can gain valuable insights into respiratory function and optimize patient care, thereby reducing the healthcare burden associated with these conditions. In addition, by integrating FOT lung mechanics data with breathomics data, we addressed a critical question in the breathomics field, enhancing our understanding of the VH influence on the recovery and interpretation of VOCs as biomarkers. This integration provides valuable insights for clinical practice,

where the reliability and clinical relevance of VOC analysis can be improved to generate more accurate diagnoses and personalized treatment plans.

Second, the differences in plasma metabolomic profiles and the identified disease signatures, which reflect metabolomic disturbance, enhance the diagnostic accuracy of the established blood biomarkers for acute cardiorespiratory conditions. Using metabolomics to identify distinct metabolic profiles in acute exacerbations of breathlessness, including AECOPD and AHF, offers an opportunity to enhance diagnostic accuracy and develop targeted interventions. The identification of specific metabolic alterations in the plasma provides valuable information for differentiating between healthy and between diseased subjects in the two disease groups. Furthermore, the investigation of SPMs as biomarkers in acute respiratory conditions opens new avenues for diagnostic and prognostic strategies. Detecting specific SPMs and understanding their correlations with disease severity, oxidative stress, and inflammation resolution can pave the way for the development of biomarkers and targeted interventions, thereby improving disease management. Thus, the integration of metabolomics into the current biomarker landscape by harnessing the potential of SPMs and further exploring and validating plasma biomarkers offers healthcare professionals an opportunity to improve diagnostic precision, monitor disease progression, and alleviate the healthcare burden associated with these conditions.

In summary, the integration of metabolomics via both targeted and non-targeted approaches with the study of lung mechanics presents valuable opportunities for improving the diagnosis and management of acute cardiorespiratory conditions. These findings have

implications for field advancement and clinical applications, offering opportunities to enhance patient outcomes.

7.4 Future work

Future research plans encompass multiple aspects, including the validation of the reported results, longitudinal assessment of these topics, and the utilization of laboratory models.

Validation is of the utmost importance to ensure the robustness and generalizability of the findings in each of my studies. To validate my results, larger-scale studies to affirm the diagnostic value of plasma biomarkers are needed. Rigorous validation protocols should be implemented to strengthen the evidence base and enhance these biomarkers' clinical utility.

Longitudinal assessment will be key in future research to understand the temporal dynamics and prognostic implications of various respiratory parameters. For projects involving the FOT and SPMs, longitudinal studies will help elucidate changes over time, to reveal the patterns and trajectories associated with disease outcomes. Longitudinal assessments will also aid in identifying early markers of disease progression or exacerbations, enabling health care providers to apply timely interventions and personalized treatment strategies.

To gain mechanistic insights, it is important to employ laboratory models to complement the clinical studies. In the context of investigating the underlying mechanisms of ventilation heterogeneity's effects on VOC emission, utilizing laboratory models will allow for controlled experiments, precise measurements, and the manipulation of variables to

explore the causal relationships between ventilation heterogeneity and known VOC metabolites.

Furthermore, integrating advanced techniques, such as intra-breath measures of respiratory impedance and airway impedance entropy, might enable further characterization of regional lung function, which could add value in identifying patterns in the differences among acute cardiorespiratory conditions, improving the clinical diagnostic value of lung function measures.

By diligently pursuing these research directions, I aim to make a meaningful scientific contribution to the development of innovative diagnostic approaches in respiratory medicine.

7.5 Concluding remarks

Overall, reporting findings, addressing limitations, and embracing interdisciplinary approaches has allowed this comprehensive analysis and exploration of plasma biomarkers, specialized pro-resolving lipid mediators, the forced oscillation technique, and volatile organic compounds in cardiorespiratory diseases to yield valuable insights and illuminate promising avenues for future research. It is my fervent hope that these endeavors will assist the medical and scientific communities in making strides toward advancing the understanding, diagnosis, and management of asthma, COPD, heart failure, and pneumonia, ultimately leading to improve outcomes and enhance the quality of care for patients worldwide.

References

1. Ibrahim W, Wilde M, Cordell R, Salman D, Ruszkiewicz D, Bryant L, et al. Assessment of breath volatile organic compounds in acute cardiorespiratory breathlessness: a protocol describing a prospective real-world observational study. *BMJ Open*. 2019;9(3):e025486.
2. Wilde MJ, Cordell RL, Salman D, Zhao B, Ibrahim W, Bryant L, et al. Breath analysis by two-dimensional gas chromatography with dual flame ionisation and mass spectrometric detection - Method optimisation and integration within a large-scale clinical study. 2019.
3. Vogelmeier CF, Criner GJ, Martinez FJ, Anzueto A, Barnes PJ, Bourbeau J, et al. Global Strategy for the Diagnosis, Management, and Prevention of Chronic Obstructive Lung Disease 2017 Report: GOLD Executive Summary. *Eur Respir J*. 2017;49(3).
4. [Available from: [https://www.who.int/news-room/fact-sheets/detail/chronic-obstructive-pulmonary-disease-\(copd\)](https://www.who.int/news-room/fact-sheets/detail/chronic-obstructive-pulmonary-disease-(copd))].
5. Mathioudakis AG, Janssens W, Sivapalan P, Singanayagam A, Dransfield MT, Jensen JS, et al. Acute exacerbations of chronic obstructive pulmonary disease: in search of diagnostic biomarkers and treatable traits. *Thorax*. 2020.
6. Barrecheguren M, Miravittles M. COPD heterogeneity: implications for management. *Multidisciplinary respiratory medicine*. 2016;11:14-.
7. Rodrigo GJ, Rodrigo C, Hall JB. Acute asthma in adults: a review. *Chest*. 2004;125(3):1081-102.
8. Global, regional, and national deaths, prevalence, disability-adjusted life years, and years lived with disability for chronic obstructive pulmonary disease and asthma, 1990-2015: a systematic analysis for the Global Burden of Disease Study 2015. *Lancet Respir Med*. 2017;5(9):691-706.
9. Kaysin A, Viera AJ. Community-Acquired Pneumonia in Adults: Diagnosis and Management. *Am Fam Physician*. 2016;94(9):698-706.
10. Kurmani S, Squire I. Acute Heart Failure: Definition, Classification and Epidemiology. *Curr Heart Fail Rep*. 2017;14(5):385-92.
11. Weintraub NL, Collins SP, Pang PS, Levy PD, Anderson AS, Arslanian-Engoren C, et al. Acute heart failure syndromes: emergency department presentation, treatment, and disposition: current approaches and future aims: a scientific statement from the American Heart Association. *Circulation*. 2010;122(19):1975-96.
12. Ponikowski P, Voors AA, Anker SD, Bueno H, Cleland JGF, Coats AJS, et al. 2016 ESC Guidelines for the diagnosis and treatment of acute and chronic heart failure: The Task Force for the diagnosis and treatment of acute and chronic heart failure of the European Society of Cardiology (ESC) Developed with the special contribution of the Heart Failure Association (HFA) of the ESC. *Eur Heart J*. 2016;37(27):2129-200.
13. Shi K, Jiang J, Ma T, Xie J, Duan L, Chen R, et al. Pathogenesis pathways of idiopathic pulmonary fibrosis in bleomycin-induced lung injury model in mice. *Respir Physiol Neurobiol*. 2014;190:113-7.
14. Liu Y, Chance MR. Pathway analyses and understanding disease associations. *Curr Genet Med Rep*. 2013;1(4).
15. Habib N, Pasha MA, Tang DD. Current Understanding of Asthma Pathogenesis and Biomarkers. *Cells*. 2022;11(17).

16. MacNee W. Pathology, pathogenesis, and pathophysiology. *Bmj*. 2006;332(7551):1202-4.
17. Chen L, Deng H, Cui H, Fang J, Zuo Z, Deng J, et al. Inflammatory responses and inflammation-associated diseases in organs. *Oncotarget*. 2018;9(6):7204-18.
18. Miller AH, Maletic V, Raison CL. Inflammation and its discontents: the role of cytokines in the pathophysiology of major depression. *Biol Psychiatry*. 2009;65(9):732-41.
19. Alberts B JA, Lewis J, et al. Helper T Cells and Lymphocyte Activation. *Molecular Biology of the Cell* 4th edition: New York: Garland Science; 2002.
20. Alberts B JA, Lewis J, et al. . Chapter 24, The Adaptive Immune System. *Molecular Biology of the Cell*: New York: Garland Science; 2002.
21. Sugimoto MA, Sousa LP, Pinho V, Perretti M, Teixeira MM. Resolution of Inflammation: What Controls Its Onset? *Front Immunol*. 2016;7:160.
22. Ortega-Gómez A, Perretti M, Soehnlein O. Resolution of inflammation: an integrated view. *EMBO Mol Med*. 2013;5(5):661-74.
23. Gilroy DW, Bishop-Bailey D. Lipid mediators in immune regulation and resolution. *Br J Pharmacol*. 2019;176(8):1009-23.
24. Rosales C. Neutrophil: A Cell with Many Roles in Inflammation or Several Cell Types? *Front Physiol*. 2018;9:113.
25. Saqib U, Sarkar S, Suk K, Mohammad O, Baig MS, Savai R. Phytochemicals as modulators of M1-M2 macrophages in inflammation. *Oncotarget*. 2018;9(25):17937-50.
26. Arpaia N, Green JA, Moltedo B, Arvey A, Hemmers S, Yuan S, et al. A Distinct Function of Regulatory T Cells in Tissue Protection. *Cell*. 2015;162(5):1078-89.
27. Iyer SS, Cheng G. Role of interleukin 10 transcriptional regulation in inflammation and autoimmune disease. *Crit Rev Immunol*. 2012;32(1):23-63.
28. Moldoveanu B, Otmishi P, Jani P, Walker J, Sarmiento X, Guardiola J, et al. Inflammatory mechanisms in the lung. *J Inflamm Res*. 2009;2:1-11.
29. Brightling CE, Barker BL. Phenotyping chronic obstructive pulmonary disease (COPD) exacerbations: realising personalised medicine. *Clinical Medicine*. 2012;12(Suppl 6):s52.
30. Bafadhel M, McKenna S, Terry S, Mistry V, Reid C, Haldar P, et al. Acute exacerbations of chronic obstructive pulmonary disease: identification of biologic clusters and their biomarkers. *Am J Respir Crit Care Med*. 2011;184(6):662-71.
31. Tinè M, Biondini D, Semenzato U, Bazzan E, Cosio MG, Saetta M, et al. Reassessing the Role of Eosinophils as a Biomarker in Chronic Obstructive Pulmonary Disease. *J Clin Med*. 2019;8(7):962.
32. Bafadhel M, Peterson S, De Blas MA, Calverley PM, Rennard SI, Richter K, et al. Predictors of exacerbation risk and response to budesonide in patients with chronic obstructive pulmonary disease: a post-hoc analysis of three randomised trials. *Lancet Respir Med*. 2018;6(2):117-26.
33. Bafadhel M, McKenna S, Terry S, Mistry V, Pancholi M, Venge P, et al. Blood eosinophils to direct corticosteroid treatment of exacerbations of chronic obstructive pulmonary disease: a randomized placebo-controlled trial. *Am J Respir Crit Care Med*. 2012;186(1):48-55.
34. Vedel-Krogh S, Nielsen SF, Lange P, Vestbo J, Nordestgaard BG. Blood Eosinophils and Exacerbations in Chronic Obstructive Pulmonary Disease. The Copenhagen General Population Study. *Am J Respir Crit Care Med*. 2016;193(9):965-74.

35. Haldar K, George L, Wang Z, Mistry V, Ramsheh MY, Free RC, et al. The sputum microbiome is distinct between COPD and health, independent of smoking history. *Respiratory Research*. 2020;21(1):183.
36. Wang Z, Bafadhel M, Haldar K, Spivak A, Mayhew D, Miller BE, et al. Lung microbiome dynamics in COPD exacerbations. *European Respiratory Journal*. 2016;47(4):1082.
37. Hurst JR. Consolidation and Exacerbation of COPD. *Med Sci (Basel)*. 2018;6(2):44.
38. Castro M, Corren J, Pavord ID, Maspero J, Wenzel S, Rabe KF, et al. Dupilumab Efficacy and Safety in Moderate-to-Severe Uncontrolled Asthma. *New England Journal of Medicine*. 2018;378(26):2486-96.
39. Nelson RK, Bush A, Stokes J, Nair P, Akuthota P. Eosinophilic Asthma. *J Allergy Clin Immunol Pract*. 2020;8(2):465-73.
40. Jatakanon A, Laloo UG, Lim S, Chung KF, Barnes PJ. Increased neutrophils and cytokines, TNF-alpha and IL-8, in induced sputum of non-asthmatic patients with chronic dry cough. *Thorax*. 1999;54(3):234-7.
41. Kuruvilla ME, Lee FE, Lee GB. Understanding Asthma Phenotypes, Endotypes, and Mechanisms of Disease. *Clin Rev Allergy Immunol*. 2019;56(2):219-33.
42. Yamasaki A, Okazaki R, Harada T. Neutrophils and Asthma. *Diagnostics (Basel)*. 2022;12(5).
43. Gibson PG, Simpson JL, Saltos N. Heterogeneity of airway inflammation in persistent asthma : evidence of neutrophilic inflammation and increased sputum interleukin-8. *Chest*. 2001;119(5):1329-36.
44. Jatakanon A, Uasuf C, Maziak W, Lim S, Chung KF, Barnes PJ. Neutrophilic inflammation in severe persistent asthma. *Am J Respir Crit Care Med*. 1999;160(5 Pt 1):1532-9.
45. Njoroge JN, Teerlink JR. Pathophysiology and Therapeutic Approaches to Acute Decompensated Heart Failure. *Circulation Research*. 2021;128(10):1468-86.
46. Levy BD, Vachier I, Serhan CN. Resolution of inflammation in asthma. *Clin Chest Med*. 2012;33(3):559-70.
47. Halade GV, Lee DH. Inflammation and resolution signaling in cardiac repair and heart failure. *EBioMedicine*. 2022;79:103992.
48. Bozinovski S, Anthony D, Vlahos R. Targeting pro-resolution pathways to combat chronic inflammation in COPD. *J Thorac Dis*. 2014;6(11):1548-56.
49. Bauer TT, Ewig S, Rodloff AC, Müller EE. Acute Respiratory Distress Syndrome and Pneumonia: A Comprehensive Review of Clinical Data. *Clinical Infectious Diseases*. 2006;43(6):748-56.
50. Kellum JA, Kong L, Fink MP, Weissfeld LA, Yealy DM, Pinsky MR, et al. Understanding the inflammatory cytokine response in pneumonia and sepsis: results of the Genetic and Inflammatory Markers of Sepsis (GenIMS) Study. *Arch Intern Med*. 2007;167(15):1655-63.
51. McCauley L, Dean N. Pneumonia and empyema: causal, casual or unknown. *J Thorac Dis*. 2015;7(6):992-8.
52. Boyd AR, Orihuela CJ. Dysregulated inflammation as a risk factor for pneumonia in the elderly. *Aging Dis*. 2011;2(6):487-500.
53. Green CE, Turner AM. The role of the endothelium in asthma and chronic obstructive pulmonary disease (COPD). *Respiratory Research*. 2017;18(1):20.

54. Singer M, Deutschman CS, Seymour CW, Shankar-Hari M, Annane D, Bauer M, et al. The Third International Consensus Definitions for Sepsis and Septic Shock (Sepsis-3). *JAMA*. 2016;315(8):801-10.
55. Mizgerd JP. Lung Infection—A Public Health Priority. *PLOS Medicine*. 2006;3(2):e76.
56. Verbrugge FH, Guazzi M, Testani JM, Borlaug BA. Altered Hemodynamics and End-Organ Damage in Heart Failure. *Circulation*. 2020;142(10):998-1012.
57. Giannitsi S, Bougiakli M, Bechlioulis A, Naka K. Endothelial dysfunction and heart failure: A review of the existing bibliography with emphasis on flow mediated dilation. *JRSM Cardiovasc Dis*. 2019;8:2048004019843047-.
58. Sies H. Oxidative Stress: Concept and Some Practical Aspects. *Antioxidants (Basel)*. 2020;9(9).
59. Mittal M, Siddiqui MR, Tran K, Reddy SP, Malik AB. Reactive oxygen species in inflammation and tissue injury. *Antioxid Redox Signal*. 2014;20(7):1126-67.
60. Wiegman CH, Michaeloudes C, Haji G, Narang P, Clarke CJ, Russell KE, et al. Oxidative stress-induced mitochondrial dysfunction drives inflammation and airway smooth muscle remodeling in patients with chronic obstructive pulmonary disease. *J Allergy Clin Immunol*. 2015;136(3):769-80.
61. Hough KP, Curtiss ML, Blain TJ, Liu RM, Trevor J, Deshane JS, et al. Airway Remodeling in Asthma. *Front Med (Lausanne)*. 2020;7:191.
62. Zhang Q, Ju Y, Ma Y, Wang T. N-acetylcysteine improves oxidative stress and inflammatory response in patients with community acquired pneumonia: A randomized controlled trial. *Medicine*. 2018;97(45).
63. Romieu I, Trenga C. Diet and obstructive lung diseases. *Epidemiol Rev*. 2001;23(2):268-87.
64. Berdnikovs S, Newcomb DC, Gebretsadik T, Snyder BM, Wiggins DA, Poleon KS, et al. Cellular and systemic energy metabolic dysregulation in asthma development—a hypothesis-generating approach. *J Allergy Clin Immunol*. 2022;149(5):1802-6.e2.
65. Ho WE, Xu YJ, Xu F, Cheng C, Peh HY, Tannenbaum SR, et al. Metabolomics reveals altered metabolic pathways in experimental asthma. *Am J Respir Cell Mol Biol*. 2013;48(2):204-11.
66. Xue M, Zeng Y, Lin R, Qu HQ, Zhang T, Zhang XD, et al. Metabolomic profiling of anaerobic and aerobic energy metabolic pathways in chronic obstructive pulmonary disease. *Exp Biol Med (Maywood)*. 2021;246(14):1586-96.
67. Lopaschuk GD, Karwi QG, Tian R, Wende AR, Abel ED. Cardiac Energy Metabolism in Heart Failure. *Circulation Research*. 2021;128(10):1487-513.
68. Kao CC, Hsu JW, Bandi V, Hanania NA, Kheradmand F, Jahoor F. Glucose and pyruvate metabolism in severe chronic obstructive pulmonary disease. *J Appl Physiol (1985)*. 2012;112(1):42-7.
69. Nagham J, Hawa E, Ebtessam I, Kenneth N. The association between blood glucose levels and hospital outcomes in patients admitted with acute exacerbations of chronic obstructive pulmonary disease. *The Southwest Respiratory and Critical Care Chronicles*. 2014;2(7).
70. Peters MC, Schiebler M, Bleecker ER, Castro M, Erzurum SC, Hastie AT, et al. Impaired Glucose Metabolism Is Associated with Asthma Severity in the Severe Asthma Research Program-3 (SARP-3) Cohort. *A31 ASTHMA: CLINICAL STUDIES I*. American Thoracic Society International Conference Abstracts: American Thoracic Society; 2019. p. A1280-A.

71. Tran DH, Wang ZV. Glucose Metabolism in Cardiac Hypertrophy and Heart Failure. *Journal of the American Heart Association*. 2019;8(12):e012673.
72. Paixão L, Caldas J, Kloosterman TG, Kuipers OP, Vinga S, Neves AR. Transcriptional and metabolic effects of glucose on *Streptococcus pneumoniae* sugar metabolism. *Front Microbiol*. 2015;6:1041.
73. Chen H, Li Z, Dong L, Wu Y, Shen H, Chen Z. Lipid metabolism in chronic obstructive pulmonary disease. *Int J Chron Obstruct Pulmon Dis*. 2019;14:1009-18.
74. Kotlyarov S, Kotlyarova A. Molecular Mechanisms of Lipid Metabolism Disorders in Infectious Exacerbations of Chronic Obstructive Pulmonary Disease. *Int J Mol Sci*. 2021;22(14).
75. Jiang T, Dai L, Li P, Zhao J, Wang X, An L, et al. Lipid metabolism and identification of biomarkers in asthma by lipidomic analysis. *Biochimica et Biophysica Acta (BBA) - Molecular and Cell Biology of Lipids*. 2021;1866(2):158853.
76. Potashnikova DM, Tvorogova AV, Saidova AA, Sotnikova TN, Arifulin EA, Lipina TV, et al. Lung lipid deposition in pneumonias of viral and non-viral aetiology. *bioRxiv*. 2023.
77. Engelen MP, Wouters EF, Deutz NE, Menheere PP, Schols AM. Factors contributing to alterations in skeletal muscle and plasma amino acid profiles in patients with chronic obstructive pulmonary disease. *Am J Clin Nutr*. 2000;72(6):1480-7.
78. Xu W, Comhair SAA, Janocha AJ, Lara A, Mavrakis LA, Bennett CD, et al. Arginine metabolic endotypes related to asthma severity. *PLOS ONE*. 2017;12(8):e0183066.
79. Arshad H, Siokis A, Franke R, Habib A, Alfonso JCL, Poliakova Y, et al. Reprogramming of Amino Acid Metabolism Differs between Community-Acquired Pneumonia and Infection-Associated Exacerbation of Chronic Obstructive Pulmonary Disease. *Cells*. 2022;11(15).
80. Narita K, Amiya E. Is branched-chain amino acid nutritional supplementation beneficial or detrimental in heart failure? *World J Cardiol*. 2021;13(6):163-9.
81. Verbanck S, Thompson BR, Schuermans D, Kalsi H, Biddiscombe M, Stuart-Andrews C, et al. Ventilation heterogeneity in the acinar and conductive zones of the normal ageing lung. *Thorax*. 2012;67(9):789.
82. Rutting S, Chapman DG, Farah CS, Thamrin C. Lung heterogeneity as a predictor for disease severity and response to therapy. *Current Opinion in Physiology*. 2021;22:100446.
83. Takahashi T, Yamada S, Tanabe K, Nakayama M, Osada N, Itoh H, et al. The effects of posture on the ventilatory responses during exercise. *J Jpn Phys Ther Assoc*. 1998;1(1):13-7.
84. Hogg JC. Pathophysiology of airflow limitation in chronic obstructive pulmonary disease. *Lancet*. 2004;364(9435):709-21.
85. Thompson BR, Douglass JA, Ellis MJ, Kelly VJ, O'Hehir RE, King GG, et al. Peripheral lung function in patients with stable and unstable asthma. *J Allergy Clin Immunol*. 2013;131(5):1322-8.
86. McNulty W, Usmani OS. Techniques of assessing small airways dysfunction. *Eur Clin Respir J*. 2014;1.
87. Young HM, Guo F, Eddy RL, Maksym G, Parraga G. Oscillometry and pulmonary MRI measurements of ventilation heterogeneity in obstructive lung disease: relationship to quality of life and disease control. *Journal of Applied Physiology*. 2018;125(1):73-85.
88. Farrow CE, Salome CM, Harris BE, Bailey DL, Berend N, King GG. Peripheral ventilation heterogeneity determines the extent of bronchoconstriction in asthma. *Journal of applied physiology*. 2017;123(5):1188-94.

89. Pisi R, Aiello M, Calzetta L, Frizzelli A, Alfieri V, Bertorelli G, et al. Ventilation Heterogeneity in Asthma and COPD: The Value of the Poorly Communicating Fraction as the Ratio of Total Lung Capacity to Alveolar Volume. *Respiration*. 2021;100(5):404-10.
90. Davis C, Sheikh K, Pike D, Svenningsen S, McCormack DG, O'Donnell D, et al. Ventilation Heterogeneity in Never-smokers and COPD:: Comparison of Pulmonary Functional Magnetic Resonance Imaging with the Poorly Communicating Fraction Derived From Plethysmography. *Academic Radiology*. 2016;23(4):398-405.
91. Tang FSM, Rutting S, Farrow CE, Tonga KO, Watts J, Dame-Carrol JR, et al. Ventilation heterogeneity and oscillometry predict asthma control improvement following step-up inhaled therapy in uncontrolled asthma. *Respirology*. 2020;25(8):827-35.
92. Kjellberg S, Houltz BK, Zetterström O, Robinson PD, Gustafsson PM. Clinical characteristics of adult asthma associated with small airway dysfunction. *Respir Med*. 2016;117:92-102.
93. Ueda T, Niimi A, Matsumoto H, Takemura M, Hirai T, Yamaguchi M, et al. Role of small airways in asthma: investigation using high-resolution computed tomography. *J Allergy Clin Immunol*. 2006;118(5):1019-25.
94. Verbanck S, Schuermans D, Noppen M, Van Muylem A, Paiva M, Vincken W. Evidence of acinar airway involvement in asthma. *Am J Respir Crit Care Med*. 1999;159(5 Pt 1):1545-50.
95. Downie SR, Salome CM, Verbanck S, Thompson B, Berend N, King GG. Ventilation heterogeneity is a major determinant of airway hyperresponsiveness in asthma, independent of airway inflammation. *Thorax*. 2007;62(8):684-9.
96. Farah CS, King GG, Brown NJ, Peters MJ, Berend N, Salome CM. Ventilation heterogeneity predicts asthma control in adults following inhaled corticosteroid dose titration. *J Allergy Clin Immunol*. 2012;130(1):61-8.
97. Gerald Teague W, Mata J, Qing K, Tustison NJ, Mugler JP, Meyer CH, et al. Measures of ventilation heterogeneity mapped with hyperpolarized helium-3 MRI demonstrate a T2-high phenotype in asthma. *Pediatr Pulmonol*. 2021;56(6):1440-8.
98. Stephen IR. COPD Heterogeneity: What This Will Mean in Practice. *Respiratory Care*. 2011;56(8):1181.
99. Linnea J, Jaro A, Leif B, Ellen T. Ventilation heterogeneity in COPD and healthy smokers relates to diffusion capacity, resistance and reactance. *European Respiratory Journal*. 2015;46(suppl 59):PA1031.
100. Inui S, Yoon SH, Doganay O, Gleeson FV, Kim M. Impaired pulmonary ventilation beyond pneumonia in COVID-19: A preliminary observation. *PLoS One*. 2022;17(1):e0263158.
101. Yoon SH, Kim M. Anterior Pulmonary Ventilation Abnormalities in COVID-19. *Radiology*. 2020;297(2):E276-e7.
102. Kee K, Stuart-Andrews C, Nilsen K, Wrobel JP, Thompson BR, Naughton MT. Ventilation heterogeneity is increased in patients with chronic heart failure. *Physiol Rep*. 2015;3(10).
103. Mountain JE, Santer P, O'Neill DP, Smith NMJ, Ciaffoni L, Couper JH, et al. Potential for noninvasive assessment of lung inhomogeneity using highly precise, highly time-resolved measurements of gas exchange. *Journal of Applied Physiology*. 2017;124(3):615-31.
104. Shimizu K, Yoshii Y, Morozumi M, Chiba N, Ubukata K, Uruga H, et al. Pathogens in COPD exacerbations identified by comprehensive real-time PCR plus older methods. *Int J Chron Obstruct Pulmon Dis*. 2015;10:2009-16.

105. Postollec F, Falentin H, Pavan S, Combrisson J, Sohier D. Recent advances in quantitative PCR (qPCR) applications in food microbiology. *Food Microbiol.* 2011;28(5):848-61.
106. Bafadhel M, Haldar K, Barker B, Patel H, Mistry V, Barer MR, et al. Airway bacteria measured by quantitative polymerase chain reaction and culture in patients with stable COPD: relationship with neutrophilic airway inflammation, exacerbation frequency, and lung function. *Int J Chron Obstruct Pulmon Dis.* 2015;10:1075-83.
107. Garibyan L, Avashia N. Polymerase chain reaction. *J Invest Dermatol.* 2013;133(3):1-4.
108. Rampini SK, Bloemberg GV, Keller PM, Büchler AC, Dollenmaier G, Speck RF, et al. Broad-range 16S rRNA gene polymerase chain reaction for diagnosis of culture-negative bacterial infections. *Clin Infect Dis.* 2011;53(12):1245-51.
109. Allaband C, McDonald D, Vázquez-Baeza Y, Minich JJ, Tripathi A, Brenner DA, et al. Microbiome 101: Studying, Analyzing, and Interpreting Gut Microbiome Data for Clinicians. *Clin Gastroenterol Hepatol.* 2019;17(2):218-30.
110. Sproston NR, Ashworth JJ. Role of C-Reactive Protein at Sites of Inflammation and Infection. *Front Immunol.* 2018;9:754-.
111. Li Y, Xie L, Xin S, Li K. Values of procalcitonin and C-reactive proteins in the diagnosis and treatment of chronic obstructive pulmonary disease having concomitant bacterial infection. *Pak J Med Sci.* 2017;33(3):566-9.
112. Butler CC, Gillespie D, White P, Bates J, Lowe R, Thomas-Jones E, et al. C-Reactive Protein Testing to Guide Antibiotic Prescribing for COPD Exacerbations. *N Engl J Med.* 2019;381(2):111-20.
113. Monadi M, Firouzjahi A, Hosseini A, Javadian Y, Sharbatdaran M, Heidari B. Serum C-reactive protein in asthma and its ability in predicting asthma control, a case-control study. *Caspian J Intern Med.* 2016;7(1):37-42.
114. Razi E, Ehteram H, Akbari H, Chavoshi V, Razi A. Evaluation of high-sensitivity C-reactive protein in acute asthma. *Tanaffos.* 2012;11(1):32-7.
115. Kalogeropoulos AP, Tang WH, Hsu A, Felker GM, Hernandez AF, Troughton RW, et al. High-sensitivity C-reactive protein in acute heart failure: insights from the ASCEND-HF trial. *J Card Fail.* 2014;20(5):319-26.
116. Stockley RA. Biomarkers in chronic obstructive pulmonary disease: confusing or useful? *Int J Chron Obstruct Pulmon Dis.* 2014;9:163-77.
117. Falsey AR, Becker KL, Swinburne AJ, Nysten ES, Snider RH, Formica MA, et al. Utility of serum procalcitonin values in patients with acute exacerbations of chronic obstructive pulmonary disease: a cautionary note. *Int J Chron Obstruct Pulmon Dis.* 2012;7:127-35.
118. Sin DD, Man SF. Why are patients with chronic obstructive pulmonary disease at increased risk of cardiovascular diseases? The potential role of systemic inflammation in chronic obstructive pulmonary disease. *Circulation.* 2003;107(11):1514-9.
119. Li Z, Yuan X, Yu L, Wang B, Gao F, Ma J. Procalcitonin-guided antibiotic therapy in acute exacerbation of chronic obstructive pulmonary disease: An updated meta-analysis. *Medicine (Baltimore).* 2019;98(32):e16775.
120. Lin C, Pang Q. Meta-analysis and systematic review of procalcitonin-guided treatment in acute exacerbation of chronic obstructive pulmonary disease. *Clin Respir J.* 2018;12(1):10-5.

121. Lindenauer PK, Shieh MS, Stefan MS, Fisher KA, Haessler SD, Pekow PS, et al. Hospital Procalcitonin Testing and Antibiotic Treatment of Patients Admitted for Chronic Obstructive Pulmonary Disease Exacerbation. *Ann Am Thorac Soc*. 2017;14(12):1779-85.
122. Price DB, Rigazio A, Campbell JD, Bleecker ER, Corrigan CJ, Thomas M, et al. Blood eosinophil count and prospective annual asthma disease burden: a UK cohort study. *Lancet Respir Med*. 2015;3(11):849-58.
123. Nayyar M, Scott S, Ahmad M. P121 Raised blood eosinophil count as a predictor of severe asthma exacerbation. *Thorax*. 2021;76(Suppl 1):A154.
124. Matucci A, Vultaggio A, Maggi E, Kasujee I. Is IgE or eosinophils the key player in allergic asthma pathogenesis? Are we asking the right question? *Respiratory Research*. 2018;19(1):113.
125. Benjamin D, Mona B, Leo K, Antony De S. Eosinophilic inflammation in COPD: from an inflammatory marker to a treatable trait. *Thorax*. 2021;76(2):188.
126. Lommatzsch M, Speer T, Herr C, Jörres RA, Watz H, Müller A, et al. IgE is associated with exacerbations and lung function decline in COPD. *Respiratory Research*. 2022;23(1):1.
127. Ricciardolo FL, Sorbello V, Ciprandi G. A pathophysiological approach for FeNO: A biomarker for asthma. *Allergol Immunopathol (Madr)*. 2015;43(6):609-16.
128. Badar A, Salem AM, Bamosa AO, Qutub HO, Gupta RK, Siddiqui IA. Association Between FeNO, Total Blood IgE, Peripheral Blood Eosinophil and Inflammatory Cytokines in Partly Controlled Asthma. *J Asthma Allergy*. 2020;13:533-43.
129. Neelamegan R, Saka V, Tamilarasu K, Rajaram M, Selvarajan S, Chandrasekaran A. Clinical Utility of Fractional exhaled Nitric Oxide (FeNO) as a Biomarker to Predict Severity of Disease and Response to Inhaled Corticosteroid (ICS) in Asthma Patients. *J Clin Diagn Res*. 2016;10(12):Fc01-fc6.
130. Use of B-Type Natriuretic Peptide (BNP) and N-Terminal proBNP (NT-proBNP) as Diagnostic Tests in Adults With Suspected Heart Failure: A Health Technology Assessment. *Ont Health Technol Assess Ser*. 2021;21(2):1-125.
131. Sujino Y, Nakano S, Tanno J, Shiraishi Y, Goda A, Mizuno A, et al. Clinical implications of the blood urea nitrogen/creatinine ratio in heart failure and their association with haemoconcentration. *ESC Heart Fail*. 2019;6(6):1274-82.
132. Serhan CN, Chiang N, Van Dyke TE. Resolving inflammation: dual anti-inflammatory and pro-resolution lipid mediators. *Nature Reviews Immunology*. 2008;8(5):349-61.
133. Levy BD, Serhan CN. Resolution of acute inflammation in the lung. *Annu Rev Physiol*. 2014;76:467-92.
134. Biernacki WA, Kharitonov SA, Barnes PJ. Increased leukotriene B4 and 8-isoprostane in exhaled breath condensate of patients with exacerbations of COPD. *Thorax*. 2003;58(4):294.
135. Ban G-Y, Kim S-H, Park H-S. Persistent Eosinophilic Inflammation in Adult Asthmatics with High Serum and Urine Levels of Leukotriene E4. *Journal of Asthma and Allergy*. 2021;Volume 14:1219-30.
136. Green SA, Malice MP, Tanaka W, Tozzi CA, Reiss TF. Increase in urinary leukotriene LTE₄ levels in acute asthma: correlation with airflow limitation. *Thorax*. 2004;59(2):100.
137. Shindo K, Hirai Y, Fukumura M, Koide K. Plasma levels of leukotriene E4 during clinical course of chronic obstructive pulmonary disease. *Prostaglandins Leukot Essent Fatty Acids*. 1997;56(3):213-7.

138. Higham A, Cadden P, Southworth T, Rossall M, Kolsum U, Lea S, et al. Leukotriene B4 levels in sputum from asthma patients. *ERJ Open Res.* 2016;2(4).
139. Fajt ML, Gelhaus SL, Freeman B, Uvalle CE, Trudeau JB, Holguin F, et al. Prostaglandin D₂ pathway upregulation: relation to asthma severity, control, and TH2 inflammation. *J Allergy Clin Immunol.* 2013;131(6):1504-12.
140. Spears M, Chaudhuri R, McSharry C, Jolly L, Thompson J, Lafferty J, et al. Elevated Sputum Prostaglandin D2 (PGD2) Concentrations In Asthma. C38 AIRWAY INFLAMMATION: FROM MECHANISMS TO NON-INVASIVE BIOMARKERS. American Thoracic Society International Conference Abstracts: American Thoracic Society; 2011. p. A4448-A.
141. Tejwani V, Villabona-Rueda AF, Khare P, Zhang C, Le A, Putcha N, et al. Airway and Systemic Prostaglandin E2 Association with COPD Symptoms and Macrophage Phenotype. *Chronic Obstr Pulm Dis.* 2023;10(2):159-69.
142. Currie GP, McLaughlin K. The expanding role of leukotriene receptor antagonists in chronic asthma. *Annals of Allergy, Asthma & Immunology.* 2006;97(6):731-42.
143. Barnes PJ. Anti-inflammatory actions of glucocorticoids: molecular mechanisms. *Clin Sci (Lond).* 1998;94(6):557-72.
144. John F, Kavitha S, Panicker S, Nair T, Indira M. Elevated levels of leukotriene B4 and thromboxane B2 distinguish chest pain of cardiac and non cardiac origin. *Indian Heart J.* 2013;65(3):295-9.
145. Gu X, Xu J, Zhu L, Bryson T, Yang XP, Peterson E, et al. Prostaglandin E2 Reduces Cardiac Contractility via EP3 Receptor. *Circ Heart Fail.* 2016;9(8).
146. Stephenson AH, Lonigro AJ, Hyers TM, Webster RO, Fowler AA. Increased concentrations of leukotrienes in bronchoalveolar lavage fluid of patients with ARDS or at risk for ARDS. *Am Rev Respir Dis.* 1988;138(3):714-9.
147. Ricciotti E, FitzGerald GA. Prostaglandins and Inflammation. *Arteriosclerosis, Thrombosis, and Vascular Biology.* 2011;31(5):986-1000.
148. Busse WW. Leukotrienes and Inflammation. *American Journal of Respiratory and Critical Care Medicine.* 1998;157(6):S210-S3.
149. Fredman G, Serhan CN. Specialized proresolving mediator targets for RvE1 and RvD1 in peripheral blood and mechanisms of resolution. *Biochem J.* 2011;437(2):185-97.
150. Harris SG, Padilla J, Koumas L, Ray D, Phipps RP. Prostaglandins as modulators of immunity. *Trends Immunol.* 2002;23(3):144-50.
151. Finney L, Wiseman D, Mackay A, Macleod M, Ritchie A, Mah J, et al. Impaired Exacerbation Recovery Is Associated With Reduced Resolvin D1 in Chronic Obstructive Pulmonary Disease. B94 DISEASE PROGRESSION AND MORBIDITY ALONG THE SPECTRUM OF COPD: FROM EARLY TO ESTABLISHED. American Thoracic Society International Conference Abstracts: American Thoracic Society; 2023. p. A4209-A.
152. Liga B, Gunta S, Normunds J, Uldis K, Agnese K, Marina B, et al. LSC 2011 Abstract: The role of lipoxin A4 in the chronic obstructive pulmonary disease. *European Respiratory Journal.* 2011;38(Suppl 55):p414.
153. L. Balode DI, A. Kislina, S. Isajevs, G. Strazda, N. Jurka, U. Kopeika, M. Bukovskis, I. Taivans (Riga, Latvia). . Chronic obstructive pulmonary disease is characterized with suppressed lipoxin A4 and increased lipoxin receptor expression in lungs. . *Eur Respir J* 2012;40: Suppl. 56, 4588.
154. Kytikova O, Novgorodtseva T, Denisenko Y, Antonyuk M, Gvozdenko T. Pro-Resolving Lipid Mediators in the Pathophysiology of Asthma. *Medicina (Kaunas).* 2019;55(6).

155. Abdulnour RE, Sham HP, Douda DN, Colas RA, Dalli J, Bai Y, et al. Aspirin-triggered resolvin D1 is produced during self-resolving gram-negative bacterial pneumonia and regulates host immune responses for the resolution of lung inflammation. *Mucosal Immunol.* 2016;9(5):1278-87.
156. Higgins G, Fustero Torre C, Tyrrell J, McNally P, Harvey BJ, Urbach V. Lipoxin A4 prevents tight junction disruption and delays the colonization of cystic fibrosis bronchial epithelial cells by *Pseudomonas aeruginosa*. *Am J Physiol Lung Cell Mol Physiol.* 2016;310(11):L1053-61.
157. Irún P, Gracia R, Piazuolo E, Pardo J, Morte E, Paño JR, et al. Serum lipid mediator profiles in COVID-19 patients and lung disease severity: a pilot study. *Sci Rep.* 2023;13(1):6497.
158. Chiurchiù V, Leuti A, Saracini S, Fontana D, Finamore P, Giua R, et al. Resolution of inflammation is altered in chronic heart failure and entails a dysfunctional responsiveness of T lymphocytes. *Faseb j.* 2019;33(1):909-16.
159. Halade GV, Kain V, Serhan CN. Immune responsive resolvin D1 programs myocardial infarction-induced cardiorenal syndrome in heart failure. *Faseb j.* 2018;32(7):3717-29.
160. Kanoh M, Inai K, Shinohara T, Tomimatsu H, Nakanishi T. Clinical implications of eicosapentaenoic acid/arachidonic acid ratio (EPA/AA) in adult patients with congenital heart disease. *Heart Vessels.* 2017;32(12):1513-22.
161. Ninomiya T, Nagata M, Hata J, Hirakawa Y, Ozawa M, Yoshida D, et al. Association between ratio of serum eicosapentaenoic acid to arachidonic acid and risk of cardiovascular disease: the Hisayama Study. *Atherosclerosis.* 2013;231(2):261-7.
162. Nambiar S, Bong How S, Gummer J, Trengove R, Moodley Y. Metabolomics in chronic lung diseases. *Respirology.* 2020;25(2):139-48.
163. Papaioannou O, Karampitsakos T, Barbayianni I, Chrysikos S, Xylourgidis N, Tzilas V, et al. Metabolic Disorders in Chronic Lung Diseases. *Front Med (Lausanne).* 2017;4:246.
164. Wishart DS. Emerging applications of metabolomics in drug discovery and precision medicine. *Nature Reviews Drug Discovery.* 2016;15(7):473-84.
165. Martinez KB, Leone V, Chang EB. Microbial metabolites in health and disease: Navigating the unknown in search of function. *J Biol Chem.* 2017;292(21):8553-9.
166. Trabado S, Al-Salameh A, Croixmarie V, Masson P, Corruble E, Fève B, et al. The human plasma-metabolome: Reference values in 800 French healthy volunteers; impact of cholesterol, gender and age. *PloS one.* 2017;12(3):e0173615.
167. Godbole S, Bowler RP. Metabolome Features of COPD: A Scoping Review. *Metabolites.* 2022;12(7).
168. Comhair SA, McDunn J, Bennett C, Fettig J, Erzurum SC, Kalhan SC. Metabolomic Endotype of Asthma. *J Immunol.* 2015;195(2):643-50.
169. Ikeda H. Plasma amino acid levels in individuals with bacterial pneumonia and healthy controls. *Clinical Nutrition ESPEN.* 2021;44:204-10.
170. Banoei MM, Vogel HJ, Weljie AM, Kumar A, Yende S, Angus DC, et al. Plasma metabolomics for the diagnosis and prognosis of H1N1 influenza pneumonia. *Critical Care.* 2017;21(1):97.
171. Nguyen M, Bourredjem A, Piroth L, Bouhemad B, Jalil A, Pallot G, et al. High plasma concentration of non-esterified polyunsaturated fatty acids is a specific feature of severe COVID-19 pneumonia. *Sci Rep.* 2021;11(1):10824.

172. More TH, Mozafari B, Märten A, Herr C, Lepper PM, Danziger G, et al. Plasma Metabolome Alterations Discriminate between COVID-19 and Non-COVID-19 Pneumonia. *Metabolites* [Internet]. 2022; 12(11).
173. Banoei MM, Vogel HJ, Weljie AM, Yende S, Angus DC, Winston BW. Plasma lipid profiling for the prognosis of 90-day mortality, in-hospital mortality, ICU admission, and severity in bacterial community-acquired pneumonia (CAP). *Critical Care*. 2020;24(1):461.
174. Albert CL, Tang WHW. Metabolic Biomarkers in Heart Failure. *Heart Fail Clin*. 2018;14(1):109-18.
175. Shah SH, Sun J-L, Stevens RD, Bain JR, Muehlbauer MJ, Pieper KS, et al. Baseline metabolomic profiles predict cardiovascular events in patients at risk for coronary artery disease. *American Heart Journal*. 2012;163(5):844-50.e1.
176. Khan SS, Kalhan R. Comorbid Chronic Obstructive Pulmonary Disease and Heart Failure: Shared Risk Factors and Opportunities to Improve Outcomes. *Ann Am Thorac Soc*. 2022;19(6):897-9.
177. Berliner D, Schneider N, Welte T, Bauersachs J. The Differential Diagnosis of Dyspnea. *Dtsch Arztebl Int*. 2016;113(49):834-45.
178. Fortis S, Luszczek ER, Weinert CR, Beilman GJ. Metabolomics in COPD Acute Respiratory Failure Requiring Noninvasive Positive Pressure Ventilation. *Canadian Respiratory Journal*. 2017;2017.
179. Loreto F, Schnitzler J-P. Abiotic stresses and induced BVOCs. *Trends in Plant Science*. 2010;15(3):154-66.
180. Amann A, Smith D. *Breath Analysis for Clinical Diagnosis and Therapeutic Monitoring*: WORLD SCIENTIFIC; 2005. 556 p.
181. EPA. Volatile Organic Compounds' Impact on Indoor Air Quality LAST UPDATED ON AUGUST 26, 2022 [Available from: <https://www.epa.gov/indoor-air-quality-iaq/volatile-organic-compounds-impact-indoor-air-quality>].
182. Haick H, Broza YY, Mochalski P, Ruzsanyi V, Amann A. Assessment, origin, and implementation of breath volatile cancer markers. *Chem Soc Rev*. 2014;43(5):1423-49.
183. de Lacy Costello B, Amann A, Al-Kateb H, Flynn C, Filipiak W, Khalid T, et al. A review of the volatiles from the healthy human body. *J Breath Res*. 2014;8(1):014001.
184. Dragonieri S, Annema JT, Schot R, van der Schee MP, Spanevello A, Carratú P, et al. An electronic nose in the discrimination of patients with non-small cell lung cancer and COPD. *Lung Cancer*. 2009;64(2):166-70.
185. Radogna AV, Siciliano PA, Sabina S, Sabato E, Capone S. A Low-Cost Breath Analyzer Module in Domiciliary Non-Invasive Mechanical Ventilation for Remote COPD Patient Monitoring. *Sensors (Basel)*. 2020;20(3).
186. Miekisch W, Schubert JK, Noeldge-Schomburg GF. Diagnostic potential of breath analysis--focus on volatile organic compounds. *Clin Chim Acta*. 2004;347(1-2):25-39.
187. Pereira J, Porto-Figueira P, Cavaco C, Taunk K, Rapole S, Dhakne R, et al. Breath analysis as a potential and non-invasive frontier in disease diagnosis: an overview. *Metabolites*. 2015;5(1):3-55.
188. Ildiko H, Peter JB, Stelios L, Peter JS, Marieann H, Anna-Carin O, et al. A European Respiratory Society technical standard: exhaled biomarkers in lung disease. *European Respiratory Journal*. 2017;49(4):1600965.
189. Amann A, Spaněl P, Smith D. Breath analysis: the approach towards clinical applications. *Mini Rev Med Chem*. 2007;7(2):115-29.

190. Phillips M, Cataneo RN, Cummin AR, Gagliardi AJ, Gleeson K, Greenberg J, et al. Detection of lung cancer with volatile markers in the breath. *Chest*. 2003;123(6):2115-23.
191. van de Kant KD, van der Sande LJ, Jöbsis Q, van Schayck OC, Dompeling E. Clinical use of exhaled volatile organic compounds in pulmonary diseases: a systematic review. *Respir Res*. 2012;13(1):117.
192. Spaněl P, Smith D. Progress in SIFT-MS: breath analysis and other applications. *Mass Spectrom Rev*. 2011;30(2):236-67.
193. Jung C, Mahmoud NSA, Alqassimi N. Identifying the relationship between VOCs emission and temperature/humidity changes in new apartments in the hot desert climate. *Frontiers in Built Environment*. 2022;8.
194. Du L, Batterman S, Godwin C, Rowe Z, Chin JY. Air exchange rates and migration of VOCs in basements and residences. *Indoor Air*. 2015;25(6):598-609.
195. Peletiri S, Rahmanian N, Mujtaba I. CO2 Pipeline design: A review. *Energies*. 2018;11:2184.
196. Ibrahim W, Carr L, Cordell R, Wilde MJ, Salman D, Monks PS, et al. Breathomics for the clinician: the use of volatile organic compounds in respiratory diseases. *Thorax*. 2021;76(5):514-21.
197. Ibrahim W, Wilde MJ, Cordell RL, Richardson M, Salman D, Free RC, et al. Visualization of exhaled breath metabolites reveals distinct diagnostic signatures for acute cardiorespiratory breathlessness. *Sci Transl Med*. 2022;14(671):eabl5849.
198. Schleiss MB, Holz O, Behnke M, Richter K, Magnussen H, Jörres RA. The concentration of hydrogen peroxide in exhaled air depends on expiratory flow rate. *Eur Respir J*. 2000;16(6):1115-8.
199. Macklem PT. The mechanics of breathing. *Am J Respir Crit Care Med*. 1998;157(4 Pt 2):S88-94.
200. Gertler R. Respiratory Mechanics. *Anesthesiol Clin*. 2021;39(3):415-40.
201. Mecham RP. Elastin in lung development and disease pathogenesis. *Matrix Biol*. 2018;73:6-20.
202. Hopkins E, Sharma S. Physiology, Functional Residual Capacity. StatPearls. Treasure Island (FL): StatPearls Publishing Copyright © 2023, StatPearls Publishing LLC.; 2023.
203. Venkataraman ST. Chapter 49 - Mechanical Ventilation and Respiratory Care. In: Fuhrman BP, Zimmerman JJ, editors. *Pediatric Critical Care (Fourth Edition)*. Saint Louis: Mosby; 2011. p. 657-88.
204. Otis AB, McKerrow CB, Bartlett RA, Mead J, McIlroy MB, Selverstone NJ, et al. Mechanical Factors in Distribution of Pulmonary Ventilation. *Journal of Applied Physiology*. 1956;8(4):427-43.
205. Mead J. Measurement of Inertia of the Lungs at Increased Ambient Pressure. *Journal of Applied Physiology*. 1956;9(2):208-12.
206. Olson DE, Dart GA, Filley GF. Pressure drop and fluid flow regime of air inspired into the human lung. *J Appl Physiol*. 1970;28(4):482-94.
207. Kaminsky DA. What does airway resistance tell us about lung function? *Respir Care*. 2012;57(1):85-96; discussion -9.
208. Ren S, Cai M, Shi Y, Xu W, Zhang XD. Influence of bronchial diameter change on the airflow dynamics based on a pressure-controlled ventilation system. *International Journal for Numerical Methods in Biomedical Engineering*. 2018;34(3):e2929.

209. Campbell M, Sapra A. Physiology, Airflow Resistance. StatPearls. Treasure Island (FL): StatPearls Publishing
Copyright © 2023, StatPearls Publishing LLC.; 2023.
210. Sériès F, Marc I. Influence of lung volume dependence of upper airway resistance during continuous negative airway pressure. *J Appl Physiol* (1985). 1994;77(2):840-4.
211. Rodarte J, Rehder K. Dynamics of Respiration. 2011.
212. Ingram R, Pedley T. Pressure-Flow Relationships in the Lungs. 2011.
213. DuBois AB, Brody AW, Lewis DH, Burgess BF. Oscillation mechanics of lungs and chest in man. *J Appl Physiol*. 1956;8.
214. Oostveen E. The forced oscillation technique in clinical practice: methodology, recommendations and future developments. *Eur Respir J*. 2003;22.
215. Coates AL, Vallinis P, Mullahoo K, Seddon P, Davis GM. Pulmonary impedance as an index of severity and mechanisms of neonatal lung disease. *Pediatr Pulmonol*. 1994;17(1):41-9.
216. Desiraju K, Agrawal A. Impulse oscillometry: The state-of-art for lung function testing. *Lung India*. 2016;33(4):410-6.
217. Lándsér FJ, Nagles J, Demedts M, Billiet L, van de Woestijne KP. A new method to determine frequency characteristics of the respiratory system. *J Appl Physiol*. 1976;41(1):101-6.
218. Marcia S, Matthew R, James T, John O-B, Salman S. Comparison of Forced and Impulse Oscillometry Measurements: A Clinical Population and Printed Airway Model Study. *European Respiratory Journal*. 2018;52(suppl 62):PA3390.
219. Schulz H, Flexeder C, Behr J, Heier M, Holle R, Huber RM, et al. Reference values of impulse oscillometric lung function indices in adults of advanced age. *PLoS One*. 2013;8(5):e63366.
220. Bellemare F, Jeanneret A, Couture J. Sex differences in thoracic dimensions and configuration. *Am J Respir Crit Care Med*. 2003;168(3):305-12.
221. Park JE, Chung JH, Lee KH, Shin KC. The effect of body composition on pulmonary function. *Tuberc Respir Dis (Seoul)*. 2012;72(5):433-40.
222. Kenneth IB, Margaret W, Roberta MG, Joan R, Mark RF, Stephen MF, et al. Respiratory impedance measured using impulse oscillometry in a healthy urban population. *ERJ Open Research*. 2021;7(1):00560-2020.
223. Braun L. Race, ethnicity and lung function: A brief history. *Can J Respir Ther*. 2015;51(4):99-101.
224. Lai S-H, Yao T-C, Liao S-L, Tsai M-H, Hua M-C, Yeh K-W, et al. Reference Value of Impulse Oscillometry in Taiwanese Preschool Children. *Pediatrics & Neonatology*. 2015;56(3):165-70.
225. Wu J, Zhang H, Shi Y, Wang J, Han Y, Zhang Q, et al. Reference values of impulse oscillometry (IOS) for healthy Chinese children aged 4–17 years. *Respiratory Research*. 2022;23(1):182.
226. Kohlhäufel M, Brand P, Scheuch G, Schulz H, Häussinger K, Heyder J. Impulse oscillometry in healthy nonsmokers and asymptomatic smokers: effects of bronchial challenge with methacholine. *J Aerosol Med*. 2001;14(1):1-12.
227. Kalchier-Dekel O, Hines SE. Forty years of reference values for respiratory system impedance in adults: 1977–2017. *Respiratory Medicine*. 2018;136:37-47.

228. Navanandan N, Hamlington KL, Mistry RD, Szeffler SJ, Liu AH. Oscillometry for acute asthma in the pediatric emergency department: A feasibility study. *Ann Allergy Asthma Immunol.* 2020;125(5):607-9.
229. Park J-H, Lee JH, Kim H-J, Jeong N, Jang H-J, Kim H-K, et al. Usefulness of impulse oscillometry for the assessment of bronchodilator response in elderly patients with chronic obstructive airway disease. *Journal of Thoracic Disease.* 2019;11(4):1485-94.
230. Klompas M, Baker M, Rhee C. What Is an Aerosol-Generating Procedure? *JAMA Surgery.* 2021;156(2):113-4.
231. Porojan-Suppini N, Fira-Mladinescu O, Marc M, Tudorache E, Oancea C. Lung Function Assessment by Impulse Oscillometry in Adults. *Ther Clin Risk Manag.* 2020;16:1139-50.
232. Wei X, Shi Z, Cui Y, Mi J, Ma Z, Ren J, et al. Impulse oscillometry system as an alternative diagnostic method for chronic obstructive pulmonary disease. *Medicine (Baltimore).* 2017;96(46):e8543.
233. David AK, Shannon JS, Kenneth IB, Peter C, Pedro LdM, Ronald D, et al. Clinical significance and applications of oscillometry. *European Respiratory Review.* 2022;31(163):210208.
234. Das V, Thorat Y, Vanjare NV, Rasam SA, Madas SJ, Kodgule RR, et al. X5 values measured on Impulse Oscillometry (IOS) help differentiate healthy, asthmatic, COPD and ILD subjects from one another. *Respiratory function technologists/scient.* 2018.
235. Bailly C, Crenesse D, Albertini M. Evaluation of impulse oscillometry during bronchial challenge testing in children. *Pediatr Pulmonol.* 2011;46(12):1209-14.
236. Schulze J, Smith HJ, Fuchs J, Herrmann E, Dressler M, Rose MA, et al. Methacholine challenge in young children as evaluated by spirometry and impulse oscillometry. *Respir Med.* 2012;106(5):627-34.
237. Batmaz SB, Kuyucu S, Arikoglu T, Tezol O, Aydogdu A. Impulse oscillometry in acute and stable asthmatic children: a comparison with spirometry. *J Asthma.* 2016;53(2):179-86.
238. Frantz S, Nihlén U, Dencker M, Engström G, Löfdahl CG, Wollmer P. Impulse oscillometry may be of value in detecting early manifestations of COPD. *Respir Med.* 2012;106(8):1116-23.
239. Crim C, Celli B, Edwards LD, Wouters E, Coxson HO, Tal-Singer R, et al. Respiratory system impedance with impulse oscillometry in healthy and COPD subjects: ECLIPSE baseline results. *Respir Med.* 2011;105(7):1069-78.
240. Galant SP, Komarow HD, Shin HW, Siddiqui S, Lipworth BJ. The case for impulse oscillometry in the management of asthma in children and adults. *Ann Allergy Asthma Immunol.* 2017;118.
241. Junichi O, Hajime K, Hiromasa O, Toshiya I, Wataru H, Masahiro K. Application of impulse oscillometry for within-breath analysis in patients with chronic obstructive pulmonary disease: pilot study. *BMJ Open.* 2011;1(2):e000184.
242. Kuo CR, Jabbal S, Lipworth B. Is small airways dysfunction related to asthma control and type 2 inflammation? *Ann Allergy Asthma Immunol.* 2018;121(5):631-2.
243. Gong SG, Yang WL, Zheng W, Liu JM. Evaluation of respiratory impedance in patients with chronic obstructive pulmonary disease by an impulse oscillation system. *Mol Med Rep.* 2014;10(5):2694-700.
244. Gonem S, Umar I, Burke D, Desai D, Corkill S, Owers-Bradley J, et al. Airway impedance entropy and exacerbations in severe asthma. *Eur Respir J.* 2012;40(5):1156-63.

245. Shi Y, Aledia AS, Galant SP, George SC. Peripheral airway impairment measured by oscillometry predicts loss of asthma control in children. *J Allergy Clin Immunol*. 2013;131(3):718-23.
246. Li Y, Chen Y, Wang P. Application of impulse oscillometry and bronchial dilation test for analysis in patients with asthma and chronic obstructive pulmonary disease. *Int J Clin Exp Med*. 2015;8(1):1271-5.
247. Song TW, Kim KW, Kim ES, Park JW, Sohn MH, Kim KE. Utility of impulse oscillometry in young children with asthma. *Pediatr Allergy Immunol*. 2008;19(8):763-8.
248. Sumner LW, Amberg A, Barrett D, Beale MH, Beger R, Daykin CA, et al. Proposed minimum reporting standards for chemical analysis. *Metabolomics*. 2007;3(3):211-21.
249. Digital service to manage high-risk chronic obstructive pulmonary disease (COPD) patients: NHS; [Available from: <https://transform.england.nhs.uk/key-tools-and-info/digital-playbooks/respiratory-digital-playbook/digital-service-to-manage-high-risk-chronic-obstructive-pulmonary-disease-copd-patients/>].
250. Mathioudakis AG, Janssens W, Sivapalan P, Singanayagam A, Dransfield MT, Jensen JS, et al. Acute exacerbations of chronic obstructive pulmonary disease: in search of diagnostic biomarkers and treatable traits. *Thorax*. 2020;75(6):520-7.
251. National Heart Failure Audit (NHFA) 2023 Summary Report (2021/22 data) [Available from: <https://www.nicor.org.uk/wp-content/uploads/2023/06/10633-NICOR-Annual-Summary-Reports-NHFA-v4-AC.pdf>].
252. Stone R, Holzhauer-Barrie J, Lowe D, McMillan V, Khan MS, Roberts M. Mortality after an acute exacerbation of COPD (AECOPD): findings from the National COPD Audit Programme. *European Respiratory Journal*. 2017;50(suppl 61):PA4969.
253. Gargiulo P, Banfi C, Ghilardi S, Magrì D, Giovannardi M, Bonomi A, et al. Surfactant-derived proteins as markers of alveolar membrane damage in heart failure. *PloS one*. 2014;9(12):e115030-e.
254. Tsutsui H, Kinugawa S, Matsushima S. Oxidative stress and heart failure. *Am J Physiol Heart Circ Physiol*. 2011;301(6):H2181-90.
255. Rosca MG, Hoppel CL. Mitochondrial dysfunction in heart failure. *Heart Fail Rev*. 2013;18(5):607-22.
256. Ptaszynska-Kopczynska K, Szpakowicz A, Marcinkiewicz-Siemion M, Lisowska A, Waszkiewicz E, Witkowski M, et al. Interleukin-6 signaling in patients with chronic heart failure treated with cardiac resynchronization therapy. *Arch Med Sci*. 2017;13(5):1069-77.
257. André S, Conde B, Fragoso E, Boléo-Tomé JP, Areias V, Cardoso J. COPD and Cardiovascular Disease. *Pulmonology*. 2019;25(3):168-76.
258. van Gestel AJ, Steier J. Autonomic dysfunction in patients with chronic obstructive pulmonary disease (COPD). *J Thorac Dis*. 2010;2(4):215-22.
259. Florea VG, Cohn JN. The Autonomic Nervous System and Heart Failure. *Circulation Research*. 2014;114(11):1815-26.
260. Ibrahim W, Wilde MJ, Cordell RL, Richardson M, Salman D, Free RC, et al. Visualization of exhaled breath metabolites reveals distinct diagnostic signatures for acute cardiorespiratory breathlessness. *Sci Transl Med*. 2022;14(671):eabl5849.
261. Carlsson G. Topology and data. *Bulletin of the American Mathematical Society*. 2009;46(2):255-308.
262. Otter N, Porter MA, Tillmann U, Grindrod P, Harrington HA. A roadmap for the computation of persistent homology. *EPJ Data Science*. 2017;6(1):17.

263. Torang A, Gupta P, Klinker DJ. An elastic-net logistic regression approach to generate classifiers and gene signatures for types of immune cells and T helper cell subsets. *BMC Bioinformatics*. 2019;20(1):433.
264. Choudhary R, Gianey HK, editors. Comprehensive review on supervised machine learning algorithms. 2017 International Conference on Machine Learning and Data Science (MLDS); 2017: IEEE.
265. Wishart DS, Feunang YD, Marcu A, Guo AC, Liang K, Vázquez-Fresno R, et al. HMDB 4.0: the human metabolome database for 2018. *Nucleic Acids Res*. 2018;46(D1):D608-D17.
266. Norman BP, Davison AS, Ross GA, Milan AM, Hughes AT, Sutherland H, et al. A Comprehensive LC-QTOF-MS Metabolic Phenotyping Strategy: Application to Alkaptonuria. *Clinical Chemistry*. 2019;65(4):530-9.
267. Fahy E, Cotter D, Sud M, Subramaniam S. Lipid classification, structures and tools. *Biochim Biophys Acta*. 2011;1811(11):637-47.
268. t'Kindt R, Telenga ED, Jorge L, Van Oosterhout AJM, Sandra P, Ten Hacken NHT, et al. Profiling over 1500 Lipids in Induced Lung Sputum and the Implications in Studying Lung Diseases. *Analytical Chemistry*. 2015;87(9):4957-64.
269. Yan F, Wen Z, Wang R, Luo W, Du Y, Wang W, et al. Identification of the lipid biomarkers from plasma in idiopathic pulmonary fibrosis by Lipidomics. *BMC Pulm Med*. 2017;17(1):174.
270. Quehenberger O, Armando AM, Brown AH, Milne SB, Myers DS, Merrill AH, et al. Lipidomics reveals a remarkable diversity of lipids in human plasma 1 [S]. *Journal of Lipid Research*. 2010;51(11):3299-305.
271. Zhang Y, Zhou Q, Ding X, Wang H, Tan G. HILIC-MS-based metabolomics reveal that *Astragalus polysaccharide* alleviates doxorubicin-induced cardiomyopathy by regulating sphingolipid and glycerophospholipid homeostasis. *Journal of Pharmaceutical and Biomedical Analysis*. 2021;203:114177.
272. Bahls M, Friedrich N, Pietzner M, Wachter R, Budde K, Hasenfuß G, et al. Heterogeneous Metabolic Response to Exercise Training in Heart Failure with Preserved Ejection Fraction. *J Clin Med*. 2019;8(5):591.
273. Kärkkäinen O, Tuomainen T, Mutikainen M, Lehtonen M, Ruas JL, Hanhineva K, et al. Heart specific PGC-1 α deletion identifies metabolome of cardiac restricted metabolic heart failure. *Cardiovascular Research*. 2018;115(1):107-18.
274. Berry CE, Wise RA. Mortality in COPD: causes, risk factors, and prevention. *Copd*. 2010;7(5):375-82.
275. Ran N, Pang Z, Gu Y, Pan H, Zuo X, Guan X, et al. An Updated Overview of Metabolomic Profile Changes in Chronic Obstructive Pulmonary Disease. *Metabolites*. 2019;9(6).
276. Naser AY, Mansour MM, Alanazi AFR, Sabha O, Alwafi H, Jalal Z, et al. Hospital admission trends due to respiratory diseases in England and Wales between 1999 and 2019: an ecologic study. *BMC Pulmonary Medicine*. 2021;21(1):356.
277. Hickey DA, Beecroft S. PCV124 - HOSPITAL ADMISSIONS FOR HEART FAILURE IN ENGLAND; AN INCREASING BURDEN ON NHS RESOURCES AND THE FOCUS OF EFFECTIVE COST CONTAINMENT. *Value in Health*. 2018;21:S113.
278. Desiraju K, Agrawal A. Impulse oscillometry: The state-of-art for lung function testing. *Lung India : official organ of Indian Chest Society*. 2016;33(4):410-6.
279. Choi IS, Koh YI, Lim H. Peak expiratory flow rate underestimates severity of airflow obstruction in acute asthma. *Korean J Intern Med*. 2002;17(3):174-9.

280. Global Strategy for the Diagnosis MaPoC. Global Initiative for Chronic Obstructive Lung Disease (GOLD). 2011.
281. Komarow HD, Myles IA, Uzzaman A, Metcalfe DD. Impulse oscillometry in the evaluation of diseases of the airways in children. *Ann Allergy Asthma Immunol.* 2011;106(3):191-9.
282. <The forced oscillation technique in clinical practice.pdf>.
283. Global Initiative for Asthma (GINA). The global strategy for asthma management and prevention, Available from <http://www.ginasthma.org> (2017).
284. Gregory G, King JB, Kenneth I. Berger, Peter Calverley, Pedro L. de Melo, Raffaele L. Dellacà, Ramon Farré, Graham L. Hall, Iulia Ioan, Charles G. Irvin, David W. Kaczka, David A. Kaminsky, Hajime Kurosawa, Enrico Lombardi, Geoffrey N. Maksym, François Marchal, Beno W. Oppenheimer, Shannon J. Simpson, Cindy Thamrin, Maarten van den Berge, Ellie Oostveen. Technical Standards for Respiratory Oscillometry. *Eur Respir J.* 2019.
285. King GG, Bates J, Berger KI, Calverley P, de Melo PL, Dellacà RL, et al. Technical standards for respiratory oscillometry. *European Respiratory Journal.* 2020;55(2):1900753.
286. Schulz H, Flexeder C, Behr J, Heier M, Holle R, Huber RM, et al. Reference values of impulse oscillometric lung function indices in adults of advanced age. *PLoS one.* 2013;8(5):e63366-e.
287. Oostveen E. Respiratory impedance in healthy subjects: baseline values and bronchodilator response. *Eur Respir J.* 2013;42.
288. Alqahtani JS, Al Rajeh AM, Aldahir AM, Aldabayan YS, Hurst JR, Mandal S. The clinical utility of forced oscillation technique during hospitalisation in patients with exacerbation of COPD. *ERJ Open Res.* 2021;7(4).
289. Terraneo S, Rinaldo RF, Sferrazza Papa GF, Ribolla F, Gulotta C, Maugeri L, et al. Distinct Mechanical Properties of the Respiratory System Evaluated by Forced Oscillation Technique in Acute Exacerbation of COPD and Acute Decompensated Heart Failure. *Diagnostics (Basel).* 2021;11(3).
290. Hantos Z. Intra-breath oscillometry for assessing respiratory outcomes. *Current Opinion in Physiology.* 2021;22:100441.
291. Sherif G, Imraan U, Daniel B, Dhananjay D, Steven C, John O-B, et al. Airway impedance entropy and exacerbations in severe asthma. *European Respiratory Journal.* 2012;40(5):1156.
292. Das S, Pal S, Mitra M. Significance of Exhaled Breath Test in Clinical Diagnosis: A Special Focus on the Detection of Diabetes Mellitus. *J Med Biol Eng.* 2016;36(5):605-24.
293. Cikach FS, Jr., Dweik RA. Cardiovascular biomarkers in exhaled breath. *Prog Cardiovasc Dis.* 2012;55(1):34-43.
294. Hyttinen M, Rautiainen P, Ruokolainen J, Sorvari J, Pasanen P. VOCs concentrations and emission rates in hospital environment and the impact of sampling locations. *Science and Technology for the Built Environment.* 2021;27(7):986-94.
295. Faulkner WB, Memarzadeh F, Riskowski G, Kalbasi A, Ching-Zu Chang A. Effects of air exchange rate, particle size and injection place on particle concentrations within a reduced-scale room. *Building and Environment.* 2015;92:246-55.
296. Wilde MJ, Zhao B, Cordell RL, Ibrahim W, Singapuri A, Greening NJ, et al. Automating and Extending Comprehensive Two-Dimensional Gas Chromatography Data Processing by Interfacing Open-Source and Commercial Software. *Analytical Chemistry.* 2020;92(20):13953-60.

297. van Vorstenbosch R, Cheng HR, Jonkers D, Penders J, Schoon E, Masclee A, et al. Systematic Review: Contribution of the Gut Microbiome to the Volatile Metabolic Fingerprint of Colorectal Neoplasia. *Metabolites*. 2023;13(1):55.
298. Phan J, Meinardi S, Barletta B, Blake DR, Whiteson K. Stable isotope profiles reveal active production of VOCs from human-associated microbes. *J Breath Res*. 2017;11(1):017101.
299. Bovey F, Cros J, Tuzson B, Seyssel K, Schneiter P, Emmenegger L, et al. Breath acetone as a marker of energy balance: an exploratory study in healthy humans. *Nutrition & Diabetes*. 2018;8(1):50.
300. Ibrahim B, Basanta M, Cadden P, Singh D, Douce D, Woodcock A, et al. Non-invasive phenotyping using exhaled volatile organic compounds in asthma. *Thorax*. 2011;66(9):804-9.
301. Phillips M, Cataneo RN, Chaturvedi A, Kaplan PD, Libardoni M, Mundada M, et al. Detection of an extended human volatome with comprehensive two-dimensional gas chromatography time-of-flight mass spectrometry. *PLoS One*. 2013;8(9):e75274.
302. Raman M, Ahmed I, Gillevet PM, Probert CS, Ratcliffe NM, Smith S, et al. Fecal microbiome and volatile organic compound metabolome in obese humans with nonalcoholic fatty liver disease. *Clin Gastroenterol Hepatol*. 2013;11(7):868-75.e1-3.
303. Garner CE, Smith S, de Lacy Costello B, White P, Spencer R, Probert CS, et al. Volatile organic compounds from feces and their potential for diagnosis of gastrointestinal disease. *Faseb j*. 2007;21(8):1675-88.
304. De Preter V, Machiels K, Joossens M, Arijis I, Matthys C, Vermeire S, et al. Faecal metabolite profiling identifies medium-chain fatty acids as discriminating compounds in IBD. *Gut*. 2015;64(3):447-58.
305. Bioassay of 1,4-dioxane for possible carcinogenicity. *Natl Cancer Inst Carcinog Tech Rep Ser*. 1978;80:1-123.
306. Kano H, Umeda Y, Kasai T, Sasaki T, Matsumoto M, Yamazaki K, et al. Carcinogenicity studies of 1,4-dioxane administered in drinking-water to rats and mice for 2 years. *Food Chem Toxicol*. 2009;47(11):2776-84.
307. Silva CL, Passos M, Câmara JS. Solid phase microextraction, mass spectrometry and metabolomic approaches for detection of potential urinary cancer biomarkers--a powerful strategy for breast cancer diagnosis. *Talanta*. 2012;89:360-8.
308. Francavilla R, Ercolini D, Piccolo M, Vannini L, Siragusa S, De Filippis F, et al. Salivary microbiota and metabolome associated with celiac disease. *Appl Environ Microbiol*. 2014;80(11):3416-25.
309. Robertson HT. Dead space: the physiology of wasted ventilation. *European Respiratory Journal*. 2015;45(6):1704.
310. Carr L, Ramsheh MY, Bryant L, Yousef A, Cordell R, Wilde M, et al. Effect of age, gender and body habitus upon exhaled breath volatiles in COPD and health. *European Respiratory Journal*. 2020;56(suppl 64):2199.
311. Haeggström JZ, Funk CD. Lipoxygenase and leukotriene pathways: biochemistry, biology, and roles in disease. *Chem Rev*. 2011;111(10):5866-98.
312. Nakamura M, Shimizu T. Leukotriene receptors. *Chem Rev*. 2011;111(10):6231-98.
313. Serhan CN. A search for endogenous mechanisms of anti-inflammation uncovers novel chemical mediators: missing links to resolution. *Histochem Cell Biol*. 2004;122(4):305-21.

314. Shimizu T. Lipid mediators in health and disease: enzymes and receptors as therapeutic targets for the regulation of immunity and inflammation. *Annu Rev Pharmacol Toxicol.* 2009;49:123-50.
315. Zhang MJ, Spite M. Resolvins: anti-inflammatory and proresolving mediators derived from omega-3 polyunsaturated fatty acids. *Annu Rev Nutr.* 2012;32:203-27.
316. Basil MC, Levy BD. Specialized pro-resolving mediators: endogenous regulators of infection and inflammation. *Nat Rev Immunol.* 2016;16(1):51-67.
317. Fredman G, Li Y, Dalli J, Chiang N, Serhan CN. Self-Limited versus Delayed Resolution of Acute Inflammation: Temporal Regulation of Pro-Resolving Mediators and MicroRNA. *Scientific Reports.* 2012;2(1):639.
318. Dalli J, Zhu M, Vlasenko NA, Deng B, Haeggström JZ, Petasis NA, et al. The novel 13S,14S-epoxy-maresin is converted by human macrophages to maresin 1 (MaR1), inhibits leukotriene A4 hydrolase (LTA4H), and shifts macrophage phenotype. *Faseb j.* 2013;27(7):2573-83.
319. Hong S, Gronert K, Devchand PR, Moussignac R-L, Serhan CN. Novel Docosatrienes and 17S-Resolvins Generated from Docosahexaenoic Acid in Murine Brain, Human Blood, and Glial Cells: AUTACOIDS IN ANTI-INFLAMMATION*. *Journal of Biological Chemistry.* 2003;278(17):14677-87.
320. Serhan CN, Clish CB, Brannon J, Colgan SP, Chiang N, Gronert K. Novel functional sets of lipid-derived mediators with antiinflammatory actions generated from omega-3 fatty acids via cyclooxygenase 2-nonsteroidal antiinflammatory drugs and transcellular processing. *J Exp Med.* 2000;192(8):1197-204.
321. Serhan CN, Hong S, Gronert K, Colgan SP, Devchand PR, Mirick G, et al. Resolvins: a family of bioactive products of omega-3 fatty acid transformation circuits initiated by aspirin treatment that counter proinflammation signals. *J Exp Med.* 2002;196(8):1025-37.
322. Serhan CN, Petasis NA. Resolvins and protectins in inflammation resolution. *Chem Rev.* 2011;111(10):5922-43.
323. Colas RA, Shinohara M, Dalli J, Chiang N, Serhan CN. Identification and signature profiles for pro-resolving and inflammatory lipid mediators in human tissue. *Am J Physiol Cell Physiol.* 2014;307(1):C39-54.
324. Croasdell A, Lacy SH, Thatcher TH, Sime PJ, Phipps RP. Resolvin D1 Dampens Pulmonary Inflammation and Promotes Clearance of Nontypeable Haemophilus influenzae. *J Immunol.* 2016;196(6):2742-52.
325. Yang A, Wu Y, Yu G, Wang H. Role of specialized pro-resolving lipid mediators in pulmonary inflammation diseases: mechanisms and development. *Respiratory Research.* 2021;22(1):204.
326. Kazani S, Planaguma A, Ono E, Bonini M, Zahid M, Marigowda G, et al. Exhaled breath condensate eicosanoid levels associate with asthma and its severity. *J Allergy Clin Immunol.* 2013;132(3):547-53.
327. Vachier I, Bonnans C, Chavis C, Farce M, Godard P, Bousquet J, et al. Severe asthma is associated with a loss of LX4, an endogenous anti-inflammatory compound. *J Allergy Clin Immunol.* 2005;115(1):55-60.
328. Ono E, Dutile S, Kazani S, Wechsler ME, Yang J, Hammock BD, et al. Lipoxin generation is related to soluble epoxide hydrolase activity in severe asthma. *Am J Respir Crit Care Med.* 2014;190(8):886-97.

329. Grumbach Y, Quynh NV, Chiron R, Urbach V. LXA4 stimulates ZO-1 expression and transepithelial electrical resistance in human airway epithelial (16HBE14o-) cells. *Am J Physiol Lung Cell Mol Physiol*. 2009;296(1):L101-8.
330. Barnig C, Cernadas M, Dutile S, Liu X, Perrella MA, Kazani S, et al. Lipoxin A4 regulates natural killer cell and type 2 innate lymphoid cell activation in asthma. *Sci Transl Med*. 2013;5(174):174ra26.
331. Haworth O, Cernadas M, Levy BD. NK cells are effectors for resolvin E1 in the timely resolution of allergic airway inflammation. *J Immunol*. 2011;186(11):6129-35.
332. Balode L, Strazda G, Jurka N, Kopeika U, Kislina A, Bukovskis M, et al. Lipoxigenase-derived arachidonic acid metabolites in chronic obstructive pulmonary disease. *Medicina*. 2012;48(6):43.
333. Croasdell A, Thatcher TH, Kottmann RM, Colas RA, Dalli J, Serhan CN, et al. Resolvins attenuate inflammation and promote resolution in cigarette smoke-exposed human macrophages. *Am J Physiol Lung Cell Mol Physiol*. 2015;309(8):L888-901.
334. Kim KH, Park TS, Kim YS, Lee JS, Oh YM, Lee SD, et al. Resolvin D1 prevents smoking-induced emphysema and promotes lung tissue regeneration. *Int J Chron Obstruct Pulmon Dis*. 2016;11:1119-28.
335. Pena KB, Ramos CO, Soares NP, da Silva PF, Bandeira AC, Costa GP, et al. The administration of a high refined carbohydrate diet promoted an increase in pulmonary inflammation and oxidative stress in mice exposed to cigarette smoke. *Int J Chron Obstruct Pulmon Dis*. 2016;11:3207-17.
336. Hsiao HM, Sapinoro RE, Thatcher TH, Croasdell A, Levy EP, Fulton RA, et al. A novel anti-inflammatory and pro-resolving role for resolvin D1 in acute cigarette smoke-induced lung inflammation. *PLoS One*. 2013;8(3):e58258.
337. Takamiya R, Fukunaga K, Arita M, Miyata J, Seki H, Minematsu N, et al. Resolvin E1 maintains macrophage function under cigarette smoke-induced oxidative stress. *FEBS Open Bio*. 2012;2:328-33.
338. Dalli J, Kraft BD, Colas RA, Shinohara M, Fredenburgh LE, Hess DR, et al. The Regulation of Proresolving Lipid Mediator Profiles in Baboon Pneumonia by Inhaled Carbon Monoxide. *Am J Respir Cell Mol Biol*. 2015;53(3):314-25.
339. Codagnone M, Cianci E, Lamolinara A, Mari VC, Nespoli A, Isopi E, et al. Resolvin D1 enhances the resolution of lung inflammation caused by long-term *Pseudomonas aeruginosa* infection. *Mucosal Immunol*. 2018;11(1):35-49.
340. Ruffin M, Brochiero E. Repair Process Impairment by *Pseudomonas aeruginosa* in Epithelial Tissues: Major Features and Potential Therapeutic Avenues. *Front Cell Infect Microbiol*. 2019;9:182.
341. Ramon S, Baker SF, Sahler JM, Kim N, Feldsott EA, Serhan CN, et al. The specialized proresolving mediator 17-HDHA enhances the antibody-mediated immune response against influenza virus: a new class of adjuvant? *J Immunol*. 2014;193(12):6031-40.
342. Morita M, Kuba K, Ichikawa A, Nakayama M, Katahira J, Iwamoto R, et al. The lipid mediator protectin D1 inhibits influenza virus replication and improves severe influenza. *Cell*. 2013;153(1):112-25.
343. Rangel Moreno J, Estrada García I, De La Luz García Hernández M, Aguilar Leon D, Marquez R, Hernández Pando R. The role of prostaglandin E2 in the immunopathogenesis of experimental pulmonary tuberculosis. *Immunology*. 2002;106(2):257-66.

344. Bormann T, Maus R, Stolper J, Jonigk D, Welte T, Gauldie J, et al. Role of the COX2-PGE(2) axis in *S. pneumoniae*-induced exacerbation of experimental fibrosis. *Am J Physiol Lung Cell Mol Physiol*. 2021;320(3):L377-l92.
345. Schmid T, Brüne B. Prostanoids and Resolution of Inflammation - Beyond the Lipid-Mediator Class Switch. *Front Immunol*. 2021;12:714042.
346. Kim N, Thatcher TH, Sime PJ, Phipps RP. Corticosteroids inhibit anti-IgE activities of specialized proresolving mediators on B cells from asthma patients. *JCI Insight*. 2017;2(3):e88588.
347. Cook NR. Quantifying the added value of new biomarkers: how and how not. *Diagnostic and Prognostic Research*. 2018;2(1):14.
348. Bafadhel M, McKenna S, Terry S, Mistry V, Reid C, Haldar P, et al. Acute Exacerbations of Chronic Obstructive Pulmonary Disease. *American Journal of Respiratory and Critical Care Medicine*. 2011;184(6):662-71.
349. Boggon R, Hubbard R, Smeeth L, Gulliford M, Cassell J, Eaton S, et al. Variability of antibiotic prescribing in patients with chronic obstructive pulmonary disease exacerbations: a cohort study. *BMC Pulm Med*. 2013;13:32.
350. Rockenschaub P, Jhass A, Freemantle N, Aryee A, Rafiq M, Hayward A, et al. Opportunities to reduce antibiotic prescribing for patients with COPD in primary care: a cohort study using electronic health records from the Clinical Practice Research Datalink (CPRD). *Journal of Antimicrobial Chemotherapy*. 2019;75(1):243-51.
351. Pouwels KB, Dolk FCK, Smith DRM, Robotham JV, Smieszek T. Actual versus 'ideal' antibiotic prescribing for common conditions in English primary care. *J Antimicrob Chemother*. 2018;73(suppl_2):19-26.


```

        xlab = "",
        col = "blue")
hist(Acute_sputum_no_HF_have_v1$`V1_PD1`,
     breaks = 9,
     main = "V1_PD1",
     xlab = "",
     col = "blue")
hist(Acute_sputum_no_HF_have_v1$`V1_MaR_2`,
     breaks = 9,
     main = "V1_MaR_2",
     xlab = "",
     col = "blue")
hist(Acute_sputum_no_HF_have_v1$`V1_MaR_1`,
     breaks = 9,
     main = "V1_MaR_1",
     xlab = "",
     col = "blue")
hist(Acute_sputum_no_HF_have_v1$age,
     breaks = 9,
     main = "age",
     xlab = "",
     col = "blue")

hist(Acute_sputum_no_HF_have_v1$v1a_blood_eos,
     breaks = 9,
     main = "v1a_blood_eos",
     xlab = "",
     col = "blue")
hist(Acute_sputum_no_HF_have_v1$v1a_blood_bnp,
     breaks = 9,
     main = "v1a_blood_bnp",
     xlab = "",
     col = "blue")
hist(Acute_sputum_no_HF_have_v1$v1a_blood_crp,
     breaks = 9,
     main = "v1a_blood_crp",
     xlab = "",
     col = "blue")

hist(Acute_sputum_no_HF_have_v1$v1a_bp_top,
     breaks = 9,
     main = "v1a_bp_top",
     xlab = "",
     col = "blue")
hist(Acute_sputum_no_HF_have_v1$v1a_temperature,
     breaks = 9,
     main = "v1a_temperature",
     xlab = "",
     col = "blue")
hist(Acute_sputum_no_HF_have_v1$v1a_heart_rate,
     breaks = 9,
     main = "v1a_heart_rate",
     xlab = "",
     col = "blue")
hist(Acute_sputum_no_HF_have_v1$v1a_resp_rate,
     breaks = 9,
     main = "v1a_resp_rate",
     xlab = "",

```

```

    col = "blue")
hist(Acute_sputum_no_HF_have_v1$v1a_spo2,
     breaks = 9,
     main = "v1a_spo2",
     xlab = "",
     col = "blue")
hist(Acute_sputum_no_HF_have_v1$v1a_vas_blness,
     breaks = 9,
     main = "v1a_vas_blness",
     xlab = "",
     col = "blue")
hist(Acute_sputum_no_HF_have_v1$v1a_vas_wheeze,
     breaks = 9,
     main = "v1a_vas_wheeze",
     xlab = "",
     col = "blue")
hist(Acute_sputum_no_HF_have_v1$v1a_emrc_admission,
     breaks = 9,
     main = "v1a_emrc_admission",
     xlab = "",
     col = "blue")
hist(Acute_sputum_no_HF_have_v1$v1a_blood_wbc,
     breaks = 9,
     main = "v1a_blood_wbc",
     xlab = "",
     col = "blue")
hist(Acute_sputum_no_HF_have_v1$v1a_blood_lymab,
     breaks = 9,
     main = "v1a_blood_lymab",
     xlab = "",
     col = "blue")
hist(Acute_sputum_no_HF_have_v1$v1a_blood_neuab,
     breaks = 9,
     main = "v1a_blood_neuab",
     xlab = "",
     col = "blue")

# all histograms into one plot
# figures arranged in x rows and x columns

par(mfrow=c(4,8))

par(mfrow=c(1,1))

# examing the normality of the data by shapiro.test

shapiro.test(Acute_sputum_no_HF_have_v1$v1a_blood_eos)
shapiro.test(Acute_sputum_no_HF_have_v1$v1a_blood_bnp)
shapiro.test(Acute_sputum_no_HF_have_v1$v1a_blood_crp)
shapiro.test(Acute_sputum_no_HF_have_v1$v1a_bp_top)
shapiro.test(Acute_sputum_no_HF_have_v1$v1a_temperature)
shapiro.test(Acute_sputum_no_HF_have_v1$v1a_heart_rate)
shapiro.test(Acute_sputum_no_HF_have_v1$v1a_resp_rate)
shapiro.test(Acute_sputum_no_HF_have_v1$v1a_spo2)
shapiro.test(Acute_sputum_no_HF_have_v1$v1a_vas_blness)
shapiro.test(Acute_sputum_no_HF_have_v1$v1a_vas_wheeze)
shapiro.test(Acute_sputum_no_HF_have_v1$v1a_emrc_admission)

```

```

shapiro.test(Acute_sputum_no_HF_have_v1$v1a_blood_wbc)
shapiro.test(Acute_sputum_no_HF_have_v1$v1a_blood_lymab)
shapiro.test(Acute_sputum_no_HF_have_v1$v1a_blood_neuab)

#####
# task 4 : clinical characteristic table (acute cohort)

# set the variable "gender" and "Diagnosis" as factor variables

Acute_sputum_no_HF_have_v1$gender <-
factor(Acute_sputum_no_HF_have_v1$gender)

Acute_sputum_no_HF_have_v1$Diagnosis <-
factor(Acute_sputum_no_HF_have_v1$Diagnosis)

library(dplyr)

# describe the data in general

describe(Acute_sputum_no_HF_have_v1)

# use the describeBy function to describe median mean SD and others by
groups

pacman::p_load(pacman, psych) # to load the "describeBy" function

describeBy(Acute_sputum_no_HF_have_v1,
Acute_sputum_no_HF_have_v1$Diagnosis)

# data marix is long, identifying the columns number can help ease the
navigation
describeBy(Acute_sputum_no_HF_have_v1[0:50],
Acute_sputum_no_HF_have_v1$Diagnosis)

# for frequancies and percentages

install.packages("cli")
Acute_sputum_no_HF_have_v1 %>% group_by(Diagnosis,gender) %>%
summarise(freq=n())
Acute_sputum_no_HF_have_v1 %>% group_by(Diagnosis,v1a_smoke) %>%
summarise(freq=n())
Acute_sputum_no_HF_have_v1 %>% group_by(Diagnosis,`Prior Abx 1=Yes, 0=No`)
%>% summarise(freq=n())
Acute_sputum_no_HF_have_v1 %>% group_by(Diagnosis,`Prior steroids`) %>%
summarise(freq=n())

# Table 4 summary by group for medians and 1st and 3rd QU by group for not
parametric data
# Measured

tapply(Acute_sputum_no_HF_have_v1$V1_RVE1 ,
Acute_sputum_no_HF_have_v1$Diagnosis, summary)
tapply(Acute_sputum_no_HF_have_v1$V1_RVD2 ,
Acute_sputum_no_HF_have_v1$Diagnosis, summary)

```

```

tapply(Acute_sputum_no_HF_have_v1$V1_RvD1 ,
Acute_sputum_no_HF_have_v1$Diagnosis, summary)
tapply(Acute_sputum_no_HF_have_v1$V1_RvD5 ,
Acute_sputum_no_HF_have_v1$Diagnosis, summary)
tapply(Acute_sputum_no_HF_have_v1$V1_LTB4 ,
Acute_sputum_no_HF_have_v1$Diagnosis, summary)
tapply(Acute_sputum_no_HF_have_v1$V1_LXA4 ,
Acute_sputum_no_HF_have_v1$Diagnosis, summary)
tapply(Acute_sputum_no_HF_have_v1$V1_LXB4 ,
Acute_sputum_no_HF_have_v1$Diagnosis, summary)
tapply(Acute_sputum_no_HF_have_v1$V1_PGD2 ,
Acute_sputum_no_HF_have_v1$Diagnosis, summary)
tapply(Acute_sputum_no_HF_have_v1$V1_PGE2 ,
Acute_sputum_no_HF_have_v1$Diagnosis, summary)
tapply(Acute_sputum_no_HF_have_v1$V1_PG2a ,
Acute_sputum_no_HF_have_v1$Diagnosis, summary)
tapply(Acute_sputum_no_HF_have_v1$V1_MaR_2 ,
Acute_sputum_no_HF_have_v1$Diagnosis, summary)
tapply(Acute_sputum_no_HF_have_v1$V1_MaR_1 ,
Acute_sputum_no_HF_have_v1$Diagnosis, summary)
tapply(Acute_sputum_no_HF_have_v1$V1_PD1 ,
Acute_sputum_no_HF_have_v1$Diagnosis, summary)

```

#adjusted

```

tapply(Acute_sputum_no_HF_have_v1$V1_RvE1_adjus_by_IS_and_weight ,
Acute_sputum_no_HF_have_v1$Diagnosis, summary)
tapply(Acute_sputum_no_HF_have_v1$V1_RvD2_adjus_by_IS_and_weight ,
Acute_sputum_no_HF_have_v1$Diagnosis, summary)
tapply(Acute_sputum_no_HF_have_v1$V1_RvD1_adjus_by_IS_and_weight ,
Acute_sputum_no_HF_have_v1$Diagnosis, summary)
tapply(Acute_sputum_no_HF_have_v1$V1_RvD5_adjus_by_IS_and_weight ,
Acute_sputum_no_HF_have_v1$Diagnosis, summary)
tapply(Acute_sputum_no_HF_have_v1$V1_LTB4_adjus_by_IS_and_weight ,
Acute_sputum_no_HF_have_v1$Diagnosis, summary)
tapply(Acute_sputum_no_HF_have_v1$V1_LXA4_adjus_by_IS_and_weight ,
Acute_sputum_no_HF_have_v1$Diagnosis, summary)
tapply(Acute_sputum_no_HF_have_v1$V1_LXB4_adjus_by_IS_and_weight ,
Acute_sputum_no_HF_have_v1$Diagnosis, summary)
tapply(Acute_sputum_no_HF_have_v1$V1_PGD2_adjus_by_IS_and_weight ,
Acute_sputum_no_HF_have_v1$Diagnosis, summary)
tapply(Acute_sputum_no_HF_have_v1$V1_PGE2_adjus_by_IS_and_weight ,
Acute_sputum_no_HF_have_v1$Diagnosis, summary)
tapply(Acute_sputum_no_HF_have_v1$V1_PG2a_adjus_by_IS_and_weight ,
Acute_sputum_no_HF_have_v1$Diagnosis, summary)
tapply(Acute_sputum_no_HF_have_v1$V1_MaR_2_adjus_by_IS_and_weight ,
Acute_sputum_no_HF_have_v1$Diagnosis, summary)
tapply(Acute_sputum_no_HF_have_v1$V1_MaR_1_adjus_by_IS_and_weight ,
Acute_sputum_no_HF_have_v1$Diagnosis, summary)
tapply(Acute_sputum_no_HF_have_v1$V1_PD1_adjus_by_IS_and_weight ,
Acute_sputum_no_HF_have_v1$Diagnosis, summary)

```

```

tapply(Acute_sputum_no_HF_have_v1$v1a_blood_eosab ,
Acute_sputum_no_HF_have_v1$Diagnosis, summary)
tapply(Acute_sputum_no_HF_have_v1$v1a_blood_bnp ,
Acute_sputum_no_HF_have_v1$Diagnosis, summary)
tapply(Acute_sputum_no_HF_have_v1$v1a_blood_crp ,
Acute_sputum_no_HF_have_v1$Diagnosis, summary)

```

```

tapply(Acute_sputum_no_HF_have_v1$v1a_emrc_admission ,
Acute_sputum_no_HF_have_v1$Diagnosis, summary)

# kruskal-Wallis test to compare nonparametric data (measured)
kruskal.test(V1_RvE1 ~ Diagnosis, data = Acute_sputum_no_HF_have_v1)
kruskal.test(V1_RvD2 ~ Diagnosis, data = Acute_sputum_no_HF_have_v1)
kruskal.test(V1_RvD1 ~ Diagnosis, data = Acute_sputum_no_HF_have_v1)
kruskal.test(V1_RvD5 ~ Diagnosis, data = Acute_sputum_no_HF_have_v1)
kruskal.test(V1_LTB4 ~ Diagnosis, data = Acute_sputum_no_HF_have_v1)
kruskal.test(V1_LXA4 ~ Diagnosis, data = Acute_sputum_no_HF_have_v1)
kruskal.test(V1_LXB4 ~ Diagnosis, data = Acute_sputum_no_HF_have_v1)
kruskal.test(V1_PGD2 ~ Diagnosis, data = Acute_sputum_no_HF_have_v1)
kruskal.test(V1_PGE2 ~ Diagnosis, data = Acute_sputum_no_HF_have_v1)
kruskal.test(V1_PG2a ~ Diagnosis, data = Acute_sputum_no_HF_have_v1)
kruskal.test(V1_MaR_2 ~ Diagnosis, data = Acute_sputum_no_HF_have_v1)
kruskal.test(V1_MaR_1 ~ Diagnosis, data = Acute_sputum_no_HF_have_v1)
kruskal.test(V1_PD1 ~ Diagnosis, data = Acute_sputum_no_HF_have_v1)

# kruskal-Wallis test to compare nonparametric data (adjusted)
kruskal.test(V1_RvE1_adjus_by_IS_and_weight ~ Diagnosis, data =
Acute_sputum_no_HF_have_v1)
kruskal.test(V1_RvD2_adjus_by_IS_and_weight ~ Diagnosis, data =
Acute_sputum_no_HF_have_v1)
kruskal.test(V1_RvD1_adjus_by_IS_and_weight ~ Diagnosis, data =
Acute_sputum_no_HF_have_v1)
kruskal.test(V1_RvD5_adjus_by_IS_and_weight ~ Diagnosis, data =
Acute_sputum_no_HF_have_v1)
kruskal.test(V1_LTB4_adjus_by_IS_and_weight ~ Diagnosis, data =
Acute_sputum_no_HF_have_v1)
kruskal.test(V1_LXA4_adjus_by_IS_and_weight ~ Diagnosis, data =
Acute_sputum_no_HF_have_v1)
kruskal.test(V1_LXB4_adjus_by_IS_and_weight ~ Diagnosis, data =
Acute_sputum_no_HF_have_v1)
kruskal.test(V1_PGD2_adjus_by_IS_and_weight ~ Diagnosis, data =
Acute_sputum_no_HF_have_v1)
kruskal.test(V1_PGE2_adjus_by_IS_and_weight ~ Diagnosis, data =
Acute_sputum_no_HF_have_v1)
kruskal.test(V1_PG2a_adjus_by_IS_and_weight ~ Diagnosis, data =
Acute_sputum_no_HF_have_v1)
kruskal.test(V1_MaR_2_adjus_by_IS_and_weight ~ Diagnosis, data =
Acute_sputum_no_HF_have_v1)
kruskal.test(V1_MaR_1_adjus_by_IS_and_weight ~ Diagnosis, data =
Acute_sputum_no_HF_have_v1)
kruskal.test(V1_PD1_adjus_by_IS_and_weight ~ Diagnosis, data =
Acute_sputum_no_HF_have_v1)

kruskal.test(v1a_blood_bnp ~ Diagnosis, data = Acute_sputum_no_HF_have_v1)
kruskal.test(v1a_blood_crp ~ Diagnosis, data = Acute_sputum_no_HF_have_v1)
kruskal.test(v1a_blood_eosab ~ Diagnosis, data =
Acute_sputum_no_HF_have_v1)
kruskal.test(v1a_emrc_admission ~ Diagnosis, data =
Acute_sputum_no_HF_have_v1)

#ANOVA for parametric data:

```

```

age.aov <- aov (age ~ Diagnosis, data = Acute_sputum_no_HF_have_v1)
summary(age.aov)

bp.aov <- aov (v1a_bp_top ~ Diagnosis, data = Acute_sputum_no_HF_have_v1)
summary(bp.aov)
Temp.aov <- aov (v1a_temperature ~ Diagnosis, data =
Acute_sputum_no_HF_have_v1)
summary(Temp.aov)
HR.aov <- aov (v1a_heart_rate ~ Diagnosis, data =
Acute_sputum_no_HF_have_v1)
summary(HR.aov)
rr.aov <- aov (v1a_resp_rate ~ Diagnosis, data =
Acute_sputum_no_HF_have_v1)
summary(rr.aov)
spo2.aov <- aov (v1a_spo2 ~ Diagnosis, data = Acute_sputum_no_HF_have_v1)
summary(spo2.aov)

VASblness.aov <- aov (v1a_vas_blness ~ Diagnosis, data =
Acute_sputum_no_HF_have_v1)
summary(VASblness.aov)
VASwheeze.aov <- aov (v1a_vas_wheeze ~ Diagnosis, data =
Acute_sputum_no_HF_have_v1)
summary(VASwheeze.aov)
EWS.aov <- aov (EWS ~ Diagnosis, data = Acute_sputum_no_HF_have_v1)
summary(EWS.aov)

WBC.aov <- aov (v1a_blood_wbc ~ Diagnosis, data =
Acute_sputum_no_HF_have_v1)
summary(WBC.aov)
lymp.aov <- aov (v1a_blood_lymab ~ Diagnosis, data =
Acute_sputum_no_HF_have_v1)
summary(lymp.aov)
neua.aov <- aov (v1a_blood_neuab ~ Diagnosis, data =
Acute_sputum_no_HF_have_v1)
summary(neua.aov)

#chi square to compare proportions and categorical variables

# creat table
table(Acute_sputum_no_HF_have_v1$Diagnosis,
Acute_sputum_no_HF_have_v1$v1a_smoke)
table(Acute_sputum_no_HF_have_v1$Diagnosis,
Acute_sputum_no_HF_have_v1$gender)

#save the table for use later
TAB0 = table(Acute_sputum_no_HF_have_v1$Diagnosis,
Acute_sputum_no_HF_have_v1$v1a_smoke)
TAB0
TAB9 = table(Acute_sputum_no_HF_have_v1$Diagnosis,
Acute_sputum_no_HF_have_v1$gender)
TAB9

# visualize the data
barplot(TAB0, legend=T, beside=T )
barplot(TAB9, legend=T, beside=T )
#do the chi-square
chisq.test(TAB0, correct=T)

```



```

tapply(sputum_have_v2_no_HF$V1_PGD2_adjus_by_IS_and_weight ,
sputum_have_v2_no_HF$Diagnosis, summary)
tapply(sputum_have_v2_no_HF$V1_PGE2_adjus_by_IS_and_weight ,
sputum_have_v2_no_HF$Diagnosis, summary)
tapply(sputum_have_v2_no_HF$V1_PG2a_adjus_by_IS_and_weight ,
sputum_have_v2_no_HF$Diagnosis, summary)
tapply(sputum_have_v2_no_HF$V1_MaR_2_adjus_by_IS_and_weight ,
sputum_have_v2_no_HF$Diagnosis, summary)
tapply(sputum_have_v2_no_HF$V1_MaR_1_adjus_by_IS_and_weight ,
sputum_have_v2_no_HF$Diagnosis, summary)
tapply(sputum_have_v2_no_HF$V1_PD1_adjus_by_IS_and_weight ,
sputum_have_v2_no_HF$Diagnosis, summary)

```

#adjusted (during the stable status)

```

tapply(sputum_have_v2_no_HF$V2_RvE1_adjus_by_IS_and_weight ,
sputum_have_v2_no_HF$V2_Diagnosis, summary)
tapply(sputum_have_v2_no_HF$V2_RvD2_adjus_by_IS_and_weight ,
sputum_have_v2_no_HF$V2_Diagnosis, summary)
tapply(sputum_have_v2_no_HF$V2_RvD1_adjus_by_IS_and_weight ,
sputum_have_v2_no_HF$V2_Diagnosis, summary)
tapply(sputum_have_v2_no_HF$V2_RvD5_adjus_by_IS_and_weight ,
sputum_have_v2_no_HF$V2_Diagnosis, summary)
tapply(sputum_have_v2_no_HF$V2_LTB4_adjus_by_IS_and_weight ,
sputum_have_v2_no_HF$V2_Diagnosis, summary)
tapply(sputum_have_v2_no_HF$V2_LXA4_adjus_by_IS_and_weight ,
sputum_have_v2_no_HF$V2_Diagnosis, summary)
tapply(sputum_have_v2_no_HF$V2_LXB4_adjus_by_IS_and_weight ,
sputum_have_v2_no_HF$V2_Diagnosis, summary)
tapply(sputum_have_v2_no_HF$V2_PGD2_adjus_by_IS_and_weight ,
sputum_have_v2_no_HF$V2_Diagnosis, summary)
tapply(sputum_have_v2_no_HF$V2_PGE2_adjus_by_IS_and_weight ,
sputum_have_v2_no_HF$V2_Diagnosis, summary)
tapply(sputum_have_v2_no_HF$V2_PG2a_adjus_by_IS_and_weight ,
sputum_have_v2_no_HF$V2_Diagnosis, summary)
tapply(sputum_have_v2_no_HF$V2_MaR_2_adjus_by_IS_and_weight ,
sputum_have_v2_no_HF$V2_Diagnosis, summary)
tapply(sputum_have_v2_no_HF$V2_MaR_1_adjus_by_IS_and_weight ,
sputum_have_v2_no_HF$V2_Diagnosis, summary)
tapply(sputum_have_v2_no_HF$V2_PD1_adjus_by_IS_and_weight ,
sputum_have_v2_no_HF$V2_Diagnosis, summary)

```

#measured (during the cute status)

```

tapply(sputum_have_v2_no_HF$V1_RvE1 , sputum_have_v2_no_HF$Diagnosis,
summary)
tapply(sputum_have_v2_no_HF$V1_RvD2 , sputum_have_v2_no_HF$Diagnosis,
summary)
tapply(sputum_have_v2_no_HF$V1_RvD1 , sputum_have_v2_no_HF$Diagnosis,
summary)
tapply(sputum_have_v2_no_HF$V1_RvD5 , sputum_have_v2_no_HF$Diagnosis,
summary)
tapply(sputum_have_v2_no_HF$V1_LTB4 , sputum_have_v2_no_HF$Diagnosis,
summary)
tapply(sputum_have_v2_no_HF$V1_LXA4 , sputum_have_v2_no_HF$Diagnosis,
summary)

```

```

tapply(sputum_have_v2_no_HF$V1_LXB4 , sputum_have_v2_no_HF$Diagnosis,
summary)
tapply(sputum_have_v2_no_HF$V1_PGD2 , sputum_have_v2_no_HF$Diagnosis,
summary)
tapply(sputum_have_v2_no_HF$V1_PGE2 , sputum_have_v2_no_HF$Diagnosis,
summary)
tapply(sputum_have_v2_no_HF$V1_PG2a , sputum_have_v2_no_HF$Diagnosis,
summary)
tapply(sputum_have_v2_no_HF$V1_MaR_2 , sputum_have_v2_no_HF$Diagnosis,
summary)
tapply(sputum_have_v2_no_HF$V1_MaR_1 , sputum_have_v2_no_HF$Diagnosis,
summary)
tapply(sputum_have_v2_no_HF$V1_PD1 , sputum_have_v2_no_HF$Diagnosis,
summary)

#measured (during the stable status )

tapply(sputum_have_v2_no_HF$V2_RvE1 , sputum_have_v2_no_HF$Diagnosis,
summary)
tapply(sputum_have_v2_no_HF$V2_RvD2, sputum_have_v2_no_HF$Diagnosis,
summary)
tapply(sputum_have_v2_no_HF$V2_RvD1 , sputum_have_v2_no_HF$Diagnosis,
summary)
tapply(sputum_have_v2_no_HF$V2_RvD5 , sputum_have_v2_no_HF$Diagnosis,
summary)
tapply(sputum_have_v2_no_HF$V2_LTB4 , sputum_have_v2_no_HF$Diagnosis,
summary)
tapply(sputum_have_v2_no_HF$V2_LXA4 , sputum_have_v2_no_HF$Diagnosis,
summary)
tapply(sputum_have_v2_no_HF$V2_LXB4 , sputum_have_v2_no_HF$Diagnosis,
summary)
tapply(sputum_have_v2_no_HF$V2_PGD2 , sputum_have_v2_no_HF$Diagnosis,
summary)
tapply(sputum_have_v2_no_HF$V2_PGE2 , sputum_have_v2_no_HF$Diagnosis,
summary)
tapply(sputum_have_v2_no_HF$V2_PG2a , sputum_have_v2_no_HF$Diagnosis,
summary)
tapply(sputum_have_v2_no_HF$V2_MaR_2 , sputum_have_v2_no_HF$Diagnosis,
summary)
tapply(sputum_have_v2_no_HF$V2_MaR_1 , sputum_have_v2_no_HF$Diagnosis,
summary)
tapply(sputum_have_v2_no_HF$V2_PD1 , sputum_have_v2_no_HF$Diagnosis,
summary)

# kruskal-Wallis test to compare nonparametric data across all groups
(adjusted)
kruskal.test(V2_RvE1_adjus_by_IS_and_weight ~ V2_Diagnosis, data =
sputum_have_v2_no_HF)
kruskal.test(V2_RvD2_adjus_by_IS_and_weight ~ V2_Diagnosis, data =
sputum_have_v2_no_HF)
kruskal.test(V2_RvD1_adjus_by_IS_and_weight ~ V2_Diagnosis, data =
sputum_have_v2_no_HF)
kruskal.test(V2_RvD5_adjus_by_IS_and_weight ~ V2_Diagnosis, data =
sputum_have_v2_no_HF)
kruskal.test(V2_LTB4_adjus_by_IS_and_weight ~ V2_Diagnosis, data =
sputum_have_v2_no_HF)
kruskal.test(V2_LXA4_adjus_by_IS_and_weight ~ V2_Diagnosis, data =
sputum_have_v2_no_HF)

```

```

kruskal.test(V2_LXB4_adjus_by_IS_and_weight ~ V2_Diagnosis, data =
sputum_have_v2_no_HF)
kruskal.test(V2_PGD2_adjus_by_IS_and_weight ~ V2_Diagnosis, data =
sputum_have_v2_no_HF)
kruskal.test(V2_PGE2_adjus_by_IS_and_weight ~ V2_Diagnosis, data =
sputum_have_v2_no_HF)
kruskal.test(V2_PG2a_adjus_by_IS_and_weight ~ V2_Diagnosis, data =
sputum_have_v2_no_HF)
kruskal.test(V2_MaR_2_adjus_by_IS_and_weight ~ V2_Diagnosis, data =
sputum_have_v2_no_HF)
kruskal.test(V2_MaR_1_adjus_by_IS_and_weight ~ V2_Diagnosis, data =
sputum_have_v2_no_HF)
kruskal.test(V2_PD1_adjus_by_IS_and_weight ~ V2_Diagnosis, data =
sputum_have_v2_no_HF)

# compare acute vs stable in each groups indivisually healthy only, COPD
only, asthma only, Pneumonia only
sputum_have_v2_no_HF_healthy <- sputum_have_v2_no_HF %>% filter(Healthy!
="N")
sputum_have_v2_no_HF_COPD <- sputum_have_v2_no_HF %>% filter(COPD!="N")
sputum_have_v2_no_HF_Asthma <- sputum_have_v2_no_HF %>% filter(Asthma!
="N")
sputum_have_v2_no_HF_Pneumonia <- sputum_have_v2_no_HF %>%
filter(Pneumonia!="N")

wilcox.test(sputum_have_v2_no_HF_healthy$V1_RvE1_adjus_by_IS_and_weight,
sputum_have_v2_no_HF_healthy$V2_RvE1_adjus_by_IS_and_weight, paired=F)
wilcox.test(sputum_have_v2_no_HF_healthy$V1_RvD2_adjus_by_IS_and_weight,
sputum_have_v2_no_HF_healthy$V2_RvD2_adjus_by_IS_and_weight, paired=F)
wilcox.test(sputum_have_v2_no_HF_healthy$V1_RvD5_adjus_by_IS_and_weight,
sputum_have_v2_no_HF_healthy$V2_RvD5_adjus_by_IS_and_weight, paired=F)
wilcox.test(sputum_have_v2_no_HF_healthy$V1_RvD1_adjus_by_IS_and_weight,
sputum_have_v2_no_HF_healthy$V2_RvD1_adjus_by_IS_and_weight, paired=F)
wilcox.test(sputum_have_v2_no_HF_healthy$V1_LTB4_adjus_by_IS_and_weight,
sputum_have_v2_no_HF_healthy$V2_LTB4_adjus_by_IS_and_weight, paired=F)
wilcox.test(sputum_have_v2_no_HF_healthy$V1_LXA4_adjus_by_IS_and_weight,
sputum_have_v2_no_HF_healthy$V2_LXA4_adjus_by_IS_and_weight, paired=F)
wilcox.test(sputum_have_v2_no_HF_healthy$V1_LXB4_adjus_by_IS_and_weight,
sputum_have_v2_no_HF_healthy$V2_LXB4_adjus_by_IS_and_weight, paired=F)
wilcox.test(sputum_have_v2_no_HF_healthy$V1_PGD2_adjus_by_IS_and_weight,
sputum_have_v2_no_HF_healthy$V2_PGD2_adjus_by_IS_and_weight, paired=F)
wilcox.test(sputum_have_v2_no_HF_healthy$V1_PGE2_adjus_by_IS_and_weight,
sputum_have_v2_no_HF_healthy$V2_PGE2_adjus_by_IS_and_weight, paired=F)
wilcox.test(sputum_have_v2_no_HF_healthy$V1_PG2a_adjus_by_IS_and_weight,
sputum_have_v2_no_HF_healthy$V2_PG2a_adjus_by_IS_and_weight, paired=F)
wilcox.test(sputum_have_v2_no_HF_healthy$V1_PD1_adjus_by_IS_and_weight,
sputum_have_v2_no_HF_healthy$V2_PD1_adjus_by_IS_and_weight , paired=F)

wilcox.test(sputum_have_v2_no_HF_COPD$V1_RvE1_adjus_by_IS_and_weight,
sputum_have_v2_no_HF_COPD$V2_RvE1_adjus_by_IS_and_weight, paired=FALSE)
wilcox.test(sputum_have_v2_no_HF_COPD$V1_RvD2_adjus_by_IS_and_weight,
sputum_have_v2_no_HF_COPD$V2_RvD2_adjus_by_IS_and_weight, paired=FALSE)

```



```

wilcox.test(sputum_have_v2_no_HF_Pneumonia$V1_PG2a_adjus_by_IS_and_weight,
sputum_have_v2_no_HF_Pneumonia$V2_PG2a_adjus_by_IS_and_weight, paired=F)
wilcox.test(sputum_have_v2_no_HF_Pneumonia$V1_PD1_adjus_by_IS_and_weight,
sputum_have_v2_no_HF_Pneumonia$V2_PD1_adjus_by_IS_and_weight , paired=F)

#####
# Task7: clinical observations vs spm (PGE2)

# Spearman correlation between 2 variables (THE DEFOLT IS 2 SIDED)

cor.test(Acute_sputum_no_HF_have_v1$v1a_blood_crp,
Acute_sputum_no_HF_have_v1$V1_PGE2_adjus_by_IS_and_weight,
method = "spearman")

cor.test(Acute_sputum_no_HF_have_v1$v1a_blood_wbc,
Acute_sputum_no_HF_have_v1$V1_PGE2_adjus_by_IS_and_weight,
method = "spearman")
cor.test(Acute_sputum_no_HF_have_v1$v1a_blood_lymab,
Acute_sputum_no_HF_have_v1$V1_PGE2_adjus_by_IS_and_weight,
method = "spearman")

cor.test(Acute_sputum_no_HF_have_v1$v1a_blood_neuab,
Acute_sputum_no_HF_have_v1$V1_PGE2_adjus_by_IS_and_weight,
method = "spearman")

cor.test(Acute_sputum_no_HF_have_v1$v1a_blood_eosab,
Acute_sputum_no_HF_have_v1$V1_PGE2_adjus_by_IS_and_weight,
method = "spearman")

# Scatter plot with correlation coefficient to the plot

sp <- ggscatter(Acute_sputum_no_HF_have_v1, x = "v1a_blood_eosab", y =
"V1_PGE2_adjus_by_IS_and_weight",
add = "reg.line", # Add regressin line
add.params = list(color = "blue", fill = "lightgray"),
ylab = "PGE2" , xlab = "Eosinophil count, x10^9/L " ,xlim=c(0.0,1.5),
ylim=c(0.0e+00,2.0e+06),# Customize reg. line
conf.int = TRUE # Add confidence interval
)
sp
sp + stat_cor(method = "spearman", label.x = 1.0, label.y = (200000))

sp1 <- ggscatter(Acute_sputum_no_HF_have_v1, x = "v1a_blood_neuab", y =
"V1_PGE2_adjus_by_IS_and_weight",
add = "reg.line", # Add regressin line
add.params = list(color = "blue", fill = "lightgray"),
ylab = "PGE2" , xlab = "Neutrophil, x10^9/L" ,xlim=c(),
ylim=c(0.0e+00,2.0e+06),# Customize reg. line
conf.int = TRUE # Add confidence interval
)
sp1
sp1 + stat_cor(method = "spearman", label.x = 17, label.y = (200000))

```


7.2 Appendix (B): SPMs Targeted Methods Optimization on LC-MS

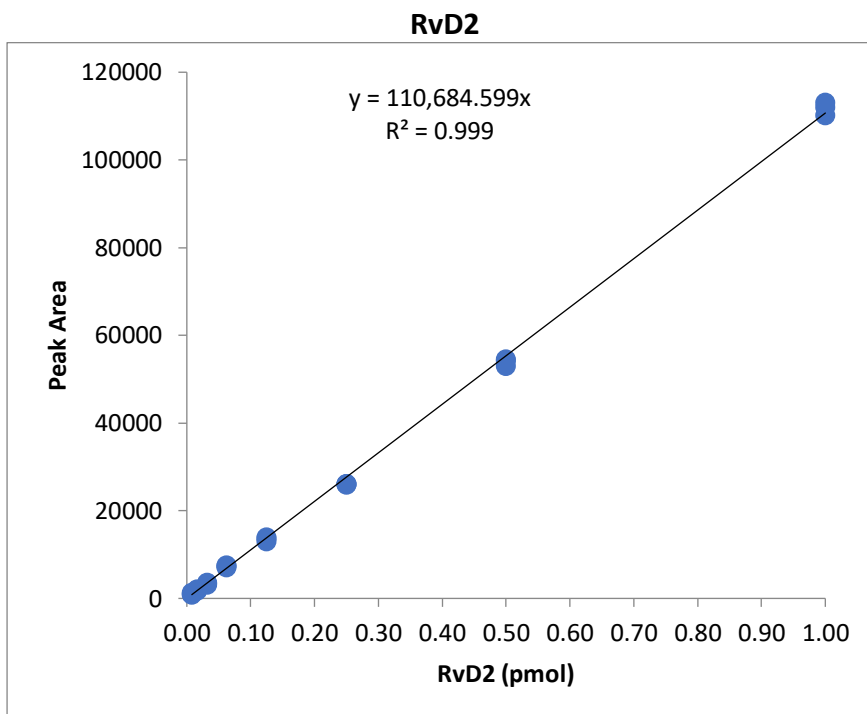
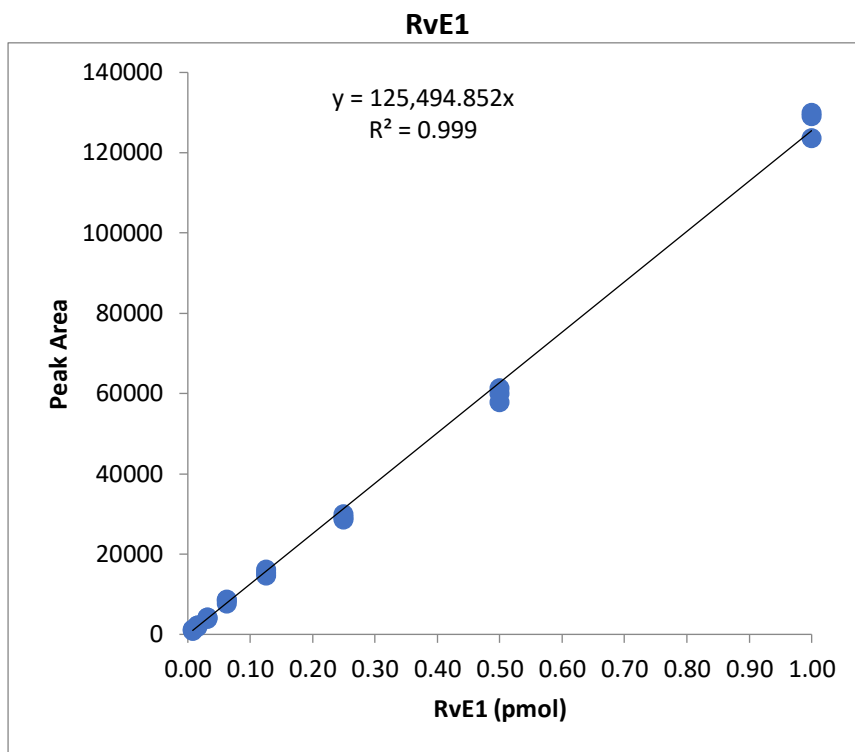
LC-ESI-MS/MS SRM lipidomics analysis

The LC-ESI-MS/MS consisted of a Waters Acquity I Class Plus Series UPLC, comprising of a binary solvent manager plus sample manager fitted with a flow through needle (FTN) connected to a Xevo TQ-XS tandem quadrupole mass spectrometer with an electrospray interface (Waters Ltd., Manchester, UK). The temperature of the electrospray source was maintained at 150 °C and the desolvation temperature at 600 °C. Nitrogen gas was used as the desolvation gas (1000 L/h) and the cone gas was set to 150 L/h. The nebulizer pressure was set at 7.0 bar. The capillary voltage was set at 0.5 kV and the cone voltage was maintained at 25 V. The SPE purified samples were dissolved in 20 µL of LC-MS grade water/methanol (60:40, v/v). A 2 µL aliquot of the SPE purified sample was injected onto a Acquity Premier Peptide BEH C18 300 Å (2.1 × 50 mm, 1.7 µm) column (Waters Ltd., Manchester, UK). The column was eluted using a gradient with solvent A, 0.1% formic acid and solvent B, acetonitrile (containing 0.1% formic acid) at a flow rate of 0.6 mL/min with a run time of 5.7 min. The following gradient was used: 0 min- 20% B, 1 min- 20% B, 4.6 min- 50% B, 5.2 min- 50% B, 5.3 min- 20% B and 5.7 min- 20% B. The column temperature was set at 40 °C using the Acquity column manager and the temperature of the samples was maintained at 6 °C in the sample manager. The samples were analysed in negative electrospray ionization mode using selected reaction monitoring (SRM). The SRM transitions monitored plus collision energies used for the different compounds were as follows: Leukotriene B4 335.4 to 195.3 *m/z* and 335.4 to 317.4 *m/z* (18 eV), Lipoxin A4 351.4 to 115.2 *m/z* and 351.4 to 217.4 *m/z* (17eV), Lipoxin B4 351.2 to 221.2 *m/z* and 351.2 to 271.3 *m/z* (17 eV), Resolvin E1 349.2 to 195.2 *m/z* and 349.2 to 107.4 *m/z* (17 eV), Resolvin D1 375.3 to 141.1 *m/z* and 375.3 to 215.4

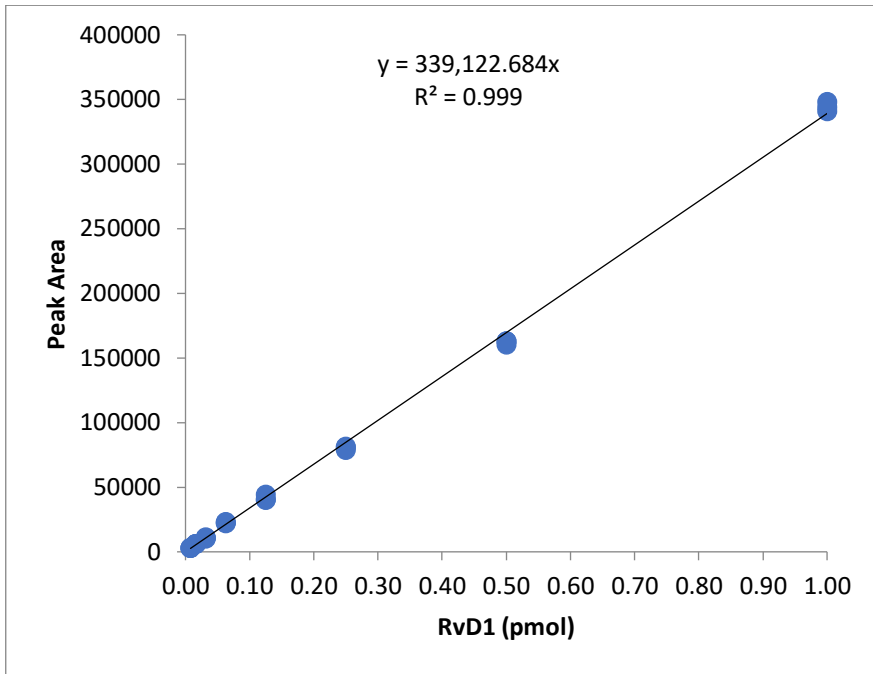
m/z (17 eV), Resolvin D2 375.4 to 141.2 *m/z* and 375.4 to 175.3 *m/z* (17 eV), Reolvin D5 359.2 to 199.3 *m/z* and 359.2 to 279.3 *m/z* (20 eV), Prostaglandin D2 351.4 to 271.4 *m/z* and 351.4 to 189.3 *m/z* (20 eV), Prostaglandin E2 351.4 to 271.4 *m/z* and 271.4 to 189.3 (20 eV), Prostaglandin F2 α 353.2 to 193.3 *m/z* and 353.2 to 247.4 *m/z* (27 eV), Maresin 1 359.4 to 113.2 *m/z* and 359.4 to 228.3 *m/z* (19 eV) Maresin 2 359.3 to 232.3 *m/z* and 359.3 to 147.3 *m/z* (19 eV), and Protectin D1 359.3 to 153.3 *m/z* and 359.3 to 206.3 *m/z* (19eV). The collision gas was argon (indicated cell pressure 3.5×10^{-3} mbar). The dwell time was set to 0.009 s and the resolution was one *m/z* unit at peak base. The data was acquired and processed using MassLynx V4.2 software.

The SRM transitions optimal collision energy data was obtained using a Micromass Quattro Premier XE (Waters Ltd., Manchester, UK) following the LC- MS/MS analysis of a 10 pmol/ μ L standard solution of each compound dissolved in LC-MS grade water/methanol (60:40, v/v). A 5 μ L aliquot of each standard solution was injected onto a Acquity UPLC BEH C18 (2.1 \times 100 mm, 1.7 μ m) column (Waters Ltd., Manchester, UK). The column was eluted using a gradient with solvent A, 0.1% acetic acid and solvent B, methanol (containing 0.1% acetic acid) at a flow rate of 0.2 mL/min with a run time of 20 min. The following gradient was used: 0 min- 40% B, 2 min- 40% B, 12 min- 95% B, 13.5 min- 95% B, 13.6 min- 40% B and 20 min- 40% B. The column temperature was set at 40 °C and the temperature of the standards was maintained at 6 °C in the sample manager. The collision gas was argon (indicated cell pressure 3.5×10^{-3} mbar). The scan time was set to 1 s and the resolution was one *m/z* unit at peak base. The data was acquired and processed using MassLynx V4.1 software.

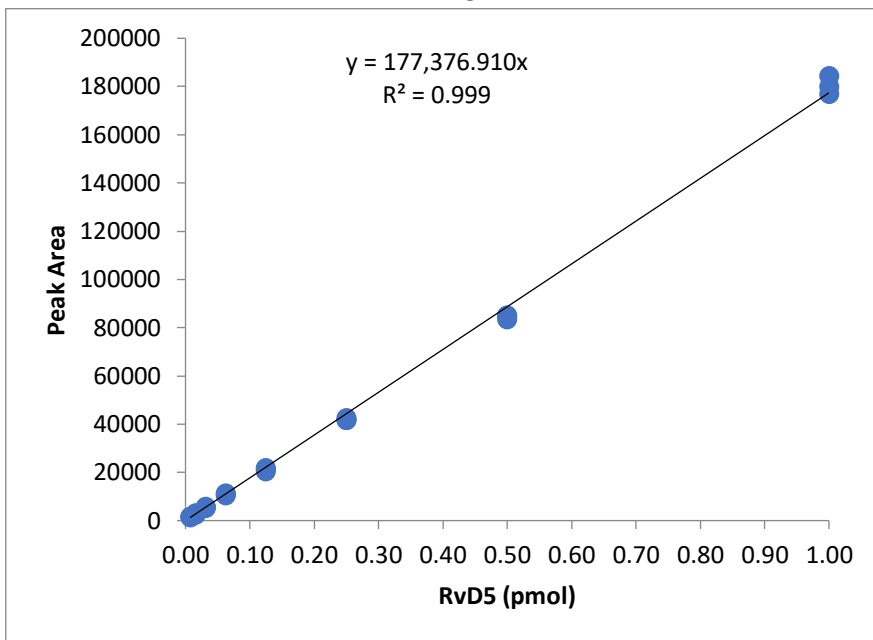
LC-ESI-MS/MS SRM calibration lines



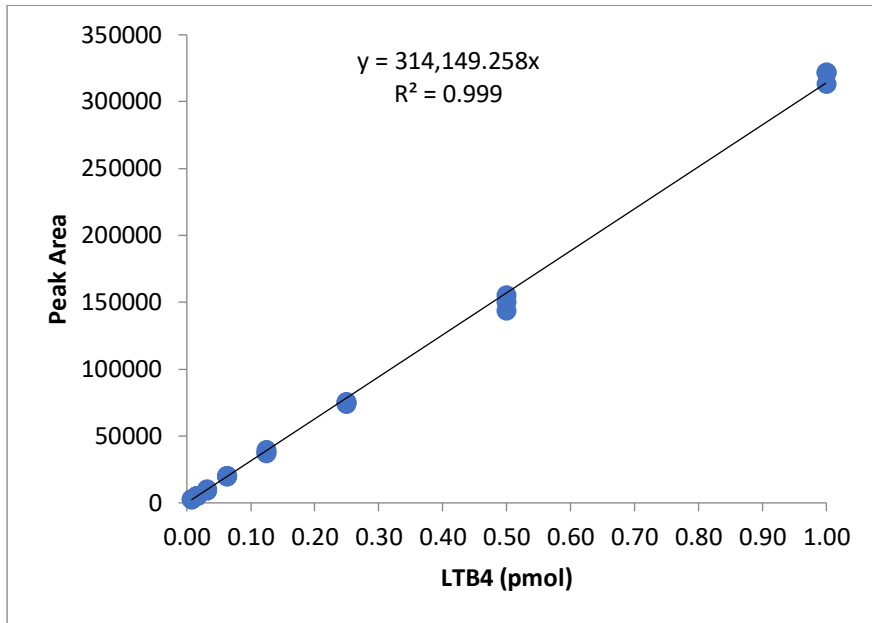
RvD1



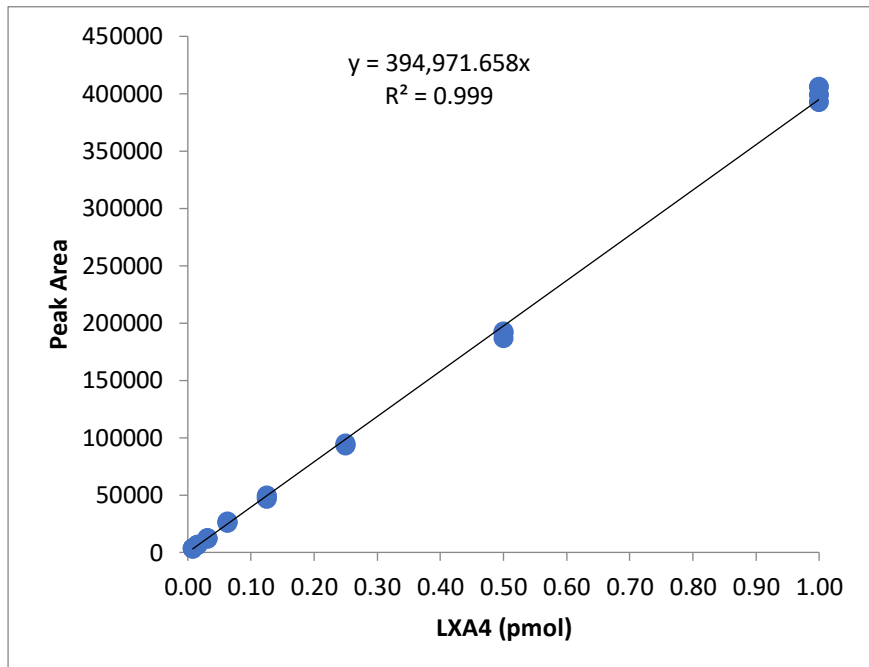
RvD5



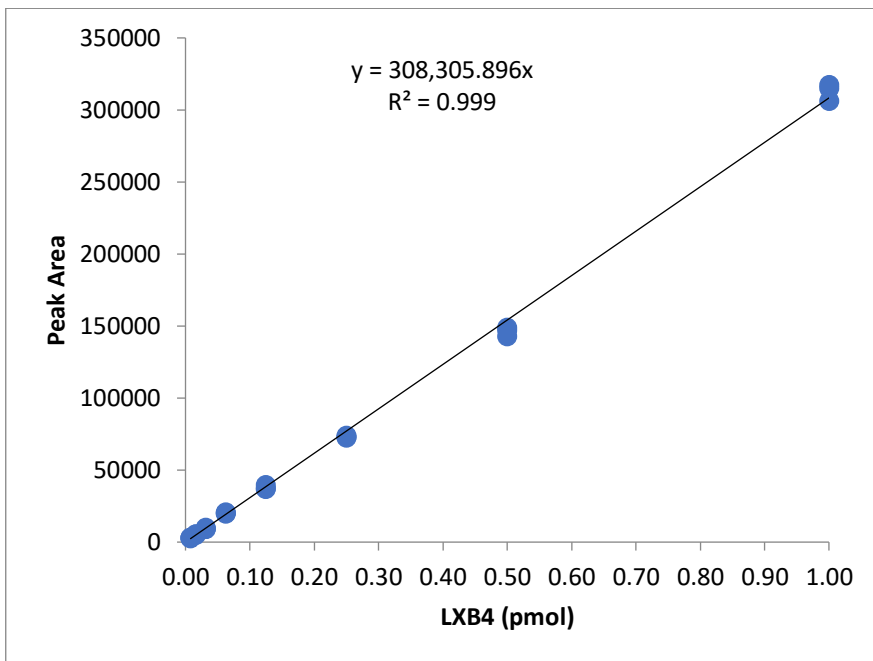
LTB4



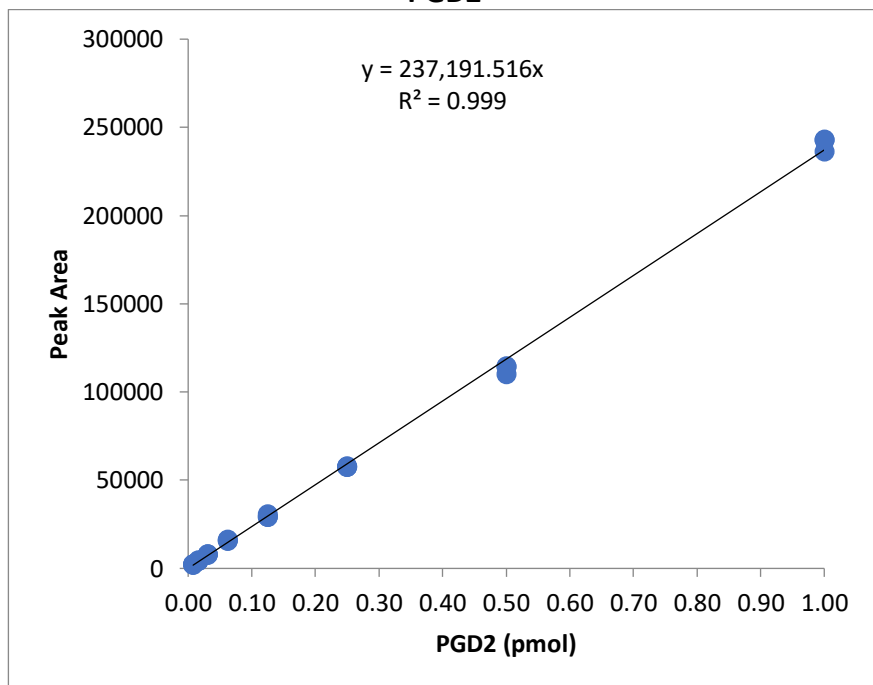
LXA4



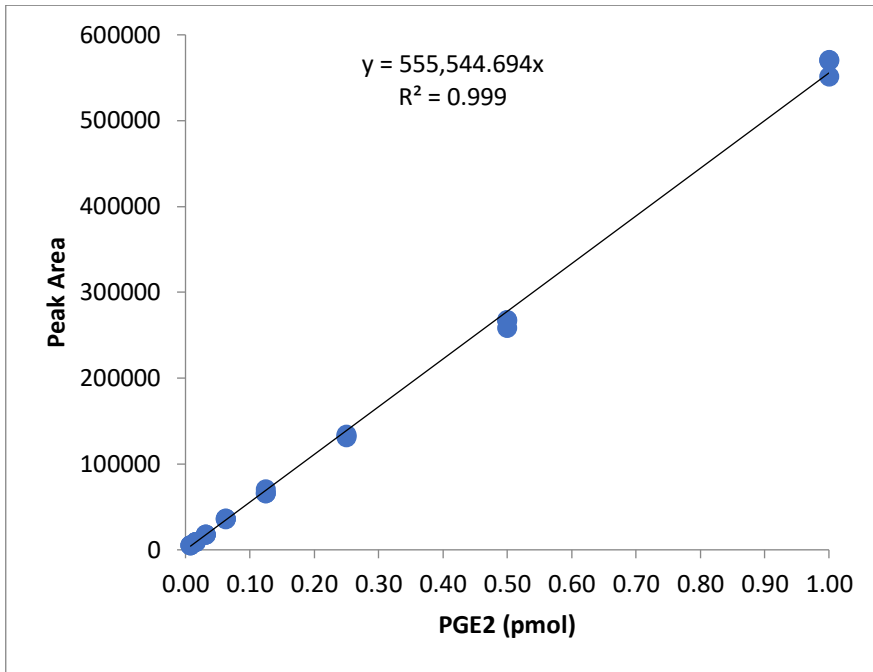
LXB4



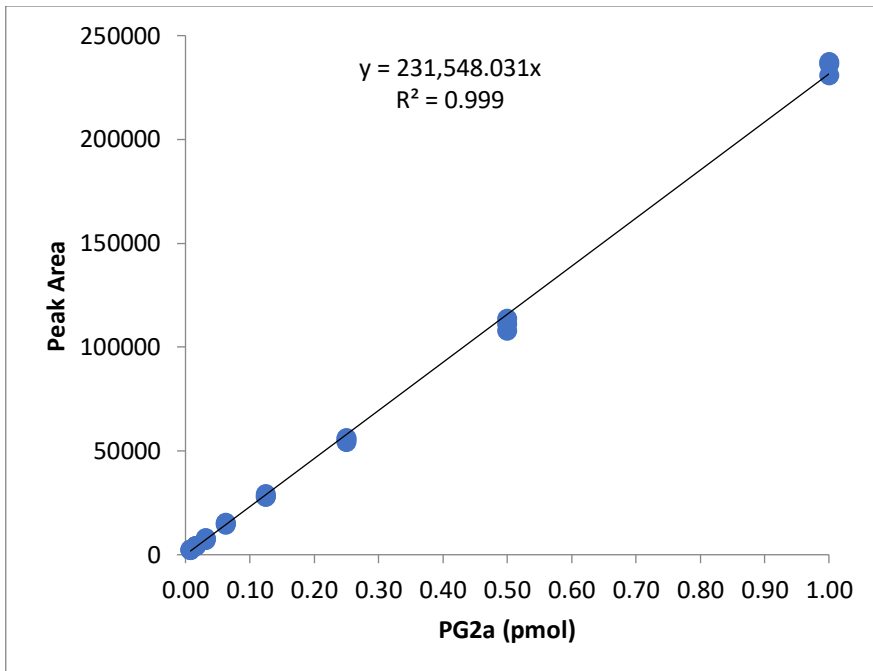
PGD2

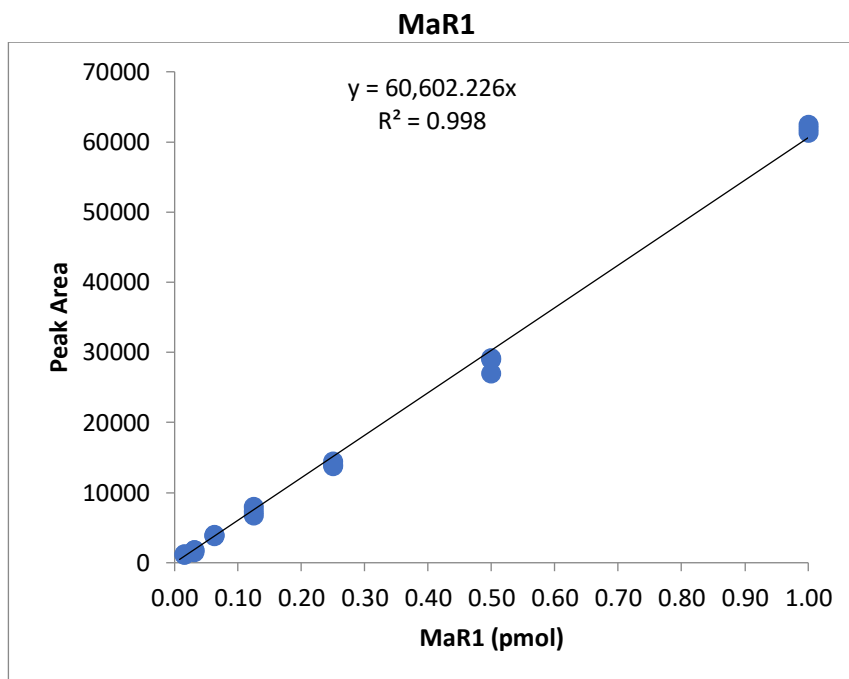
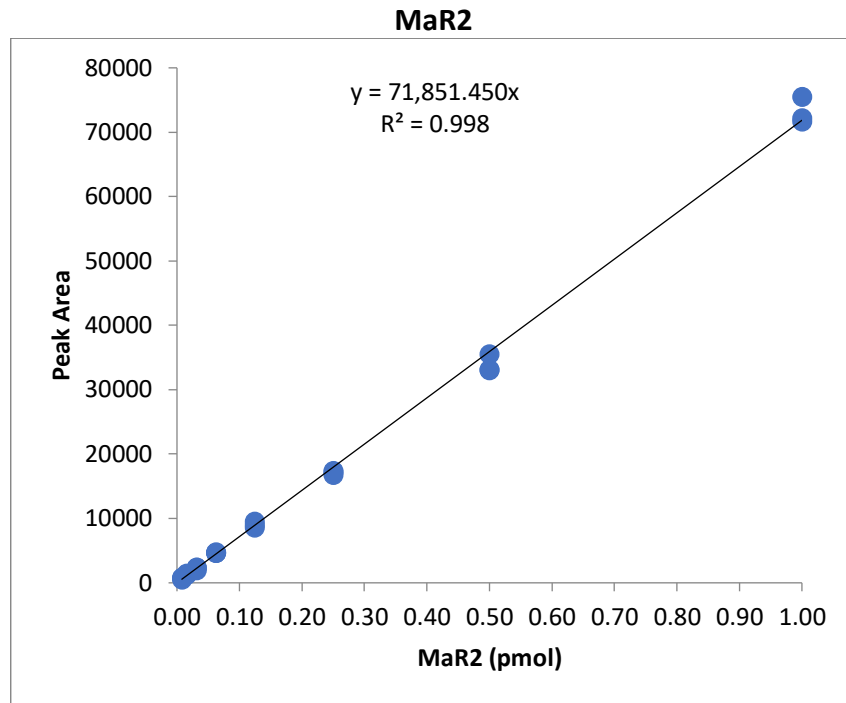


PGE2

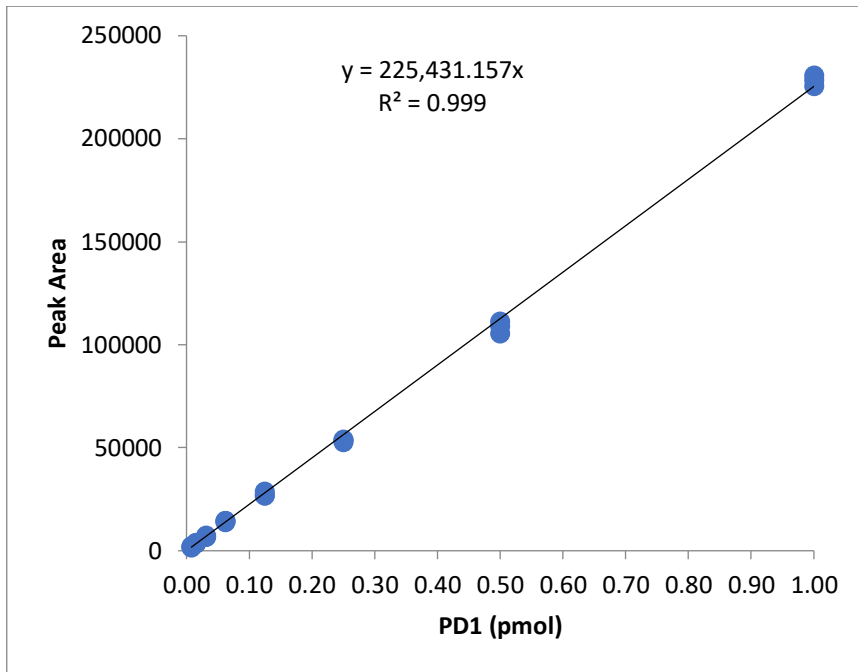


PG2a





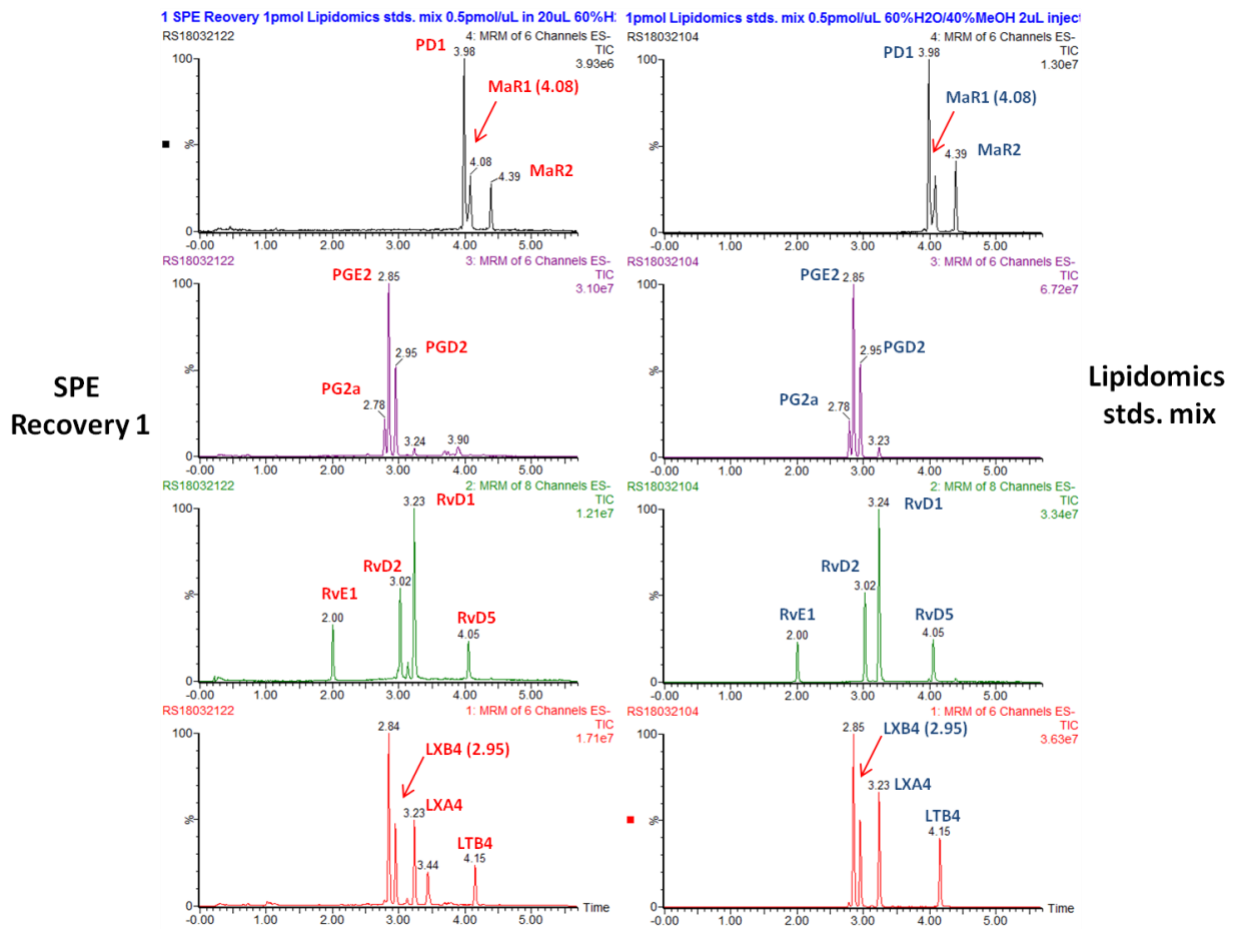
PD1



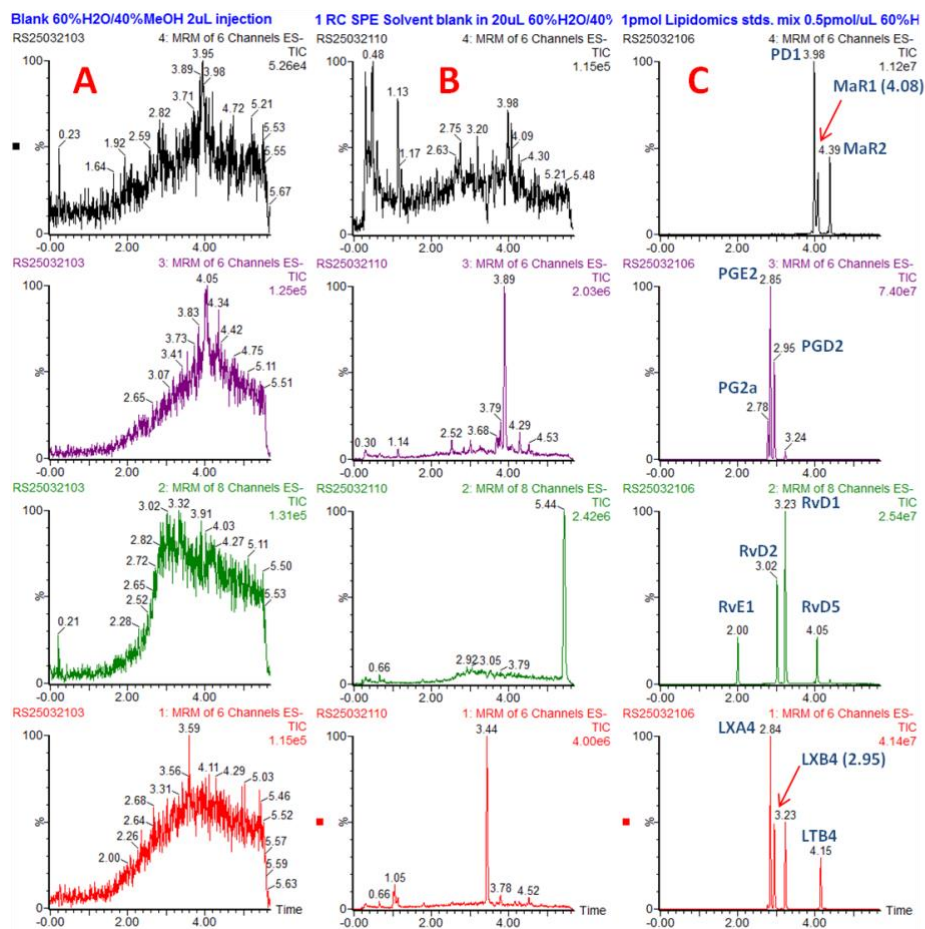
LC-ESI-MS/MS SRM LOD and LOQ

Std.		LOD	S/N		LOQ	S/N
RvE1		0.488fmol	3.7		0.977fmol	8.2
RvD2		0.977fmol	3.4		1.953fmol	11.5
RvD1		0.488fmol	3.3		0.977fmol	9.9
RvD5		0.977fmol	3.9		1.953fmol	9.6
LTB4		0.488fmol	4.0		0.977fmol	10.4
LXA4		0.244fmol	3.7		0.488fmol	9.2
LXB4		1.953fmol	3.4		3.906fmol	12.0
PGD2		0.488fmol	3.3		0.977fmol	7.4
PGE2		0.488fmol	3.6		0.977fmol	9.3
PG2a		1.953fmol	3.6		3.906fmol	10.1
MaR2		0.244fmol	3.3		0.488fmol	9.0
MaR1		0.977fmol	3.3		1.953fmol	12.6
PD1		0.244fmol	3.8		0.488fmol	12.0

LC-ESI-MS/MS SRM chromatograms for SPE recovery



LC-ESI-MS/MS SRM chromatograms for solvent blanks

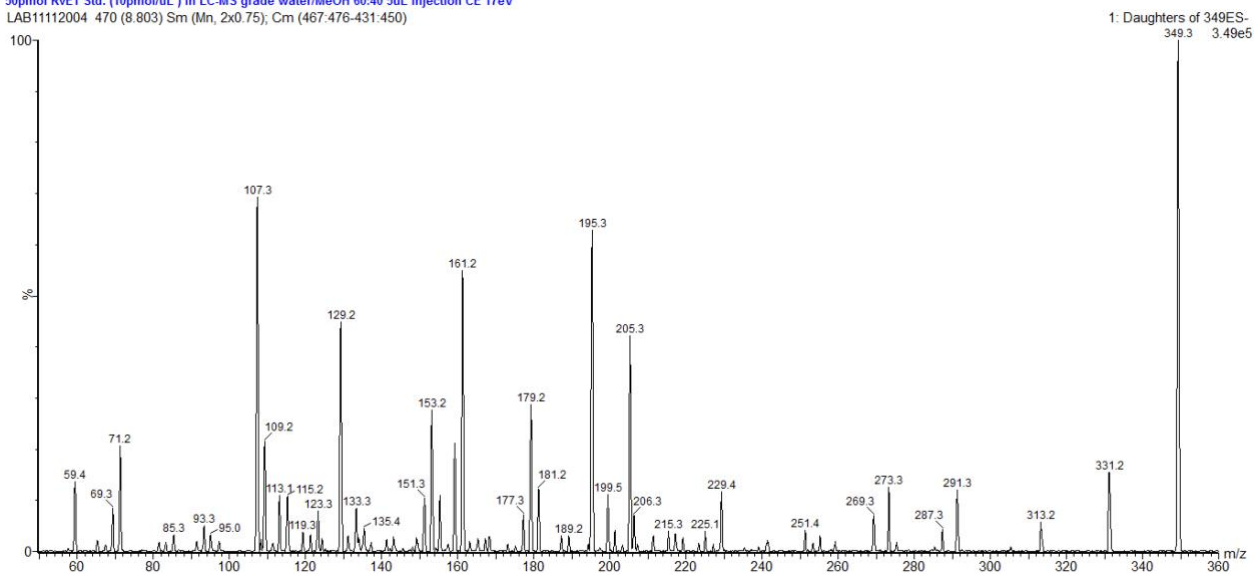


- A** Blank injection
- B** SPE Blank solvents
- C** Lipidomics stds. mix

LC-ESI-MS/MS Lipidomics standards product ion spectra

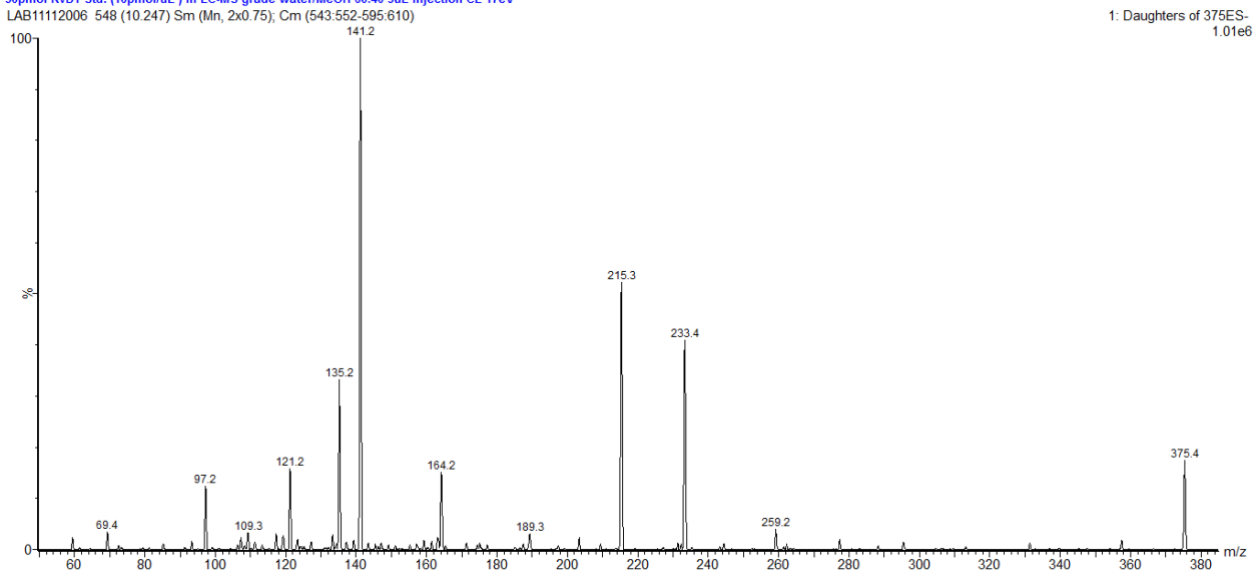
RvE1

50pmol RvE1 Std. (10pmol/uL) in LC-MS grade water/MeOH 60:40 5uL injection CE 17eV
LAB11112004 470 (8.803) Sm (Mn, 2x0.75); Cm (467-476-431-450)



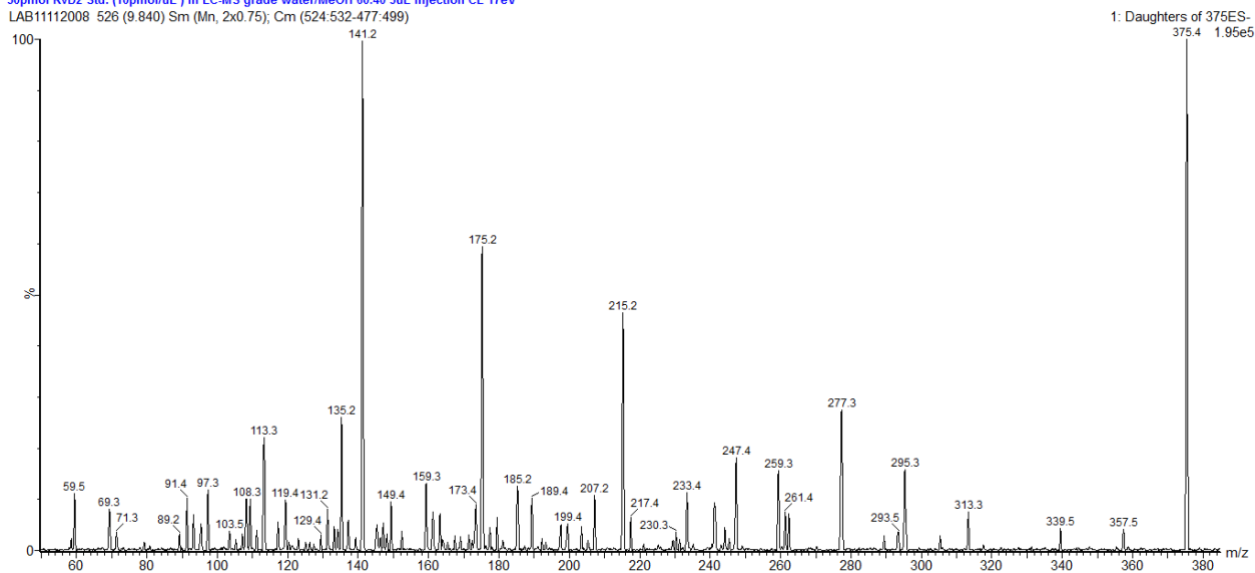
RvD1

50pmol RvD1 Std. (10pmol/uL) in LC-MS grade water/MeOH 60:40 5uL injection CE 17eV
LAB11112006 548 (10.247) Sm (Mn, 2x0.75); Cm (543-552-595-610)



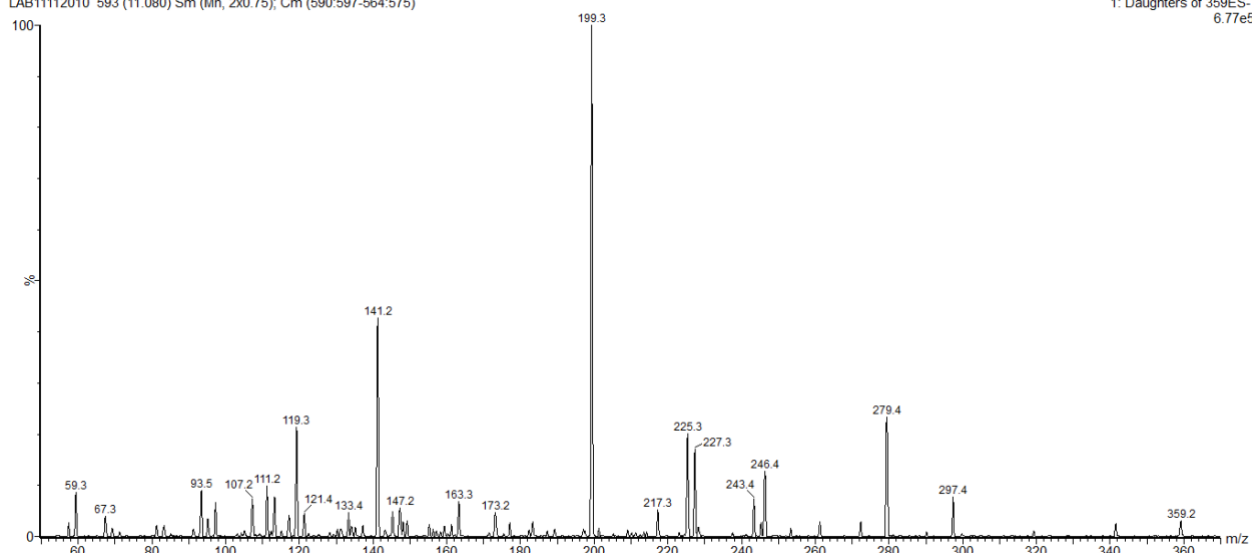
RvD2

50pmol RvD2 Std. (10pmol/ μ L) in LC-MS grade water/MeOH 60:40 5 μ L injection CE 17eV
LAB11112008 526 (9.840) Sm (Mn, 2x0.75); Cm (524.532-477.499)



RvD5

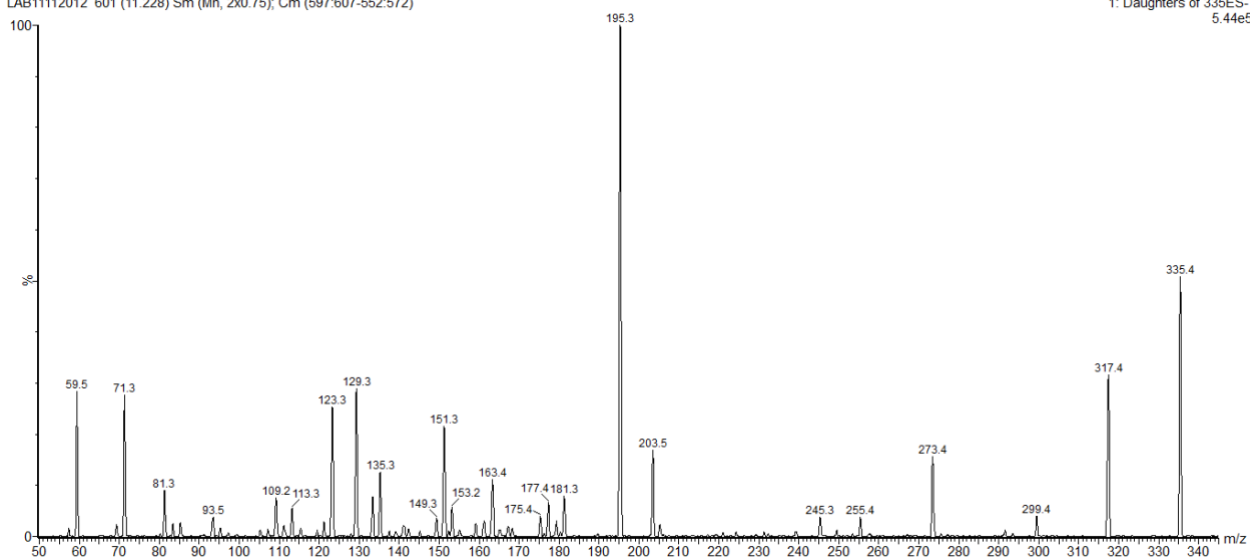
50pmol RvD5 Std. (10pmol/ μ L) in LC-MS grade water/MeOH 60:40 5 μ L injection CE 20eV
LAB11112010 593 (11.080) Sm (Mn, 2x0.75); Cm (590.597-564.575)



LTB4

50pmol LTB4 Std. (10pmol/ μ L) in LC-MS grade water/MeOH 60:40 5 μ L injection CE 18eV
LAB11112012 601 (11.228) Sm (Mn, 2x0.75); Cm (597:607-552:572)

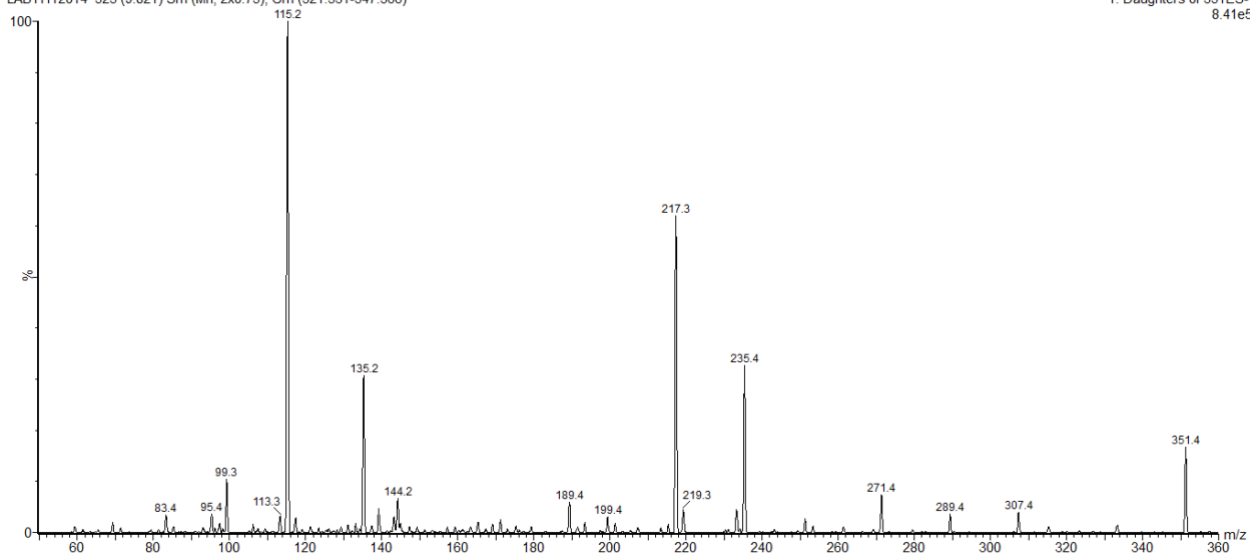
1: Daughters of 335ES-
5.44e5



LXA4

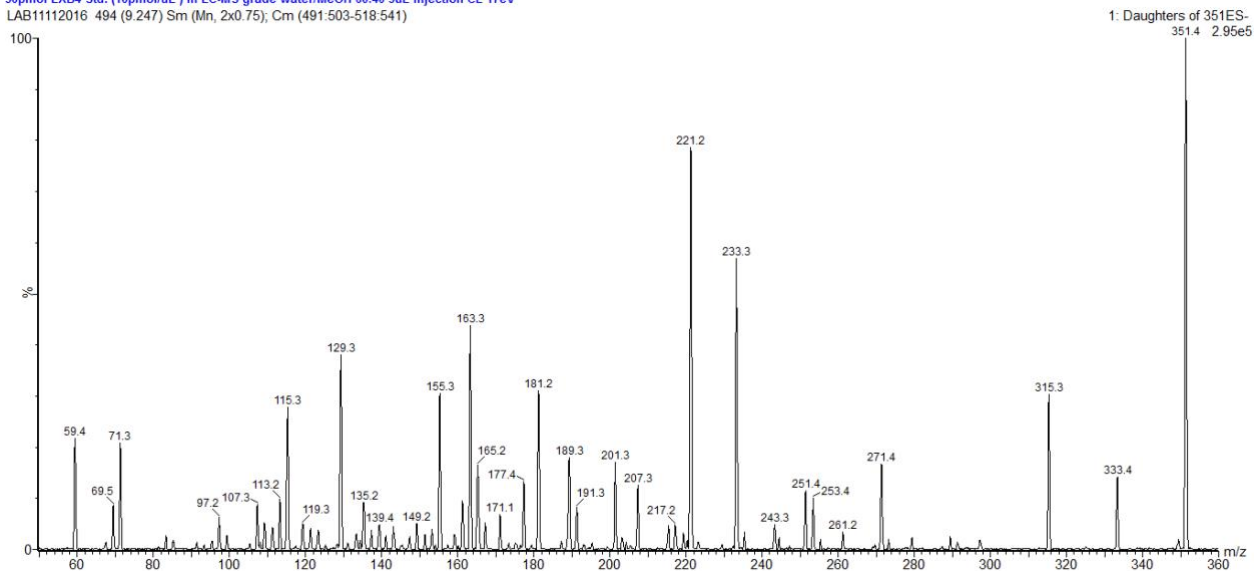
50pmol LXA4 Std. (10pmol/ μ L) in LC-MS grade water/MeOH 60:40 5 μ L injection CE 17eV
LAB11112014 525 (9.821) Sm (Mn, 2x0.75); Cm (521:531-547:566)

1: Daughters of 351ES-
8.41e5



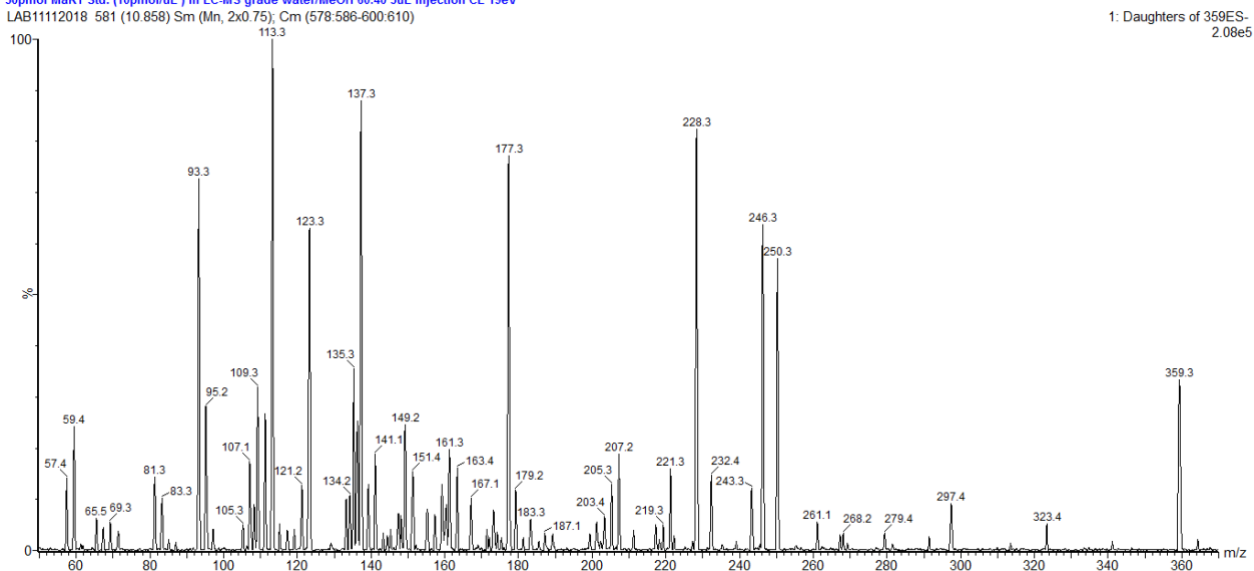
LXB4

50pmol LXB4 Std. (10pmol/uL) in LC-MS grade water/MeOH 60:40 5uL injection CE 17eV
LAB11112016 494 (9.247) Sm (Mn, 2x0.75); Cm (491-503-518:541)



MaR1

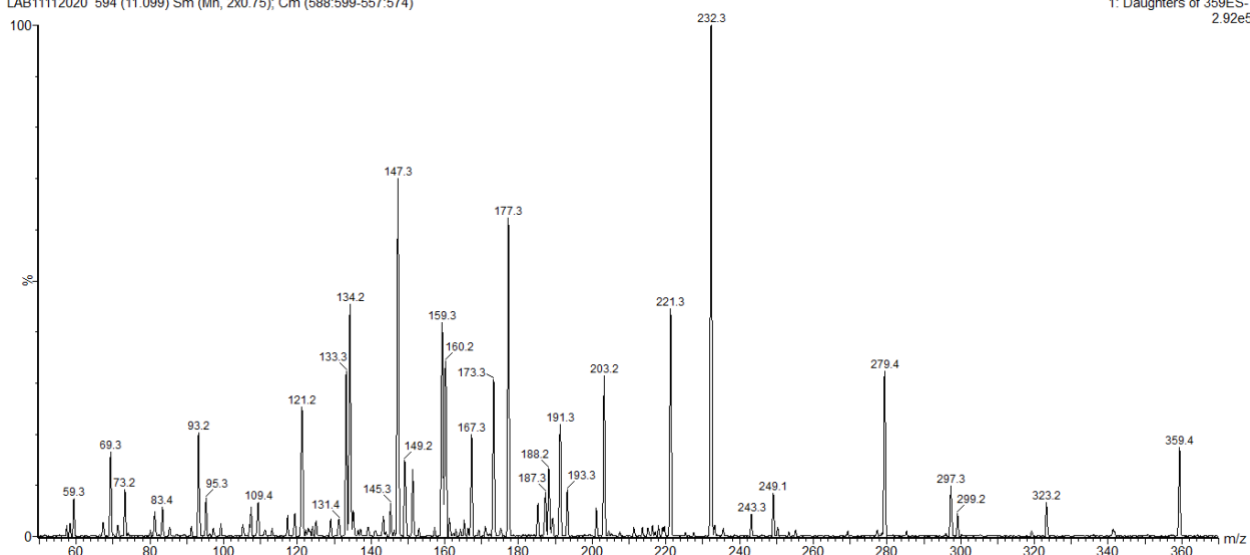
50pmol MaR1 Std. (10pmol/uL) in LC-MS grade water/MeOH 60:40 5uL injection CE 19eV
LAB11112018 581 (10.858) Sm (Mn, 2x0.75); Cm (578-586-600:610)



MaR2

50pmol MaR2 Std. (10pmol/ μ L) in LC-MS grade water/MeOH 60:40 5 μ L injection CE 19eV
LAB11112020 594 (11.099) Sm (Mn, 2x0.75); Cm (588:599-557:574)

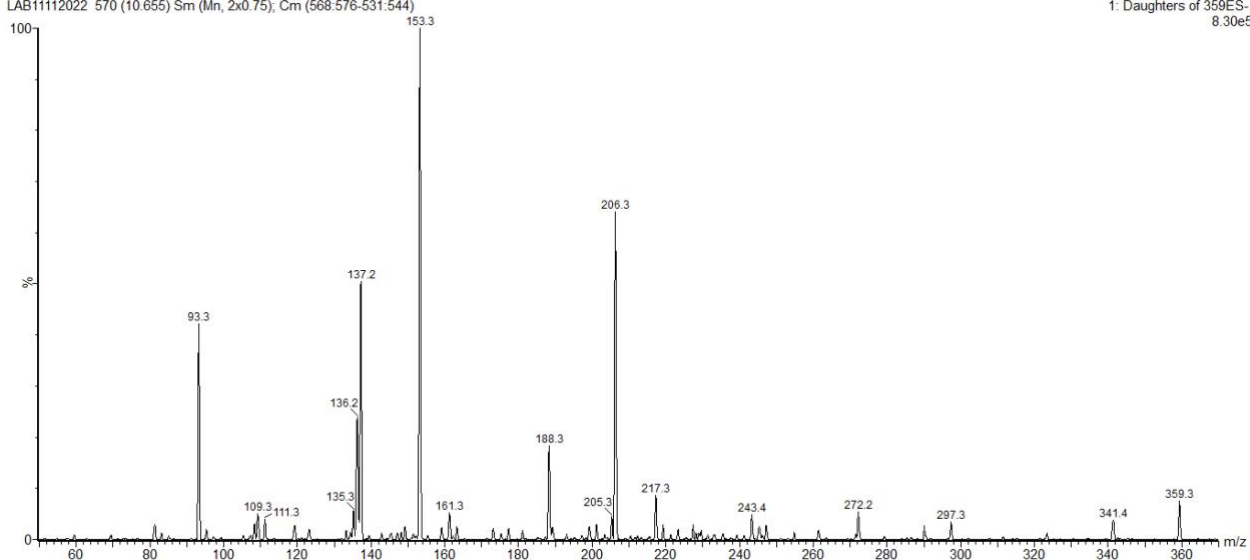
1: Daughters of 359ES-
2.92e5



PD1

50pmol PD1 Std. (10pmol/ μ L) in LC-MS grade water/MeOH 60:40 5 μ L injection CE 19eV
LAB11112022 570 (10.655) Sm (Mn, 2x0.75); Cm (568:576-531:544)

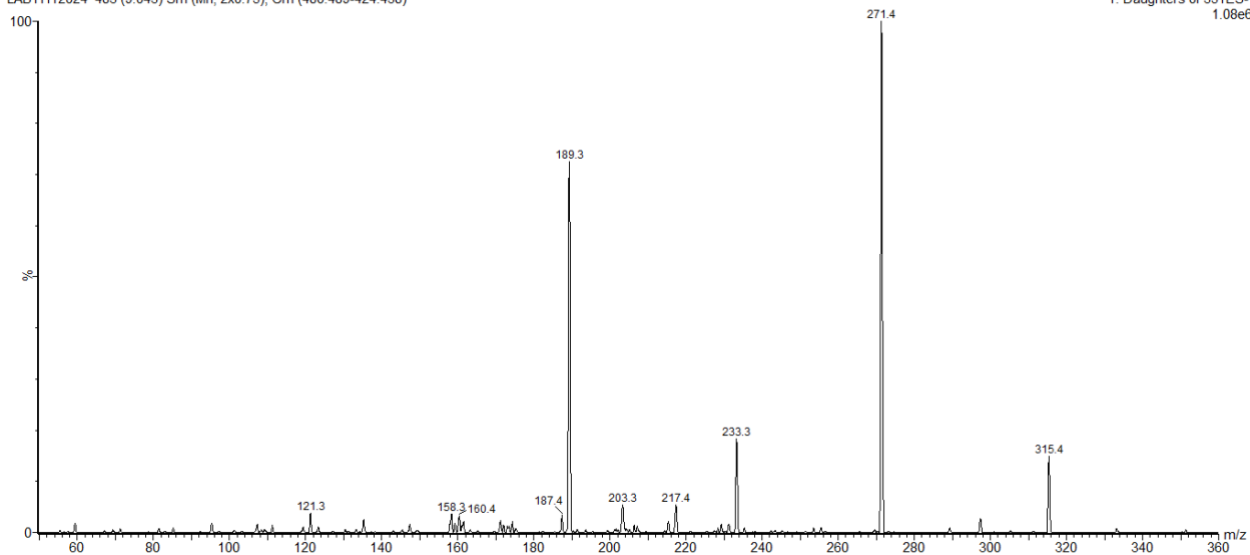
1: Daughters of 359ES-
8.30e5



PGD2

50pmol PGD2 Std. (10pmol/uL) in LC-MS grade water/MeOH 60:40 5uL injection CE 20eV
LAB11112024 483 (9.043) Sm (Mn, 2x0.75); Cm (480-489-424-438)

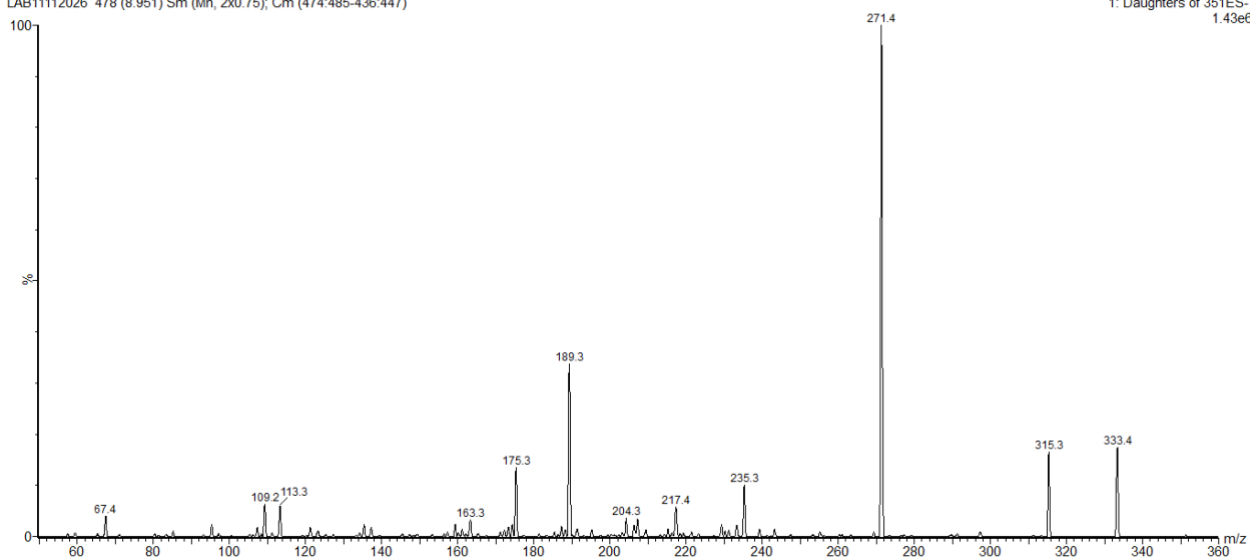
1: Daughters of 351ES-
1.08e6



PGE2

50pmol PGE2 Std. (10pmol/uL) in LC-MS grade water/MeOH 60:40 5uL injection CE 20eV
LAB11112026 478 (8.951) Sm (Mn, 2x0.75); Cm (474-485-436-447)

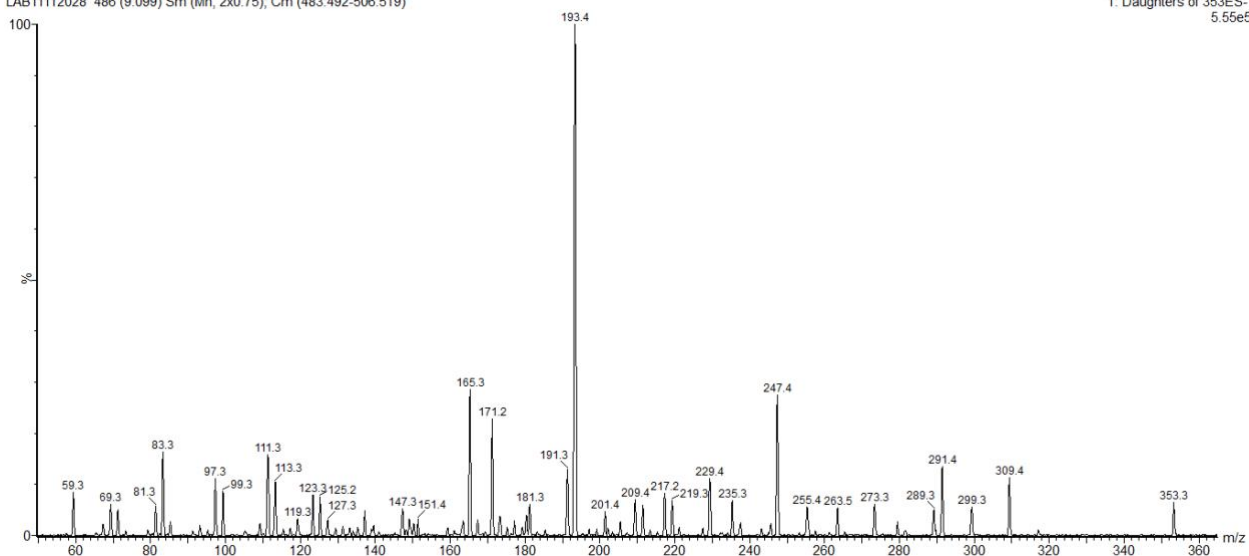
1: Daughters of 351ES-
1.43e6



PGF2a

50pmol PGF2a Std. (10pmol/uL) in LC-MS grade water/MeOH 60:40 5uL injection CE 27eV
LAB11112028 486 (9.099) Sm (Mn, 2x0.75); Cm (483-492-506-519)

1: Daughters of 353ES-
5.55e5



Lipidomics standards (from Cayman Chemical) preparation

Standard Synonym	Resolvin E1 RvE1	Resolvin D1 RvD1	Resolvin D2 RvD2	Resolvin D5 RvD5	Leukotriene B ₄ LTB ₄
Catalogue no.	10007848	1012554	10007279	10007280	20110
Solution/Solid	EtOH	EtOH	EtOH	EtOH	EtOH
Average Mwt.	350.5	376.5	376.5	360.5	336.5
Accurate Mwt.	350.2093	376.2250	376.2250	360.2301	336.2301
µg/250µL/500µL	25	25	25	25	25
mol/µL	1.4265E-10	2.6560E-10	2.6560E-10	2.7739E-10	2.9718E-10
pmol/µL	142.65	265.60	265.60	277.39	297.18
10pmol/µL solution (µL) plus 40%MeOH/60%H ₂ O (µL)	14.02 185.98	7.53 192.47	7.53 192.47	7.21 192.79	6.73 193.27
1pmol/µL solution (µL) plus 40%MeOH/60%H ₂ O (µL)	20.00 180.00	20.00 180.00	20.00 180.00	20.00 180.00	20.00 180.00
Collision Energy	17eV	17eV		20eV*	18eV
Diagnostic m/z ions (ESI -ve)	349.3 331.5 205.3 195.2 161.2 107.2	375.1 232.9 215.1 163.9 135.0 141.0		279.2 199.2 141.1	335.1 317.2 195.1 129.0 115.0 111.5
Standard Synonym	Lipoxin A ₄ LXA ₄	Lipoxin B ₄ LXB ₄	Maresin 1 MaR1	Maresin 2 MaR2	Protectin D1 PD1
Catalogue no.	90410	90420	10878	16369	10010390
Solution/Solid	EtOH	EtOH	EtOH	EtOH	EtOH
Average Mwt.	352.5	352.5	360.5	360.5	360.5
Accurate Mwt.	352.2250	352.2250	360.2301	360.2301	360.2301
µg/250µL/100µL	25	25	25	25	25
mol/µL	2.8369E-10	2.8369E-10	2.7739E-10	2.7739E-10	1.3870E-10
pmol/µL	283.69	283.69	277.39	277.39	138.70
10pmol/µL solution (µL) plus 40%MeOH/60%H ₂ O (µL)	7.05 192.95	7.05 192.95	7.21 192.79	7.21 192.79	14.42 185.58
1pmol/µL solution (µL) plus 40%MeOH/60%H ₂ O (µL)	20.00 180.00	20.00 180.00	20.00 180.00	20.00 180.00	20.00 180.00
Collision Energy	17eV		19eV		
Diagnostic m/z ions (ESI -ve)	351.2 251.1 235.1 145.6 114.9		359.1 250.0 246.1 221.0 140.9 113.6		

Standard Synonym	Prostaglandin D₂ PGD₂	Prostaglandin E₂ PGE₂	Prostaglandin F_{2α} PGF_{2α}	
Catalogue No.	12010	14010	16010	
Solution/Solid	solid (1mg)	solid (5mg)*	solid (1mg)	*Dissolved in 1mL of 40%MeOH/60%H ₂ O
Average Mwt.	352.5	352.5	354.5	
Accurate Mwt.	352.2250	352.225	354.2406	
mg/mL dissolved in 40%MeOH/60%H₂O	1	1	1	
mol/mL	2.8369E-06	2.8369E-06	2.8209E-06	
μmol/mL	2.8369	2.8369	2.8209	
nmol/μL	2.8369	2.8369	2.8209	
10pmol/μL solution (μL) plus 40%MeOH/60%H₂O (μL)	3.53 996.48	3.53 996.48	3.55 996.46	
1pmol/μL solution (μL) plus 40%MeOH/60%H₂O (μL)	50 450	50 450	50 450	
Collision Energy	20eV	20eV	27eV	
Diagnostic m/z ions (ESI -ve)	351.1 315.0 271.3 233.1 189.1	351.8 333.1 315.2 271.1 188.9	353.2 309.2 281.1 253.0 193.1	

Lipidomics standards percentage Waters HLB columns SPE recovery

Title: Running Standards to optimize sample preparation method

Date: 13 June 22

Objective: Testing drying the samples in TurboVap larger tubes vs Transfer to a smaller 1 ml tubes.

Testing Full water tank (water touching the outer wall of test tube walls) vs lower water level (water not touching the tube walls)

Samples annotations:

1 ST Standard Test done with water tank 5.5 L. When methyl format < 1 ml samples transferred to a 1 ml tube (Discovery)

2 ST Standard Test done with water tank 5.5 L. When methyl format < 1 ml samples transferred to a 1 ml tube (Replication)

3 ST Standard Test done with water tank 7.5 L. samples completely dried in the larger test tubes (Discovery)

4 ST Standard Test done with water tank 7.5 L. samples completely dried in the larger test tubes (Replication)

7 ST Standard Test done with water tank 5.5 L. samples completely dried in the larger test tubes (Discovery)

8 ST Standard Test done with water tank 5.5 L. samples completely dried in the larger test tubes (Replication)

Results: Refer to the table below

Conclusion : Recovery rate significantly higher when the equipment is utilized (31% - 81%) compared to the manual method (22% to 50 %). MaR2 have the lowest recovery rate of all the studied compounds.

Recovery rate significantly higher when 37 degrees water doesn't touch the tubes outer walls.

Recovery rate % increased when samples were transferred to a small tubes compared to drying the samples in large tube however relative variability between injections are significantly lower in large tube (0.1% - 2.2%). compared to the small tubes (3.7% - 34.1%).

Sample injection	1 ST			2 ST			3 ST			4 ST			5 ST			6 ST		
	a	b	c	a	b	c	a	b	c	a	b	c	a	b	c	a	b	c
RvE1	74.2	61.6	54.9	61.7	63.1	62.8	53.2	52.1	44.9	55.2	55.7	55.9	68.4	70.5	82.5	68.5	66.0	66.9
	63.6			62.6			53.5			55.6			69.0			67.1		
RvD2	68.1	69.2	64.5	59.2	58.3	59.2	35.2	36.8	37.4	41.1	41.4	41.3	53.7	52.3	52.9	56.8	56.3	56.0
	67.3			58.9			36.5			41.3			53.0			56.4		
RvD1	78.8	76.1	66.7	63.6	60.7	61.6	36.9	36.2	37.6	41.5	41.2	41.9	53.8	53.9	54.4	58.5	58.2	59.0
	73.9			62.0			36.9			41.5			54.0			58.6		
RvD5	40.7	42.5	45.0	45.3	46.2	50.3	22.8	21.6	23.8	26.4	27.8	25.1	38.0	38.4	39.5	51.7	52.2	51.5
	42.7			47.3			22.8			26.4			38.6			51.8		
LTB4	35.2	41.3	44.2	49.9	52.0	50.2	22.6	21.9	21.2	26.6	25.7	25.6	35.7	37.4	35.4	49.2	47.7	48.3
	40.3			50.7			21.9			26.0			36.2			48.4		
LXA4	60.2	56.0	54.8	56.6	58.4	58.4	36.2	37.0	37.2	40.1	40.5	41.4	52.7	51.7	51.4	54.7	53.1	52.8
	57.0			57.8			36.8			40.7			51.9			53.5		
LXB4	83.1	66.2	62.4	66.7	68.5	70.1	46.9	47.6	48.1	51.3	49.9	50.5	68.1	69.1	66.6	67.8	65.7	67.2
	70.5			68.4			47.5			50.5			67.9			66.9		
PGD2	94.9	73.8	71.7	72.7	74.6	75.1	50.8	52.1	51.3	55.3	54.8	55.6	75.7	73.5	73.4	72.3	72.4	72.0
	80.1			74.1			51.4			55.2			74.2			72.2		
PGE2	97.6	74.3	71.0	72.8	76.3	74.8	53.3	54.2	53.9	58.6	57.5	59.0	79.2	78.7	78.3	79.1	79.1	79.0
	81.0			82.6			53.8			58.4			78.8			79.1		
PG2a	96.1	69.6	65.2	69.5	70.2	76.0	52.2	54.5	53.2	59.0	58.6	56.8	77.0	78.7	76.1	75.3	74.2	77.0
	77.0			71.9			68.2			58.1			77.3			75.5		
MaR2	17.1	34.2	33.0	34.4	34.3	33.8	12.0	11.7	12.5	15.6	15.4	15.0	22.3	23.1	22.8	42.3	40.9	40.9
	28.1			34.1			12.1			15.3			22.7			41.4		
MaR1	34.7	42.1	46.4	46.0	49.4	49.5	21.7	22.4	21.8	27.6	26.3	27.5	37.1	37.6	34.6	51.5	51.7	49.6
	41.1			48.3			22.0			27.1			36.4			51.0		
PD1	44.9	52.0	51.5	53.8	51.5	53.4	23.2	23.9	23.7	28.7	29.6	27.3	38.9	40.4	39.5	57.1	54.6	55.6
	49.5			52.9			23.6			28.5			39.6			55.8		

Title: Running Standards to optimize sample preparation method

Date: 17 Oct 22

Objective: Practice standards run

Testing drying the samples in TurboVap larger tubes vs Transfer to a smaller 1 ml tubes.

Samples annotations:

- 1 ST Standard Test done with water tank 5.5 L. samples completely dried in the larger test tubes
- 2 ST Standard Test done with water tank 5.5 L. samples completely dried in the larger test tubes
- 3 ST Standard Test done with water tank 5.5 L. samples completely dried in the larger test tubes
- 4 ST Standard Test done with water tank 5.5 L. samples completely dried in the larger test tubes
- 5 ST Standard Test done with water tank 5.5 L. samples completely dried in the larger test tubes

- 6 ST Standard Test done with water tank 5.5 L. When methyl format < 1 ml samples transferred to a 1 ml tube
- 7 ST Standard Test done with water tank 5.5 L. When methyl format < 1 ml samples transferred to a 1 ml tube
- 8 ST Standard Test done with water tank 5.5 L. When methyl format < 1 ml samples transferred to a 1 ml tube
- 9 ST Standard Test done with water tank 5.5 L. When methyl format < 1 ml samples transferred to a 1 ml tube
- 10 ST Standard Test done with water tank 5.5 L. When methyl format < 1 ml samples transferred to a 1 ml tube

Results: Refer to the table below

Conclusion : The average recovery rate for the samples per method range between 53% (MaR1) to 85% (RvE1) compared to (31% - 81%) on the previous run on 13/6/22.

Recovery rate % increased when samples were transferred to a small tubes (samples 6-10) compared to drying the samples in large tube (samples 1-5) which is consistence with the observations of the previous run on 13/6/22.

Sample injection	1 ST			2 ST			3 ST			4 ST			5 ST			Average
	a	b	c	a	b	c	a	b	c	a	b	c	a	b	c	
RvE1	73.5	74.7	77.9	65.8	61.5	60.3	69.4	72.6	71.1	74.3	72.6	76.3	80.9	79.8	84.7	
	75.4			62.6			71.1			74.4			81.8			73.0
RvD2	55.9	59.3	61.8	57.3	58.5	56.9	73.3	73.1	72.2	69.0	67.8	69.2	72.1	77.1	78.0	
	59.0			57.5			72.9			68.6			75.7			66.8
RvD1	47.9	53.3	55.5	53.8	54.0	54.4	71.1	71.4	71.8	66.6	65.8	65.2	66.9	72.8	72.9	
	52.2			54.0			71.4			65.9			70.9			62.9
RvD5	42.4	63.4	72.0	64.6	62.6	61.8	90.1	88.7	89.4	75.7	73.2	74.1	74.8	88.6	89.7	
	59.3			63.0			89.4			74.3			84.4			74.1
LTB4	27.2	46.5	56.4	56.5	54.4	52.8	80.9	81.0	80.2	68.8	67.4	68.5	66.3	74.7	76.3	
	43.4			54.6			80.7			68.2			72.4			63.9
LXA4	40.8	51.7	55.0	55.9	53.5	53.2	69.3	69.5	69.0	63.6	62.8	62.6	60.9	66.9	67.6	
	49.2			54.2			69.2			63.0			65.1			60.2
LXB4	53.0	60.8	64.6	60.4	56.8	55.7	70.4	70.4	70.5	68.1	67.3	68.0	70.3	76.6	77.0	
	59.5			57.6			70.4			67.8			74.6			66.0
PGD2	52.9	63.1	64.5	59.0	56.2	55.0	69.0	68.9	70.2	67.2	67.4	67.3	72.8	78.2	78.4	
	60.2			56.7			69.4			67.3			76.5			66.0
PGE2	62.4	70.6	74.8	64.9	60.8	60.1	73.8	71.1	73.8	75.3	75.5	75.9	84.2	87.5	87.8	
	69.3			61.9			72.9			75.5			86.5			73.2
PG2a	60.3	69.7	71.8	63.3	57.0	55.6	72.6	77.4	75.5	73.6	73.0	72.3	81.0	90.0	90.2	
	67.3			58.6			75.2			73.0			87.1			72.2
MaR2	29.6	36.1	53.6	47.1	47.6	45.1	74.6	74.7	75.5	62.0	57.4	58.4	55.2	64.4	68.4	
	39.8			46.6			74.9			59.3			62.7			56.6
MaR1	41.5	61.3	68.6	59.8	61.6	57.4	90.2	86.5	86.4	74.4	69.8	72.5	72.3	83.6	86.9	
	57.1			59.6			87.7			72.3			80.9			71.5
PD1	39.6	52.3	59.6	54.6	54.2	54.4	83.2	83.1	83.0	71.4	68.4	68.6	71.3	80.3	80.1	
	50.5			54.4			83.1			69.5			77.2			66.9

7.3 APPENDIX (C): Postponed work due to COVID- 19 impact

Research Study Title: Validation of exhaled breath metabolomics signatures in COPD exacerbation subtypes.

Study Protocol

The objectives fit in the published Ember protocol which are to define volatile biomarkers of acute exacerbation, AECOPD in this particular study. Thus, this study will be performed under published EMBER study protocol; Exhaled Breath Metabolomic Biomarkers in the Acutely Breathless Patient, *Ibrahim et. al* (1). Ethically approved by The National Research Ethics Service Committee East Midlands (REC number: 16/LO/1747). Integrated Research Approval System (IRAS) 198921. The necessary amendment to the current EMBER study protocol will be made and submit for updates approvals to include:

- additional subject- up to 100 in the acute COPD patients category to the recruitment plan
- As current protocol approvals run until December 2021, it will be recommended to request extending the protocol to cover the 18 months proposed for the study duration.
- For inclusion criteria, to include bacterial COPD exacerbation as been defined in the study population. For exclusion criteria, exclude patients who are unable to produce sputum samples. matched controls”
- To add the Breath SPEC sampler to the list of the study breath analysis devices.
- Possibly, removing the need for senior decision maker review as inclusion criteria. Ember current inclusion criteria stated “Diagnosed with acute breathlessness as one of the primary indicator reasons by the clinical acute care team. This is not a requirement for healthy subjects or matched controls. One of the indicator provisional diagnoses identified in section 7.1 following senior review by the clinical acute care team. This is not a requirement for healthy subjects or controls”

Background and Significance

the therapeutic approaches for acute exacerbation of COPD (AECOPD) remained standardized in the clinical setting. These treatments usually consist of bronchodilators, systemic corticosteroids and antibiotics administration.(5) Thus, biomarkers to stratify therapeutic approaches in AECOPD is needed. In the EMBER project of breath metabolomic profiling, results suggest that breath volatiles can distinct clinical conditions of patients who present with acute breathlessness including acute asthma, COPD, pneumonia and HF. Studying all comers with breathlessness a bilaminar data developed in the embers study, under preparation for manuscript, identified breath print of infection in pneumonia and AECOPD. These signatures showed an association with high and low CRP cases with high sensitivity and specificity for bacterial infection.(1, 2) **This EMBER’s prospective sub-study aims** to validate these signatures early at the beginning of the care pathway in bacterial exacerbation of AECOPD. figure 1. **Clinical significance** lays in the potential ability of breath volatiles to influence the clinical decision making to stratify treatments including antibiotics and antiinfection agents in patients with AECOPD which in turn improves clinical outcomes in COPD patients and reduce associated complications from the unnecessary administration of medications.

Objectives

The objectives of this project fit in the published EMBER protocol which is to define volatile biomarkers of acute exacerbation

Primary Objective

Validating breath biomarkers that are sensitive and specific to bacterial acute exacerbation subtypes of COPD.

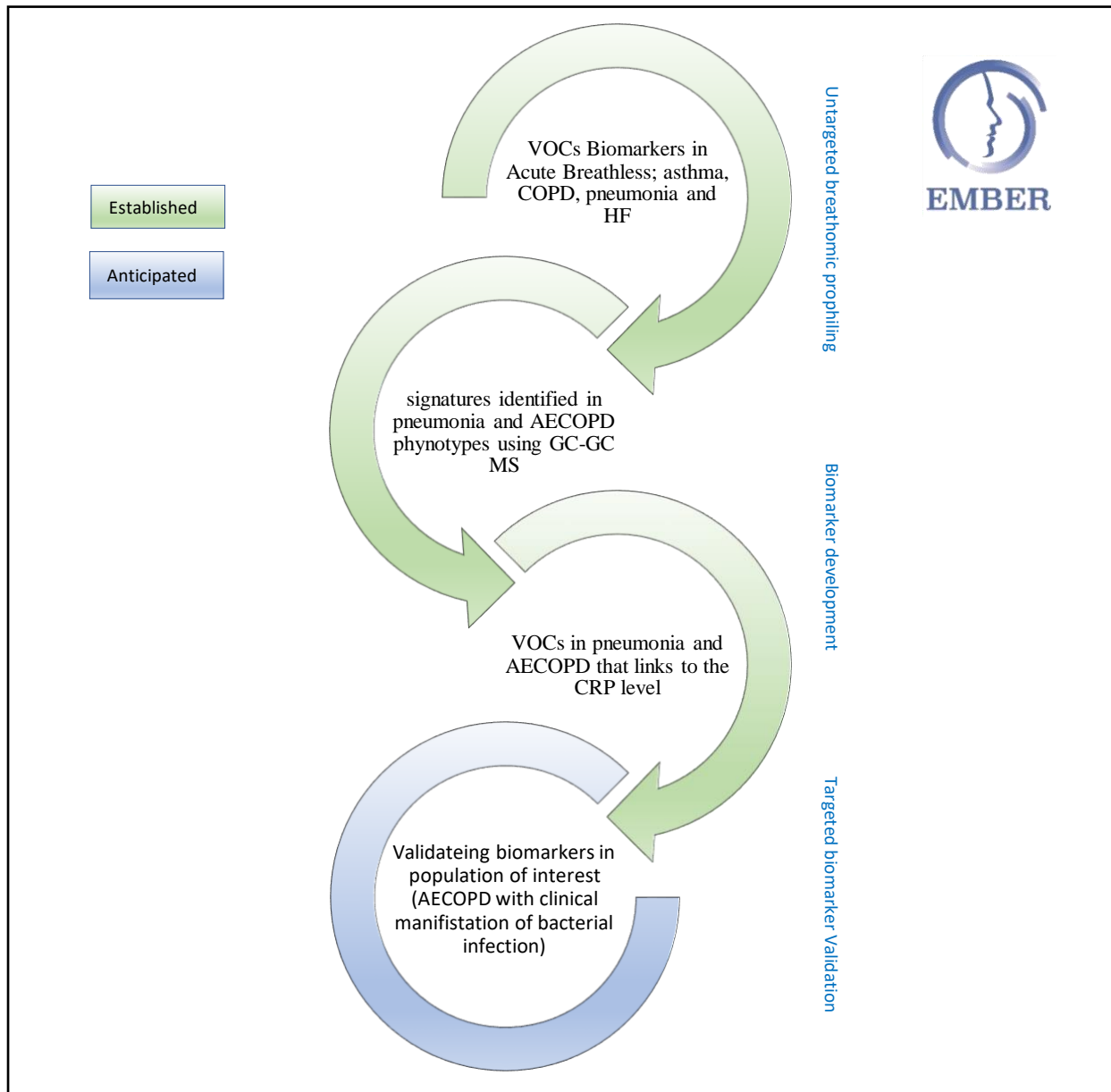
Secondary Objectives

- Associating the breath biomarkers sensitive and specificity with existing diagnostic measures of bacterial exacerbation including baseline C-reactive protein and culture positivity for bacterial infection.
- Comparing the quality of the proposed test according to patient's prior antibiotic exposure at presentation (to address a major confounder).

Potential Objective

This exploratory objective is subject to funding, using metagenomic research tool to perform detailed quantitative microbiome in sputum sample for a sub-group of patients with high CRP indicating a high bacteria load to link these findings with the proposed VOCs as a marker of bacterial infection.

Fig. flow chart presenting the context of the future work proposed in this sub-study within the EMBER established framework:



Study design/methodology

Study Design

This is an acute prospective observational and point of care diagnostic accuracy study.

Study Duration and targeted sample size:

Study duration is 18 months to total. Estimated recruitment time to target 50-100 subject will be 12 months starting from Jan 2021 through Dec 2021 (to recruited 2.5 patients/ week based on a 40 week per year). Additional 6 months will be utilized for data analysis and reporting.

Study Schedule:

Events Describing is available in EMBER protocol, a summary provided in figure3.

Study Population

Adult patients with a documented or reported history of COPD who arrive at Glenfield hospital CDU respiratory unit with a clinical manifestations of bacterial COPD exacerbation. defined by one or more of the following criteria:

- CRP of More than 50.0 mg/dL indicates a severe elevation and an evidence of acute bacterial infections (blood usually taken at triage or EME results are expected within 4-6 hours)
- Reported Sputum purulence within last 24 hours of admission using sputum color chart.
- Evidence of consolidation on chest X-ray.

Inclusion /Exclusion Criteria

There will be no valuations to the original inclusion and exclusion criteria at the current version of EMBER study protocol, With the addition of (amendments will be proposed) the enrichment of AECOPD patients presented with a manifestation of bacterial mediated exacerbation as an Inclusion Criteria. Moreover, to exclude patients who are unable to produce spontaneous sputum sample as there will be inability to confirm the diagnosis of LRTI with the suggested reference standard.

Method:

Over twelve months, a target of (n) = 50- 100 subjects selected through a consecutive sampling will be enrolled. Patients will be admitted to the CDU at Glenfield hospital via the standard streaming of medical emergency care pathways at the University Hospitals of Leicester National Health Service Trust. Upon arriving at the triage a member of the healthcare team, usually a nurse, will assign patients to either a respiratory or cardiac unit for initial patient assessment and to be seen by the senior decision maker later at the pathway care. Enrollment will occur early on in the pathway. Subjects' data collection and sampling will be performed at three sampling points; at visit 1, reflecting acute disease status at triage unit, at visit 2, reflecting the stable status at hospital discharge, and at visit 3, reflecting the recovery level and chronic status of the disease (described in ember protocol as the next clinic follow-up appointment for participants at least 6-weeks post exacerbation event and up to 6 months).

A Spontaneous sputum samples and a breath test will be performed at each sampling point using a Point of Care non- invasive Breath SPEC device. Additional samples will be collected using the Reciva method to be send to the lab for a GC-GC MS targeted analysis. Based on the Index test, bacteria associated AECOPD will be defined as; the present of bacterial infection based on VOCs biomarkers in exhaled breath Diagnosis will be confirm using as reference standards based on the current gold standards in the clinical practice guidelines to identify bacterial infection. Based on the reference standards bacteria-associated exacerbations will be identify with positive sputum culture results for common bacterial infections, elevated CRP level, or sputum color. Clinical information and breath test outcomes will be available to the assessors of the reference standard.

Outcome measures for primary Objectives:

STARD guidelines for diagnostic accuracy studies will be utilized to deliver transparent and comprehensive quality reporting. The index test will be assessed against the reference test to determine the prevalence of true positive, false negative, false positive, and true negative figure 1. Then, the potential discriminative ability of breath test to phenotype AECOPD with

LRTI can be quantified by the measures of diagnostic accuracy such as sensitivity and specificity, predictive values, likelihood ratios, the area under the ROC curve, Youden's index, and diagnostic odds ratio. (347)

Outcome measures for secondary Objectives:

Further evaluation of the Index test against the reference test according to three distinguished groups based on history of antibiotic treatment received within the last two weeks before admission; group (1) antibiotic exposed, group (2) antibiotic naïve, group (3) regardless of antibiotics exposure. volatiles biomarkers will linked to CRP level, sputum culture results, sputum color changes, and chest x-ray by conducting measures for quantifying added value e.g. Difference in ROC curves.

Variables and Data Collection:

Data will be collect within routine clinical care using the EMBER CRF. Summary available in table.1.

Table 1. Data collection per sampling points.

Data Collection	Time point		
	Visit 1	Visit 2	Visit 3
Written Informed Consent	X		
Collection of Demographic Data (age, gender, height, wight, ethnicity, smoking status)	X		
Time and date of admission/ discharge/ follow up assessment	X	X	X
Patient physiological triage categories	X		
Samples collections:			
Point of care breath biomarkers for pneumonia VOCs set	X	X	X
Breath samples collection for GC-GC MS	X	X	X
Spontaneous sputum	X	X	X
Data collection from clinical case notes in Patient Electronic Health Records:			
primary diagnosis for the current admission	X		
30/ 60-day hospital re-admission.			X
Hospital mortality rate	X		
CRP	X	X	X
Blood eosinophils	X	X	X
VAS of breathlessness	X	X	X
CBC, and neutrophils count	X		
Present of consolidation in chest X - ray imaging	X	X	X
COPD assessment tool (CAT)	X	X	X
DECAF scores	X		
Sputum cultures results			
Medication usage within last two weeks:			

Antibiotic	X	X	X
Corticosteroids (ICSs) and Systemic Steroids	X	X	X

Statistical Analysis Plan:

Sample size determination:

Prevalence of bacterial infection mediated exacerbation in COPD from a published work was used to estimate sample size. *Pafadhal Mona et al., 2011* identified three clusters phenotypes in 182 exacerbation events from 86 patients as following: COPD exacerbation associated with a bacterial infection 55% (defined as a positive bacterial pathogen on routine culture or a total aerobic CFU $\geq 10^7$ cells), virus 29% (defined as positive sputum viral PCR with or without positive bacterial pathogen on routine culture), or eosinophilic airway inflammation 28% (defined as $> 3\%$ nonsquamous cells). (348) Furthermore, 60% to 70% of all AECOPD had an antibiotic prescription on the same day of consultations in primary care (349-351).

Considering 60% as the percentage of antibiotic exposure in all AECOPD, this leaves 40% with no antibiotic exposure. Thus, we assume a prevalence of AECOPD with bacterial infection of 55% in which 33% will be expected to have a prior to admission antibiotic treatment:

- 33% of patients will have bacterial exacerbation and be antibiotic exposed.
 $.60 \times .55 = .33^*$
- 22.0% of patients will have bacterial exacerbation and be antibiotic naïve.
 $.40 \times .55 = .22^*$

* might slightly differ, because of the potential bias that patients present with clinical manifestation of bacterial infection are more likely to receive antibiotic treatment

In this specific project, we aim to recruit (n)= 50 up to 100 subjects. There is a risk of not recruiting the population of interest if the study based on recruitment of all AECOPD comes and to have an underpowered study to identify sensitive and specific biomarkers. This might be due to the possibility of having a false negative diagnosis based on sputum culture caused by technique limited sensitive or prior antibiotic exposure. Therefore, this study will aim to enrich the bacterial infection phenotype on AECOPD to increase the prevalence of the population of interest. By applying the proposed criteria in the study population, we are estimating at least 7 of 10 patients to have infection increasing the prevalence of 55% up to 70%. Table 2. provides a sample size calculation for proposed prevalence ranges powered to identify sensitive and specific biomarkers ($\geq 80\%$) of LRTI in AECOPD with a precision of 10% and 95% confidence.

Table 2. sample size calculation tables

20% prevalence, 10% precision				30% prevalence, 10% precision			
Sensitivity	Sample Size	Specificity	Sample Size	Sensitivity	Sample Size	Specificity	Sample Size
0.8	307	0.8	77	0.8	205	0.2	88
0.81	296	0.81	74	0.81	198	0.2	85
0.82	284	0.82	71	0.82	189	0.2	81
0.83	271	0.83	68	0.83	181	0.2	78
0.84	258	0.84	65	0.84	173	0.2	74
0.85	245	0.85	61	0.85	164	0.2	70
0.86	231	0.86	58	0.86	155	0.2	67
0.87	217	0.87	54	0.87	145	0.2	63
0.88	203	0.88	51	0.88	136	0.2	58
0.89	188	0.89	47	0.89	126	0.2	54
0.9	173	0.9	43	0.9	116	0.2	50
55% prevalence, 10% precision				60% prevalence, 10% precision			
Sensitivity	Sample Size	Specificity	Sample Size	Sensitivity	Sample Size	Specificity	Sample Size
0.8	112	0.8	137	0.8	103	0.8	154
0.81	107	0.81	131	0.81	99	0.81	148
0.82	103	0.82	126	0.82	95	0.82	142
0.83	99	0.83	120	0.83	91	0.83	136
0.84	94	0.84	115	0.84	87	0.84	130
0.85	89	0.85	109	0.85	82	0.85	123
0.86	84	0.86	103	0.86	78	0.86	116
0.87	79	0.87	97	0.87	73	0.87	109
0.88	74	0.88	90	0.88	68	0.88	102
0.89	68	0.89	84	0.89	63	0.89	95
0.9	63	0.90	77	0.9	58	0.9	87
0.91	58	0.91	70	0.91	53	0.91	79
0.92	52	0.92	63	0.92	48	0.92	71
0.93	46	0.93	56	0.93	42	0.93	63
0.94	40	0.94	49	0.94	37	0.94	55
0.95	34	0.95	41	0.95	31	0.95	46
65% prevalence, 10% precision				70% prevalence, 10% precision			
Sensitivity	Sample Size	Specificity	Sample Size	Sensitivity	Sample Size	Specificity	Sample Size
0.8	95	0.8	176	0.8	88	0.8	205
0.81	91	0.81	169	0.81	85	0.81	198
0.82	88	0.82	162	0.82	81	0.82	189
0.83	84	0.83	155	0.83	78	0.83	181
0.84	80	0.84	148	0.84	74	0.84	173
0.85	76	0.85	140	0.85	70	0.85	164
0.86	72	0.86	133	0.86	67	0.86	155
0.87	67	0.87	125	0.87	63	0.87	145
0.88	63	0.88	116	0.88	58	0.88	136
0.89	58	0.89	108	0.89	54	0.89	126
0.9	54	0.9	99	0.9	50	0.9	116
0.91	49	0.91	90	0.91	45	0.91	105
0.92	44	0.92	81	0.92	41	0.92	95
0.93	39	0.93	72	0.93	36	0.93	84
0.94	34	0.94	62	0.94	31	0.94	73
0.95	29	0.95	53	0.95	27	0.95	61
75% prevalence, 10% precision				80% prevalence, 10% precision			

Sensitivity	Sample Size	Specificity	Sample Size	Sensitivity	Sample Size	Specificity	Sample Size
0.8	82	0.8	246	0.8	77	0.8	308
0.81	79	0.81	237	0.81	74	0.81	296
0.82	76	0.82	227	0.82	71	0.82	284
0.83	73	0.83	217	0.83	68	0.83	272
0.84	69	0.84	207	0.84	65	0.84	259
0.85	66	0.85	196	0.85	62	0.85	245
0.86	62	0.86	186	0.86	58	0.86	232
0.87	58	0.87	174	0.87	55	0.87	218
0.88	55	0.88	163	0.88	51	0.88	203
0.89	51	0.89	151	0.89	48	0.89	189
0.9	47	0.9	139	0.90	44	0.90	173
0.91	42	0.91	126	0.91	40	0.91	158
0.92	38	0.92	114	0.92	36	0.92	142
0.93	34	0.93	101	0.93	32	0.93	126
0.94	29	0.94	87	0.94	28	0.94	109
0.95	25	0.95	73	0.95	23	0.95	92

Figure 2. STARD flow diagram for patients included in the study for undergoing Breath sampling procedures.

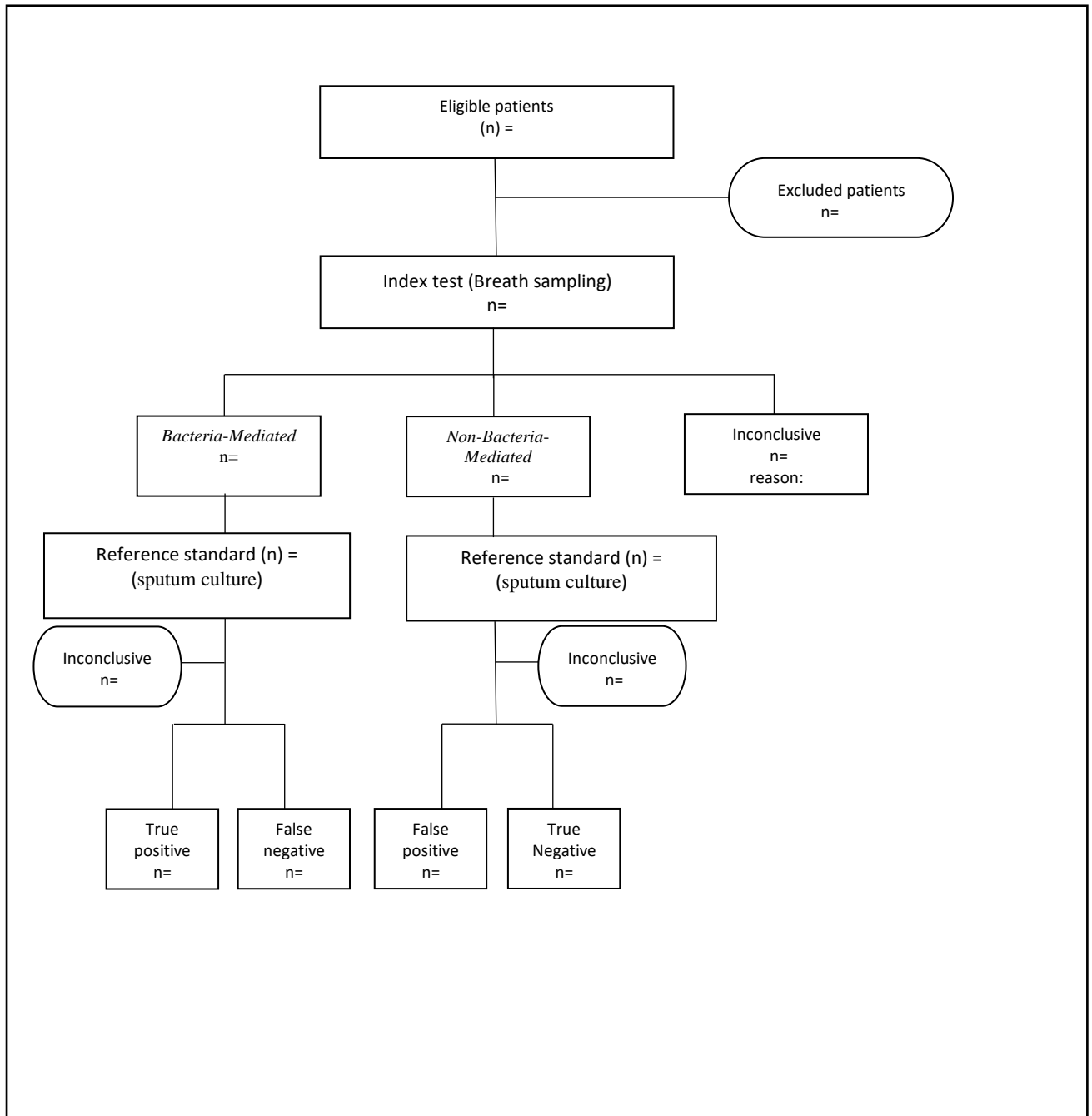
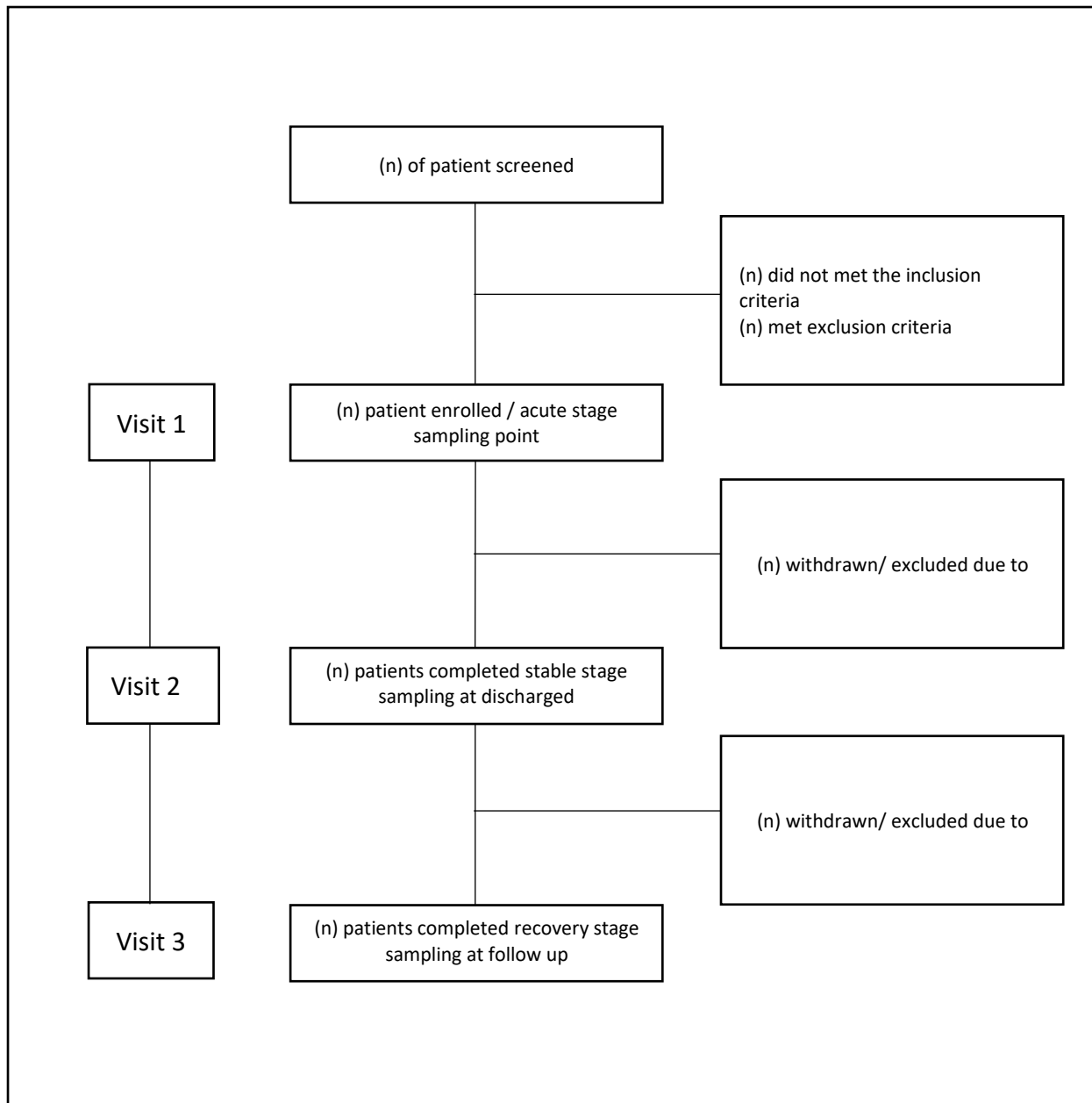


Figure 3. Flow chart of study events and sampling points.



Topic: Review article on metabolomics in COPD with LRTI (with or without pneumonia)

Background and review questions:

- COPD phenotypes prevalence and mortality (with a focus on phenotype related to LRTI with and without pneumonia)
- COPD, LRTI, pneumonia Overlaying and co- existing:

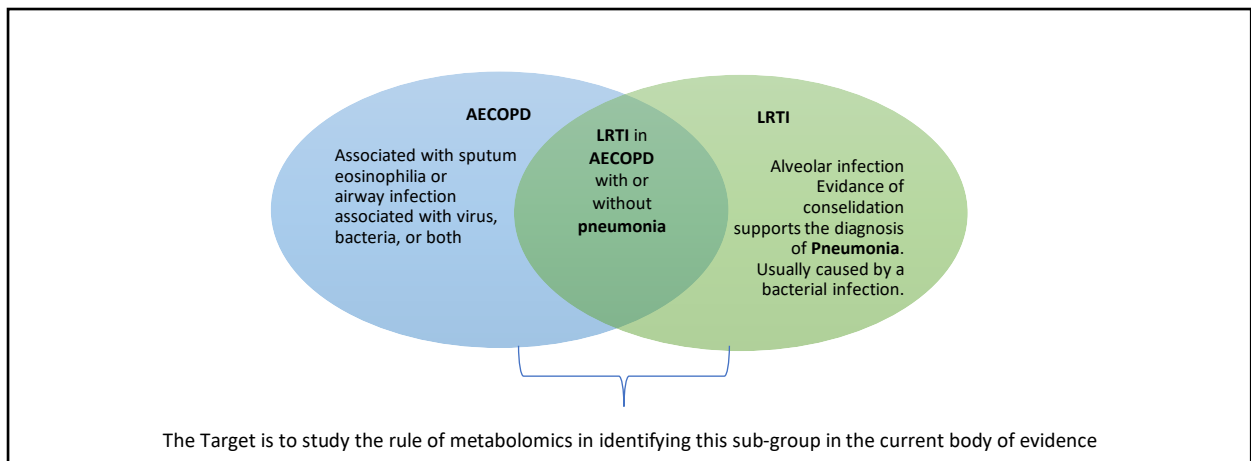


Figure 2. clinical overlap between AECOPD, LRTI, and pneumonia

- Topic significance and Clinical Relevance: Current approach in diagnosis and limitation. What metabolomics can offer to support clinical decision making related to diagnosis, prognosis, treatment response, phenotyping, and pathogenesis identification.

Searching strategy protocol

Inclusion criteria:

- 1- Human adult subjects studies examining metabolomics in COPD or/and LRTI (with or without pneumonia).
2. The use of NMR or MS platforms technique to identify metabolites with a targeted and/or untargeted approach.
3. All types of biological samples will be included (plasma, serum, breath, urine, blood, EBC, Lung tissue sample, Other samples).

Exclusion criteria:

- 1- Animal models.
- 2- Participants who did not meet recognized clinical criteria for diagnosis of COPD, LRTI, or pneumonia.
3. Pediatric populations studies.
4. Editorials, Reviews, and Case-reports.
5. Studies with abstract published only.
6. Secondary data.

Outcome(s)

The main outcome will be a thorough assessment of metabolic pathway (altered pathogenesis), common and significant metabolites (biomarkers) that differentiate COPD/ LRTI phenotypes.

Data extraction

Data variables include: study location, year of publication, sample size, study population, characteristics of participants (age, sex, and ethnicity), timeline of study (if there is any follow up), type of biospecimens samples, platform, statistical methods, analytic technique, study outcomes summary of key findings (identified biological metabolites, pathways, significant versus nonsignificant, effect sizes, and direction of effect).

Data synthesis

This review will take a qualitative approach. We will provide a narrative synthesis of the findings and provide a table of key study characteristics. It is anticipated that models developed for metabolites - for example - discrimination between COPD phenotypes will differ upon which they are based. As a result it might be inappropriate to combine these for a pooled area under the curve value. Presentation and analysis might be split according to phenotype (eosinophilic and non-eosinophilic); analytical methods (gas chromatography-mass spectrometry and electronic nose); statistical methods (discriminative models and cluster analyses); or study aim/outcome (diagnosis, pathway, phenotyping).

Database Search

Using PubMed and Ovid MEDLINE will be conducted to include papers published in English from 2000 and later. No restrictions on study designs will be applied initially. Within some included studies there might be a control (healthy) or comparison disease groups (other than COPD, LRTI, or pneumonia). We also expect some studies with longitude approach looking at the metabolites in the acute, recovery and chronic status and any differences between high and low symptom individuals (severity). Appendix1. Indicate Full searching strategies used.

Searches will use a combination of the following terms as keywords:

(breathomics, metabolomic/s, Metabolomic profile/ing, metabolite/s, Metabolism/s, volatile organic compounds, metabolomic compounds, chronic obstructive pulmonary disease, AECOPD, exacerbation of COPD, Acute exacerbation of chronic obstructive pulmonary disease, LRTI, Lower respiratory tract infection, Pneumonia, Consolidation)

MEDLINE search strategy:

First Concept:

1. exp Metabolomics/ (16829)
2. Metabolom* .mp. (39353)
3. Metabolite* .mp. (280696)
4. Breathomic .mp. (63)
5. Volatile organic compounds .mp. or Volatile organic compounds/ (15664)
6. 1 or 2 or 3 or 4 or 5 (312516)

Second Concept:

7. exp Pulmonary Disease, Chronic Obstructive/ (56185)
8. COPD .mp. (47966)
9. Acute Exacerbation of COPD .mp. (916)
10. Acute Exacerbation of Chronic Obstructive Pulmonary Disease .mp. (1020)
11. AECOPD .mp. (1171)
12. ACOPD .mp. (3)

Third Concept:

13. 7 or 8 or 9 or 10 or 11 or 12 (74520)
14. LRTI .mp. (1256)
15. lower respiratory tract infection .mp. (3108)
16. exp Respiratory Tract Infection/ (383671)

Fourth Concept:

17. Exp Pneumonia/ (118355)
18. Pneumonia .mp. (183116)
19. Consolidation .mp. (30087)
20. 14 or 15 or 16 (385200)
21. 17 or 18 or 19 (214645)

Combined Concept:

22. 13 or 20 or 21 (538007)

23. 6 and 22 (1639)

Limits:

24. Limit 23 to (English language and human and "all adult (19 plus years)") (466)

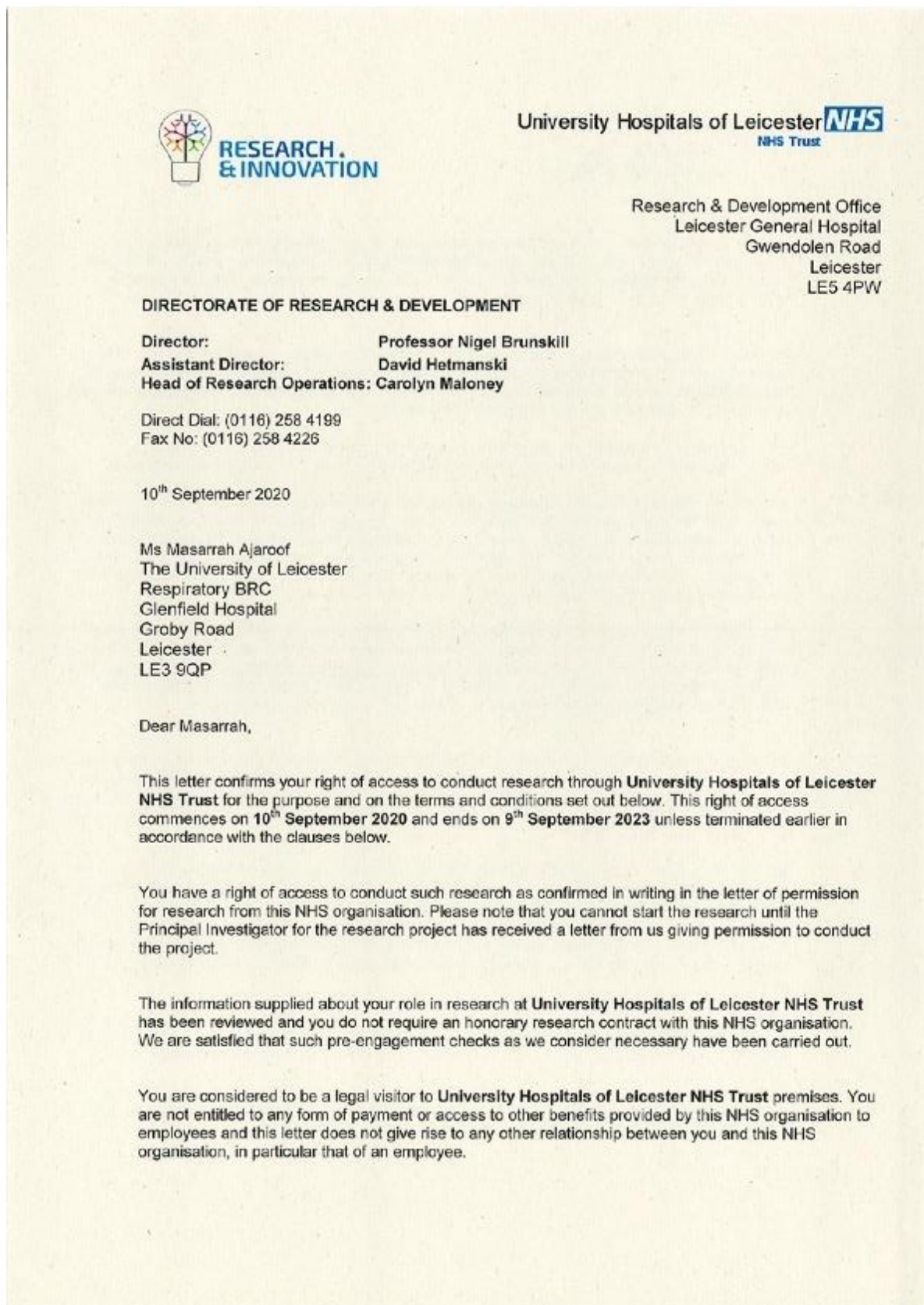
Limits:

25. Limit 25 to yr = "2010-Current"

PubMed Search Strategy:

```
((((COPD OR Pulmonary Disease Chronic Obstructive OR Acute Exacerbation of COPD OR Acute Exacerbation of Chronic Obstructive Pulmonary Disease OR AECOPD) AND ((y_10[Filter]) AND (clinicaltrial[Filter]) AND (fft[Filter]) AND (humans[Filter]) AND (english[Filter]) AND (alladult[Filter])))) OR (((LRTI OR lower respiratory tract infection OR Respiratory Tract Infection) AND ((y_10[Filter]) AND (clinicaltrial[Filter]) AND (fft[Filter]) AND (humans[Filter]) AND (english[Filter]) AND (alladult[Filter])))) OR (((Pneumonia OR Consolidation) AND ((y_10[Filter]) AND (clinicaltrial[Filter]) AND (fft[Filter]) AND (humans[Filter]) AND (english[Filter]) AND (alladult[Filter])))) AND (((Metabolomics OR Metabolom* OR Metabolite OR Breathomic OR Volatile organic compounds) AND ((y_10[Filter]) AND (clinicaltrial[Filter]) AND (fft[Filter]) AND (humans[Filter]) AND (english
```

7.4 APPENDIX (D): Additional documents; Research passport, certificates for Good Clinical Practice (GCP) training, research essentials and informed consent training





RESEARCH & INNOVATION

While undertaking research through University Hospitals of Leicester NHS Trust, you will remain accountable to your Employer **University of Leicester** but you are required to follow the reasonable instructions of **Prof Salman Siddiqui** in this NHS organisation or those given on her/his behalf in relation to the terms of this right of access.

Where any third party claim is made, whether or not legal proceedings are issued, arising out of or in connection with your right of access, you are required to co-operate fully with any investigation by this NHS organisation in connection with any such claim and to give all such assistance as may reasonably be required regarding the conduct of any legal proceedings.

You must act in accordance with **University Hospitals of Leicester NHS Trust** policies and procedures, which are available to you upon request, and the Research Governance Framework.

You are required to co-operate with **University Hospitals of Leicester NHS Trust** in discharging its duties under the Health and Safety at Work etc Act 1974 and other health and safety legislation and to take reasonable care for the health and safety of yourself and others while on **University Hospitals of Leicester NHS Trust** premises. You must observe the same standards of care and propriety in dealing with patients, staff, visitors, equipment and premises as is expected of any other contract holder and you must act appropriately, responsibly and professionally at all times.

You are required to ensure that all information regarding patients or staff remains secure and *strictly confidential* at all times. You must ensure that you understand and comply with the requirements of the NHS Confidentiality Code of Practice (<http://www.dh.gov.uk/assetRoot/04/06/92/54/04069254.pdf>) and the Data Protection Act 1998. Furthermore you should be aware that under the Act, unauthorised disclosure of information is an offence and such disclosures may lead to prosecution.

You should ensure that, where you are issued with an identity or security card, a bleep number, email or library account, keys or protective clothing, these are returned upon termination of this arrangement. Please also ensure that while on the premises you wear your ID badge at all times, or are able to prove your identity if challenged. Please note that this NHS organisation accepts no responsibility for damage to or loss of personal property.

We may terminate your right to attend at any time either by giving seven days' written notice to you or immediately without any notice if you are in breach of any of the terms or conditions described in this letter or if you commit any act that we reasonably consider to amount to serious misconduct or to be disruptive and/or prejudicial to the interests and/or business of this NHS organisation or if you are convicted of any criminal offence. Your substantive employer is responsible for your conduct during this research project and may in the circumstances described above instigate disciplinary action against you.

University Hospitals of Leicester NHS Trust will not indemnify you against any liability incurred as a result of any breach of confidentiality or breach of the Data Protection Act 1998. Any breach of the Data Protection Act 1998 may result in legal action against you and/or your substantive employer.

If your current role or involvement in research changes, or any of the information provided in your Research Passport changes, you must inform your employer through their normal procedures. You must also inform your nominated manager in this NHS organisation.



**RESEARCH
& INNOVATION**

Yours sincerely

**Lisa Wann
R&I Manager**

**cc: Copy to University of Leicester HR
Tina Larder HR UHL
Prof Salman Siddiqui UHL
Copy for File**

CERTIFICATE OF ACHIEVEMENT

Masarrah aljaroof

has completed the course:

Introduction to Good Clinical Practice (GCP) eLearning

July 21, 2020

Modules Completed

- Introduction to Health and Social Care Research
- Good Clinical Practice
- Informed Consent
- Data Collection and Documentation
- Safety Reporting
- Summary

Doctoral College, University of Leicester

This is to certify that

Masarrah Y.H. Aljarroof

has successfully completed

Research Essentials Online

on

11 April 2020



Certificate of Completion

Masarrah Aljarroof

has completed

Informed Consent

on

13 August 2020 Online Delivery

AIMS

- Understand the ethical and legislative frameworks that underpin the research consent process
- Understand the principles and responsibilities of consent in clinical research
 - Develop an understanding of the research consent process
- Gain an insight into the added protection required for vulnerable groups
 - Build confidence in participating in the research consent process

Improving the health and wealth of the nation through research